FlowDike-D

Influence of wind and current on wave run-up and wave overtopping

Final report

Dipl.-Ing. Stefanie Lorke[1]
Dr.-Ing. Antje Bornschein[2]
Univ.-Prof. Dr.-Ing. Holger Schüttrumpf[1]
Prof. Dr.-Ing. habil. Reinhard Pohl[2]

Aachen and Dresden, April 2012

[1] Institute of Hydraulic Engineering and Water Resources Management, RWTH Aachen University, Germany

[2] Institute of Hydraulic Engineering and Technical Hydromechanics, TU Dresden, Germany

Following partners and authors are responsible for this report:

IWW (RWTH Aachen): Stefanie Lorke, Holger Schüttrumpf
IWD (TU Dresden): Antje Bornschein, Reinhard Pohl

The authors would like to thank the following researchers who have contributed to the project and report:
Stefan Carstensen, Jens Kirkegard, Flemming Schlütter, DHI Hørsholm, Denmark
Jentsje W. van der Meer, Van der Meer Consulting, Netherlands
Babette Scheres, Anja Brüning, RWTH Aachen University, Germany
Stefano Gilli, Torsten Heyer, Nadine Krüger, Technische Universität Dresden, Germany
Ladislav Dvorak, Miroslav Spano, Jaromir Riha, Technical University Brno, Czechia
Stefan Werk, Technical University Braunschweig, Germany

Table of contents

List of figures

Annex

List of tables

Annex

List of symbols

Letters

a	[-]	correction factor single overtopping events
a_d	[-]	dilatations correction factor
a_r	[-]	coefficient depending at least on the dike slope to determine the influence factor γ_β
b	[-]	inclination of the slope of the graph (regression curve)
b_r	[-]	coefficient depending at least on the dike slope to determine the influence factor γ_β
c	[m/s]	wave velocity
c_1	[-]	empirical parameters to determine the run-up height
c_2	[-]	empirical parameters to determine the run-up height
c_3	[-]	empirical parameters to determine the run-up height
c_2*	[-]	parameter for describing the layer thickness
$c_{g,rel}$	[m/s]	relative group velocity of waves
c_h	[-]	empirical coefficient determined by model tests concerning flow depth on crest
c_v	[-]	empirical coefficient determined by model tests
d	[m]	flow depth, water depth
d_b	[m]	flow depth at breaker point without wind
$d_{b(wind)}$	[m]	flow depth at breaker point with wind
$d_{channel}$	[m]	width of the overtopping channel
f	[Hz]	frequency
f_p	[Hz]	spectral peak frequency
g	[m/s²]	acceleration due to gravity (= 9.81 m/s²)
h*	[-]	dimensionless flow depth on seaward dike crest

$h_{2\%}$	[m]	flow depth on dike crest exceeded by 2% of the incoming waves
h_{crest}	[m]	layer thickness (flow depth) on dike crest
k	[rad/m]	wave number $k = \frac{2\pi}{\omega}$
m_0	[m²/s]	zero order moment of spectral density
$m_{0,inc}$	[m²/s]	energy density of the incident wave spectrum
$m_{0,refl}$	[m²/s]	energy density of the reflected wave spectrum
m_{-1}	[m²]	minus first moment of spectral density
m_n	[m²/s^n]	n^{th} moment of spectral density
p	[-]	probability of wave overtopping event
p_{br}	[-]	coefficient for deterministic and probabilistic design, breaking waves
p_{nbr}	[-]	coefficient for deterministic and probabilistic design, breaking waves
q	[m³/(sm)]	mean overtopping rate per meter structure width
q^*	[-]	dimensionless overtopping discharge
$q_{\beta=0°}$	[m³/(sm)]	overtopping rate with angle of wave attack $\beta = 0°$
$q_{\beta\neq0°}$	[m³/(sm)]	overtopping rate with angle of wave attack $\beta > 0°$
s	[-]	wave steepness s = H/L
$s_{m-1,0}$	[-]	wave steepness defined by $s_{m-1,0} = H_{m0}/L_{m-1,0}$
t_{end}	[s]	analyzing end time of the test
t_{start}	[s]	analyzing start time of the test
u	[m/s]	wind velocity
u_{10}	[m/s]	wind velocity 10 m above still water level
v	[m/s]	current velocity parallel to the dike crest
$v_{2\%}$	[m/s]	flow velocity on dike crest exceeded by 2% of the incoming waves
v_{crest}	[m/s]	overtopping velocity (flow velocity) on the dike crest
$v_{crest,no\ wind}$	[m/s]	flow velocity on the dike crest, wind $u_{10} = 0$ m/s
$v_{crest,wind}$	[m/s]	flow velocity on the dike crest, wind $u_{10} \neq 0$ m/s

v_n	[m/s]	current velocity in the direction of wave propagation
x	[m]	horizontal coordinate parallel to the dike crest
y	[m]	horizontal coordinate perpendicular to the dike crest
z	[m]	vertical coordinate

Capital letters

C	[-]	coefficient
C_r	[-]	average reflection coefficient
C_ξ	[-]	parameter considering infl. of shallow foreshore, roughness, obliqueness
Fr_{crest}	[-]	Froude number at the crest
Fr_{wave}	[-]	Froude number of the wave
H	[m]	wave height
H_{m0}	[m]	significant wave height from spectral analysis
$H_{m0,dike\ toe}$	[m]	significant wave height from spectral analysis at toe of the dike
$H_{m0,wave\ generator}$	[m]	significant wave height from spectral analysis in front of wave generator
H_{max}	[m]	measured maximum wave height
H_s	[m]	significant wave height (defined as highest one-third of wave heights)
H_{WM}	[m]	wave height, adjusted at the wave machine
K_R	[-]	reflection coefficient
L	[m]	wave length in direction of wave propagation
$L_{0m-1,0}$	[m]	deep water wave length based on $T_{m-1,0}$
L_{0p}	[m]	wavelength corresponding to T_p and deep water conditions
L_m	[m]	wavelength corresponding to T_m
$L_{m-1,0}$	[m]	deep water wave length $L_{m-1,0} = \frac{T_{m-1,0}}{2\pi}$
L_p	[m]	wavelength corresponding to T_p
L_s	[m]	airy wave length corresponding to T_s

N	[-]	number of incoming waves
P_{OW}	[-]	probability of overtopping per wave
Q_0	[-]	interception with the y-axis
R_{c*}	[-]	dimensionless freeboard height
R^2	[-]	coefficient of determination
R_c	[m]	freeboard height of the structure
R_u	[m]	run-up level, vertical measured with respect to the SWL
$R_{u2\%}$	[m]	run-up height exceeded by 2% of the incoming waves
$R_{u2\%;\beta=0°}$	[m]	run-up height exceeded by 2% of the incoming waves with $\beta = 0°$
$R_{u2\%;\beta>0°}$	[m]	run-up height exceeded by 2% of the incoming waves with $\beta > 0°$
$R_{ux\%}$	[m]	run-up level exceeded by x% of incoming waves
Re_{wave}	[-]	Reynold number of the wave
Re_{crest}	[-]	Reynold number at the crest
SJ(f)	[m²/Hz]	JONSWAP-energy-density-spectrum
SP(f)	[m²/Hz]	Phillips-spectrum describing the decreasing part of the graph
SPM(f)	[m²/Hz]	energy density spectrum of Pierson-Moskowitz
T	[s]	wave period
T_m	[s]	mean wave period (here: from time-domain analysis)
T_0	[s]	deep water wave period
$T_{m0,1}$	[s]	average wave period defined by $T_{m0,1} = m_0/m_1$
$T_{m0,2}$	[s]	average wave period defined by $T_{m0,2} = m_0/m_2$
$T_{m-1,0}$	[s]	spectral wave period defined by $T_{m-1,0} = m_{-1}/m_0$
T_p	[s]	spectral peak wave period
U	[V]	voltage (measured value)
V	[m³]	overtopping volume per wave
V'	[m³/s]	overtopping volume per meter wave

V_{lc}'	[m³/m]	volume per meter wave considering the channel width of the load cell
V_{ov}	[m³]	overtopping volume during one test
V_{Pump}	[m³]	volume, pumped out of the overtopping tank
V_{vh}'	[m³/m]	volume per meter wave considering data of wave gauges and micro propeller
V_i	[m³]	volume in the overtopping tank at time t_i
We_{crest}	[-]	Weber number at the crest

Greek letters

α	[°]	slope of the front face of the structure
α	[-]	Phillips-constant $\alpha = 8.1 \cdot 10\text{-}3$
β	[°]	angle of wave attack relative to normal on structure; perpendicular wave attack: $\beta = 0°$; oblique wave attack: $\beta \neq 0°$
β'	[°]	ratio of angle of wave attack and dike parallel wave attack
β_e	[°]	angle of wave energy relative to normal on structure
γ	[-]	peak raising factor [-] $\gamma = 3.3$ for mean JONSWAP-spectrum
γ	[-]	correction factor considering run-up and overtopping design
γ_b	[-]	correction factor for a berm considering run-up and overtopping design
γ_{cu}	[-]	correction factor to take the influence of current v_x into account
γ_f	[-]	correction factor for surface roughness considering run-up and ov. design
γ_β	[-]	correction factor for oblique wave attack considering run-up and ov. design
$\gamma_{\beta,cu}$	[-]	correction factor to take the influence of angle of wave attack current v_x into account
γ_v	[-]	correction factor for a vertical wall on the slope
γ_w	[-]	correction factor to take the influence of wind into account
Δt	[s]	duration of a wave overtopping event
ΔV_i	[l]	difference of the volume in the tank during pumping interval
ξ_{eq}	[-]	surf similarity parameter considering influence of a berm

$\xi_{m-1,0}$	[-]	surf similarity parameter based on $s_{m-1,0}$
ξ_p	[-]	surf similarity parameter based on H_s and L_{0p}
ξ_{tr}	[-]	surf similarity parameter describing transition between br. and non-br. waves
ν	[m²/s]	dynamic viscosity
ν_{crest}	[m/s]	velocity at the crest
σ_0	[N/m]	surface tension
ω_{abs}	[rad/s]	absolute angular frequency
ω_{rel}	[rad/s]	relative angular frequency

List of abbreviations

br	breaking wave conditions
fd 1	FlowDike 1 – 1:3 sloped dike
fd 2	FlowDike 2 – 1:6 sloped dike
nbr	non-breaking wave conditions
SWL	still water level
w1	wave condition number 1
w2	wave condition number 2
w3	wave condition number 3
w4	wave condition number 4
w5	wave condition number 5
w6	wave condition number 6
wcI	wave characteristics I
wc II	wave characteristics II
WL	water level

1 Introduction

A variety of structures has been built in the past to protect the adjacent areas during high water levels and storm surges from coastal or river flooding. It is common practice to build smooth sloped dikes as well as steep or vertical walls as flood protection structures. The knowledge of the design water level with a certain return interval, wind surge, wave run-up and/or wave overtopping is used to determine the crest height of these structures.

The incoming wave parameters at the toe of the structure are relevant for the freeboard design in wide rivers, estuaries and at the coast. At rivers these are probably influenced by local wind fields and sometimes by strong currents - occurring at high water levels mostly parallel to the structure. In the past no investigations were made on the effects of current and the combined effects of wind and current on wave run-up and wave overtopping. Only a few papers, dealing with wind effects, are publicized. To achieve an improved design of structures these effects should not be neglected, otherwise the lack of knowledge may result in too high and expensive structures or in to low flood protection structure which results in a higher risk of flooding.

The aim of the research project presented is to achieve better understanding about the influence of current and wind on wave run-up and wave overtopping by experimental investigations in an offshore wave basin. Data from previous KFKI projects “Oblique wave attack at sea dikes” and “Loading of the inner slope of sea dikes by wave overtopping” and from the CLASH-database are at hand for comparison purposes. They represent a set-up with perpendicular and oblique wave attack but without wind and without longshore current.

The research dealt with the wave run-up and wave overtopping due to long-crested waves on a dike slope with a smooth surface. The experimental set-up includes different longshore current velocities and onshore wind speeds, two different dike crest levels and various wave directions.

The experimental investigations were performed within two test phases in 2009 at DHI in Hørsholm, Denmark. In the first test phase (EU-HYDRALAB-III project FlowDike) a 1:3 sloped dike (FlowDike 1) was investigated, while a 1:6 sloped dike (FlowDike 2) was tested in the second test phase (BMBF-KFKI project FlowDike-D, 03KIS075 (IWW), 03KIS076 (IWD)). The compilation of both test phases, using the results for the 1:3 dike as well as the results for the 1:6 dike, is done within the project FlowDike-D.

A first overall view of the experimental procedure and a more detailed description of the model set-up as well as the used measurements are given in section 2 and 3. After presenting the literature review and the method of analyzing data of the wave field (section 4) and of the wave run-up and wave overtopping (section 5), the data processing of the raw data is given in section 6 for the different measurements. Section 7 presents the analysis of the wave field which includes the verification of a homogeneous wave field at the dike toes and the description of the influence of current on the measured wave field. The analyses on wave run-up and wave overtopping have been done in section 8, which includes the analyses of wave run-up measurements, determination of mean overtopping discharges, evaluation of flow processes on dike crests and single overtopping events. Finally a conclusion and outlook is given in section 9.

2 Experimental procedure

2.1 Overview of test program

The investigation was focused on long crested waves which were created using JONSWAP spectrum (see section 2.2). The test program covered model tests with and without current and with and without wind for normal and oblique wave attack. Table 2.1 presents a summary of the test program. The angle of wave attack covers a range of 0° to 45°. The maximum flow velocity was 0.4 m/s and the maximum wind speed was 10 m/s. Normal wave attack is here equal to an angle of $\beta = 0°$. Waves with a positive angle of wave attack propagate in the direction of the current, while waves with a negative angle of wave attack are directed against the current.

Table 2.1 Summary of the test program and test configurations.

freeboard height R_C [m]	1:3 dike: 0.10 and 0.20 1:6 dike: 0.05 and 0.15						
wave height H_s [m] and wave period T_p [s]	1:3 dike: H_s	0.07	0.07	0.10	0.10	0.15	0.15
	T_P	1.474	1.045	1.76	1.243	2.156	1.529
	1:6 dike: H_s	0.09	0.09	0.12	0.12	0.15	0.15
	T_P	1.67	1.181	1.929	1.364	2.156	1.525
angle of wave attack β [°]	-45	-30	-15	0	+15	+30	
current v_x [m/s]	0.00	0.15	0.30	0.40 (only 1:6 dike)			
wind velocity measured at the dike crest u [m/s]	1:3 dike		0	5	10		
	1:6 dike		0	4	8		

The test program did consider dikes with different slopes too. In whole 119 tests were performed on a 1:3 sloped dike and 152 tests were done on a 1:6 sloped dike (for details see Table°2.2 and Table 2.3. Extensive tables with all tests and the associated test number as well as boundary conditions are given in Annex E (1:3 sloped dike) and Annex F (1:6 sloped dike).

Table°2.2 Matrix of test configurations, 1:3 sloped dike (tests regarding the influence of wind are marked by a number (wind velocity [m/s]) in the cell, □ = tests were not carried out, ■ = test were carried out applying wave characteristics I (cf. Table 2.4), flow depth 0.50 m (see section 2.2)).

Current [m/s]	-45	-30	-15	0	+15	+30
0.40						
0.30	■	■	■	5 10	■	5 10
0.15	■	■	■	■	■	■
0.00	■	5 10	■	5 10	■	5 10

Wave direction [°]

Table 2.3 Matrix of test configurations, 1:6 sloped dike (tests regarding the influence of wind are marked by a number (wind velocity [m/s]) in the cell, □ = tests were not carried out, ■ = test were carried out applying wave condition I (cf. Table 2.4), flow depth 0.50 m, ■ tests were carried out with wave characteristics II (cf. Table 2.5), flow depth 0.55 m (see section 2.2)).

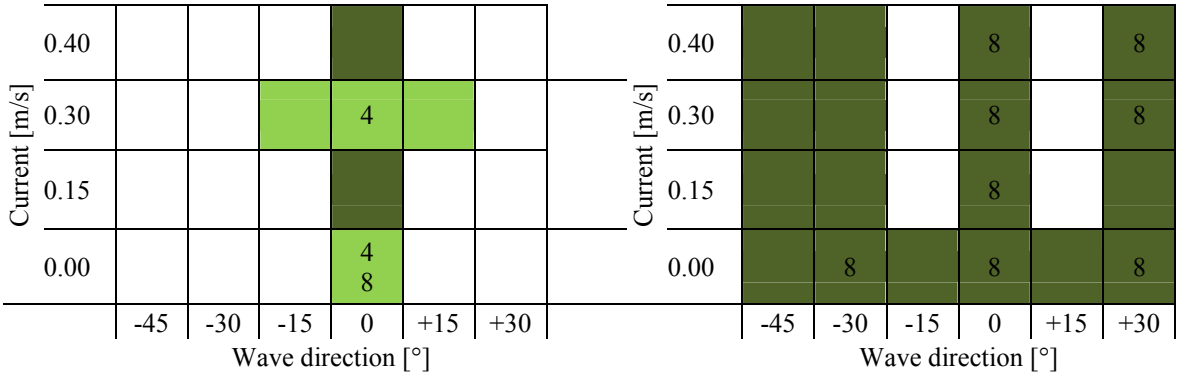

2.2 Wave parameters

Each tested combination of a certain angle of wave attack, a current velocity (including no current) and a wind velocity (including no wind) provides the framework for six tests with six different sea states. Each sea state is characterized by a significant wave height H_s and a peak period T_p. The DHI wave synthesizer (DHI WASY WATER & ENVIRONMENT, 2007) was applied to generate the time-dependent wave height according to the formulas of JONSWAP spectra (cf. section 4.1) so that one test includes at least 1000 approaching waves (cf. Annex D).

Table 2.4 Wave parameters of wave characteristics I (wc I)

wave no. [-]	H_S [m]	T_P [s]	$T_{m-1,0} \approx \frac{T_p}{1.1}$ [s]	$L_{m-1,0} = \frac{g \cdot T_{m-1,0}^2}{2\pi}$ [m]	$s_{m-1,0} = \frac{H_s}{L_{m-1,0}}$ [-]	$\xi = \frac{tan\alpha}{\sqrt{s_{m-1,0}}}$ dike slope		duration of 1000 waves [min]
						1:3 [-]	1:6 [-]	
w1	0.07	1.474	1.340	2.803	0.025	2.109	1.055	25
w2	0.07	1.045	0.950	1.409	0.050	1.496	0.748	17
w3	0.10	1.76	1.600	3.997	0.025	2.107	1.054	29
w4	0.10	1.243	1.130	1.994	0.050	1.488	0.744	21
w5	0.15	2.156	1.960	5.998	0.025	2.108	1.054	36
w6	0.15	1.529	1.390	3.017	0.050	1.495	0.747	25

The waves characterized in Table 2.4 were tested during the first part of the test program using a 1:3 sloped dike and a water depth of 0.50 m (FlowDike 1). Different wave parameters as well as two different water depths of 0.50 m and 0.55 m have been chosen during the second part of the test program in order to get a significant overtopping rate. The associated wave characteristics I are given in Table 2.4 whereas wave characteristics II are presented in Table 2.5.

Table 2.5 Wave parameters of wave characteristics II (wc II)

wave no. [-]	H_S [m]	T_P [s]	$T_{m-1,0} \approx \frac{T_p}{1.1}$ [s]	$L_{m-1,0} = \frac{g \cdot T_{m-1,0}^2}{2\pi} \cdot$ [m]	$s_{m-1,0} = \frac{H_s}{L_{m-1,0}}$ [-]	$\xi = \frac{tan\alpha}{\sqrt{s_{m-1,0}}}$ dike slope 1:6 [-]	duration of 1000 waves [min]
w1	0.09	1.670	1.518	3.599	0.025	1.054	28
w2	0.09	1.181	1.074	1.800	0.050	0.745	20
w3	0.12	1.929	1.754	4.801	0.025	1.054	32
w4	0.12	1.364	1.240	2.401	0.050	0.745	23
w5	0.15	2.156	1.960	5.998	0.025	1.054	36
w6	0.15	1.525	1.386	3.001	0.050	0.745	25

A fully developed sea state could only be created within a certain domain of the basin because of the limited length of the wave machine. In addition the influence of the current and the obliqueness of wave attack restricted the dike section which was reliable for measurement. Therefore it was necessary to install different set-up configurations to ensure parallel measurement of run-up and overtopping. Table 2.6 gives an overview of all six test set-ups. Detailed information for every test set-up is given in the Annex (Figure-annex 1 to Figure-annex 6).

Table 2.6 Overview of different model set-ups depending on the considered angle of wave attack.

angle of wave attack [°]	1:3 sloped dike [-]	1:6 sloped dike [-]
-15, 0, +15	set-up 1	set-up 4
+30	set-up 2	set-up 5
-30, -45	set-up 3	set-up 6

2.3 Short overview of the data storage management

For each test of a test series a process file (*.xls) was generated. One process file includes i.e. the graphics for the spectral energy density, wave height distribution, as well as some exceedance curves for flow velocities and layer thickness. Preliminary results of processed data are explained by means of test s1_01_00_w1_00_00 (reference test, 1:3 sloped dike) in section 6.

The filename includes the main information, such as set-up number, test series, current, wave number, wind speed and angle of wave attack. The template was defined as follow:

s1	_	01	_	00	_	w1	_	00	_	00w
set-up no. [-]		test series no. [-]		current (velocity) [cm/s]		wave no. [-]		wind (generation) [Hz]		angle of wave attack* [°]

*indices: “m” or “w”: with the current (+); “p” or ”a”: against the current (-); [“m” and “p” are old terms]

3 Model construction and instrumentation

3.1 Configuration

3.1.1 Shallow water basin

The Danish Hydraulic Institute (DHI) in Hørsholm, Denmark provided a shallow water wave basin as test facility for the hydraulic model tests. It was 35 m long, 25 m wide and could be flooded to a maximum water depth of 0.9 m. At the eastern long side an 18 m long multidirectional wave generator composed of 36 segments (paddles) was installed (see Figure 3.1). The 0.5 m wide and 1.2 m high segments can be used to generate multidirectional, long or short crested waves. The applied DHI software included procedures for active wave absorption. An automatic control system called AWACS (Active Wave Absorption Control System) used the measured data of the actual water depth at each paddle to identify and absorb reflected waves.

Wind machines were used to introduce wind as an influence parameter. They could generate a homogenous wind field over the free water surface. Six wind machines were placed in front of the wave generator 0.8 m above the basin floor.

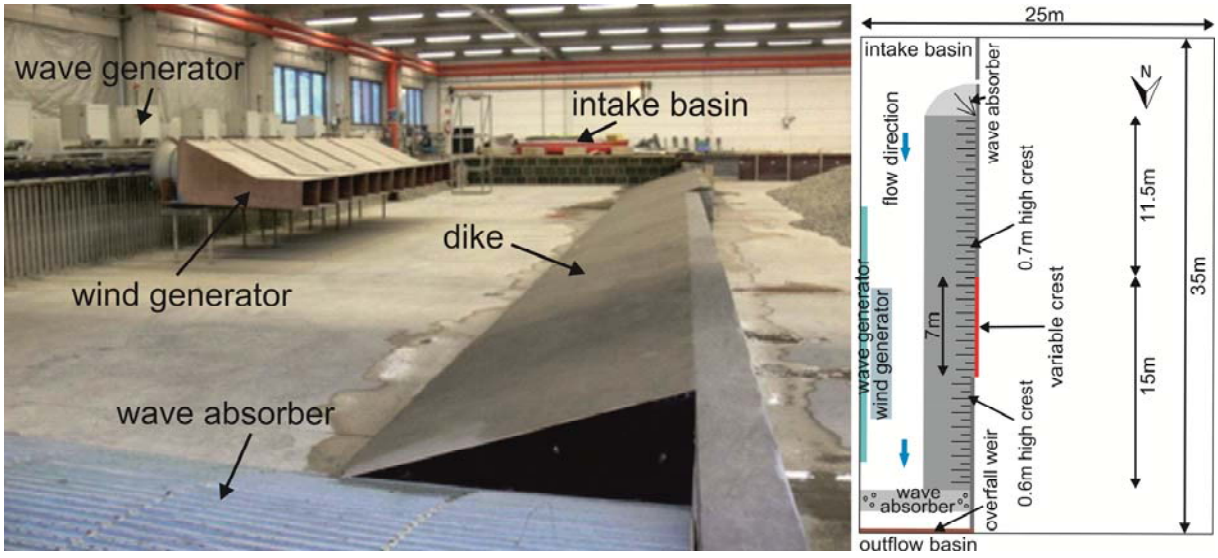

Figure 3.1 Completed dike slope (view from downstream), wave generator (paddles) and wind generator (fans) on the left side.

An adjustable weir at the downstream end was used to ensure a constant water depth in the basin. To create a longshore current a closed water cycle was initiated. The pumped water discharge was adjusted for each current velocity so that the chosen water depth was assured. Three rows of beverage crates at the upstream end were used to straighten the inflow and to provide aligned and parallel streamlines within the channel (see Figure 3.2). Wave absorbers at the upstream and downstream end ensured minimal reflection and diffraction. At the upstream end gravel heap was placed whereas at the downstream end metallic wave absorber was used (see Figure 3.2).

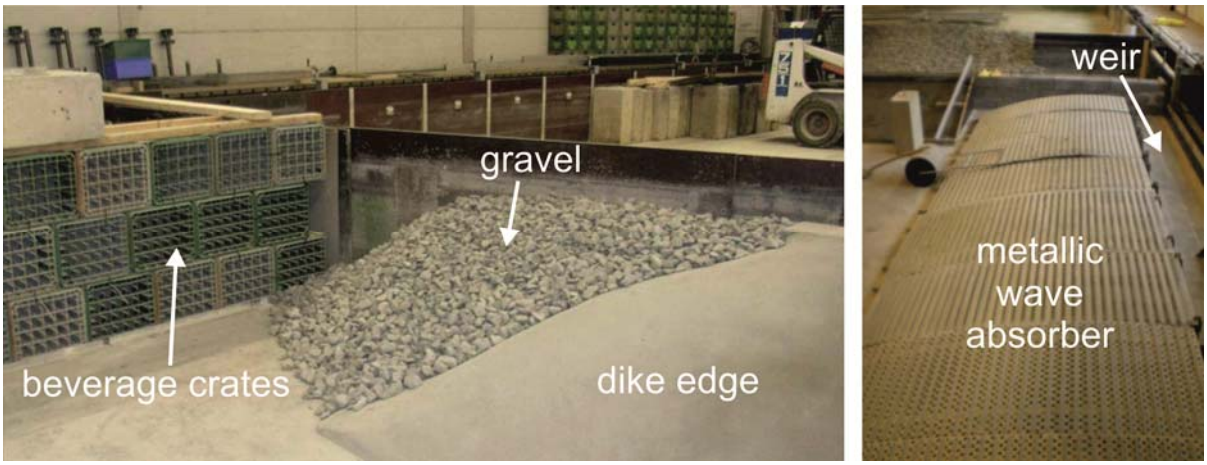

Figure 3.2 left: upstream edge of the dike with wave absorption and beverage racks; right: metallic wave absorber in front of the weir

All sensor signals were sampled and put into storage by using the DHI Wave Synthesizer. During FlowDike 1 a sampling frequency of 25 Hz was used whereas during FlowDike 2 a sampling frequency of 40 Hz was adapted according to the signal resolution of the pressure sensors. All acquired data were stored in *.dfs0- and *.daf-files.

After all measurement devices have been installed the whole basin in front of and behind the dike section was flooded. Therefore all additional equipment like data acquisition, amplifier, computer and spotlights, which were situated behind the dike, needed to be placed on platforms. An overall view of the data acquisition during FlowDike 2 is illustrated by Figure 3.3.

Figure 3.3 Platform with data acquisition; Stand with amplifier and A/D converter

3.1.2 Construction of the 1:3 sloped dike – FlowDike 1

The toe of the 1:3 sloped dike was situated at a distance of 6.0 m from the wave generator. The complete dike structure was 26.5 m long. Its length was determined by the domain where the fully developed sea state reaches the dike slope considering the different wave directions (see Annex Figure-annex 1 to Figure-annex 3).

The model dike looked like half a dike. A brick wall formed the landward side and the 0.28 m wide dike crest. On the seaward side a core of compacted gravel was covered with a 50 mm concreted layer.

The dike was divided into two sections. Each section had a different dike height. Hence two different freeboard heights could be investigated at the same time. The first dike section had a crest height of

0.6 m and was 15 m long. Downstream the second dike section with a dike height of 0.7 m and a length of 11.5 m was situated. In addition a variable crest of plywood was used to extend the part of the 0.7 m high dike by 7 m (see Figure 3.1 and Figure 3.4). This was required for the different set-up configuration during the test program. To avoid different roughness coefficients between the concrete layer of the dike and the structure of the variable crest all plywood parts were covered with a fine layer of sand.

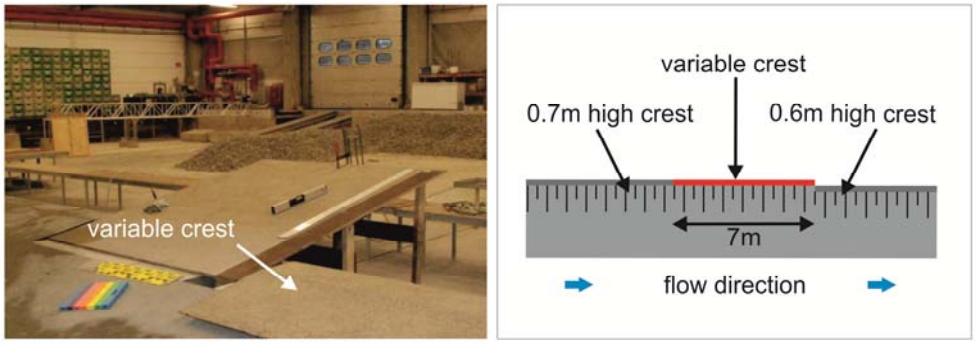

Figure 3.4 Run-up board and variable crest during construction (left); arrangement of the two dike sections (left)

The overtopping water was sampled by four overtopping units out of plywood which were mounted at the landward edge of the crest. A cross-section of one overtopping unit is given in Figure 3.5. Two units have been installed at the lower and two at the higher dike part. The overtopping water was lead into an overtopping channel and then into the overtopping tank. The overtopping water in each tank was measured by a load cell and water level gauges in each tank. Standard pumps in the tanks were used to empty the tanks during and after each test (see section 3.2.7). External boxes were constructed to contain the overtopping tanks, load cells and water level gauges and prevent these devices from uplift.

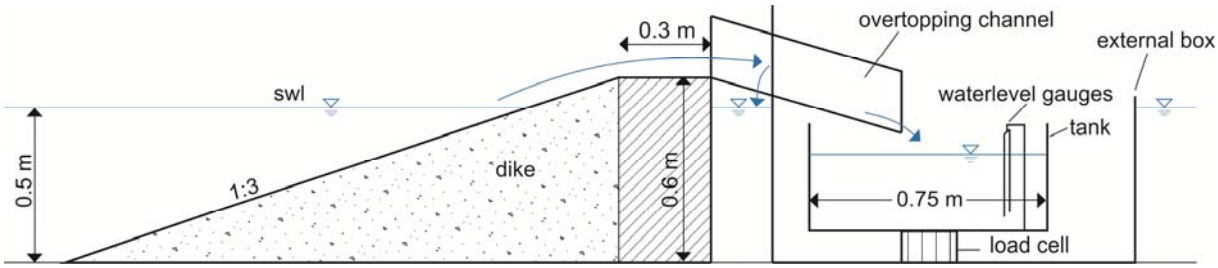

Figure 3.5 Cross section of overtopping unit exemplary for the 0.6 m high dike

For the wave run-up a so called “run-up board” out of plywood (2 m x 2.5 m) was mounted on top of the concrete crest to facilitate the up rush measurement by a capacity gauge and video analysis. This plate could be moved easily in its position during the changes of set-ups. The gap between run-up board and crest edge was filled either with a wooden piece and silicone or with a cement cover. To get films with a better contrast the wave run-up board was enlightened by a 2000-W-spotlight which was positioned such as the light met the run-up board within an angle of 120° to the optical axis of the digital cameras. On the left side of the run-up plate a digital radio controlled clock with a 0.4 m x 0.4 m display was positioned due to the purpose of synchronizing the measurements (Figure 3.6). Additionally two step gauges with a length of 1 m each have been installed on the 0.7 m high dike.

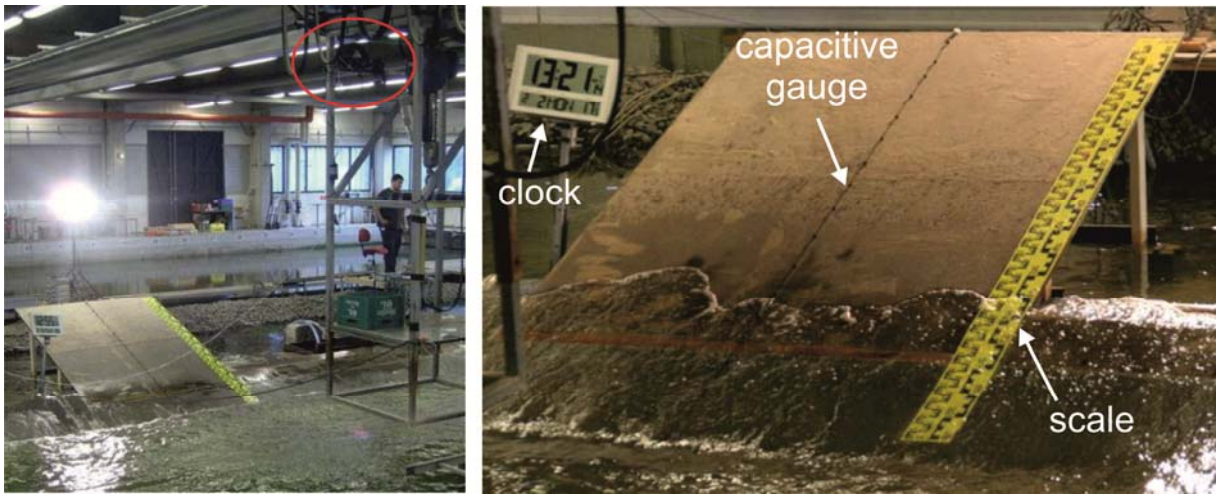

Figure 3.6 Wave run-up board and rack with both digital cameras marked with a red circle (left); capacitive gauge, clock and scale (right)

3.1.3 Construction of 1:6 sloped dike – FlowDike 2

Some details were changed for the FlowDike 2 test phase in comparison to the set-up of the first investigations of FlowDike 1 (1:3 sloped dike). Overtopping units, run-up board and variable crest remained mostly in the same shape or were reused.

Figure 3.7 View from the upstream inlet of the 1:6 sloped dike set-up, wind machines and wave gauges in front of the dike

In order to keep the line where the still water level (SWL) reaches the dike slope at the same position as during the FlowDike 1 tests the toe of the 1:6 sloped dike was situated at a distance of 4.5 m from the wave generator. Due to the smoother slope of the dike the channel cross section was smaller during FlowDike 2 than during FlowDike 1. The length of the dike remained 26.5 m depending on the section where a fully established sea state reached the dike slope.

3.2 Measurements

3.2.1 Overview

An overview of the shallow water basin is given in Figure 3.8 (1:3 sloped dike) and Figure 3.9 (1:6 sloped dike). Flow direction of the current (blue arrows) was from left to right. The area marked in light yellow indicates the domain where the fully developed sea state occurred depending of the angle

of wave attack. The position of all used measurement devices is marked and explained within the drawings. They are listed below in alphabetical order and are described in detail in the following sections. If there were changes in measurement devices between the tests on the 1:3 sloped dike and the 1:6 sloped dike they are explained too.

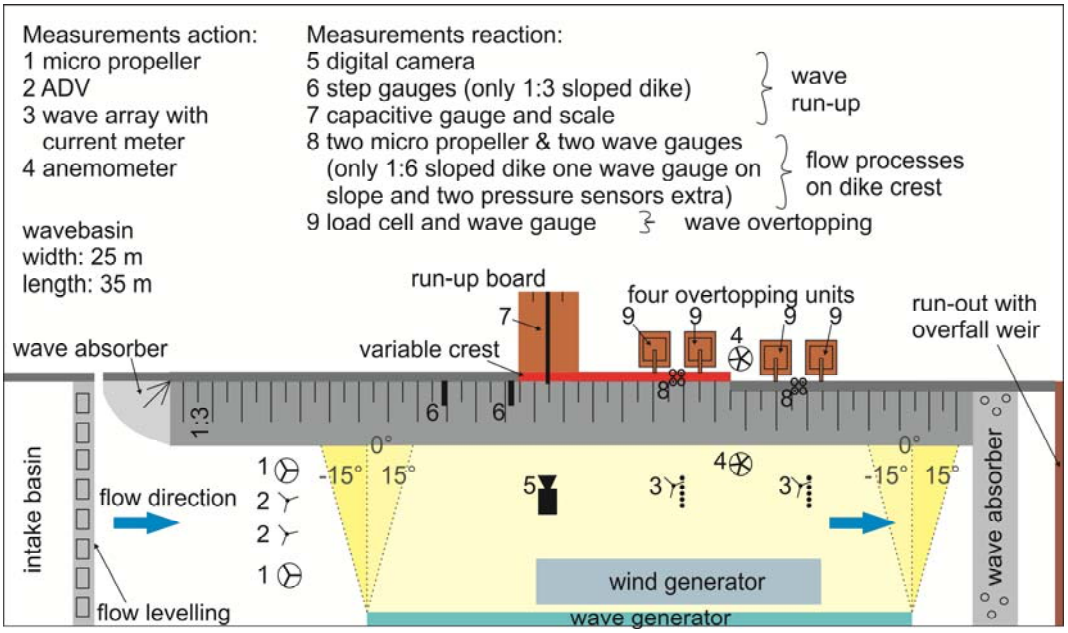

Figure 3.8 Model set-up 1 (FlowDike 1) with instruments and flow direction (1:3 sloped dike)

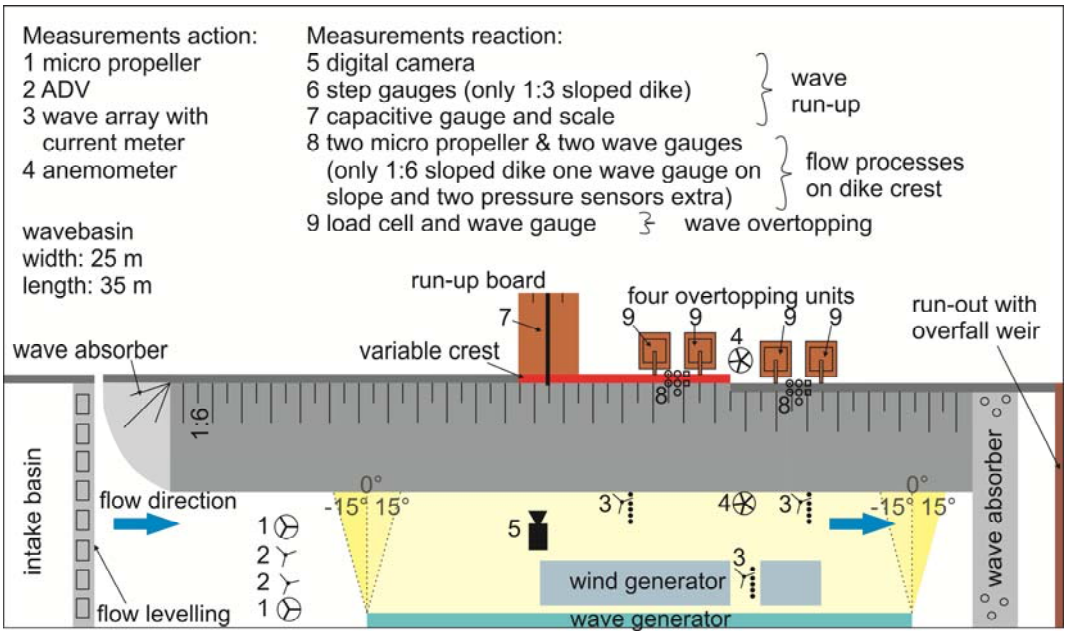

Figure 3.9 Model set-up 4 (FlowDike 2) with instruments and flow direction (1:6 sloped dike)

Anemometer (TSI)

Wind velocity was measured by two anemometers. They were provided by DHI and installed in the model set up. These thin transducers with a small window for the sensor were able to record a range of 0 V – 10 V (0 m/s – 20 m/s) with a sampling frequency of 5 Hz.

Capacitive gauge

The capacitive gauge on a run-up plate was used to get quantitative data of time-dependent wave run-up and down. The main part a 3.5 m long capacitor was formed by one insulated and one non insulated wire. Air or water between the two wires forms the dielectric fluid. The scale of the voltage value ranged from 0 V to 5 V. A sampling frequency of 25 Hz was applied.

The capacitive gauge was insensitive to environmental conditions like changes in water temperature but it depends on the model set-up especially on the wire length and the mounting height. That is why the calibration was repeated for each model set-up.

Current meter (Acoustic Doppler Velocity meter (ADV), Minilab SD-12, Vectrino)

Different devices were applied to measure current velocity at different location in the shallow water basin. Both ADV's and Vectrino are single point Doppler current meters. The current velocity is measured using the Doppler Effect. The sampling frequency was set to 25 Hz and a nominal velocity range of ±1 m/s. The Minilab SD-12 is an ultrasonic current meter. It contains a transducer, a reflector and four receivers that measure the velocity from time difference between the send and received signal. The resolution of this current meter is 1 mm/s.

Digital Cameras

The flow processes on the run up board were recorded by means of digital cameras too. The data analysis to obtain the run-up height could then be done later after the model tests. Two digital cameras were used for FlowDike 1 as well for FlowDike 2 but with different picture resolution and different frame rates.

Load cell

The cubic shaped weighing equipment had a height of 0.1 m and was mounted beneath the overtopping tank. They were used to measure the amounts of overtopping water. Data analysis was focused on the z-component with a maximum capacity of 2150 N (≈ 220 kg). Due to its accuracy (≤ 0.05 %) it was used to detect single overtopping events.

Micro propeller (Schiltknecht)

Vane anemometers of Schildknecht, Switzerland were used to measure flow velocity on the dike crest. The vane rotation is closely linear to flow velocity and is unaffected by pressure, temperature, density and humidity. During FlowDike 1 model tests a MiniWater 20 Micro was used. Its measuring range lay between 0.04 m/s and 5 m/s and its accuracy was 2% of the full scale. The calibration of the micro propeller was done by the partner from Braunschweig (LWI) before using them in the Hydralab project. For each device a calibration curve (voltage versus velocity) was determined (see Figure annex 7 in the Annex). Several MiniWater 6 Micro anemometers have been provided by DHI for FlowDike 2 tests. Their measuring range is identical to that of the MiniWater 20 Micro. The calibration was done in the model set-up by DHI (see calibration curves in Figure-annex 8).

Pressure sensors

Overtopping flow depth on the dike crest was measured by pressure sensors only on the 1:6 sloped dike. The head of these water resistant devices was installed as such as to have them flush with the

surface of the dike crest. The measuring range of the pressure sensors was 25 mV for 0.75 m water column. The voltage outputs for a constant calibration of 0.1 m per 1 Volt worked within a full scale accuracy of ±0.1%.

Step gauges

The step gauges which were additionally applied to quantify the wave run-up had a total length of 1 m and included 4 successive parts with 24 electrodes and a continuous wire. Wave run-up was detected by a signal when a short cut was caused between electrode and wire. A constant distance between the pins of 0.01 m gives a vertical precision of 0.0032 m regarding a 1:3 sloped dike. This device was only applied during FlowDike 1 and has not been evaluated yet.

Thermometer

It was essential for some measurement devices e.g. wave gauges to assure a constant water temperature during the test. A significant change in water temperature could be caused by pumping in order to create a longshore current velocity. The water temperature was monitored during all tests.

Wave gauges, water level gauges

Wave gauges and water level gauges were applied to measure water surface elevation and to gain data about the wave field and the flow depth on the crest. These sensors detect a change in water depth by means of change of conductivity between two thin, parallel stainless steel electrodes. An analog output signal is taken from the Wave Meter conditioning module, where the wave gauge is connected to, and compiled in the data acquisition system. Each wave gauge array included five wave gauges and one velocity meter. Calibration was only valid for a constant water temperature and had to be repeated if the water temperature deviated more than 0.5°C, generally at the beginning of each test day. Hereby a calibration factor of 0.1 m per 1 Volt was used. As an exception the calibration factor for the small wave gauges on the crest was 0.1 m per 0.5 Volt during FlowDike 1.

3.2.2 Wave field (wave gauges, ADV)

To analyze the wave field the water surface elevation as well as flow velocity has to be measured. These values were determined by two wave gauge arrays of 5 wave gauges (with a length of 0.6 m each) and a current meter. An overall view given in Figure 3.10 and Figure 3.11 demonstrates that each of them is orthogonal aligned between the wave machine and the dike. Each array was assigned to one crest height and placed at the toe of the structure positioned between the two overtopping channels.

Non-equal distances between the single gauges of the wave gauge arrays were necessary for the reflection analysis. That is why the wave gauges were placed at 0.00 m, 0.40 m, 0.75 m, 1.00 m and 1.10 m from the first wave gauge along a line. A current meter, ADV or Minilab SD-12, was positioned close to one wave gauge of the array. Reflection and crossing analysis were carried out for each array and its associated velocity meter.

In order to observe the development of the wave field while propagating through the longshore current a third wave gauge array, which was placed in front of the wave generator, was added to the model set-up of the 1:6 sloped dike. A vectrino was assigned as current meter to this array. The two other wave gauge arrays were situated in similar positions as in FlowDike 1 (1:3 sloped dike). The distance between the two wave gauge arrays at the dike toe and the one near the wave generator was 1.1 m.

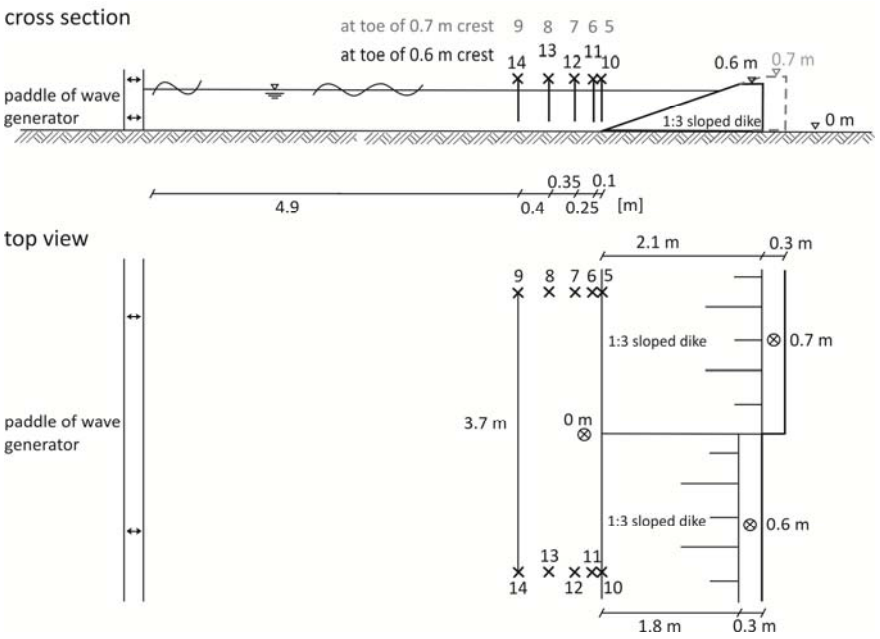

Figure 3.10 Configuration of the wave gauge arrays exemplary on the 1:3 sloped dike (cross sectional and top view)

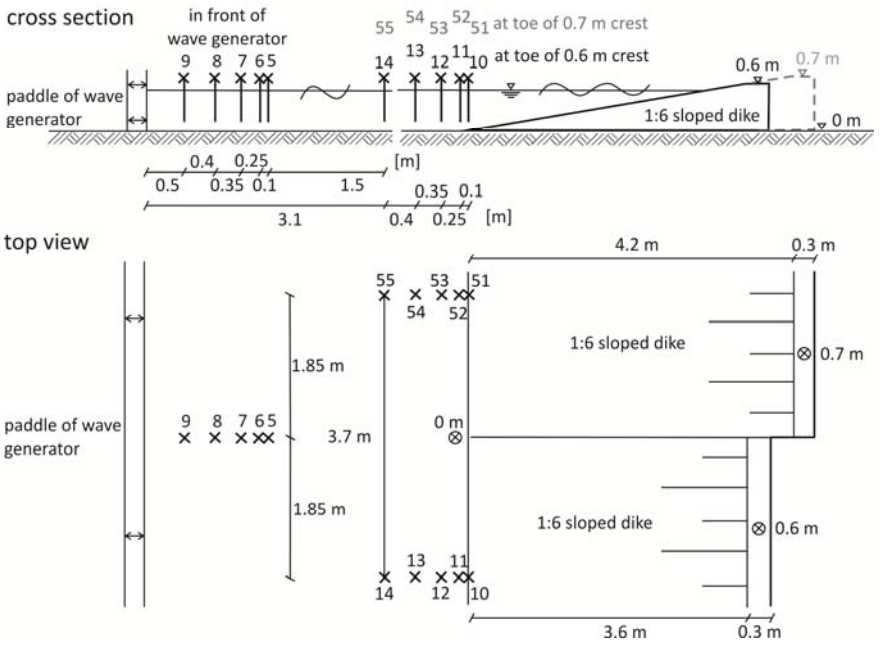

Figure 3.11 Configuration of the wave gauge arrays exemplary on the 1:6 sloped dike (cross sectional and top view)

3.2.3 Wind field (wind machine, Anemometer)

During the tests a wind field was generated by six wind machines using wind turbines. Wind direction was towards the dike and perpendicular to the dike crest. In order to create a homogeneous wind field on the dike slope and crest the distances between the six wind machines were not equally spaced (0.38 m – 0.45 m – 0.50 m – 0.45 m – 0.38 m).

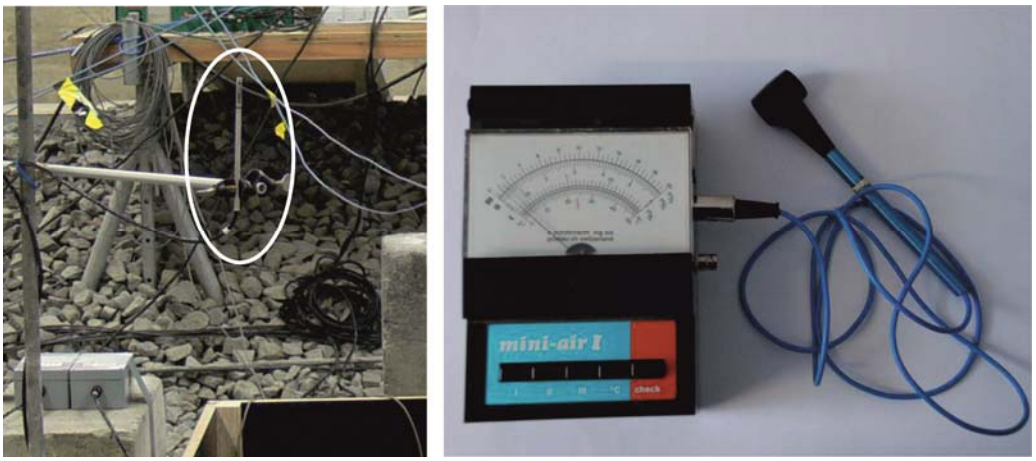

Figure 3.12 Anemometer (left) and fan wheel for air velocity measurement (right)

During the tests two different wind velocities have been created by setting two different propeller revolutions per second at the wind generators. To verify, if the wind field was spatially homogeneous, the wind velocity was measured along the dike crest with a fan wheel (see Figure 3.12). The results are given in Figure 3.13 and Figure 3.14.

All measurement results prove a homogeneously distributed wind field. The average wind velocity in FlowDike 2 (1:6 sloped dike) was slightly lower than in FlowDike 1 (1:3 sloped dike). This was caused by the larger distance between the wind generator and the dike crest.

To control wind velocity during tests two anemometers for velocity measurements provided by DHI were installed in the model set up (see in the annex Figure-annex 1 to Figure-annex 3). One was situated 2 m in front of the dike toe and the second was placed above the crest. Both measured within a height of 1 m above the basin ground, just in the middle between the overtopping unities for each crest as shown in Figure 3.12.

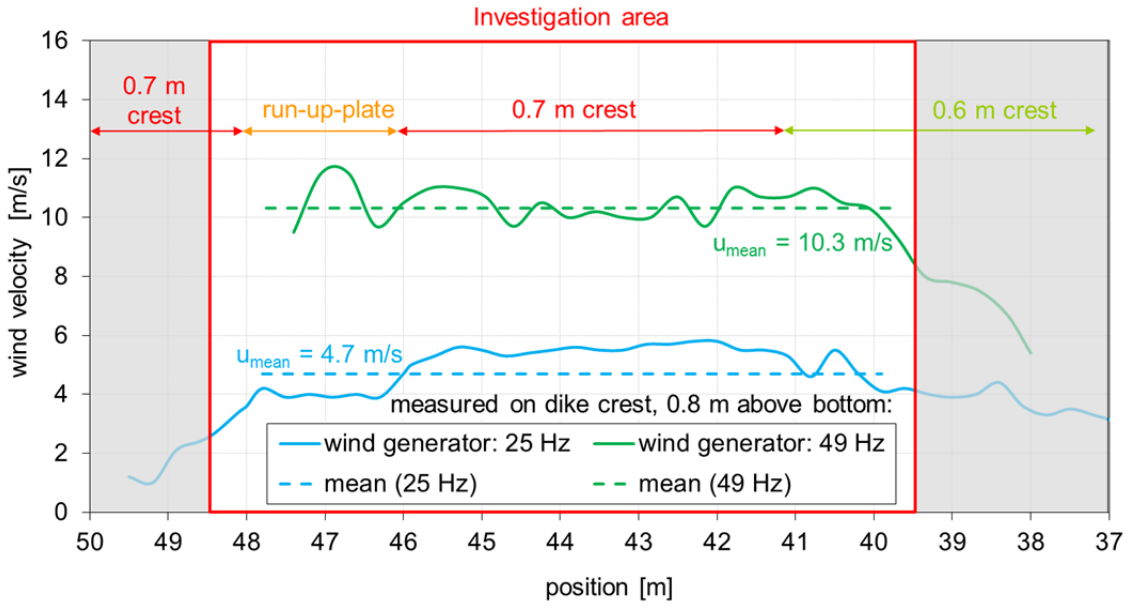

Figure 3.13 Wind velocity distribution for a frequency of 25 Hz and 49 Hz (1:3 sloped dike)

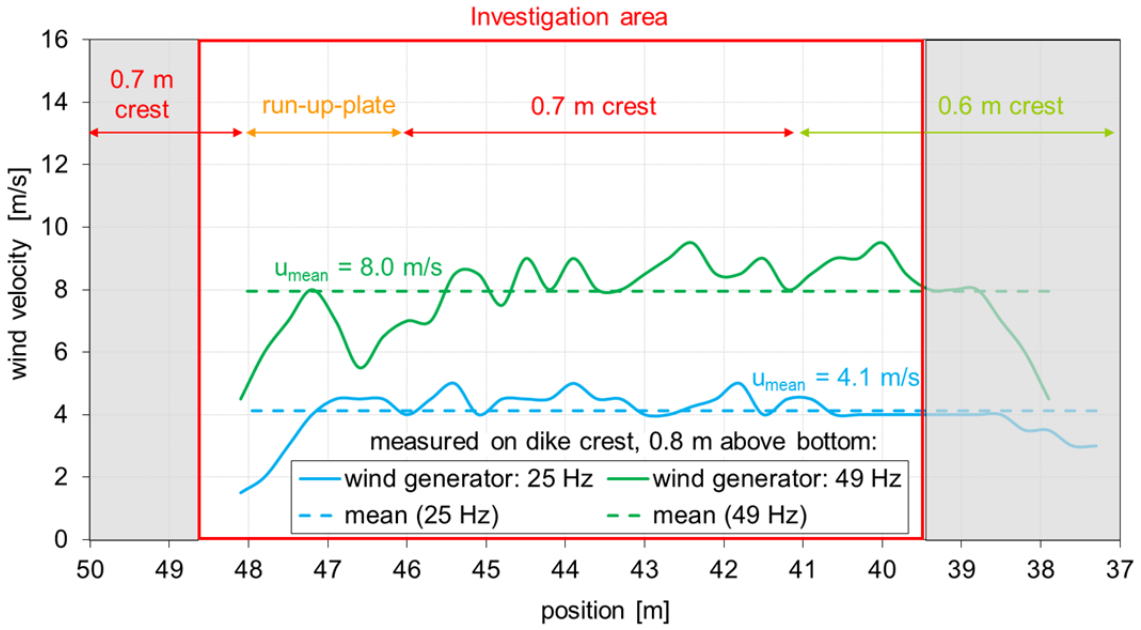

Figure 3.14 Wind velocity distribution for a frequency of 25 Hz and 49 Hz (1:6 sloped dike)

3.2.4 Current (weir, ADV, micro propeller)

Current velocities were controlled with two ADV's (a blue and a black one) and two big micro propellers. All these devices were fixed on a beam, which was situated 2 m upstream the wave machine (Figure 3.15). The velocity was measured at a height of 2/3 water depth (circa 33 cm above the basin bottom) where an average velocity within the depth profile was assumed. Both ADV's were placed in a distance of 2 m and 3.5 m from the dike toe. For a better knowledge of the velocity distribution in the cross section two micro propellers were installed additionally, within a distance of 1.5 m, besides the ADV's.

Figure 3.15 Beam upstream the wave machine (on the left side), flow direction from right to left; ADV; Micro propeller (FlowDike 1)

The position of the beam was not changed between FlowDike 1 and FlowDike 2. The positions of all devices applied in FlowDike 2 are shown in Figure 3.16.

Table 3.1 Pumped discharge, weir height and associated current velocity.

Dike slope [-]	Water depth [m]	discharge [m³/s]	Weir height [m]	Current velocity [m/s]
1:3 sloped dike	0.5 0.5	0.6 1.12	0.387 0.321	0.15 0.3
1:6 sloped dike	0.55 0.55 0.55	0.43 0.83 1.1	0.442 0.382 0.337	0.15 0.3 0.4

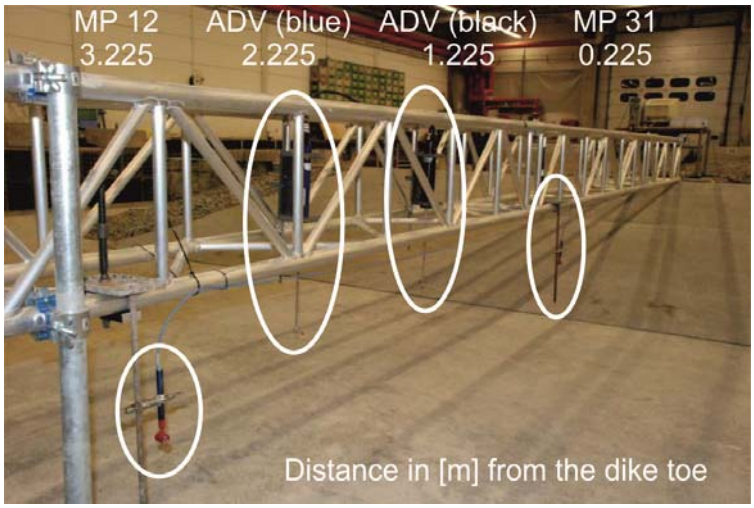

Figure 3.16 Beam upstream the wave machine with current devices (FlowDike 2)

An example of measured current velocity of the ADVs before starting the wave generator for a test with a current of 0.15 m/s is given in Figure 3.22. These ADVS have been installed at the middle of the beam in the flow channel (cf. Figure 3.16). The micro propeller did not give a clear signal.

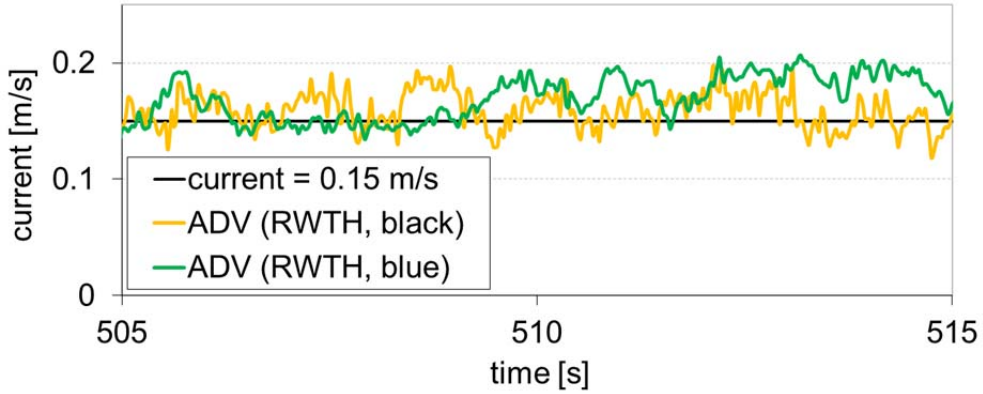

Figure 3.17 Signal of current meter (test s4_35 with 15 m/s current)

At the beginning of each test day, the velocity measurements at all probes started when the current was stabilized. A constant flow velocity was considered when the average of the mean values did not deviate more than 0.05 m/s from each other.

3.2.5 Wave run-up (capacitive gauge, camera, step gauge)

In order to observe and measure wave run-up a 2 m wide and 2.5 m long ply-wood plate was installed as an extension of the dike slope (Figure 3.19). Its surface was covered with sand which was fixed by means of shellac to provide a similar surface roughness as of concrete slope.

At the right side of the run-up board an adhesive tape with a black/yellow or black/white pattern was put on as the gauge board (see Figure 3.18). This gauge had two different scales in the FlowDike 1 set-up. The original scale with its 0.01 m long sections showed the oblique wave run-up height. The distances at the second scale were multiplied with a factor depending on the dike slope and represented the vertical run-up height.

A capacitive gauge was mounted in the middle of the run-up board. Its capacitor (Figure 3.18) was formed by two electrodes - one insulated and one non insulated wire each 3.5 m long. They were mounted on the run-up plate orthogonally to the dike base. One end was installed about 0.25 m above the bed which is equal to 0.25 m below still water level (SWL). The other end was fitted at the highest point of the run-up plate. Thus it is possible to measure both the wave run-up and the run-down. To avoid a water film between the two electrodes after a wave runs down several rubber bands assure a constant distance of about 5 mm between the two wires.

The air or the water between the two wires was the dielectric fluid. Because the permittivity of water is 80 times greater than that of air, the variation of the water level produced a measurable variation of the electrical value of the capacitor. A transducer allowed loading and unloading the capacitor 25 times per second which is equal to a sampling frequency of 25 Hz. Each value of the time constant of the capacitor τ would be transmitted to an A/D-converter as a voltage value. The digital signal which came out of the A/D-converter would be transmitted to the data collection unit and put in storage together with the signals of the other measurement equipment.

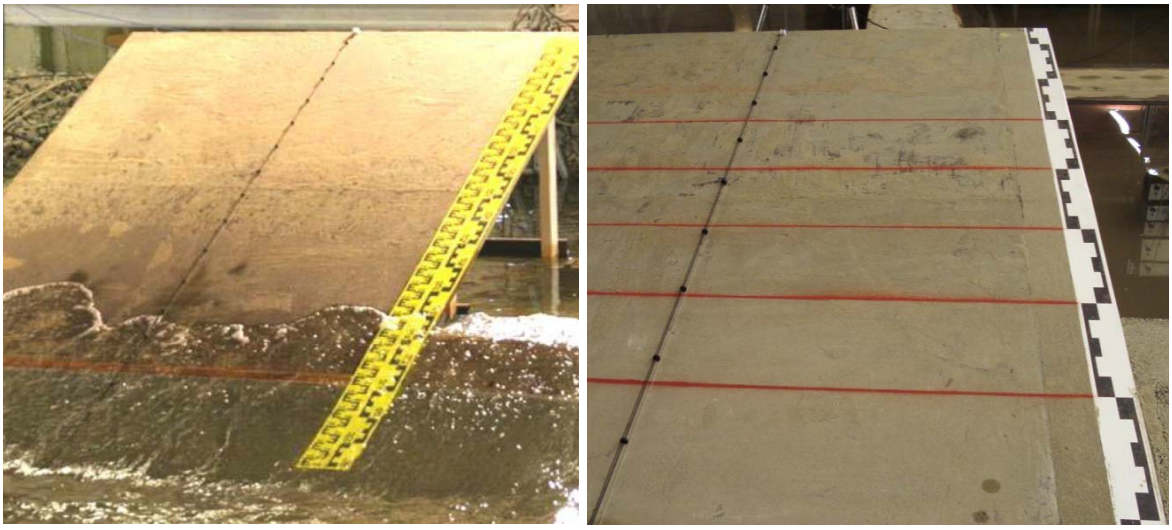

Figure 3.18: Capacitive gauge and visual gauge on the run-up board (left: FlowDike 1, right: FlowDike 2).

In addition to the capacitive gauge the wave run-up height was measured by two digital gauges (*step gauges)* each 1.5 m long. They were mounted at the 0.7 m high dike slope within a distance of 2.2 m. It was only possible to measure the wave run-up till the dike crest with these gauges. These devices were not applied during FlowDike 2. There is no analysis available concerning the step gauges yet.

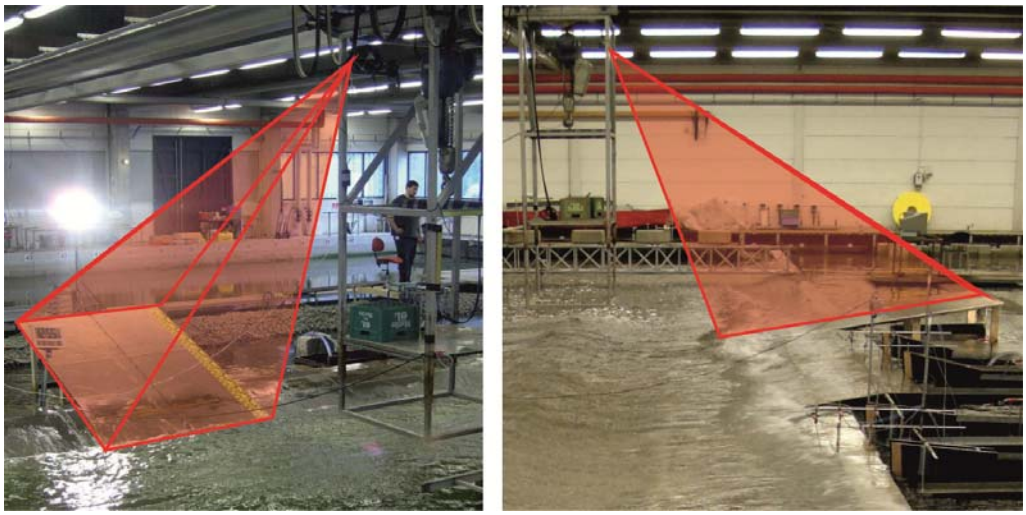

Figure 3.19 Wave run-up plate and rack with both digital cameras (left: FlowDike 1, right: FlowDike 2)

Two digital video cameras were used to record in parallel the wave run-up (Figure 3.20). Both were mounted on a rack about 4 m above the ground (Figure 3.19). The rack was fixed at a laboratory crane to make the positioning of the two cameras very easy.

In the FlowDike 1 model set-up a digital camera and SONY camcorder were applied. The digital camera was a compact, professional USB 2.0 camera from VRmagic GmbH which is suitable for industrial purposes. The used model VRmC-3 + PRO contained a 1/3 inch-CMOS-sensor which could record 69 frames per second. The picture resolution of 754 x 482 pixels was adequate for measurement purposes in the model tests presented herein. The camera was suitable for recording very fast motions like wave run-up on slopes. One benefit of this camera was the possibility to transmit the data to the computer directly by the high speed USB 2.0 interface and without any additional frame grabber hardware. The recorded films were AVI-files. These files were automatically analyzed after the end of the model tests.

Figure 3.20: Left: USB-camera, Right: Both cameras mounted on a rack in the FlowDike 1 model set-up

The SONY Camcorder (Model: *DCR-TRV900E PAL*) had a 3CCD (*Charge Coupled Device*, ¼ inch). The objective had a focal distance between 4.3 mm and 51.6 mm and a 12 times optical zoom. The camcorder was employed as a redundant system in the event of a USB-camera malfunction. The camcorder used mini cassettes to store its films. Choosing the LP-modus the record time of the mini

cassettes could be extended to 90 minutes. Because of test durations between 17 and 34 minutes the cassettes were able to store between 2 and 4 test films. For analysis purposes the films on mini cassettes had to be transformed into AVI-files. This is very time expensive and that is why USB camera was chosen as the main system though the SONY camcorder has a better resolution.

In FlowDike 2 both cameras were replaced by two others with better picture resolution. Since the image-processing algorithm works with grey-level images, one color camera was replaced with a more powerful monochrome camera (1/2“ Progressive-scan-CCD sensor (*Charge Coupled Device*, 1/2 inch) JAI CM-140 GE of Stemmer Imaging). Its resolution of 1392 x 1040 pixels with 4.65 µm pixel size allows producing pictures of the run-up plate with a precision of 0.5 mm. The second camera (a color area scan camera) was used for documentation purpose. It had the same features like the monochrome one but the output-files are three times greater (about 2.6 GB/min). The same objectives as in FlowDike 1 were reused.

A benefit of these cameras was their Gigabit Ethernet (C3 series) interface, which allowed placing the laptop in the office room outside the very humid air of the laboratory hall. Laptop and camera were connected with a 30 m cable. In addition the interface allowed a three times higher transfer rate. The MATLAB algorithm was upgraded considering the new output-file format.

To get films with a better contrast the wave run-up board was enlightened by a 2000 W-spotlight which was positioned such as the light met the run-up plate within an angle of 120 ° to the optical axis of the digital cameras. For the purpose of synchronizing all measurements a digital radio controlled clock with a 0.4 m x 0.4 m display was positioned on the left side of the run-up plate (Figure 3.19).

Stored video data had a compacted AVI-format (*Codec VRMM*) with 10 frames per second.

3.2.6 Overtopping velocity and layer thickness (micro propeller, wave gauge, pressure sensor)

To measure the flow processes on the dike crest, the width of the crest was enlarged to 0.3 m in the region where the measurement devices have been installed. Hence the flow processes are comparable with former investigations.

Micro propellers (*Schiltknecht*) and small wave gauges (0.2 m long) were applied in FlowDike 1 to record flow velocities and flow depths on the crest. A testing section included two small micro propellers combined with two wave gauges between the two overtopping boxes at the seaward and the landward edge of the dike crest (see Figure 3.21). An example of measured data is given in Figure 3.22. They provide a good basis to distinguish between single overtopping events.

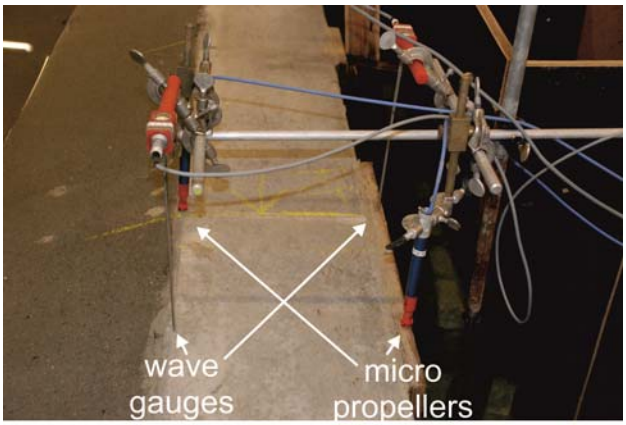

Figure 3.21 Measurement of velocity and depth of flow on the crest

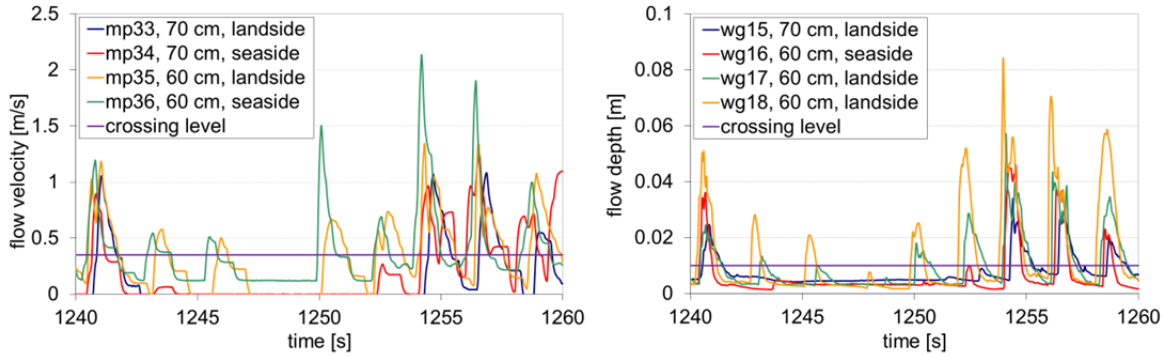

Figure 3.22 Micro propeller (left) and wave gauge (right) measurement for a sequence (s1_03_30_w5_00_00)

Pressure sensors were used to measure flow depth additionally in FlowDike 2. Furthermore all devices were situated 0.03 m from each crest edge, so a distance of 0.24 m was kept between the aligned seaward and landward devices. To investigate the influence of the seaward edge another wave gauge was placed perpendicular onto the slope. The flow depth of the up rushing wave was measured in a horizontal distance of about 0.12 m downstream the crest edge (Figure 3.23 and Figure 3.24).

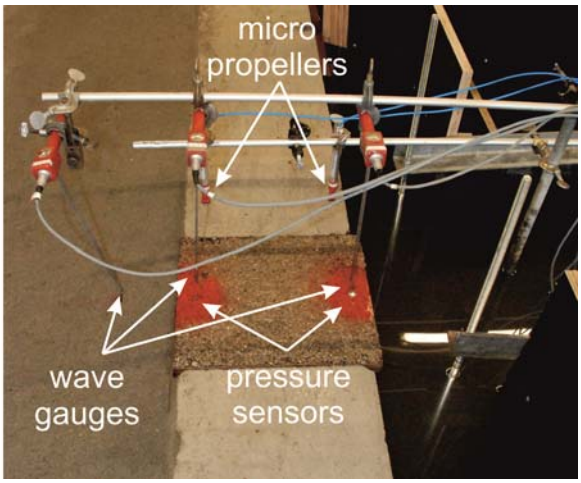

Figure 3.23 Measurement of pressure, velocity and depth of flow on the crest

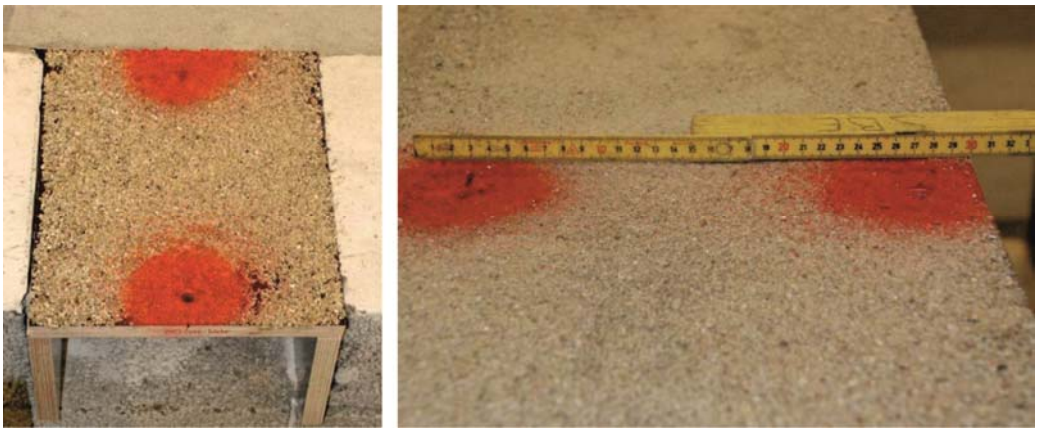

Figure 3.24 Plywood boxes and drilled holes for pressure sensors

3.2.7 Overtopping water volume (load cell, pump)

Wave overtopping volume was measured by four similar overtopping units - two per crest section. Each overtopping unit consisted of an overtopping channel, an external box, a tank, a load cell and a water level gauge. The tank (0.35 m x 0.75 m x 0.75 m) was mounted on a load cell of 0.10 m height. This load cell was placed on the bottom of the separate watertight external box (0.55 m x 1.02 m x 1.18 m), which was built to avoid uplift of the tanks and load cells, when the shallow water basin was flooded. To avoid entering splash water into the overtopping tank next to the overtopping channel, the wall of the external box next to the dike was extended. A rectangular overtopping channel with a 0.10 m wide cross section led the incoming water into the tank, where its weight was recorded by the load cell over the time. The cross-section of an overtopping unit is sketched in Figure 3.25.

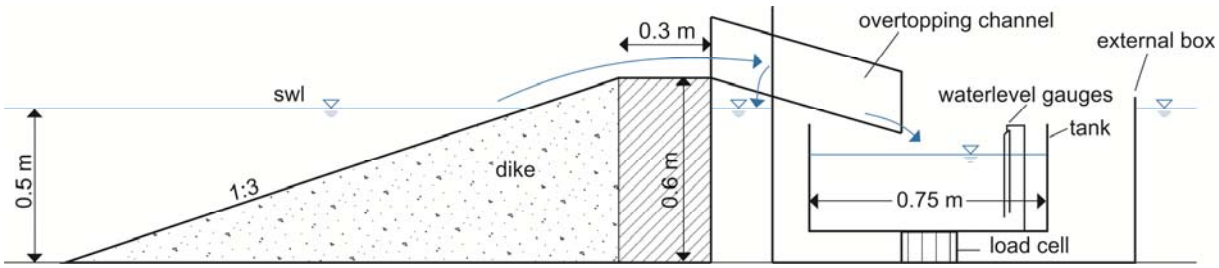

Figure 3.25 Cross-section of the overtopping unit on the 1:3 sloped dike

Because of the thick plywood parts (0.018 m) for all tests of set-up 1 an inlet cross sectional width of 0.118 m was assumed. During the preliminary construction work to prepare for set-up 2 the edges of the channel were sharpened. That is why a 0.10 m inner width is assumed for all other tests.

A wave gauge (0.60 m length) was placed in every tank to gain redundant data regarding the water elevation. But wave gauge data could not be used to detect single overtopping events due to the disturbed water level.

The overtopping boxes were not capable to capture the whole overtopped water volume for each test of approximately 30 min. Therefore a pump (standard pump) with a predetermined sufficient flow was placed within each tank. All four pumps were connected with the data acquisition via a switch, so start and end time of pumping could easily be detected. This allowed recalculating the lost amount of water during the pumping time.

Figure 3.26 Overtopping units with channel and measurement devices for flow depth and flow velocity measurements

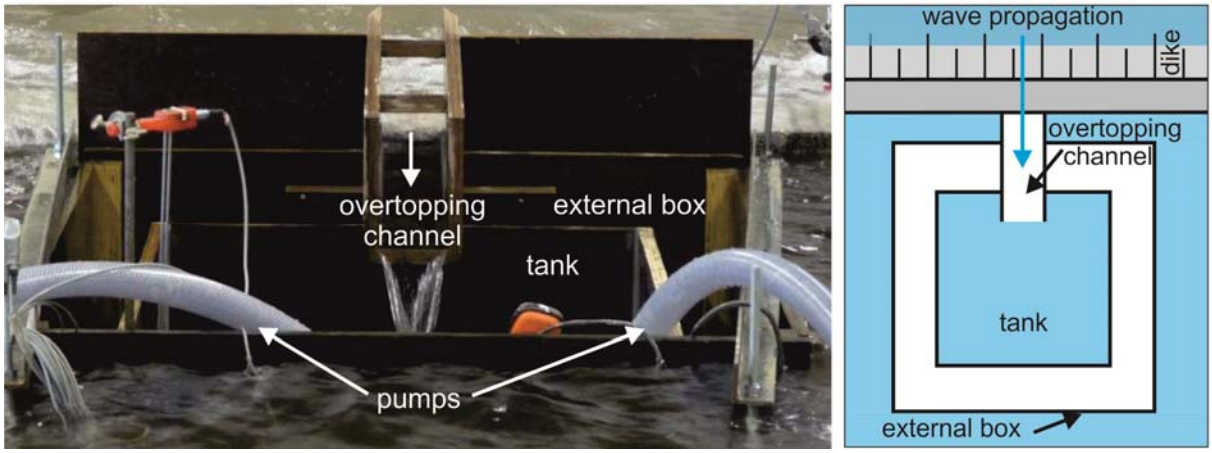

Figure 3.27 Overtopping unit seen from behind the dike

3.3 Calibration

3.3.1 Gauge scale adaptation

After fixing the adhesive gauge tape on the run-up board the scale was longer because of its elasticity. In order to control possible changes, a post measurement was conducted. As a result the label of 2.9 m was placed at a distance of 2.923 m from the zero-point which is equal to an extensibility of 0.8 %. In the end the measured wave run-up is to short and has to be corrected.

Assuming a linear correlation between the original and the extended scale the following formula was obtained to match both:

$$length_{correct}[m] = a_d \cdot length_{board}[m] \quad (3.1)$$

with $a_d = 1{,}0087$ dilatations correction factor [-]

The even little difference has to be considered in the post processing and the data analysis using AVI-files from the camera (see 6.3.1).

3.3.2 Capacitive run-up gauge

The measurement results of the 18 resistance wave gauges were influenced by water temperature and salinity. That's why one had to calibrate these gauges twice a day.

Otherwise the capacitive gauge was non-sensitive to these environmental conditions. The calibration was conducted only one time before the test start. Therefore three test with regularly waves with a mean wave height of H = 0.10 m, 0.15 m and 0.20 m were run.

As the result of a linear regression with 20 values ($R^2 = 0.9985$) the following equation was obtained:

$$WL\,[m] = 0.3748 \cdot voltage\,[V] + 0.4047 \tag{3.2}$$

Than the wave run-up height R could be calculated as the difference between water level WL and the still water level SWL:

$$R\,[m] = WL\,[m] - SWL\,[m] \tag{3.3}$$

Equation (3.2) depends on the model set-up especially on the wire length and the mounting height. That is why the calibration has to be repeated for each model set-up (see equation (3.4) to (3.7)).

$$WL\,[m] = 0.3674 \cdot voltage\,[V] + 0.2279 \quad (R^2 = 0.9977, \text{set-up 2}) \tag{3.4}$$

$$WL\,[m] = 0.3708 \cdot voltage\,[V] + 0.4095 \quad (R^2 = 0.9977, \text{set-up 3}) \tag{3.5}$$

$$WL\,[m] = 0.1179 \cdot voltage\,[V] + 0.5092 \quad (R^2 = 0.9945, \text{set-up 4 and 5}) \tag{3.6}$$

$$WL\,[m] = 0.117 \cdot voltage\,[V] + 0.5224 \quad (R^2 = 0.9788, \text{set-up 6}) \tag{3.7}$$

3.3.3 Pumps

Within each overtopping box a pump with a predetermined sufficient flow was installed. The capacity of each pump was determined before each test period (FlowDike 1 and FlowDike 2). Therewith the lost amount of water during the pumping time and the whole overtopping amount were determinable. The calibration has been done by formula (3.8). The corresponding calibration factors for each pump are given in Table 3.2 (1:3 sloped dike) and Table 3.3 (1:6 sloped dike).

$$Q\,[l/s] = \text{calibration factor} \cdot voltage\,[V] \tag{3.8}$$

Table 3.2 Calibration factors of pumps situated in overtopping tanks (used on 1:3 sloped dike)

Pump no.	placed in overtopping box…	Calibration factor
45	behind 0.7 m high dike, upstream (lc37)	1.7845
46	behind 0.7 m high dike, downstream (lc39)	1.4010
47	behind 0.6 m high dike, upstream (lc41)	1.5942
48	behind 0.6 m high dike, downstream (lc43)	1.5943

Table 3.3 Calibration factors of pumps situated in overtopping tanks (used on 1:6 sloped dike)

Pump no.	placed in overtopping box…	Calibration factor
45	behind 0.7 m high dike, upstream (lc37)	1.7335
46	behind 0.7 m high dike, downstream (lc39)	1.5996
47	behind 0.6 m high dike, upstream (lc41)	1.6799
48	behind 0.6 m high dike, downstream (lc43)	1.7456

3.3.4 Micro propellers

The micro propellers have been calibrated based on formula (3.9). The calibration factors for all micro propellers are listed in Table 3.4 (FlowDike 1) and Table 3.5 (FlowDike 2). The corresponding detailed calibration curves are given in Annex G.

$$\text{velocity}\,[\text{m/s}] = \text{calibration factor} \cdot \text{voltage}\,[\text{V}] \tag{3.9}$$

Table 3.4 Calibration factors of micro propellers in flow direction from LWI, TU Braunschweig (used on 1:3 sloped dike)

Micro propeller no.	Calibration factor in flow direction
31	0.8616
32	1.0900
33	0.8296
34	0.4871
35	0.4687
36	0.4913

Table 3.5 Calibration factors of micro propellers from RWTH Aachen University (used on 1:6 sloped dike)

	Calibration factor	
Micro propeller no.	in flow direction	against flow direction
33	0.1989	0.2119
34	0.1630	0.1644
35	0.1900	0.1967
36	0.1591	0.1650

3.4 Model and scale effects

3.4.1 Model effects

Model effects could be caused by boundaries of the test facility which do not represent natural boundary conditions or by inadequate wave spectra creation. The FlowDike-D tests did not reproduce a specific natural dike. Nevertheless the results can be devolved to natural relations.

Model effects regarding FlowDike-D tests might be caused by

- wave reflection at the model boundaries
- distance between wave generator and dike (basin width)
- width of the run-up board
- inlet of the overtopping channel (shape, geometry)

In order to mitigate wave reflection different devices were installed within the shallow water basin as described in section 3.1.1. Due to the relatively short distance between the wave generator and the dike wave reflection influenced the incoming sea state. Therefore wave generation includes an algorithm to absorb reflected waves. It should be mentioned that this algorithm was not operational during FlowDike 2 (1:6 sloped dike) due to technical problems. In case of very oblique wave attack the up rushing waves might not develop their full run-up height in a few tests because of the limited run-up board width. To ensure low turbulence during the wave overtopping process the edges of the overtopping channel were sharpened after the first test series.

3.4.2 Scale effects

The current research project was applied to consider the influence of wind and current on wave run-up and wave overtopping. In a first step the tests can be considered as prototype tests. In a second step the

model set-up can be seen as a reduced model of a natural dike. That's why a relatively smooth surface on the dike slope was applied.

To ensure the similarity between the model and the prototype, the geometric similarity, the kinematic similarity and the dynamic similarity have to be considered. The geometric similarity assures the scaling of the design and the wave heights end lengths. The kinematic similarity describes the relation of the time scale for example of the wave period. More difficult is to ensure the dynamic similarity which includes the model laws by Froude, Reynolds, Weber, Thoma and Cauchy. The model law by Cauchy includes the equality of the elasticity and the inertia force. Thoma considers the inertia forces and pressure. Both Thoma and Chauchy are negligible for free surface applications.

The main complexity in scaling the wind tests is the different theory which has to be used for wind and water waves. Wind has to be scaled according to Reynolds, whereas waves are scaled according to the Froude-law. The law of Weber considers the interface between water and air. These three theories cannot be combined. That is why only few investigations considering the influence of wind on wave overtopping by means of physical model tests have been done (GONZÁLEZ-ESCRIVA, 2006). Therefore the influence of wind on wave run-up and wave overtopping is analyzed only qualitative in the project FlowDike-D.

Regarding DE ROUCK ET AL. (2002) the roughness of the dike surface does only influence scaling for porous dikes. Therefore this factor is negligible in this study with a smooth dike.

The model laws by Froude, Reynolds and Weber have been already analyzed in detail by SCHÜTTRUMPF (2001). The same procedure is used to determine the influence of the surface tension (Weber). According to LE MÉHAUTÉ (1976) the influence of the surface tension on scale effects of the incoming wave field is negligible for water depths higher 0.02 m and wave periods higher 0.35 s. Both conditions are achieved in the current project. Therefore the influence of the surface tension has to be determined only for the flow depth during wave run-up and wave overtopping processes.

Based on SCHÜTTRUMPF(2001) the scale effect of the surface tension is described using the following formulae:

$$\frac{1}{2} = \frac{1}{c_2^* \cdot Fr_{crest}^{\ 2}} + \frac{1}{We_{crest}} \tag{3.10}$$

$$Fr_{crest} = \frac{v_{crest}}{\sqrt{g \cdot h_{crest}}} \tag{3.11}$$

$$We_{crest} = \frac{v_{crest}^{\ 2} \cdot h_{crest} \cdot \rho_w}{\sigma_0} \tag{3.12}$$

with: Fr_{crest} Froude number at the crest [-]

We_{crest} Weber number at the crest [-]

c_2^* parameter for describing the layer thickness [-]

v_{crest} velocity at the crest [m/s]

h_{crest} layer thickness at the crest [m]

σ_0 surface tension, *here:* σ_0 = 0.0732 N/m for a temperature of 16.5°

Figure 3.28 shows the Froude number against the Weber number using formula (3.10). The Weber number describes the influence of surface tension on the flow process. The different graphs are based on different parameters c_2^*. All graphs show constant values of the Froude number for Weber numbers higher than 10.

The parameter describing the layer thickness c_2* is set to 0.4 for FlowDike 1 (1:3 sloped dike) and to 0.7 for FlowDike 2 (1:6 sloped dike). The accordingly calculated data are plotted with red and blue data points and have Weber numbers higher than 10 (except one value). So the surface tension has no effect on the overtopping events on the dikes.

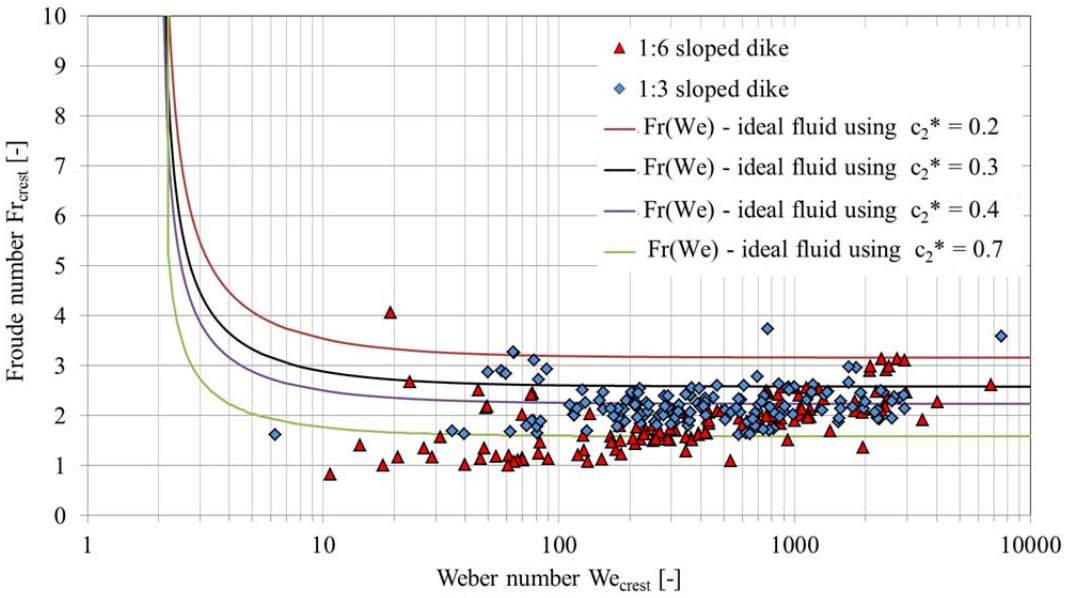

Figure 3.28 Influence of surface tension on the dike crest

The influence of the viscosity has to be analyzed for the wave propagation as well as for the wave overtopping process. Both numbers Froude and Reynolds have been determined using the formula by SCHÜTTRUMPF (2001). The results should clarify if the viscosity has to be considered during data analysis:

Wave propagation:

$$Fr_{wave}^2 = \left[1 - \frac{1}{2 \cdot \sqrt{Re_{wave} \cdot kd}}\right]^2 \quad \text{with} \quad kd = \frac{2\pi \cdot d}{L_{m-1,0}} \tag{3.13}$$

$$Re_{wave} = \frac{c \cdot d}{\nu} \tag{3.14}$$

$$Fr_{wave} = \frac{c}{\sqrt{g \cdot d}} \tag{3.15}$$

with: Fr_{wave} Froude number of the wave [-]

Re_{wave} Reynolds number of the wave [-]

d flow depth, water depth [m]

$L_{m-1,0}$ deep water wave length based on $T_{m-1,0}$[m]

c wave velocity [m/s]

ν dynamic viscosity [m²/s]

Wave overtopping processes:

$$Fr_{crest} = \sqrt{\frac{1}{\left(1 - \frac{64}{4 \cdot Re_{crest} \cdot c_2}\right)}} \tag{3.16}$$

$$Re_{crest} = \frac{2 \cdot \left(R_{u2\%} - R_C\right)^2}{\left(\nu \cdot T\right)} \tag{3.17}$$

$$Fr_{crest} = \frac{v_{crest}}{\sqrt{g \cdot h_{crest}}} \tag{3.18}$$

$$c_2 = \frac{c_2^*}{n} \text{ with } \begin{matrix} c_2^* = 0.4 \text{ and } n = 3 \text{ for } 1:3 \text{ sloped dike} \\ c_2^* = 0.7 \text{ and } n = 6 \text{ for } 1:6 \text{ sloped dike} \end{matrix} \tag{3.19}$$

with: Fr_{crest} Froude number on the crest [-]

Re_{crest} Reynolds number on the crest [-]

$R_{u2\%}$ run-up height exceeded by 2% of the incoming waves [m]

R_C freeboard height of the structure [m]

ν dynamic viscosity [m²/s]

T wave period [s]

v_{crest} velocity at the crest [m/s]

h_{crest} layer thickness at the crest [m]

c_2^* parameter for describing the layer thickness [-]

As shown in Figure 3.29 viscosity does only have an influence on wave evolution if Reynolds number is lower than 10^4. Therefore no influence on the results of the wave field are expected because Reynolds number for the FlowDike 1 and FlowDike 2 tests were higher than 10^6.

The influence of the viscosity on the wave overtopping process is shown in Figure 3.30. Subsequently the viscosity does not influence the wave overtopping process for Reynolds numbers higher than 1000, which was observed for nearly all tests.

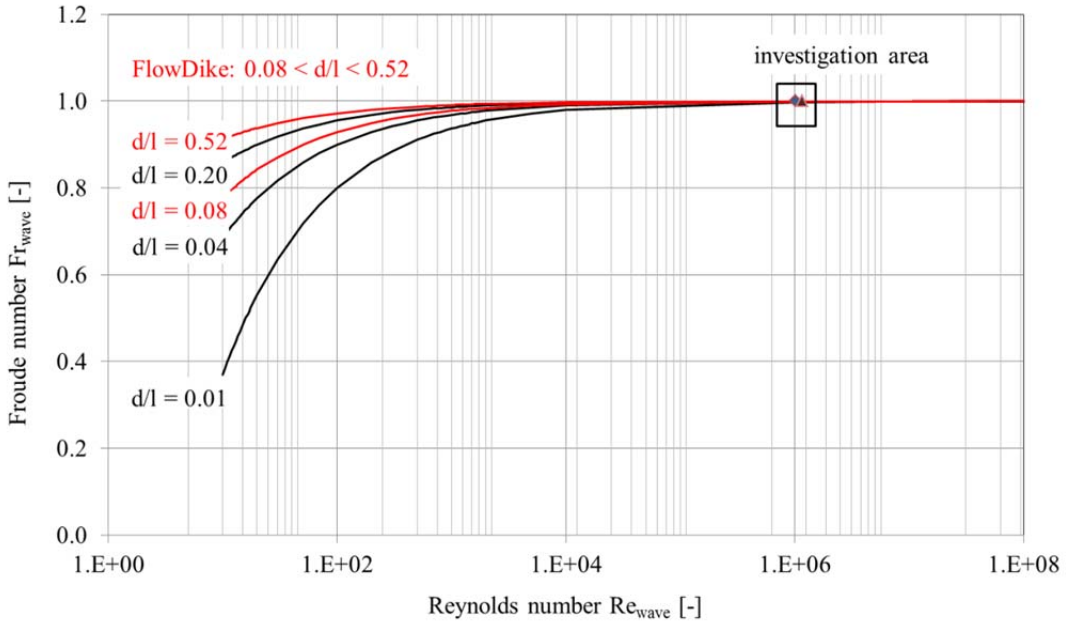

Figure 3.29 Influence of viscosity on wave evolution

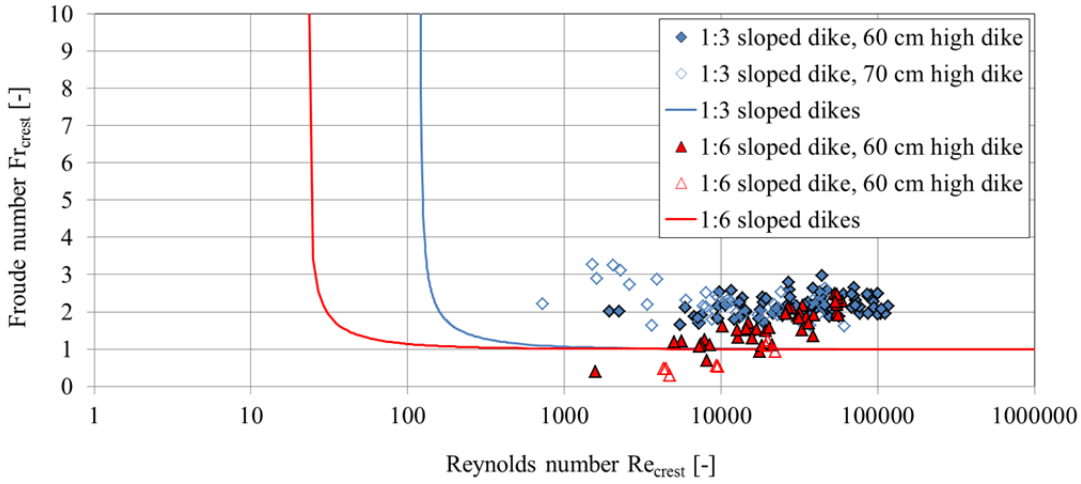

Figure 3.30 Influence of viscosity on wave overtopping processes

4 Wave field – Literature review and method of analyzing data

4.1 Wave spectrum

First investigations on wave spectra were done by PHILLIPS (1958) and served as basis for an investigation on fully developed sea state by Pearson and Moskowitz (1964). Its results are still used in off-shore design. During the Joint-North-Sea-Wave-Project (JONSWAP) developing wind seas were analyzed. Main aim of that project was to describe a wave spectrum in a development phase as well as its behavior in shallow water. Hence the so called JONSWAP spectrum was developed. The also often used TMA spectrum is based on the JONSWAP spectrum and applicable for shallow water conditions.

The JONSWAP spectrum is the most common used spectrum in current research projects. To guarantee comparability this spectrum was applied in the FlowDike 1 and FlowDike 2 tests and will be presented in more detail. The theoretical JONSWAP spectrum can be described with energy density S as a function of the frequency f and a JONSWAP portion θ_J, which determines the maximum energy in the spectrum. The JONSWAP spectrum $S_J(f)$ can be determined using the formula (4.1) based on the formula of PEARSON-MOSKOWITZ (4.3) and of PHILLIPS (4.5) (cf. MALCHEREK, 2010):

$$S_J(f) = S_{PM}(f) \cdot \Theta_J\left(f, f_P, \gamma, \sigma_a, \sigma_b\right) \tag{4.1}$$

with $S_J(f)$ energy density, JONSWAP spectrum [m²/Hz]

$S_{PM}(f)$ energy density, Pierson-Moskowitz spectrum [m²/Hz]

θ_J JONSWAP coefficient describing the maximum energy density [-]

$$\Theta_J = \gamma^{\exp\left(\frac{-(f-f_p)^2}{2\sigma^2 \cdot f_p^2}\right)} \tag{4.2}$$

γ peak raising factor [-] $\gamma = 3.3$ for mean JONSWAP spectrum

σ form parameter describing the forward peak width [-]

$f < fp \rightarrow \sigma = 0{,}07$

$f > fp \rightarrow \sigma = 0{,}09$

$$S_{PM}(f) = S_p(f) \cdot \Theta_{PM}\frac{f}{f_p} \tag{4.3}$$

with $S_{PM}(f)$ energy density, Pierson-Moskowitz spectrum [m²/Hz]

$S_P(f)$ Phillips spectrum describing the decreasing part of the graph [m²/Hz]

θ_{PM} Pierson-Moskowitz parameter describing the spectrum [-]

$$\Theta_{PM} = \exp\left(-\frac{5}{4}\cdot\left(\frac{f}{f_p}\right)^{-4}\right) \tag{4.4}$$

with f_p peak frequency [Hz]

$$S_p(f) = \frac{\alpha \cdot g^2}{(2\pi)^4 \cdot f^5} \tag{4.5}$$

with α Phillips constant $\alpha = 8.1 \cdot 10^{-3}$ [-]

f frequency [Hz]

4.2 Wave and current interaction

4.2.1 General

The model tests were performed with and without a longshore current. Since the wave propagation is different in flowing water and in still water, it is required to interpret the following results with respect to the interaction of waves and current (TRELOAR, 1986). Two main aspects have to be considered while interpreting the results:

- current induced shoaling: absolute and relative wave parameters
- current induced wave refraction: energy propagation

The wave propagation path can be divided into two parts. The first part reaches from the wave generator to the dike toe. The second part extends from the dike toe to the dike crest.

4.2.2 Current induced shoaling

If a wave propagates on a current, a distinction has to be made between relative and absolute wave parameters and can be described by using the wave celerity. The relative wave celerity is the celerity relative to an observer who moves with the current, while the absolute celerity is defined as the velocity compared to a stationary observer and the ground, respectively.

The wave gauge arrays at the toe of the dike measured the wave field with its absolute parameters. According to HEDGES (1987), TRELOAR (1986) and HOLTHUIJSEN (2007) waves act only with its relative parameters. To determine the relative wave period $T_{rel,m-1,0}$ from the measured absolute wave period $T_{abs,m-1,0}$, the absolute angular frequency ω_{abs} has to be equalized to the sum of the relative angular frequency ω_{rel} and the corresponding constituent of the current ($k \cdot v_n$) (cf. HOLTHUIJSEN, 2007):

$$\omega_{abs} = \omega_{rel} + k_{rel} \cdot v_{\beta} \tag{4.6}$$

with ω_{abs} absolute angular frequency [rad/s]

ω_{rel} relative angular frequency [rad/s]

k_{rel} relative wave number [rad/m]

v_{β} component of current velocity in the direction of wave propagation [m/s]

d flow depth [m]

The absolute angular frequency can be determined using the measured absolute spectral wave period $T_{abs,m-1,0}$

$$T_{abs,m-1,0} = \frac{m_{-1}}{m_0} \tag{4.7}$$

with m_{-1} minus first moment of spectral density [m²]

m_0 zero order moment of spectral density [m²/s]

and the following formula:

$$\omega_{abs} = \frac{2\pi}{T_{abs,m-1,0}} \tag{4.8}$$

The relative angular frequency ω_{rel} is also defined as

$$\omega_{rel} = \sqrt{g \cdot k_{rel} \cdot \tanh(k_{rel} \cdot d)} \tag{4.9}$$

By using eq. (4.6) and (4.9), the relative wave number k_{rel} can be determined iteratively by using the measured absolute wave period $T_{abs,m-1,0}$ (4.7), the known flow depth d and the current velocity in the direction of wave propagation v_β, which is defined as:

$$v_\beta = v_x \cdot \sin\beta \tag{4.10}$$

with the current velocity parallel to the dike v_x and the angle of wave attack β relative to a line perpendicular to the shore.

The relative angular frequency ω_{rel} can be calculated using equation (4.9). Assuming deep water conditions the relative wave period $T_{rel,m-1,0}$ and the relative wave length $L_{rel,m-1,0}$ are determinable using the following formulae:

$$T_{rel,m-1,0} = \frac{2\pi}{\omega_{rel}} \tag{4.11}$$

$$L_{abs,m-1,0} = g \cdot \frac{\left(L_{abs,m-1,0}\right)^2}{2\pi} \tag{4.12}$$

As shown in Figure 4.1, the relative wave period $T_{rel,m-1,0}$ decreases compared to the absolute wave period if a wave propagates against a current and increases if a wave propagates with a current (cf. formula (4.6) and (4.11)).

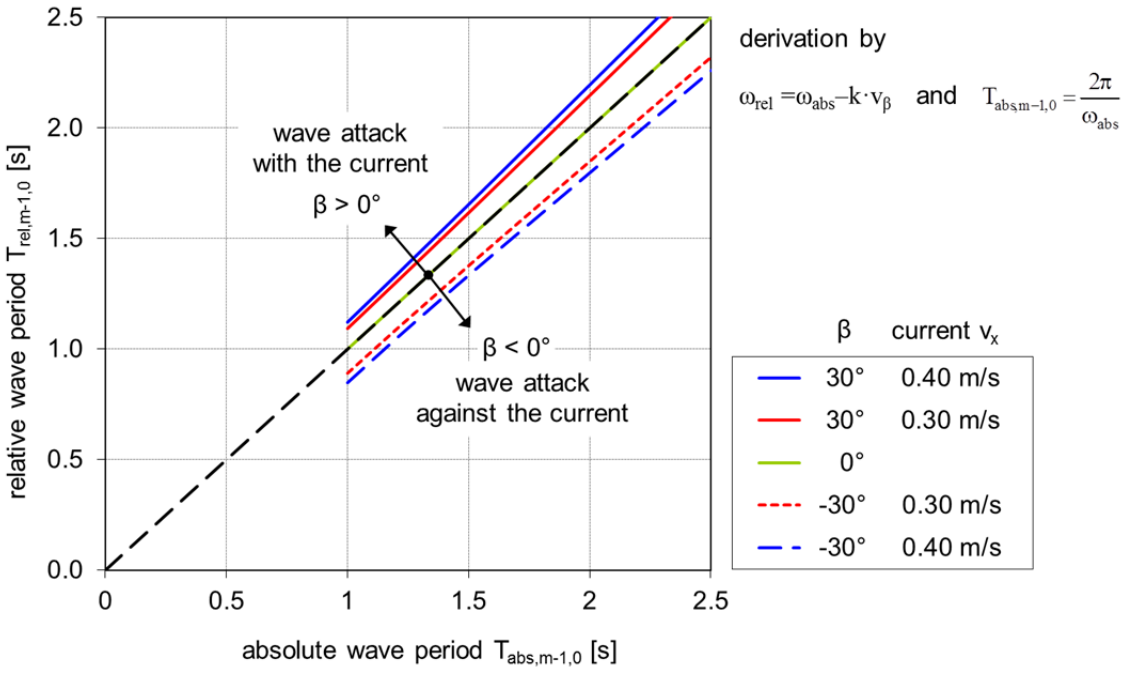

Figure 4.1 Absolute wave period $T_{abs,m-1,0}$ against relative wave period $T_{rel,m-1,0}$, water depth d = 0.5 m

4.2.3 Current induced wave refraction

Figure 4.2 shows schematically the combination of the two vectors for the current and the wave direction for negative (left) and positive (right) angles of wave attack. The dashed arrow describes the relative direction of the wave attack generated by the wave generator and the corresponding angle β. The dotted arrow indicates the direction of the longshore current. According to HOLTHUIJSEN (2007) the current does not change the angle of wave attack but its energy direction by the combination of the two vectors current velocity v_x and relative group velocity $c_{g,rel}$ marked with the corresponding arrow. As shown in Figure 4.2, negative angles of wave attack lead to a smaller absolute value of the angle of wave energy β_e whereas positive angles of wave attack lead to a higher angle of wave energy β_e than the angle of wave attack β.

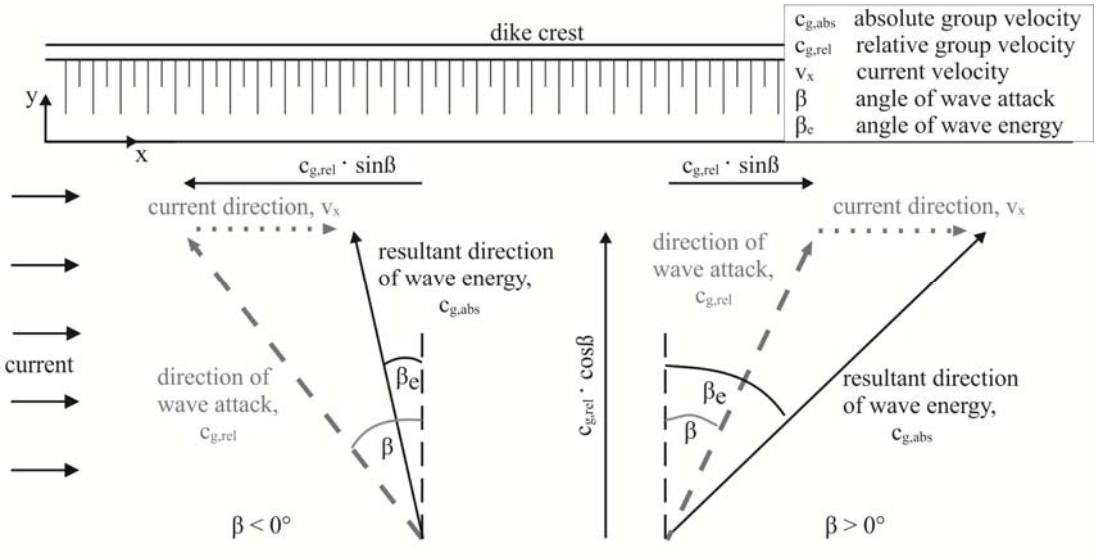

Figure 4.2. Interaction between wave direction and current

The angle of wave energy β_e is determined by the relative group velocity $c_{g,rel}$, the angle of wave attack β and the current velocity v_x by the trigonometrical function (cf. Figure 4.2):

$$\tan\beta_e = \frac{c_{g,rel} \cdot \sin\beta + v_x}{c_{g,rel} \cdot \cos\beta} \tag{4.13}$$

Herein the relative group velocity $c_{g,rel}$ is determined by the following formula:

$$c_{g,rel} = \frac{\partial\omega}{\partial k} = \frac{\partial\left(\sqrt{g \cdot k \cdot \tanh(k \cdot d)}\right)}{\partial k} \tag{4.14}$$

which leads to:

$$c_{g,rel} = 0.5 \cdot \frac{\omega_{rel}}{k}\left(1 + \frac{2 \cdot k \cdot d}{\sinh(2 \cdot k \cdot d)}\right) \tag{4.15}$$

Figure 4.3 shows how a current influences the angle of wave energy. On the abscissa the current is plotted. The ordinate shows the angle of wave attack (dashed line) and the angle of wave energy (continuous line). The graphs show different angles of wave attack with and against the current. For all angles of wave attack the angle of wave energy increases significantly depending on the current velocity. For currents higher than 4 m/s the changes in the angle of wave attack are lower and converge against 90° which is the direction of the current. For negative angles of wave attack (against

the current, green and blue graph) the changing of the angle of wave energy is more significant than for the positive angles of wave attack (with the current, orange graph).

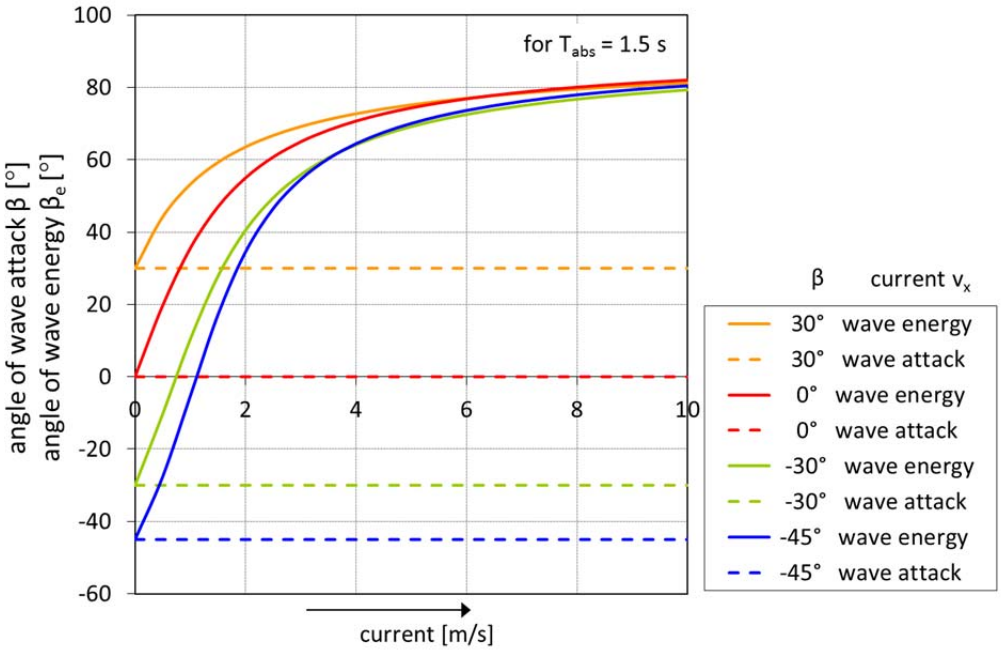

Figure 4.3 Angle of wave energy β_e divided by angle of wave attack β against the current for different angles of wave attack, water depth d = 0.5 m, T_{abs} = 1.5 s

4.3 Influence of wind on waves

In the current research project the waves are induced by a wave generator. But the mechanically induced wind might change the wave parameters at the dike toe and influences the breaking process as well. GALLOWAY (1989) carried out wave observations at coasts to determine the influence of the wind direction on breaking waves. Wind in the direction of wave propagations leads to previous breaking of the waves which become surging waves. DE WAAL ET AL. (1996) included this knowledge in a formula for wave overtopping by reducing the breaker flow depth d_b. He determined the wind influenced flow depth $d_{b(wind)}$ at the breaker point to:

$$\frac{d_{b(wind)}}{d_b} = \left(1 + p \cdot \frac{u_{10}}{\sqrt{g \cdot d_b}}\right)^2 \tag{4.16}$$

with d_b flow depth at breaker point without wind [m]

u_{10} wind velocity 10 m above still water level [m/s]

$$p = \frac{v_{crest,wind} - v_{crest,no\ wind}}{u_{10}} \approx 0.03 \text{ percentage by DE WAAL ET AL. (1996)} \tag{4.17}$$

with $v_{crest,wind}$ flow velocity on the dike crest, wind $u_{10} \neq 0$ m/s [m/s]

$v_{crest,no\ wind}$ flow velocity on the dike crest, wind $u_{10} = 0$ m/s [m/s]

5 Wave run-up and wave overtopping – Literature review and method of analyzing data

5.1 Delimitation of literature review

Wave run-up is the rush of water up a structure as a result of wave attack. Wave overtopping is the mean discharge of water in l/(s·m) that passes over a structure due to wave attack and should be limited to a tolerable amount. Analysis of wave run-up and wave overtopping were performed mostly for coastal areas in the past. First investigations have been carried out before 1935 (see WASSING, 1957 and GIBSON, 1930). In the meantime, many experimental, numerical, theoretical and field investigations were performed. Extensive studies on perpendicular wave run-up and overtopping and some investigations on oblique wave run-up are available.

The main aspects which were investigated on wave run-up and wave overtopping can be listed as follows:

- geometry of the dike (inclination, berm)
- long and short crested waves
- regular and spectral wave attack, natural sea spectrum
- normal and oblique wave attack
- dike constitution (roughness, permeability)
- kind of investigation (experimental (laboratory, field), numerical, theoretical)

In the FlowDike-D project long crested waves characterized by a JONSWAP spectrum were investigated (cf. section 2.2 and 4.1). The following sections include a more detailed literature review about the main aspects investigated in FlowDike 1 and FlowDike 2 concerning wave run-up and wave overtopping:

- normal wave attack including influence of spectrum
- influence of oblique wave attack
- influence of wind
- method of analyzing data
- flow processes

The complete new aspect - the influence of a longshore current on wave run-up and wave overtopping - was not investigated in any project before. Concerning the influence of wind on wave run-up and wave overtopping only a few investigations have been published (cf. section 5.4).

5.2 Wave run-up and wave overtopping under perpendicular wave attack

5.2.1 Wave run-up

The wave run-up height was investigated by several authors. HUNT (1959) gave 4 basic formulae describing the wave run-up height R considering regular waves:

$$R = C \cdot \sqrt{H \cdot L_0} \cdot \tan\alpha \qquad \text{with} \quad C = 1.0 \tag{5.1}$$

$$R = C \cdot \sqrt{H \cdot g} \cdot T \cdot \tan\alpha \text{ with} \quad C = 1/(2\cdot\pi)^{0.5} \approx 0.4 \tag{5.2}$$

$$R = C \cdot \sqrt{H} \cdot T \cdot \tan\alpha \quad \text{with} \quad C = 1.25 \tag{5.3}$$

$$\frac{R}{H} = C \cdot \frac{\tan\alpha}{\sqrt{H \cdot L_0}} = C \cdot \xi \text{ with} \quad C = 1.0 \tag{5.4}$$

with C coefficient [-]

H wave height [m]

L_o wave length [m]

T wave period [s]

α inclination of the structure [°]

To analyze model tests with sea state these formulae had to be modified. Formula (5.4) is most commonly used here according to GRÜNE & WANG (2000). Exemplary the formula by VAN DER MEER & JANSSEN (1994) is given:

$$\frac{R_{u,2\%}}{H_{m0}} = C_\xi \cdot \xi_{eq} \quad \text{with} \quad C_\xi = 1.6 \cdot \gamma_b \cdot \gamma_f \cdot \gamma_\beta \quad \text{and} \quad \xi_{eq} = \gamma_b \cdot \frac{\tan\alpha}{\sqrt{\frac{2\pi \cdot H_{m0}}{g \cdot T_p^2}}} \tag{5.5}$$

with its maximum value

$$\frac{R_{u,2\%}}{H_{m0}} = 3.2 \cdot \gamma_b \cdot \gamma_f \cdot \gamma_\beta \tag{5.6}$$

with $R_{u,2\%}$ wave run-up height which is exceeded by 2% of all waves [m]

H_{m0} significant wave height from spectral analysis

C_ξ parameter considering infl. of shallow foreshore, roughness, oblique wave attack [-]

ξ_{eq} surf similarity parameter, parameter considering influence of a berm [-]

γ_b parameter covering influence of a berm [-]

γ_f parameter covering influence of surface roughness [-]

γ_β parameter covering influence of wave direction (angle β) [-]

A similar version is given in the EUROTOP-MANUAL (2007) with different correction parameters. It is the main commonly used formula for wave run-up:

$$\frac{R_{u,2\%}}{H_{m0}} = c_1 \cdot \gamma_b \cdot \gamma_f \cdot \gamma_\beta \cdot \xi_{m-1,0} \tag{5.7}$$

with its maximum value

$$\frac{R_{u,2\%}}{H_{m0}} = \gamma_b \cdot \gamma_f \cdot \gamma_\beta \cdot \left(c_2 - \frac{c_3}{\sqrt{\xi_{m-1,0}}} \right) \tag{5.8}$$

with

c_1, c_2, c_3 empirical parameters with $c_2 = c_1 \cdot \xi_{tr} + c_3 / \xi_{tr}$ [-]

for average $R_{u,2\%}$: $c_1 = 1.65$, $c_2 = 4.0$, $c_3 = 1.5$

ξ_{tr} surf parameter describing the transition between breaking and non-breaking waves [-]

5.2.2 Wave overtopping

The wave overtopping rate is a significant parameter to design flood protection structures. Wave overtopping is a dynamic process with a variable volume of overtopped water during a period of time. The wave overtopping amount depends mainly on the wave parameters and water level at the dike toe as well as the geometry of the flood protection structure. Mostly the wave overtopping rate q is specified in liter per second and meter dike length or the dimensionless overtopping rate including the wave parameters.

Several formulae are used to determine the mean dimensionless overtopping rate q_* [-]. Most of them are given as:

$$q_* = a \cdot \exp\left(-b \cdot R_{c*}\right) \tag{5.9}$$

or

$$q_* = a \cdot \left(1 - R_{c*}\right)^{-b} \tag{5.10}$$

with a best-fit coefficient; for $R_{c*} = 0$ is $a = q_*$ (dimensionless overtopping rate) [-]

b best-fit coefficient [-]

R_{c*} dimensionless freeboard height [-]

Several authors have presented formulae for the dimensionless overtopping rate q_* and the dimensionless freeboard height R_{c*}. In Table 5.1 these formulae are given from investigations on sloped dike and irregular waves. The following parameters are used:

H_s significant wave height [m]

T_m mean wave period [s]

T_p peak wave period [s]

R_c freeboard height [m]

$R_{2\%}$ run-up exceeded by 2% of the incoming waves [m]

L_m wave length corresponding to T_m [m]

L_p wave length corresponding to T_p [m]

L_s airy wave length corresponding to T_s [m]

ξ_p surf similarity parameter using H_s and L_{0p} [-]

L_{0p} wave length corresponding to T_p and deep water conditions [m]

α slope of the structure [-]

γ influence factor of berm, permeability, roughness, oblique wave attack, shallow water [-]

For more formulae regarding vertical walls and regular waves see SCHÜTTRUMPF (2001).

Table 5.1 Recommended dimensionless overtopping rate q_* and dimensionless freeboard height R_{c*} for sloped structures and irregular waves (modified according to HEDGES & REIS, 1998)

Reference		Dimensionless overtopping rate q_*	Dimensionless freeboard height R_{c*}	Correlation between q_* and R_{c*}
OWEN	1982	$\frac{q}{T_m \cdot g \cdot H_s}$	$\frac{R_c}{T_m \cdot \sqrt{g \cdot H_s}}$	$q_* = a \cdot \exp(-b \cdot R_*)$
BRADBURY & ALLSOP	1988	$\frac{q}{T_m \cdot g \cdot H_s}$	$\frac{R_c^2}{T_m \cdot \sqrt{g \cdot H_s^3}}$	$q_* = a \cdot (R_*)^{-b}$
AHRENS &HEIMBAUGH	1988	$\frac{q}{\sqrt{g \cdot H_s^3}}$	$\frac{R_c}{(H_s^2 \cdot L_p)^{1/3}}$	$q_* = a \cdot \exp(-b \cdot R_*)$
SAWARAGI ET AL.	1988	$\frac{q^*}{\sqrt{g \cdot L_s \cdot H_s^2}}$	$\frac{R_c}{H_s}$	-
AMINTI& FRANCO	1988	$\frac{q}{T_m \cdot g \cdot H_s}$	$\frac{R_c}{H_s}$	$q_* = a \cdot (R_*)^{-b}$
PEDERSEN &BURCHARTH	1992	$\frac{q \cdot T_m}{L_m^2}$	$\frac{R_c}{H_s}$	$q_* = a \cdot (R_*)^{-b}$
DE WAAL & VAN DER MEER	1992	$\frac{q}{\sqrt{g \cdot H_s^3}}$	$\frac{R_{2\%} - R_c}{H_s}$	$q_* = a \cdot \exp(-b \cdot R_*)$
VAN DER MEER, SMITH ET AL.; VAN DER MEER & JANSSEN	1993; 1994; 1995	$\frac{q}{\sqrt{g \cdot H_s^3}} \frac{\sqrt{\tan\alpha}}{\xi_p}$ for $\xi_p < 2$ $\frac{q}{\sqrt{g \cdot H_s^3}}$ for $\xi_p > 2$	$\frac{R_c}{H_s} \frac{1}{\xi_p} \frac{1}{\gamma}$ for $\xi_p < 2$ $\frac{R_c}{H_S} \frac{1}{\gamma}$ for $\xi_p > 2$	$q_* = a \cdot \exp(-b \cdot R_*)$
FRANCO ET AL.	1994	$\frac{q}{\sqrt{g \cdot H_S^3}}$	$\frac{R_c}{H_s}$	$q_* = a \cdot \exp(-b \cdot R_*)$
SCHÜTTRUMPF	2001	$\frac{q}{\sqrt{2g \cdot H_S^3}} \cdot \frac{1}{\xi_m}$	$\frac{R_c}{H_s}$	$q_* = a \cdot \exp(-b \cdot R_*)$
EUROTOP-MANUAL	2007	$\frac{q}{\sqrt{g \cdot H_{m0}^3}}$	$\frac{R_c}{H_{m0}} \frac{1}{\gamma}$	$q_* = a \cdot \exp(-b \cdot R_*)$

The formula first applied by VAN DER MEER (1993) for the dimensionless overtopping rate q_* and the dimensionless freeboard height R_{c*} is the most common form and is used for comparison with the results presented in this report (cf. formula (5.13)).

The mean overtopping rate by the EURTOP-MANUAL (2007) is determinable using deterministic or probabilistic approaches based on several investigations. The probabilistic design formula is used for comparing measurements. Therefore a 95 % confidence range is included. Designs of dike structures are based on the following deterministic approach. Both deterministic and probabilistic designs are based on the following formulae (5.11) and (5.12) for breaking and non-breaking wave conditions. The smaller value indicates breaking or non-breaking wave conditions. VAN DER MEER (1993) distinguished between breaking and non-breaking waves by using the surf-similarity-parameter ξ_p. It should be mentioned, that the adapted formulae in this work are stated for short crested waves, but within the model tests only long crested waves were generated. This has to be considered for comparison of the analysis.

Breaking wave conditions:

$$q_* = \frac{q}{\sqrt{g \cdot H_{m0}^3}} = \frac{0.067}{\sqrt{\tan\alpha}} \cdot \gamma_b \cdot \xi_{m-1,0} \cdot \exp\left(- b_{br} \cdot \frac{R_c}{\xi_{m-1,0} \cdot H_{m0} \cdot \gamma_b \cdot \gamma_f \cdot \gamma_\beta \cdot \gamma_\nu} \right) \tag{5.11}$$

probabilistic design: $b_{br} = 4.75$ deterministic design: $b_{br} = 4.3$

Non-breaking wave conditions:

$$q_* = \frac{q}{\sqrt{g \cdot H_{m0}^3}} = 0.2 \cdot \exp\left(- b_{nbr} \cdot \frac{R_c}{H_{m0} \cdot \gamma_f \cdot \gamma_\beta} \right) \tag{5.12}$$

probabilistic design: $b_{nbr} = 2.6$ deterministic design: $b_{nbr} = 2.3$

with
- q mean overtopping discharge per meter structure width [m³/s/m]
- α slope of the front face of the structure [°]
- R_c crest freeboard of structure [m]
- γ_b correction factor for a berm [-]
- γ_f correction factor for permeability and roughness of the structure [-]
- γ_β correction factor for oblique wave attack [-]
- γ_υ correction factor for a vertical wall on the slope [-]
- b_{br} coefficient for deterministic and probabilistic design, breaking waves [-]
- b_{nbr} coefficient for deterministic and probabilistic design, non-breaking waves

With $\frac{R_{u,2\%}}{c_1} = \xi_{m-1,0} \cdot H_{m0} \cdot \gamma_b \cdot \gamma_f \cdot \gamma_\beta$ (cf. formula (5.7) and EURTOP-MANUAL 2007) and $c_1 = 1.65$ the dimensionless overtopping rate results in:

$$\underbrace{\frac{q}{\sqrt{g \cdot H_{m0}^3}} \frac{\sqrt{\tan\alpha}}{\gamma_b \cdot \xi_{m-1,0}}}_{q_*} = \underbrace{0.067}_{Q_0} \cdot \exp\left(- \underbrace{4.75}_{b} \cdot \frac{1.65 \cdot R_c}{\underbrace{\gamma_\upsilon \cdot R_{u,2\%}}_{R_*}} \right) \tag{5.13}$$

This relation gives the probabilistic curves for overtopping calculation using the following factors (see also graphs in the EUROTOP-MANUAL (2007):

- breaking waves: $Q_0 = 0.067$; $b_{br} = -4.75$
- non-breaking waves: $Q_0 = 0.2$; $b_{nbr} = -2.6$

5.2.3 Influence of analyzed spectrum

In OUMERACI ET AL. (2000) physical model tests investigating the influence of the wave spectra were presented. Herein regular waves, TMA spectra (single peak), JONSWAP spectra (single and double peak) and measured multi peak spectra were investigated. The spectra differ not only in the peak period but also in the energy density of the spectrum. The energy of a spectrum is more significant for the run-up and overtopping measurements than the peak period. So the spectral period is defined as

$$T_{m-1,0} = \frac{m_{-1}}{m_0} \tag{5.14}$$

Concerning the statistical wave parameters, GRÜNE & WANG (2000) observed a low sensitivity of the wave height as well as freeboard height to the wave period T. It was suggested to use the mean period T_m or the spectral period $T_{m-1,0}$ instead of the peak period (GRÜNE & WANG, 2000).

5.3 Wave run-up and wave overtopping under oblique wave attack

Several investigations were done by analyzing the influence of different angles of wave attack on wave run-up and overtopping. This aspect is described by an influence factor γ_β considering the following ratios for the run-up height and the overtopping rate:

$$\gamma_\beta = \frac{\left(\frac{R_{u2\%}}{H_{m0}}\right)_{\beta>0°}}{\left(\frac{R_{u2\%}}{H_{m0}}\right)_{\beta=0°}} \tag{5.15}$$

$$\gamma_\beta = \frac{q_{\beta>0°}}{q_{\beta=0°}} \tag{5.16}$$

with γ_β influence factor [-]

β angle of wave attack ($\beta = 0°$ for perpendicular wave attack) [°]

H_{m0} measured incident wave height [m]

$R_{u2\%;\beta>0°}$ run-up height exceeded by 2% of the incoming waves with $\beta > 0°$

$R_{u2\%;\beta=0°}$ run-up height exceeded by 2% of the incoming waves with $\beta = 0°$

$q_{\beta>0°}$ overtopping rate with angle of wave attack $\beta > 0°$

$q_{\beta=0°}$ overtopping rate with angle of wave attack $\beta = 0°$

First investigations concerning this aspect on smooth sloped dikes were done by WASSING (1957) with regular waves using the following formula for the influence factor:

$$\gamma_\beta = \frac{1+\cos\left(\frac{\beta\cdot\pi}{180°}\right)}{2} \tag{5.17}$$

Field measurements have been done by WAGNER & BÜRGER (1973) on different dike slopes (1:2.7; 1:3; 1:3.3; 1:3.6). The following formula for the influence factor was found:

$$\gamma_\beta = 0.35 + 0.65\cdot\cos\left(\frac{\beta\cdot\pi}{180°}\right) \tag{5.18}$$

Further investigations with regular waves were done by TAUTENHAIN ET AL. (1982)on a 1:6 sloped dike for angles of wave attack up to 60°. An increasing wave overtopping rate while increasing the angle of wave attack up to 30° was determined. An increase of the overtopping rate was also determined by OWEN (1980) for vertical structures and JUHL & SLOTH (1994) for breakwaters. The formula for the influence factor for the obliquity by TAUTENHAIN ET AL. (1982) is given by

$$\gamma_\beta = \cos\left(\frac{\beta\cdot\pi}{180°}\right)\cdot\sqrt[3]{2-\cos^3\left(2\cdot\frac{\beta\cdot\pi}{180°}\right)} \tag{5.19}$$

DE WAAL & VAN DER MEER (1992) investigated this influence on 1:2.5 and 1:4 sloped dikes with and without berms for angles of wave attack up to 80°. Different formulae were determined for long and short crested waves. For short crested waves different influence factors were determined for wave run-up and wave overtopping (cf. formulae (5.20) and (5.21)). The influence of short crested waves is less than for long crested waves.

$$\begin{aligned} &\beta < 10° && \Rightarrow \quad \gamma_\beta = 1 \\ &10° \le \beta \le 50° && \Rightarrow \quad \gamma_\beta = \cos^2(\beta - 10) \\ &\beta > 10° && \Rightarrow \quad \gamma_\beta = 0.6 \end{aligned} \qquad \text{for long crested waves} \tag{5.20}$$

$$\begin{aligned} &\text{run}-\text{up}: && \gamma_\beta = 1 - 0.0033\cdot\beta \\ &\text{overtopping}: && \gamma_\beta = 1 - 0.0022\cdot\beta \end{aligned} \qquad \text{for short crested waves} \tag{5.21}$$

OUMERACI ET AL. (2002) do not distinguish between long and short crested waves in the investigations for determining the formulae for the influence factor. Investigations have been done on a 1:3 and 1:6 sloped dike. The formulae, different for the two investigated dike slopes, are based on the formula by WAGNER & BÜRGER (1973):

$$\gamma_\beta = 0.10 + 0.90\cdot\cos\left(\frac{\beta\cdot\pi}{180°}\right) \quad \text{for the 1:3 sloped dike} \tag{5.22}$$

$$\gamma_\beta = 0.35 + 0.65\cdot\cos\left(\frac{\beta\cdot\pi}{180°}\right) \quad \text{for the 1:6 sloped dike} \tag{5.23}$$

The following formula is based on investigations by KORTENHAUS (2009) on 1:3 and 1:6 sloped dikes. For both dike slopes only one formula was defined:

$$\gamma_\beta = 1.00 + 0.0076\cdot\beta \tag{5.24}$$

Table 5.2 summarizes the main formulae for the influence factor γ_β considering investigations on smooth dike slopes. The corresponding graphs are given in Figure 5.1. It was discussed in the literature that the influence factor > 1 by TAUTENHAIN ET AL. (1982) was caused by measurement uncertainties. For angles of wave attack < 40° all listed authors except TAUTENHAIN ET AL. (1982) and KORTENHAUS (2009) give similar characteristics of γ_β. For angles of wave attack higher than 40° the curves describing the influence on wave run-up and wave overtopping given by different authors diverge significantly.

Table 5.2 Summary of formula for the influence factor γ_β of former investigations on smooth dike slopes

author	**year**	**slope of the structure and roughness of its surface**	**kind of waves**	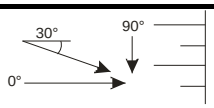 **influence factor γ_β**
WASSING	1957		regular waves	$\frac{1+\cos\left(\frac{\beta\cdot\pi}{180°}\right)}{2}$
TAUTEN-HAIN ET AL.	1982	1:6 sloped dike d = 0,35m	regular single waves	$\cos\left(\frac{\beta\cdot\pi}{180°}\right)\cdot\sqrt[3]{2-\cos^3\left(2\cdot\frac{\beta\cdot\pi}{180°}\right)}$ β < 60°
DE WAAL & VAN DER MEER; EUROTOP-MANUAL	1992; 2007	1:2.5 and 1:4 sloped dike; with and without berm	long crested waves	1; $0 \le \beta < 10$ $\cos^2(\beta\text{-}10)$; $10 \le \beta \le 50$ 0.6; $\beta > 50$
			short crested waves	$1-0.0033\cdot\beta$ (ov) $1-0.0022\cdot\beta$ (run − up)
OUMERACI ET AL.	2002	1:3 sloped dike	long and short crested waves	$0.1+0.90\cdot\cos\left(\frac{\beta\cdot\pi}{180°}\right)$
		1:6 sloped dike		$0.35+0.65\cdot\cos\left(\frac{\beta\cdot\pi}{180°}\right)$
KORTEN-HAUS ET AL.	2009	1:3 and 1:6 sloped dike	breaking and non-breaking waves	$1.0-0.0076\cdot\beta$

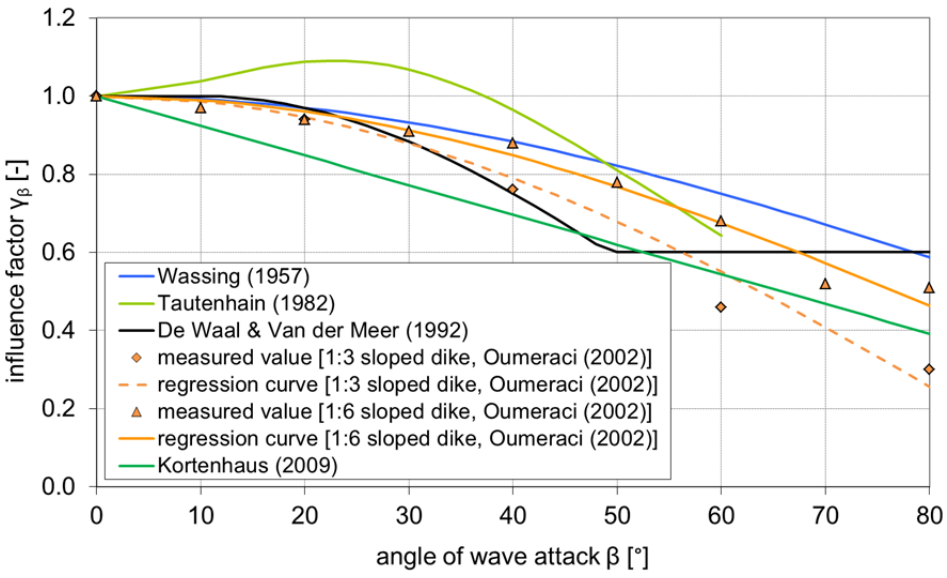

Figure 5.1 Angle of wave attack against influence factor γ_β of former investigations

5.4 Wave run-up and wave overtopping influenced by wind

The influence of onshore wind on wave run-up is a much younger research topic than current-wave-interaction. One reason might be that it is more complicated to transfer the results of physical model tests into prototype conditions because the scaling laws of Froude (wave propagation, wave run-up), Reynolds (shear forces) and Weber (interface between water and air) do not correspond and cannot be fulfilled in one model set-up. Nevertheless it is commonly assumed that onshore wind has an increasing effect on wave run-up. Single reasons for that are that onshore wind pushes the water up the slope and the velocity in the wave run-up tongue increases. In addition the effect of downwash on the subsequent wave might be reduced. Other changes can be distinguished in the breaking process. Wind induces an earlier breaking of the waves and a change of the breaking type as well as of the breaking point on the slope. These effects have been summarized but could only partly be quantified by GONZÁLES-ECRIVÁ (2006).

Different hydraulic model tests were conducted to investigate the influence of wind on wave run-up (e. g. WARD ET AL. 1996, MEDINA 1998). The chosen facilities were flumes and monochromatic waves were studied. Wind speed created by wind machines ranged between 6.5 m/s and 16 m/s. Whereas WARD ET AL. (1996) studied single slope structures the investigation of MEDINA (1998) considered complex breakwater cross sections and the wave run-up was observed e. g. at a vertical wall on the crest. In general it was found that lower wind speeds ($w < 6$ m/s) have no significant effect on wave run-up whereas higher wind speeds increases the wave run-up height substantially. This effect can be observed on smooth as well as on rough slope surfaces. In the case of flatter slopes the increasing effect is less. WARD ET AL. (1996) stated a linear increase of the equivalent wave run-up height (maximum wave run-up adjusted for the increase in still water level due to onshore wind) with the incident wave height for wind speed > 12 m/s. But if the wind induces wave breaking before the waves reach the test structure the wave run-up decreases with increasing incident wave height.

The OPTICREST-project was focused on storm induced wave run-up and collected prototype measurement data as well as model test results (DE ROUCK ET AL. 2001). Two prototype locations the Zeebrugge Breakwater (Belgium) and the Petten Sea-Defense (Netherlands) were investigated. While the first structure is a rubble mound breakwater the measured wave run-up height is strongly influenced by the permeability and the roughness of the slope surface. The second structure is a dike with a smooth impermeable surface but a berm and a long shallow foreshore. Mainly the foreshore has a significant influence on the measured wave run-up height. Most of the model tests did not include a wind generation. Also the conformity between physical model and prototype was ensured by applying the wave spectra measured in the prototype. Altogether these measurement results are not appropriate for comparison with the FlowDike model tests.

GONZÁLES-ECRIVÁ (2006) found that wind increases the energy of the wave spectrum slightly but no differences in the spectral width could be distinguished.

Especially for small overtopping rates and vertical structures the effect of wind might be significant (DE WAAL ET AL., 1996). The influence of wind can be neglected for high overtopping rates and/or low wind velocities (WARD ET AL., 1996) but information on wind influence on wave overtopping is still scarce.

The main problem to consider wind experimentally and to quantify its effect is the inaccurate scaling of wind in small scale model tests. YAMASHIRO ET AL. (2006) recommend to scale the prototype wind by a factor 1/3 but the experiments are restricted to a model scale of 1/45.

5.5 Method of analyzing data on wave run-up and wave overtopping

5.5.1 General

A similar approach as in the EURTOP-MANUAL (2007) has been used to analyze the data and to derive influencing factors regarding angle of wave attack, wind and current. The EURTOP-MANUAL (2007) distinguishes between formulae for wave run-up and wave overtopping, for breaking and non-breaking wave conditions.

5.5.2 Wave run-up

Usually the influence of different factors on wave run-up height could be determined using a formula which was originally suggested by HUNT (1959) and then upgraded in EURTOP-MANUAL (2007) with different correction parameters:

$$\frac{R_{u2\%}}{H_{m0}} = c_1 \cdot \gamma_b \cdot \gamma_f \cdot \gamma_\beta \cdot \xi_{m-1,0} \tag{5.25}$$

with its maximum:

$$\frac{R_{u2\%}}{H_{m0}} = \gamma_f \cdot \gamma_\beta \cdot \left(c_2 - \frac{c_3}{\sqrt{\xi_{m-1,0}}} \right) \tag{5.26}$$

with $R_{u2\%}$ wave run-up height which is exceeded by 2% of all wave run-ups [m]

γ_b parameter which covers the influence of a berm [-]

γ_f parameter which covers the influence of surface roughness [-]

γ_β parameter which covers the influence of wave direction (angle β) [-]

$\xi_{m-1,0}$ surf similarity parameter based on $s_{m-1,0}$ [-]

$s_{m-1,0}$ wave steepness based on H_{m0} and $L_{m-1,0}$ [-]

$L_{m-1,0}$ deep water wave length based on $T_{m-1,0}$ [m]

$T_{m-1,0}$ spectral wave period [s]

H_{m0} significant wave height from spectral analysis [m]

The empirical parameters c_1, c_2 and c_3 are dimensionless and defined as follow:

$$c_2 = c_1 \cdot \xi_{tr} + c_3 / \xi_{tr} \tag{5.27}$$

with ξ_{tr} surf similarity parameter describing the transition between breaking and non-breaking waves [-]

For a prediction of the average run-up height $R_{u2\%}$ the following values $c_1 = 1.65$, $c_2 = 4.0$ and $c_3 = 1.5$ should be used.

5.5.3 Wave overtopping

The EURTOP-MANUAL (2007) is the base of the analysis of wave overtopping in the current research project (cf. previous section 5.2). Therefrom formulae (5.11) can be used to calculate the average overtopping discharge q in liter per second and per meter dike length for given geometry and wave condition based on the van der Meer & Janssen formulae (cf. Table 5.1). The non-breaking condition

limits the overtopping discharge to a maximum value, see formula (5.12). The smallest value of both equations should be taken as the result.

Contrary to EURTOP-MANUAL (2007), no difference is made in formula (5.13) between the influence factor for obliquity γ_β for wave run-up and wave overtopping. In the current report one influence factor γ_β valid for both wave run-up and overtopping will be determined.

In a first step the influence factor γ_β were determined separately for wave run-up and wave overtopping. Later on they were compared and one valid parameter for both wave run-up and wave overtopping was established.

5.6 Flow processes on dike crests

Nowadays, the research on wave run-up and wave overtopping intends to describe also the flow processes on the crest. SCHÜTTRUMPF (2001) and VAN GENT (2002) describe these processes related to wave run-up and wave overtopping by flow parameters such as flow depth $h_{2\%}$ and flow velocity $v_{2\%}$. A formula resulting from a simplified energy equation is given to determine the flow depths on the seaward dike crest $h_{2\%}$ which are exceeded by 2% of the incoming waves with the formula

$$\frac{h_{2\%}}{H_s} = c_h \cdot \frac{R_{u2\%} - R_c}{H_s} \quad [-] \tag{5.28}$$

with H_s significant wave height [m]

$R_{u2\%}$ run-up height exceeded by 2% of the incoming waves [m]

R_c freeboard height [m]

c_h empirical coefficient determined by model tests[-]

Additionally flow velocities on the seaward dike crest $v_{2\%}$ are given by

$$\frac{v_{2\%}}{\sqrt{g \cdot H_s}} = c_v \cdot \sqrt{\frac{R_{u2\%} - R_c}{H_s}} \quad [-] \tag{5.29}$$

c_v empirical coefficient determined by model tests [-]

Experimental investigations on the overtopping flow parameters were performed in small and large wave flumes but the three dimensionality of the process was not investigated so far.

6 Data processing

6.1 Remarks

As described previously the raw data were acquired every $\Delta t = 0.04$ sec ($f_s = 25$ Hz) for FlowDike 1 and every $\Delta t = 0.025$ sec ($f_s = 40$ Hz) for FlowDike 2.

The Wave Synthesizer included in the software package Mike Zero by DHI was used as data processing tool for reflection and crossing analysis. MATLAB scripts were used to calculate the average overtopping rates from the available ascii-files (*.daf) and to determine the time depended run-up from the available *.avi-files.

6.2 Wave field

In frequency domain the wave parameters were analyzed using a reflection analysis. For this analysis the methods and definitions described by BENDAT & PIERSOL (1993) were used. Herein the reflection coefficient C_r was determined at the same time. The time-series of water level elevation were transformed and analyzed by a Fourier-transformation giving the spectral energy density S(f) for measured, incident and reflected wave. Based on the moments m_n of the spectral densities, the following characteristic wave parameters can be calculated:

- wave height $H_{m0} = 4 \cdot \sqrt{m_0}$ [m]
- spectral wave period $T_{m-1,0} = \frac{m_{-1}}{m_0}$ [s] with m_{-1} minus first moment of spectral density [m²]

  and m_0 zero order moment of spectral density [m²/s]

Determining the wave field in time domain, a zero-down crossing was applied, whereby single wave events were detected. The number of detected events (waves) N of each wave gauge is the result of the crossing analysis. From the certain quantity N of the measured surface elevation, the maximum wave height H_{max} (peak to peak decomposition) and the mean wave period T_m (event duration), can be calculated. These values are the average of all wave gauges contributing to one of the wave gauge arrays. Other averages for characteristic height parameters, such as the significant wave height $H_S = H_{1/3}$, have not been analyzed.

For data analysis the following parameters were distinguished to be analyzed in a first step:

- Frequency domain: H_{m0}, T_p, C_r, $T_{m-1,0}$
- Time domain: H_{max}, T_m, N
- Plots: time series, energy density, reflection function

These signals were determined by two wave gauge arrays of 5 wave gauges (with a length of 0.6 m each) and a current meter. An overall view and further details how the measurement devices were positioned and about the differences between FlowDike 1 and FlowDike 2 are given in section 3.2.2.

In the previous sections it was mentioned, that a JONSWAP spectrum was used for the investigations. A typical raw data signal of the wave gauges 9 to 5 is given in Figure 6.1 for 20 s. The shift between the peaks of each wave gauge is due to the defined distances between the wave gauges in each wave

gauge array. These defined distances have to be input in MikeZero preliminary to the reflection analysis. The array positioning was not changed in case of oblique wave attack. So the distances have to be recalculated with a factor of the cosine of the angle of wave attack.

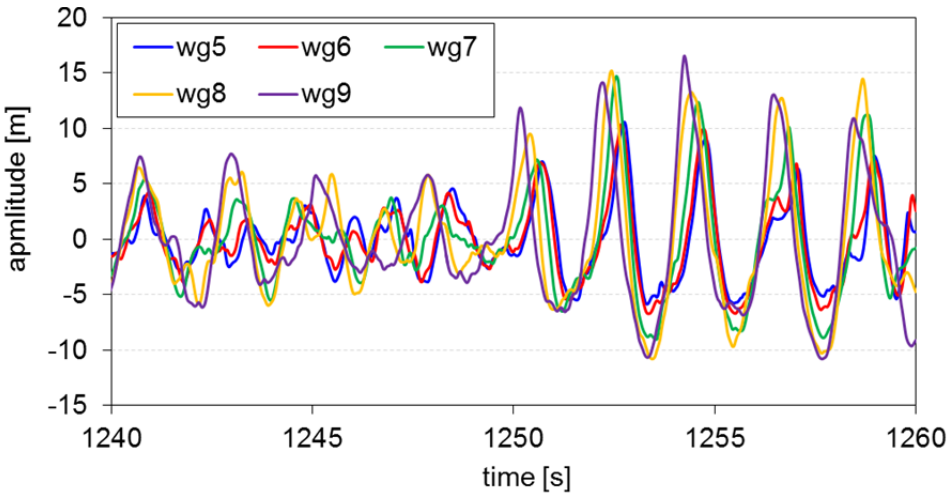

Figure 6.1 Raw data for wave gauges 9 to 5 for 20 seconds; test s1_03_30_w5_00

6.3 Wave run-up

6.3.1 Capacitive gauge

The values measured by the capacitive gauge have been stored with all values from other devices such as wave gauges, anemometers, micro propellers and ADV in the central data storage directly. The unit of these values is Volt and the time series format is *.dsf0. The latter is a binary code developed by DHI.

Equations (3.1) to (3.7) have been used to calculate the time-dependent run-up height in meter considering the model set-up.

During the analysis it has been found that the still-water-level in some test records was higher at the end of the test ($t = t_{END}$) than at the beginning ($t = t_0$). The difference was about 1 cm. The reason was that after the first waves run up little water remained between the two wires above the ring-shaped distance pieces. The effect did only occur when the water had enough time to evaporate from the wires for instance overnight and the wires were totally dry before the tests began. This effect was easily identifiable and has been considered within the data analysis.

6.3.2 Video film analysis

To create wave run-up time series from video films a MATLAB procedure has been used. The maximum run-up in each frame was identified as described in the following paragraphs. In order to get the run-up time series the recording time of the frame has to be assigned to the detected run-up in it.

In the first step of the procedure it was detected in which parts (pixel) of the frame a movement has taken place which is visible by changes in pixel brightness. Therefore the difference between two frames in sequence was calculated. The difference is equal zero if there was no movement and unequal zero if there was a movement. A variable threshold (threshold for image difference, see “Parameter” in Figure 6.5) has been used to adjust the sensitivity in detection of pixels with significant brightness difference. As a result a new black/white frame was created. Pixels with a significant change in pixel

brightness were defined as white pixels and all other as black pixels. Figure 6.2 shows as an example a video frame in grey scale and an according frame in black and white which represents the change in pixel brightness between the two sequent frames. The wave front is easily detectable but there are white pixels right above the up-rushing water front which are caused by water from the previous wave flowing down the run-up board. Furthermore there are white pixels above in the middle of the run-up board which indicates light reflected on the capacitive gauge. The reflections are in general characterized by a size of only one pixel or very few pixels. Therefore it was necessary to define a so called “minimum region” by determining a “minimum wave crest width” and a “minimum wave crest height” to avoid false detection of reflections as upmost wave tongue. The setting of these two parameters is possible within the left section “Parameter” of the designed MATLAB interface (see Figure 6.5). A “minimum wave crest width” of 5 pixels (FlowDike 1, 1:3 sloped dike) and 20 pixels (FlowDike 2, 1:6 sloped dike) was sufficient in most cases. The “minimum wave crest height” was set to 1 pixel (FlowDike 1) and 5 pixels (FlowDike2) respectively.

In the next step every line of the black/white frame was checked beginning in the left above corner of the frame and continuing in right and downwards direction. If the routine find a minimum region (FlowDike 1: 5 contiguous pixels; FlowDike 2: 100 contiguous pixels) this was defined as the maximum run-up tongue (green triangle in Figure 6.2).

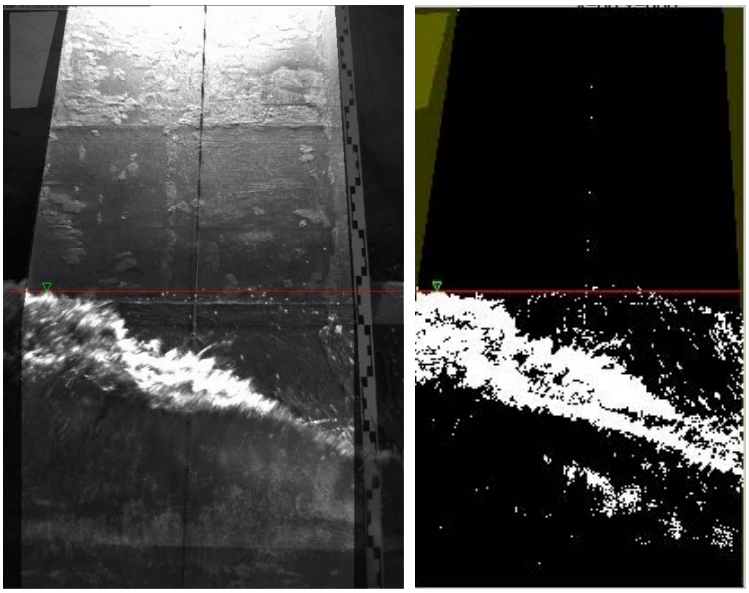

Figure 6.2 Left: video frame with the detected position of the upmost wave tip on the run-up plate (red line with green triangle), right: associated picture displaying the difference in pixel brightness between the frame at the left side and its following frame in the video film (test s5_22_15_w6_00_30w)

The last step in the procedure was to calculate the run-up height value in meter out of the run-up height in pixel. Here a nonlinear function was used because the image plane was not parallel to the run-up board. This was due to the optical distortion within the camera lens and due to the effects of perspective.

This nonlinear function has to be determined for each video film before the analysis was conducted. Therefore several data are used. At first one had to click on the gauge scale in the video frame displaced within the designed MATLAB interface (Figure 6.5). The obtained data set [cm; pixel] is visible as a table in the left and below corner there (“gauge scale”). Another used value was the still-water-level. One had to determine its height above level zero of the gauge scale in the set “Parameter”

as “SWL” (see Figure 6.5, left and middle). Another needed parameter was the dilatations correction factor. Its determination has been described in section 3.3.1. All these data has been used to obtain a polynomial function of degree 3 to calculate R [m] out of R [pixel].

During the data analysis it was considered to get more data on basis of the existing video films. Therefore an advanced data analysis routine was developed. Within this routine the run-up height for 10 stripes each representing the tenth part of the run-up board width (see Figure 6.3) was determined. A further benefit was that the run-up data detected at the smaller stripes a more similar to the data measured by the capacitive gauge (see section 8.2.1).

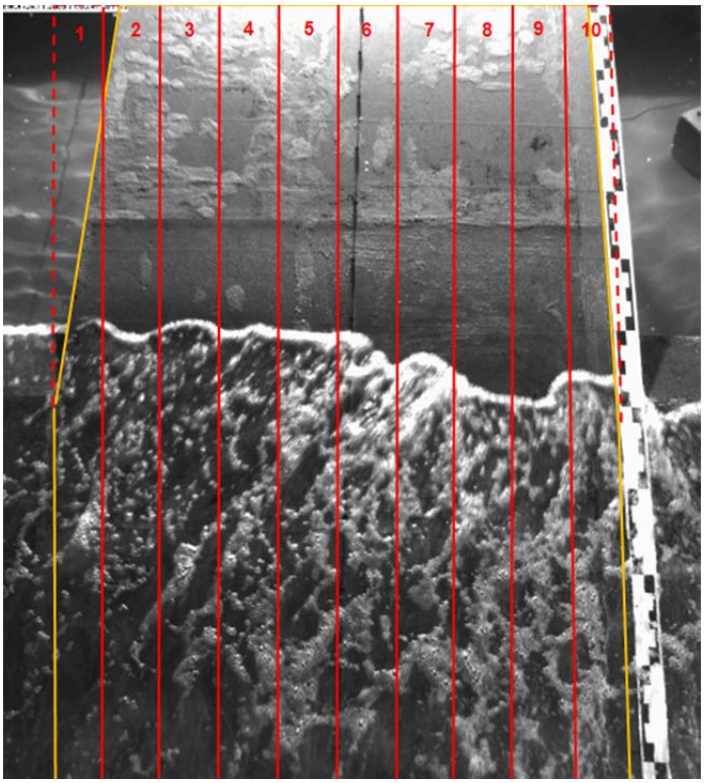

Figure 6.3 Definition of 10 stripes for advanced run-up data analysis within the MATLAB interface.

By this it was possible to get 10 wave run-up time series for each video film and not only one (see Figure 6.4). The two stripes at the left and the right edge of the run-up board (stripe 1 and stripe 10) were not used in data analysis because the water there flows partially sidewards and this lessens the detected run-up height.

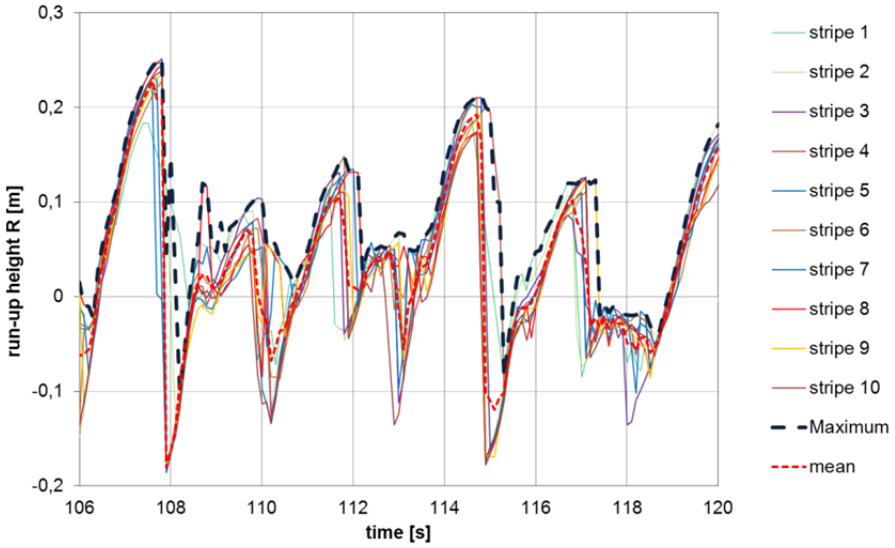

Figure 6.4 Run-up height depending on time for 10 stripes of the run-up plate.

Before one could start the film analysis procedure several parts of the video frames had to be excluded from analysis due to reasons explained in the following paragraphs. The size and the location of the excluded frame regions had to be determined for each video film because it could be possible that the location of the camera was changed between two model tests.

The parts at the left and the right side of the pictures for instance are not necessary for data analysis because they only include things which were located behind the run-up board. These parts were “cut out” by means of a tool which was integrated in the designed MATLAB interface (left below in Figure 6.5). These parts are marked with a darker color.

For FlowDike 1 tests (1:3 sloped dike) an almost perpendicular bar, which is marked with a lighter color in Figure 6.5 has to be excluded due to repeated reflections almost always after the up-rushing water runs down. The reflections were originated by a ceiling lamp. A third region is shaped like a horizontal bar and is also marked with a lighter color in Figure 6.5. This bar covers the boundary between the dike slope and the run-up board. Water drops remain there due to very small roughness elements and could be detected as wave tips although the wave front is already below.

In order to get a photo documentation of the model tests every single test and every device has been photographed during test program. Due to its smooth surface camera flash lights were reflected on the gauge scale and false detections of wave run-up could be created. That’s why the gauge scale at the right side of the run-up plate was excluded from video film analysis too.

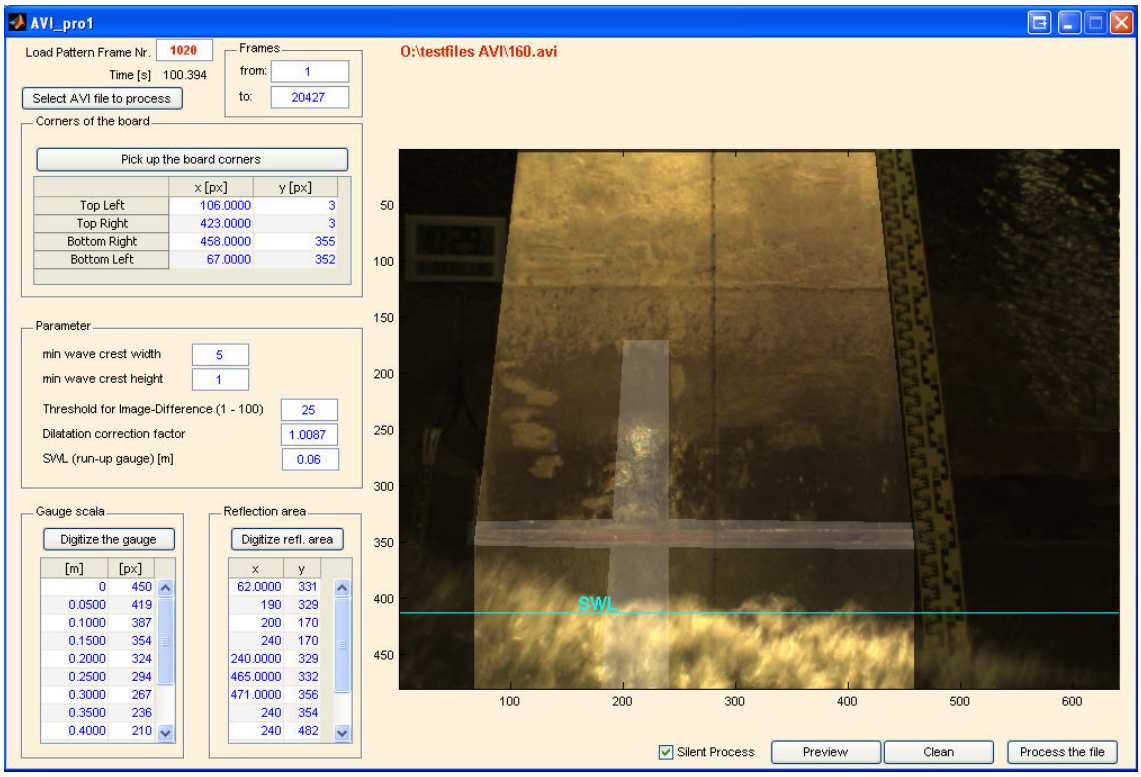

Figure 6.5 MATLAB interface which was used to analyze video films

Further errors were eliminated from data results manually. Sometimes there were falsely detected wave run-up heights due the moving shadow of members of staff who cross the light which illuminated the run-up board (Figure 6.6, left and middle). In other cases a malfunction of the cameras (chip or memory malfunction) did cause horizontal displaced bars within the frames which constrained data extraction (Figure 6.6, right).

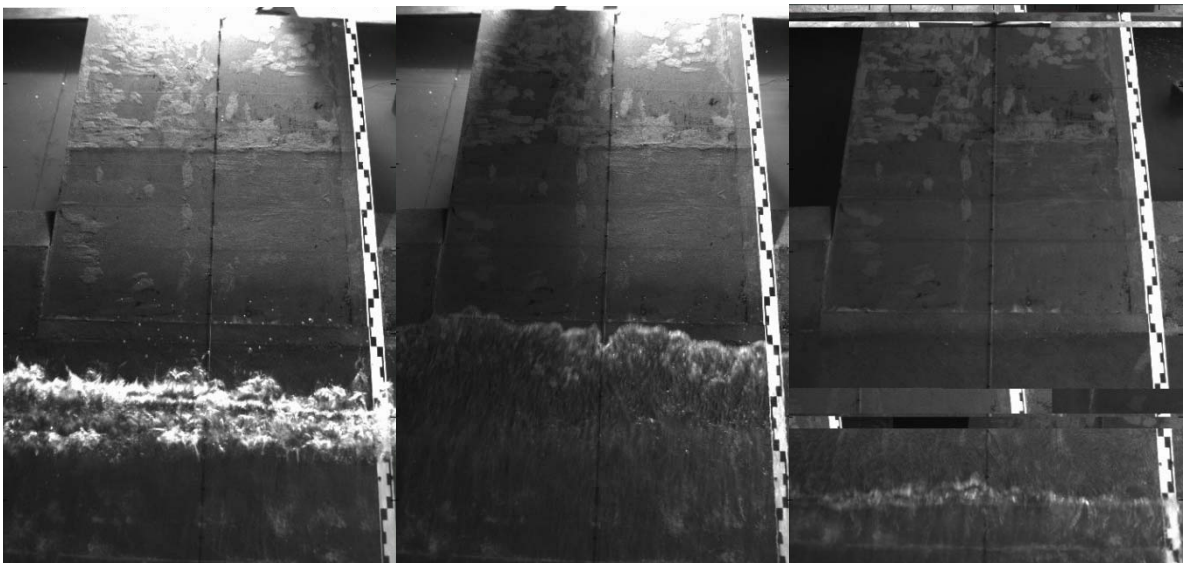

Figure 6.6 Left and middle: moving shadow between frame 2480 and 2500 in test s4_04a_30_w1_00_00, Right: A horizontal displaced bar in the avi-file of test s4_03_00_w1_49_00

The detected wave run-up height could be visualized within the videos films in order to verify the detection process. This is marked with a red line and a green triangle in Figure 6.2. During the video analysis for FlowDike 1 (1:3 sloped dike) every frame was transformed into grey scale and there was

no visualization on the screen in order to get a higher detection speed. Therefore the procedure was started in batch modus.

6.3.3 Determination of $R_{u2\%}$

Wave run-up height is defined as vertical difference between the still water level (SWL) and the maximum elevation of the run-up tongue. But every wave of a sea state causes a different run-up height. Within literature or design standards the value $R_{u2\%}$ is often used. This is the run-up height which is exceeded by only 2 % of all waves arriving at the toe of the considered structure.

To calculate $R_{u2\%}$ based on run-up time series for both measurement devices (capacitive gauge, video films) a MATLAB procedure has been programmed (see section 6.3.1). The wave run-up height $R_{u2\%}$ is determined with a crossing analysis using a threshold level different from zero. This was chosen out of practical reasons. Not all smaller events can be detected but it avoids losing higher run-up events when the down rushing water after a run-up event still remains above SWL until the next wave rushes up (see section 8.2.1).

The crossing level was always chosen so that at least n = 500 run-up events and their maximum run-up height could be detected. These n maximum values were than sorted in descending order. According to the number of incoming waves per test of approximately N = 1000 the wave run-up height $R_{u2\%}$ is defined as the minimal value of the highest $k = 0.02 \cdot N = 20$ run-up events.

6.4 Wave overtopping

For the following analysis the amount of overtopping water was calculated. This is visible exemplary in Figure 6.9 (left). Here the graph for loadcell 41 and loadcell 43 are unequal.

In Figure 6.7 the wave overtopping amount measured during one test is displayed. Here the descending part indicates the pumping of water. The signals given in Figure 6.7 (right) demonstrate the measurements of the load cells for wave by wave overtopping during 5 seconds.

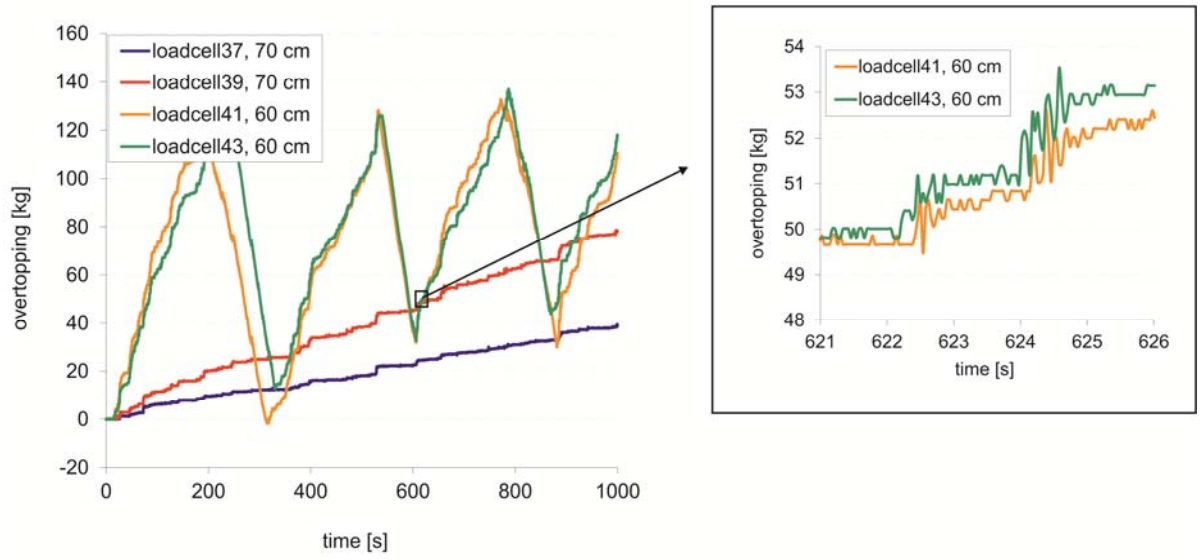

Figure 6.7 Overtopping measurement for a sequence of 1000 s (left) and for a sequence of 20 s (right); test no. 162 (s1_11_15_w5_00_00)

The wave overtopping was calculated by adding the pumped water volumes (recalculation from known pump capacity and working period) to the collected amount within the tank. Figure 6.8 shows the relevant parameters for the determination of the overtopping rate. The overtopping volume during the whole test can be determined by the following formula:

$$\begin{aligned} V_{ov} &= \Delta V_1 + (V_{Pump} - \Delta V_2) + \Delta V_3 \\ &= V_2 - V_1 + V_{Pump} - (V_2 - V_3) + V_4 - V_3 \\ &= V_4 - V_1 + V_{Pump} \end{aligned} \tag{6.1}$$

with V_{ov} overtopping volume during one test [m³]

V_{Pump} volume, pumped out of the overtopping tank [m³]

ΔV_i difference of the volume in the tank during pumping interval [m³]

V_i volume in the overtopping tank at time t_i [m³]

The volume V_{pump} which was pumped out of the overtopping tank can be calculated as the product of the pumping time t_{Pump} and the pump capacity (cf. Annex B and Annex C).

The overtopping rate q is determined by dividing the overtopping volume V_{ov} by the test duration and the width of the overtopping channel $d_{channel}$. The overtopping channel was 0.1 m wide except during set-up 1 with 0.118 m width.

$$q = \frac{V_{ov}}{(t_{end} - t_{start}) \cdot d_{channel}} \tag{6.2}$$

with q overtopping rate [m³/(m·s)]

t_{start} analyzing start time of the test [s]

t_{end} analyzing end time of the test [s]

$d_{channel}$ width of the overtopping channel [m]

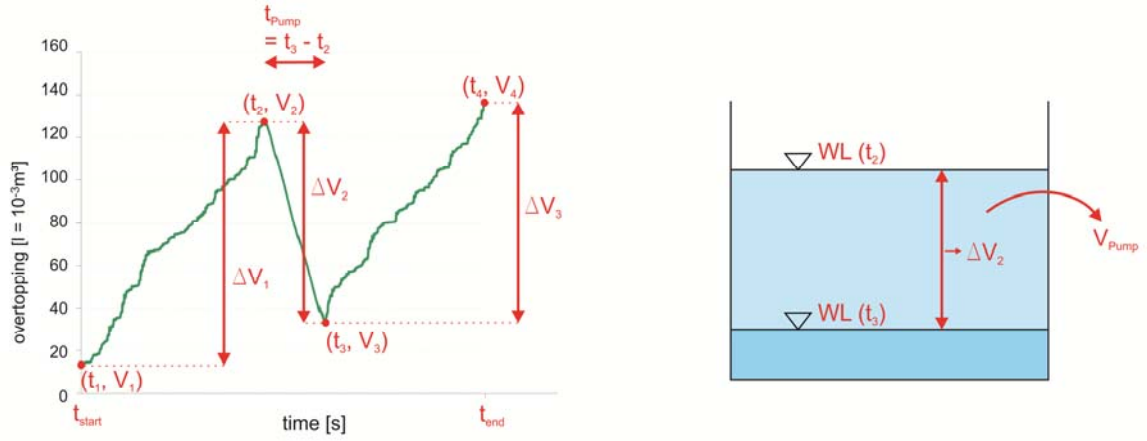

Figure 6.8 Parameters for the determination of overtopping rate

Figure 6.9 shows the overtopping raw data and the calculated overtopping discharge of test no. 144. The final overtopping amount of load cell 43 is 65 kg. In the given test the overtopping rate for load cell 43 with t_{end} = 1350 s is

q = 65 l/(1350 s · 0.118 m) = 0.408 l/(s·m)

The measurement error of the load cell is smaller than 0.05 % which corresponds to 0.11 kg considering the maximum measuring range of approximately 220 kg (2150 N). For the presented test no. 144 no significant overtopping amount on the 0.7 m crest could be measured. For all tests a overtopping rate beneath 0.02 l/(s·m) will be assumed to be negligible.

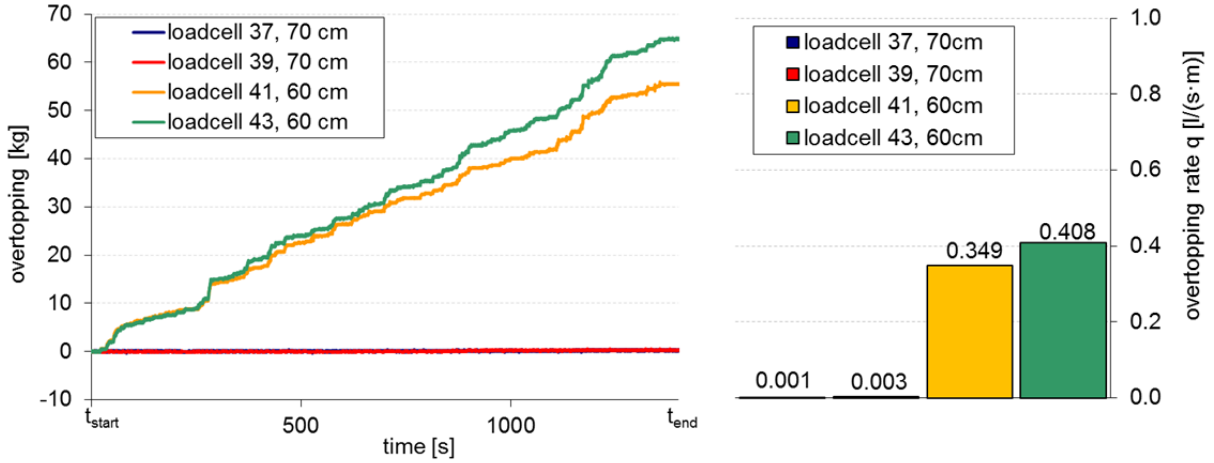

Figure 6.9 Overtopping raw data (left) and calculated overtopping discharge (right); test no. 144 (s1_01_00_w1_00_00)

6.5 Flow processes on crest

6.5.1 Flow velocity on the crest

One part of the presented project was focused on the analysis and description of single overtopping events. Therefore, the process of overtopping on the dike crest was analyzed in detail too. Micro propellers data were processed using crossing analysis. Different threshold levels (0.1 Volt and 1 Volt, see Figure 6.10) were selected to identify the number of overtopping events.

Crossing analysis with a defined threshold was done for the measurement devices on the crest. Here the micro propellers were measuring the flow velocity on the crest at the seaward and the landward edge. As described earlier, statistical characteristics were determined as a relation of detected events and number of waves.

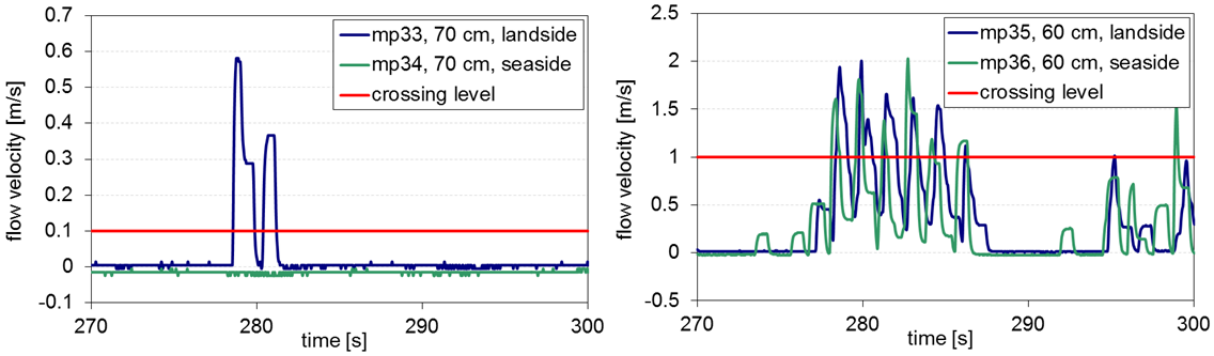

Figure 6.10 Raw data and crossing level of flow velocity on the dike crest measured by micro propellers (mp); on 0.7 m high dike crest (left); on 0.6 m high dike crest (right); test no. 144 (s1_01_00_w1_00_00)

The measured velocity was depicted by means of an exceedance curve (see Figure 6.11). Here, values were calculated by adding the threshold and multiplication of the voltage readings with the defined

calibration factor (see Annex). For the presented test no 144 the 2%-value for the velocities on the 0.6 m high dike are 1.2 m/s (mp 35) and 1.33 m/s (mp 36). For the 0.7 m high dike some items were only detected for the seaward side, but do not give any useful results regarding an overtopping velocity. Therefore it has to be concluded that no significant overtopping process during the test occurred. This fits well with the results from the analysis of the overtopping amount of water.

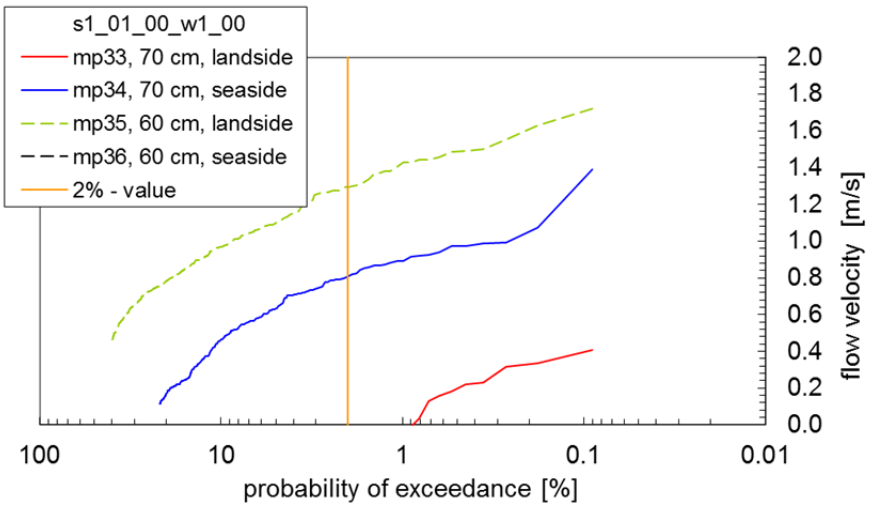

Figure 6.11 Exceedance curves for flow velocity on dike crest measured by micro propellers (mp); test no. 144 (s1_01_00_w1_00_00)

6.5.2 Flow depth on the crest

The procedure in layer thickness data processing was similar to the methods used on measurement results of flow velocities. The data from the DHI Wave Synthesizer was already given with the unit meter. Therefore no calibration had to be added.

As mentioned above for the micro propellers data in test no. 144, only few items for the 0.7 m crest were detected (see the raw data in Figure 6.12). Figure 6.13 illustrates exceedance curve of flow depth for both crest heights. Due to the different freeboard heights, the layer thickness on the 0.7 m high dike crest is lower than on the 0.6 m high dike crest. It becomes obvious that the flow depth decreases along the flow process over the dike crest, since the wave gauges on the landward edge give smaller values than the ones on the seaward side. The 2%-values of the layer thickness on the 0.6 m crest are 0.017 m (wg 17) and 0.026 m (wg 16).

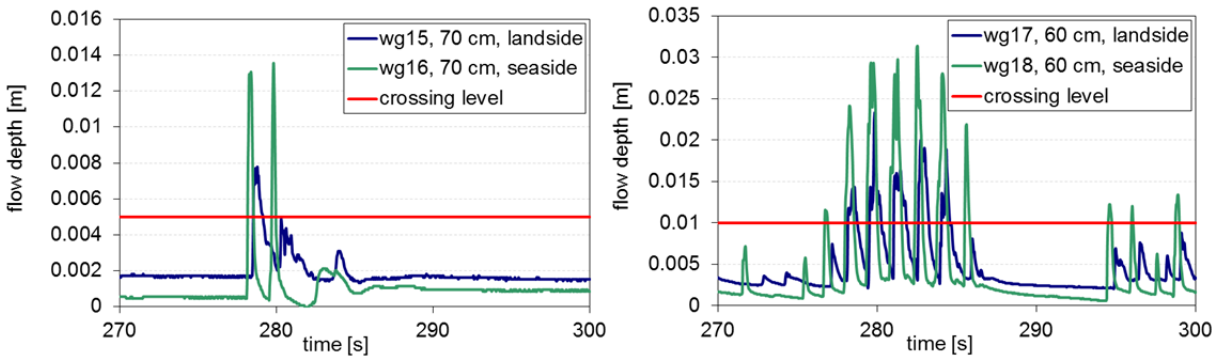

Figure 6.12 Raw data with crossing level for flow depth on the dike crest measured by wave gauges (wg), 0.7 m high dike crest (left); 0.6 m high dike crest (right); test no. 144 (s1_01_00_w1_00_00)

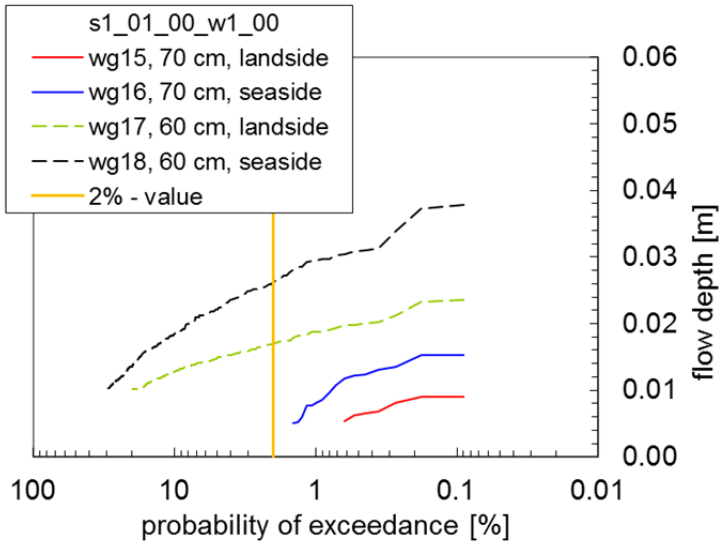

Figure 6.13 Exceedance curves for flow depth on the crest measured by wave gauges (wg); test no. 144 (s1_01_00_w1_00_00)

7 Analysis of wave field and breaking processes

7.1 General

To analyze the wave evolution in front of the dike, the results from reflection and zero-down-crossing analysis were evaluated. The reflection analysis was done in frequency domain, the zero-down-crossing analysis in time domain. The main analyzed data of the wave field are summarized in Annex H and Annex I.

First the verification of the measurements is reviewed in section 7.2. The composition of the wave parameters used for the analysis on wave run-up and wave overtopping are given in section 7.5. Section 7.6 gives the influence of the current on these wave parameters.

7.2 Verification of measurements

7.2.1 General

The measurements of the wave field had to be verified. Therefore the signals of the wave gauges recorded over the first seconds of the reference test were compared. Afterwards the zero-down-crossing analysis is described to see the distribution of the input signal of each wave gauge array. This signal should be Rayleigh distributed (HOLTHUIJSEN, 2007). To verify the correctness of the reflection analysis the spectral moments of the measured, reflected and incident waves will be compared among each other. On the basis of the reflection analysis the wave parameters of the incident waves, used for the analysis on wave run-up and wave overtopping, will be determined. Additionally the wave breaking will be analyzed while comparing the reflection coefficient and the surf similarity parameter.

7.2.2 Wave gauge signal

Measurement devices for the wave field are described in section 3.1 and 3.2.2. In Figure 7.1 and Figure 7.2 the signals recorded during the first seconds of the reference test with wave no. 5 (no current, no wind, perpendicular wave attack) are given for all wave gauges. Data at the dike toe of the 0.6 m high dike as well as the 0.7 m high dike for FlowDike 1 (1:3 sloped dike) are presented in Figure 7.1. Figure 7.2 illustrates the data of three wave gauge array of the FlowDike 2 set-up (1:6 sloped dike). The first was located in front of the wave generator and the other two at the dike toe of the 0.6 m high dike and the 0.7 m high dike.

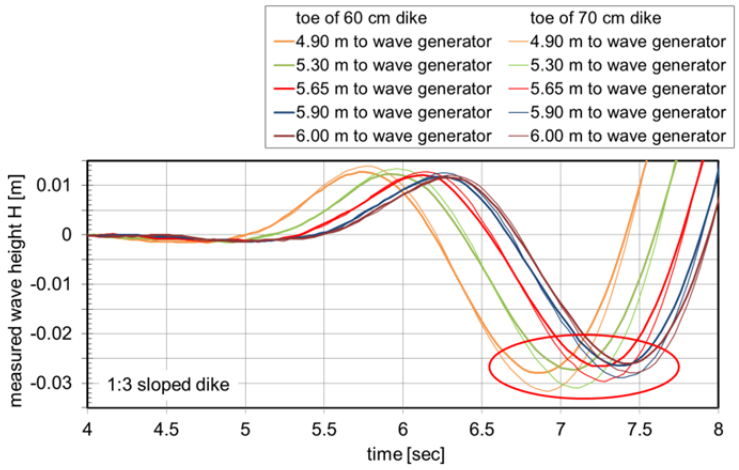

Figure 7.1 Signal of wave gauges exemplary for the reference test, wave spectrum no. 5; 1:3 sloped dike

During the first seconds only incident waves were measured, because reflection did not start until the first waves arrived at the sloped dike. It was expected that the measured value of water surface elevation would only differ in time but not in height between the different wave gauges. The graphs should be only moved along the x-axis (time). But the graphs show different developments. There are maximum differences in water level elevation of 15 % (marked by a red ellipse in Figure 7.1 and Figure 7.2, orange and green graphs). Due to these unexpected measurement data of wave gauges, the incoming waves are analyzed in more detail.

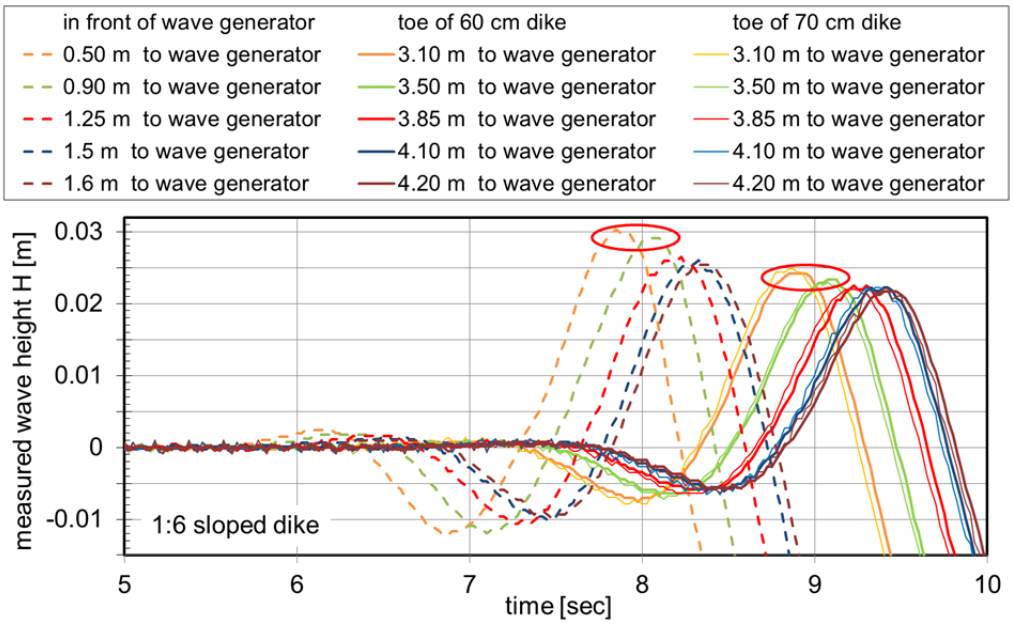

Figure 7.2 Signal of wave gauges exemplary for the reference test, wave spectrum no. 5; 1:6 sloped dike

7.2.3 Measured wave heights

As a result of the zero-down-crossing analysis of the measured wave heights H in time domain, Figure 7.3 depicts the Rayleigh distribution of wave heights exemplarily for the wave gauge array at the toe of 0.7 m high and 1:6 sloped dike. The Rayleigh distribution is common for the analysis of JONSWAP spectra in deep water. The abscissa is fitted to a Rayleigh scale by means of the relation:

$$x' = \sqrt{-\ln\left(1 - \frac{100 - x}{100}\right)} \qquad (7.1)$$

with x probability of exceedance [%]

x´ probability of exceedance – Rayleigh distributed [%]

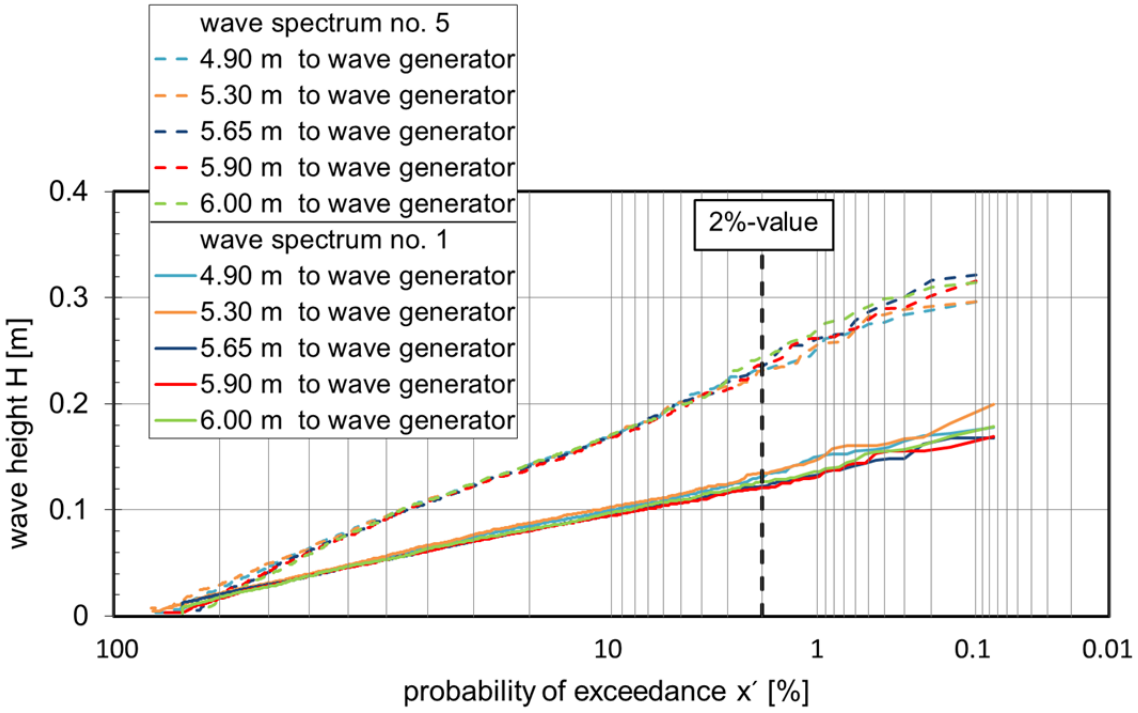

Figure 7.3 Linear distribution of wave height H over a Rayleigh scale for a Jonswap spectrum exemplarily for the wave gauges at the toe of the 0.7 m dike on the 1:6 sloped dike (wave no. 1 and wave no. 5)

The Rayleigh distributed x-values are the reason why a linear trend was found. The similarity of their shape indicates the homogeneous arrangement for both wave gauge arrays.

The wave height exceeded by 2 % of the waves $H_{2\%}$ in [m] is a dimension for the homogeneity of the wave field as well as the correct measuring of the wave gauges. Figure 7.4 and Figure 7.5 show the standard deviation of the wave heights $H_{2\%}$ of each wave gauge array for different tests (w1 to w6). The standard deviations of $H_{2\%}$ of the tests on the 1:6 sloped dike are mainly smaller than 0.01 m. The comparative high standard deviation for the wave spectra 5 (steepest analyzed wave in this project, 1:3 sloped dike) and wave spectra 6 (1:6 sloped dike, 15° wave attack) can be traced back to prematurely breaking waves caused by superposition of incident and reflected wave. This has to be considered while interpreting the results on wave run-up and wave overtopping.

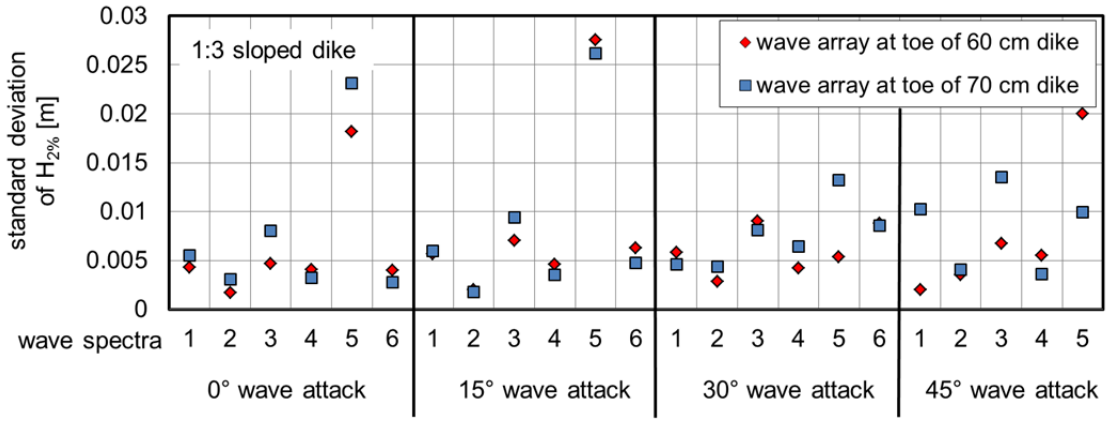

Figure 7.4 Standard deviation of $H_{2\%}$-values; 1:3 sloped dike; zero-down-crossing analysis considering five wave gauges

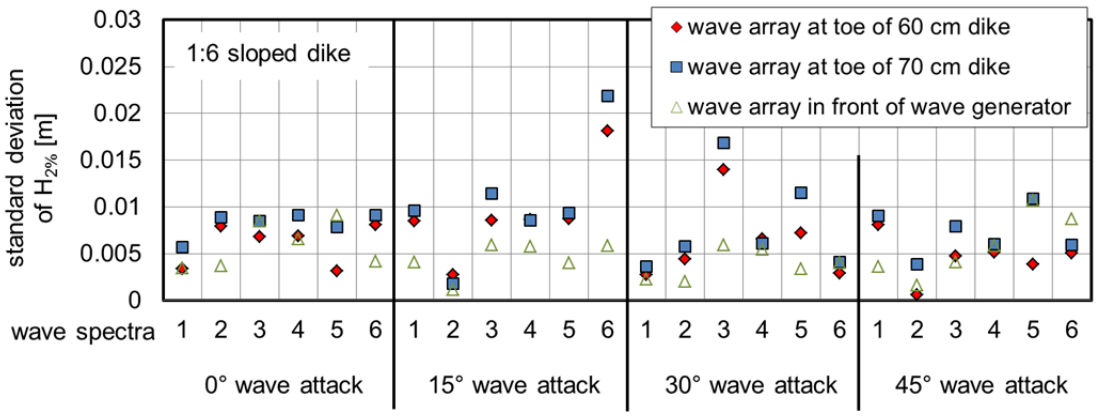

Figure 7.5 Standard deviation of $H_{2\%}$-values; 1:6 sloped dike; zero-down-crossing analysis considering five wave gauges

7.2.4 Reflection analysis - frequency domain

The wave field was analyzed with the described method in section 6.2. From the reflection analysis, which is performed in frequency domain, the plotted distribution of energy density (reference tests, wave no. 1 and 5, toe at the 0.6 m high dike) in Figure 7.6 corresponds to the theoretical assumption for a JONSWAP spectrum as a single peaked spectrum. The determined reflection coefficients and surf similarity parameters of all tests are described in more detail in section 7.3.

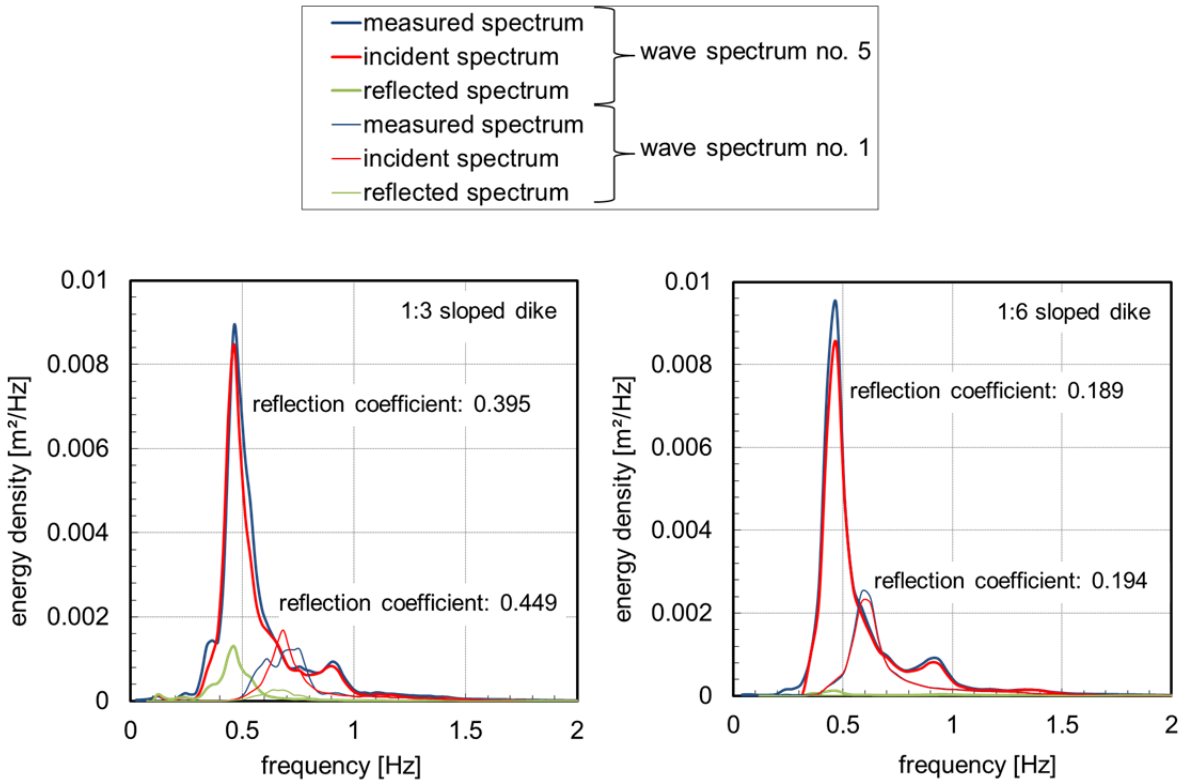

Figure 7.6 Energy density spectrum in front of 0.6 m crest of the 1:3 sloped dike (left) and 1:6 sloped dike (right); three wave gauges analyzed

The reflection analysis was performed twice. First all five wave gauges were used. Secondly only three wave gauges of each wave gauge array were considered. The wave heights H_{m0} of these wave gauges as a result of the reflection analysis are plotted for each wave gauge array in Figure 7.7 for the reference test on the 1:3 sloped dike. The left figure shows the wave heights from the analysis of five

wave gauges, the left figure from three wave gauges. Figure 7.8 shows the analyzed data for the 1:6 sloped dike.

The wave gauges are listed in direction of wave propagation (from left to right). The different graphs show the wave heights of the six analyzed wave spectra w1 to w6. Uniform wave heights are determinable for each wave gauge, except wave heights of the wave spectra w5 on the 1:3 sloped dike. These wave heights decrease in wave direction. As an explanation two photos of the beginning of the breaking process of some waves during the wave spectra w5 on the 1:3 sloped dike (flow depth 0.5 m) are given in Figure 7.9. The corresponding surf similarity parameters are described in more detail in section 7.3. A large difference in wave heights is obvious for wave spectra 5 (1:3 and 1:6 sloped dike). Also the first two wave gauges of the analysis using five wave gauges give different wave heights (left graphs in Figure 7.7 and Figure 7.8).

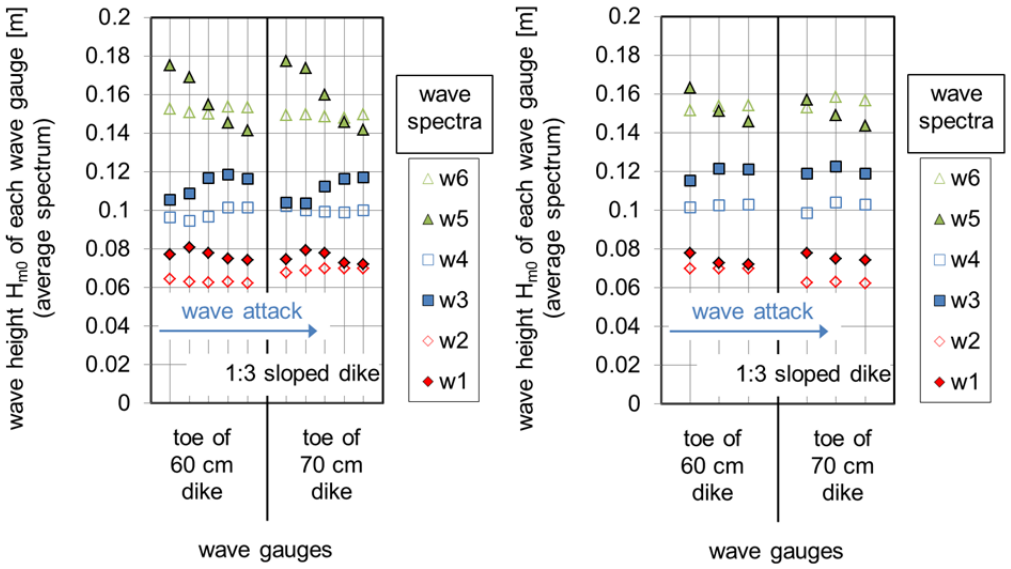

Figure 7.7 Wave height H_{m0} of the analyzed wave gauges - reflection analysis with five wave gauges (left) and reflection analysis with three wave gauges (right); reference test on 1:3 sloped dike

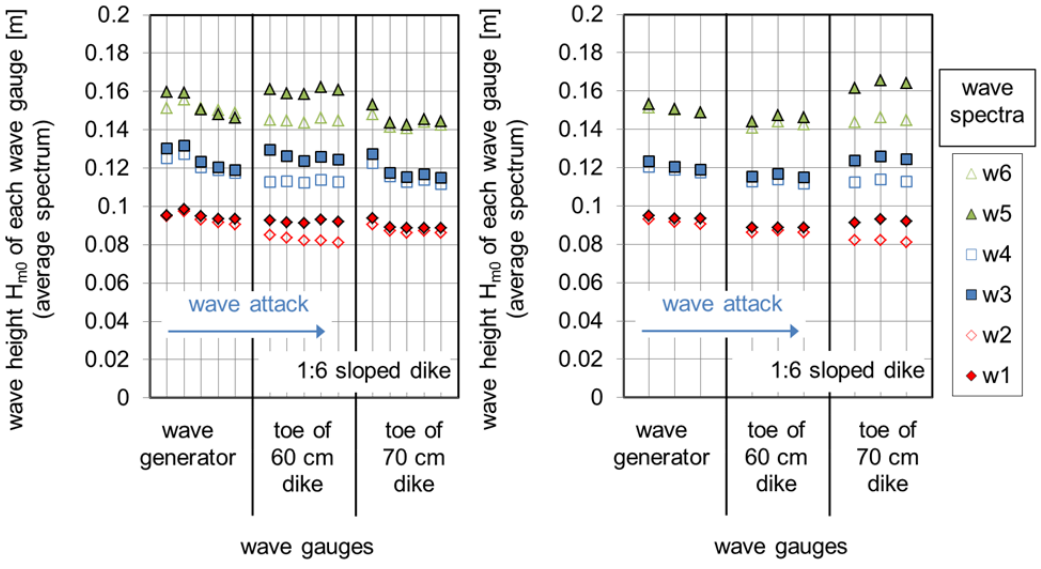

Figure 7.8 Wave height H_{m0} of the analyzed wave gauges - reflection analysis with five wave gauges (left), reflection analysis with three wave gauges (left); reference test on 1:6 sloped dike

Figure 7.9 Beginning of breaker process of waves (wave propagation from right to left)

Under consideration of wave reflection one value H_{m0} for each wave gauge array was obtained. Figure 7.10 gives the significant wave heights H_{m0} of the incident wave of the reference tests from the reflection analysis with five wave gauges. The wave gauge arrays at the toe of the two dike heights give quite similar significant wave heights H_{m0} for each test phase (1:3 and 1:6 sloped dike). The right graph for the 1:6 sloped dike includes the wave heights in front of the wave generator. For the wave number 6 the wave height in front of the wave generator differs slightly from the wave heights at the toe of the dike. The maximum deviation of 0.01 m appears for wave spectrum number 5 (H_s = 0.15 m).

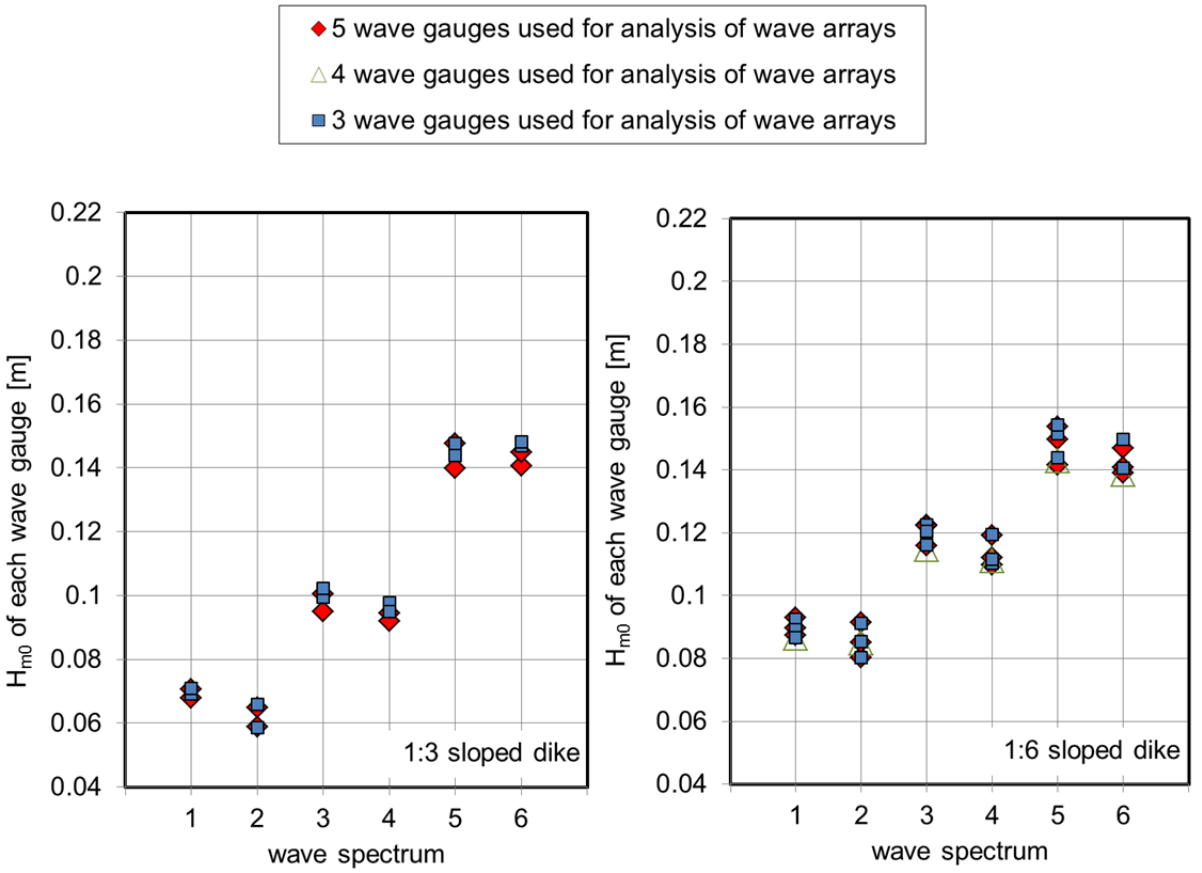

Figure 7.10 Significant incident wave height H_{m0} for the reference model tests calculated for each wave gauge array and the six wave spectra

The spectral wave heights H_{m0} are determined for every test at the toe of the 0.6 m high dike and at the toe of the 0.7 m high dike. These two wave heights are plotted against each other in Figure 7.11. The black graph demonstrates equal x and y values. The best fit lines of the wave heights on the 1:3 and

1:6 sloped dike correspond well with that graph. For both tests phases (1:3 and 1:6 sloped dike) the coefficient of determination of the two best-fit-lines is equal or higher than 0.90. Therefore both wave heights can be used for the following analyses on wave run-up and wave overtopping.

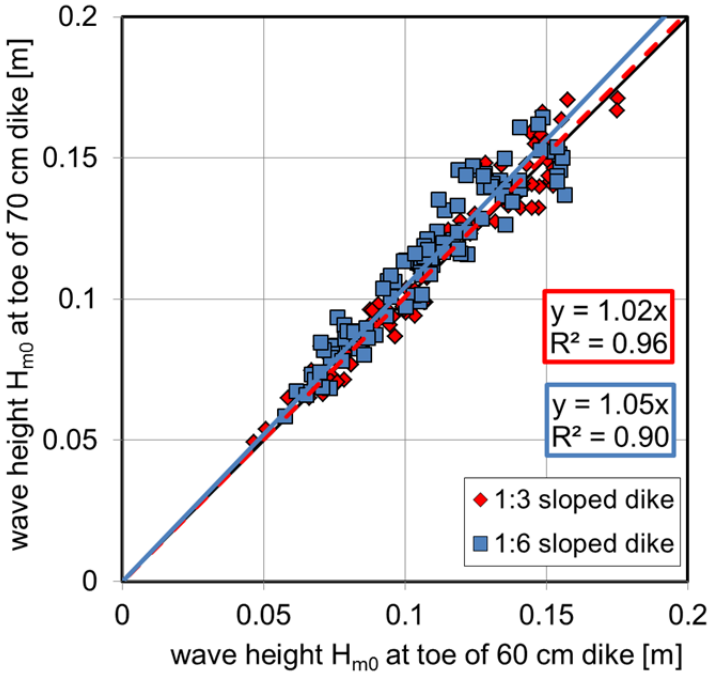

Figure 7.11 Spectral wave heights H_{m0} in front of 0.6 m high dike against wave heights H_{m0} in front of 0.7 m high dike; five wave gauges analyzed

The zeroth moment of the average spectrum, which is equal to the measured spectrum, the zeroth moment of the incident spectrum and of the reflected spectrum has been determined for every test. In Figure 7.12 and Figure 7.13 the zeroth moment of the average wave spectrum is plotted against the sum of the incident and reflected spectrum. It should be:

$$m_{0,average} = m_{0,incident} + m_{0,reflected} \tag{7.2}$$

Figure 7.12 shows the results for the analysis using five wave gauges which scatter less than the results of the analysis using only three wave gauges (cf. Figure 7.13). In the left graphs of these figures the data points of the reference test are filled with a color and correspond well with the line of perfect equality. The data points in the right graphs of the two figures show the results for all test without current and wind but with oblique wave attack. Therefore small deviations in comparison to the line of perfect equality are noticeable.

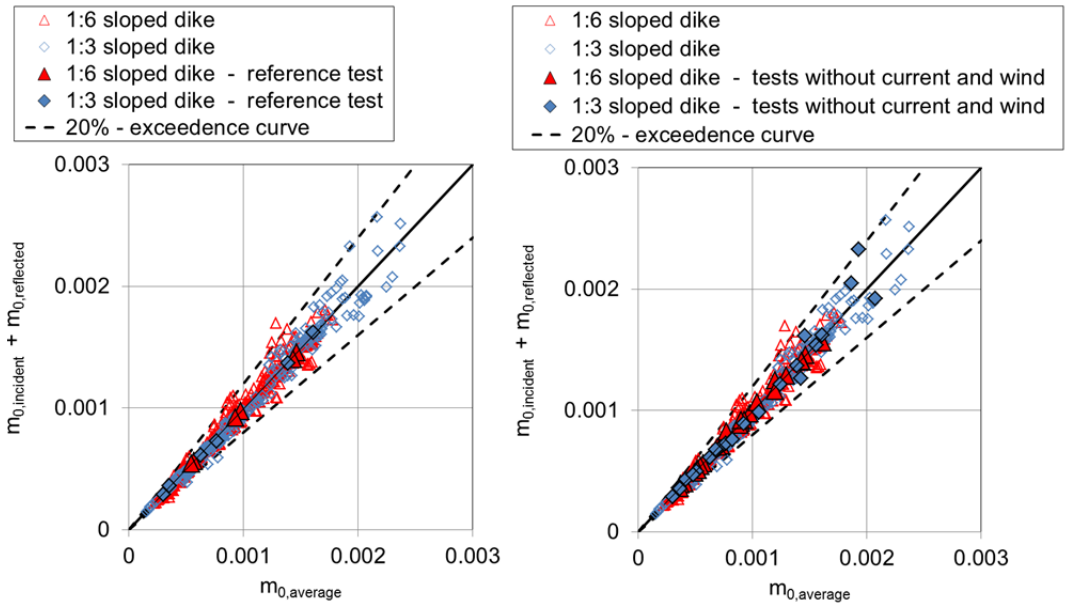

Figure 7.12 $m_{0,average}$ as a function of the sum of $m_{0,incident}$ and $m_{0,reflected}$, analysis with 5 wave gauges

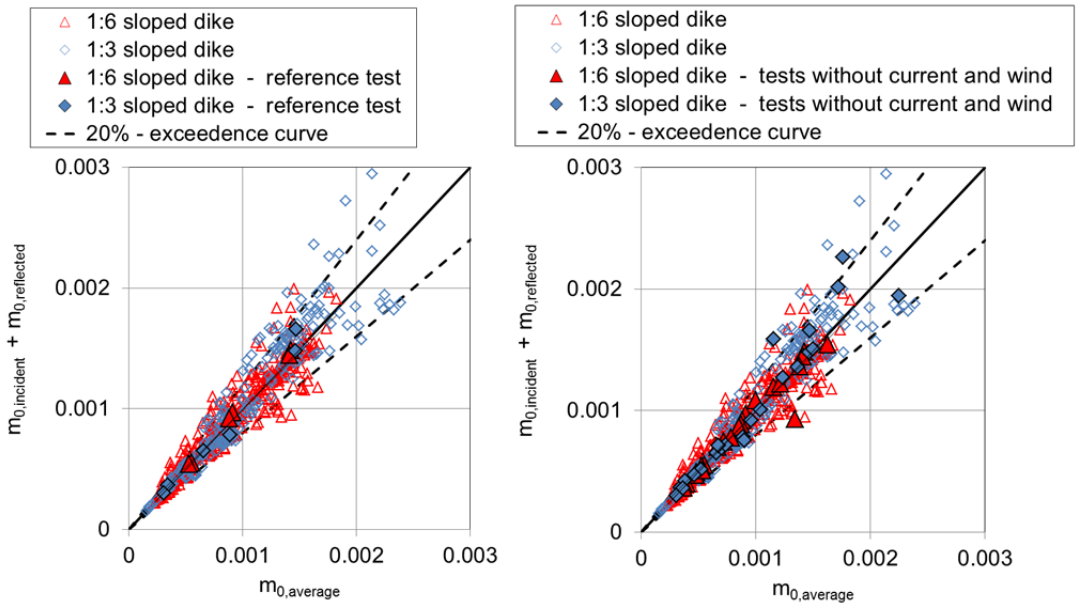

Figure 7.13 $m_{0,average}$ as a function of the sum of $m_{0,incident}$ and $m_{0,reflected}$, analysis with 3 wave gauges

Many parameters, like the dimensionless run-up height and the dimensionless overtopping rate, are calculated using the spectral wave period $T_{m-1,0}$ which is defined as

$$T_{m-1,0} = \frac{m_{-1}}{m_0} \quad [s] \tag{7.3}$$

with m_{-1} minus first moment of spectral density [m²]

m_0 zero order moment of spectral density [m²/s]

As shown in the literature review of section 4.1 the simplification for the spectral moment $T_{m-1,0}$ is often used:

$$T_{m-1,0} = \frac{T_p}{1.1} \quad [s] \tag{7.4}$$

with T_p peak period [s]

Figure 7.14 shows the calculated spectral wave period $T_{m-1,0} = m_{-1}/m_0$ against the peak period T_p. The green graph shows the approximated function $T_{m-1,0} = T_p/1.1$. For both analyses, using five or three wave gauges for the reflection analysis, the data points agree well with the approximated function. For further analyses the exact value of the calculated spectral period $T_{m-1,0} = m_{-1}/m_0$ will be used.

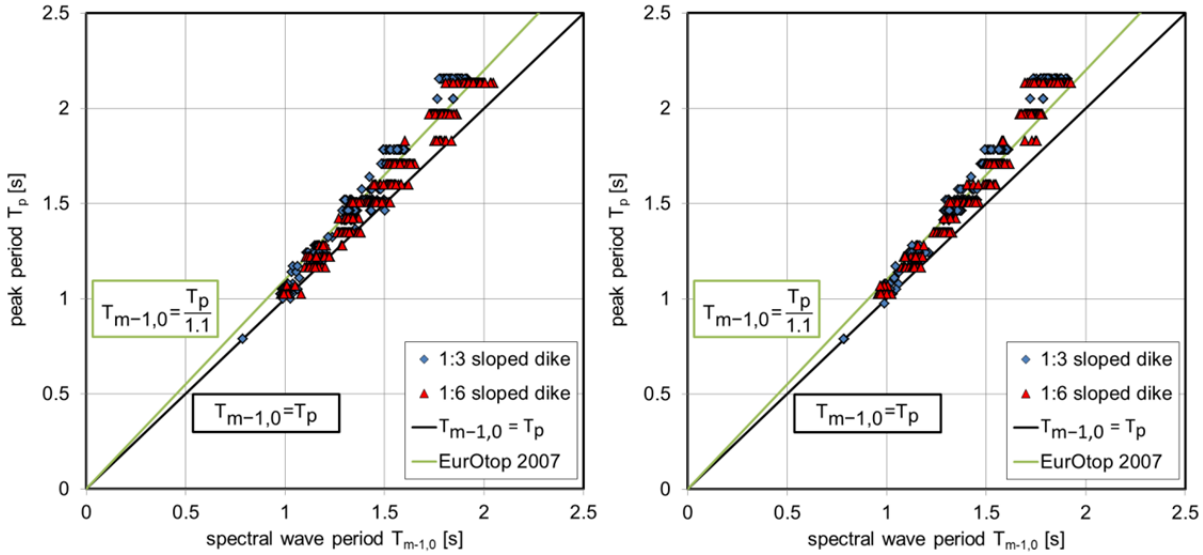

Figure 7.14 Spectral wave period $T_{m-1,0}$ against peak period T_p (left: refl. analysis using five wave gauges. right: refl. analysis using three wave gauges)

7.3 Wave breaking

In Figure 7.19 and Figure 7.22 the surf similarity parameter $\xi_{m-1,0}$ is plotted against the reflection coefficients K_R for the reference tests on the 1:3 and 1:6 sloped dike. The data points filled with color are the data points of the investigations on the 1:3 sloped dike. The reflection coefficients for the 1:6 sloped dike are lower because of less reflection. The reflection coefficients K_R of the FlowDike 1 and FlowDike 2 tests are slightly higher than given by BATTJES (1974) with:

$$K_R = 0.1 \cdot \xi^2 \quad [-] \tag{7.5}$$

The surf similarity parameter was determined using the formula (7.6). The reflection coefficient is given by formula (7.7). Thereby no distinction was made between perpendicular and oblique wave attack.

$$\xi_{m-1,0} = \frac{\tan\alpha}{\sqrt{s_{m-1,0}}} = \frac{\tan\alpha}{\sqrt{\frac{H_{m0}}{L_{m-1,0}}}} \quad [-] \tag{7.6}$$

$$K_R = \sqrt{\frac{m_{0,refl}}{m_{0,inc}}} \quad [-] \tag{7.7}$$

with $m_{0,refl}$ Energy density of the reflected wave spectrum [m²/s]

$m_{0,inc}$ Energy density of the incident wave spectrum [m²/s]

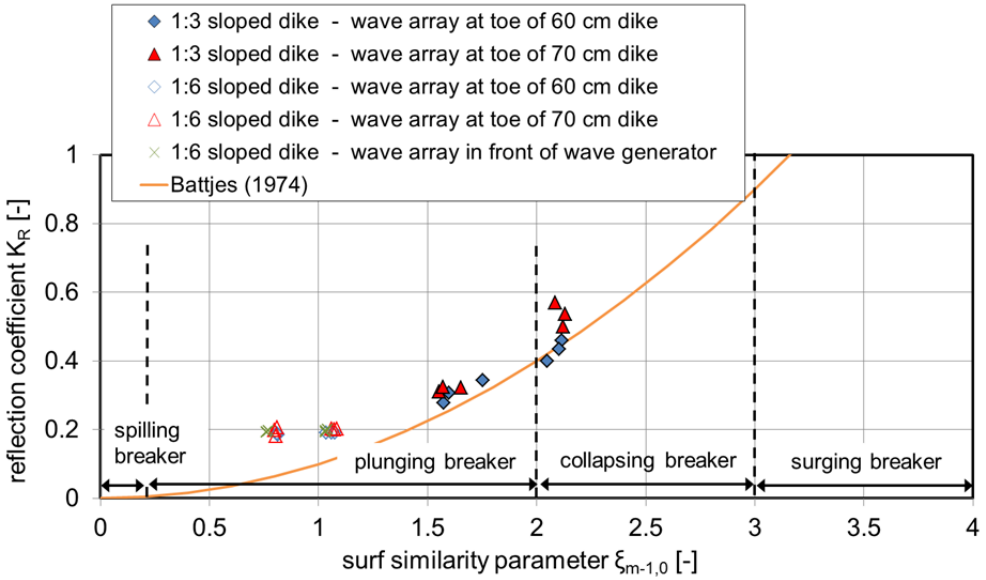

Figure 7.15 Surf similarity parameter $\xi_{m-1,0}$ against reflection coefficient K_R for reference tests; reflection analysis using five wave gauges

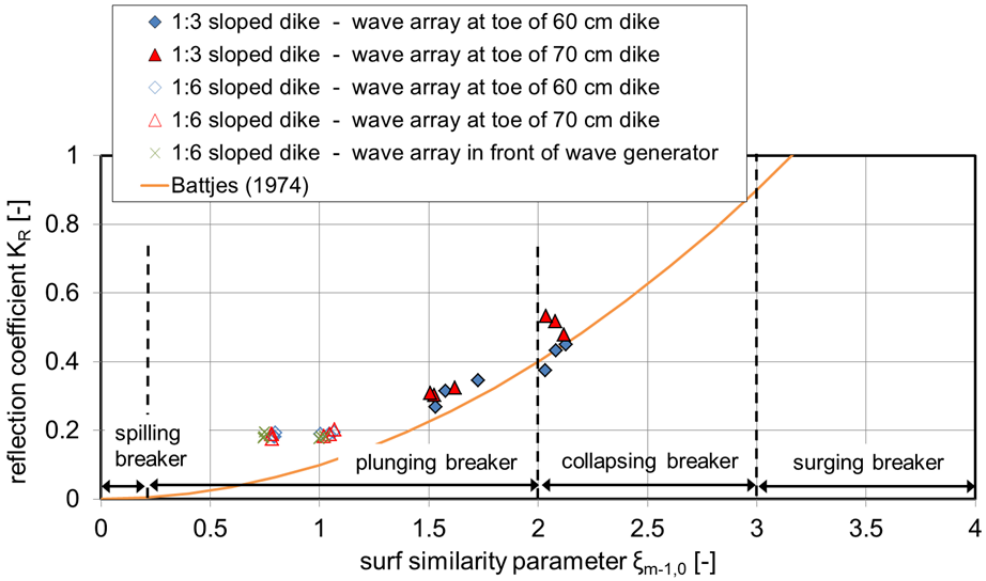

Figure 7.16 Surf similarity parameter $\xi_{m-1,0}$ against reflection coefficient K_R for reference tests; reflection analysis using three wave gauges

Figure 7.17 shows the surf similarity parameter as a function of the reflection coefficient for all tests without current and wind but considering different angles of wave attack. The reflection coefficients K_R on the 1:6 sloped dike ($\xi_{m-1,0} > 1.3$) correspond well with the reflection coefficients of the reference test. The reflection coefficients K_R on the 1:3 sloped dike ($\xi_{m-1,0} > 1.3$) are higher than the values from the reference test.

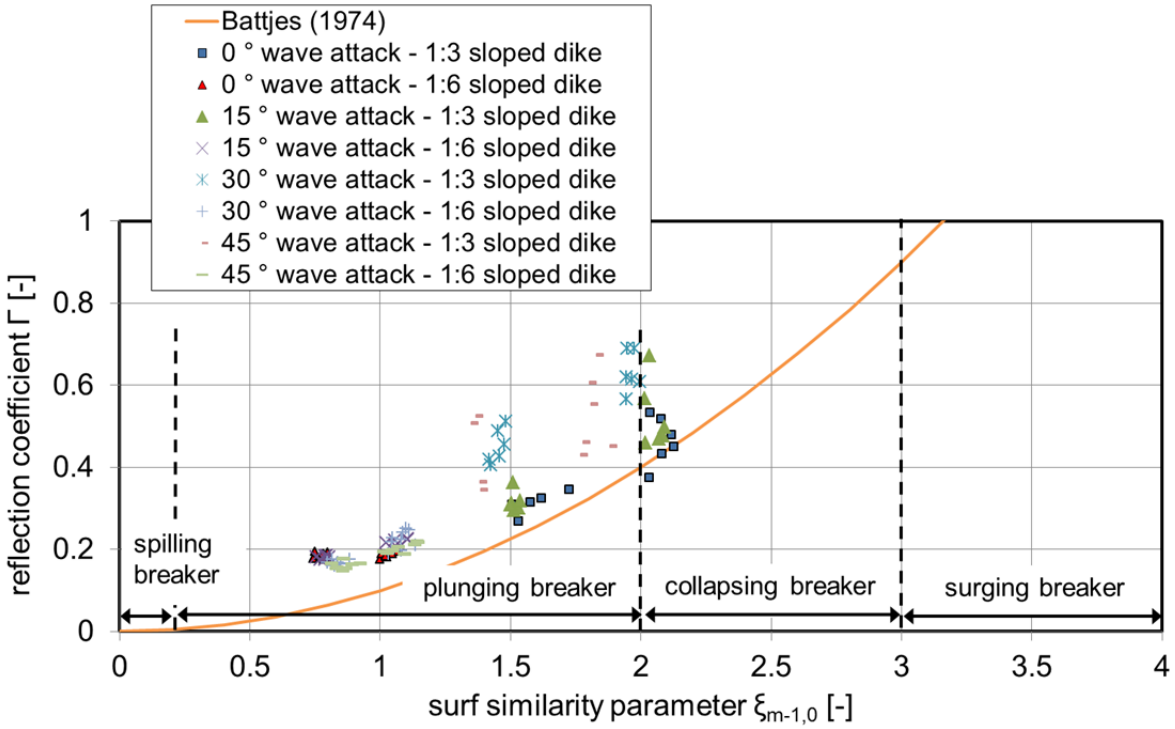

Figure 7.17 Surf similarity parameter $\xi_{m-1,0}$against reflection coefficient K_R for tests without current and wind, oblique wave attack; reflection analysis using three wave gauges

In Figure 7.18 and Figure 7.19 the surf similarity parameters $\xi_{m-1,0}$ are plotted against the reflection coefficients K_R for all tests using five and three wave gauges for the reflection analysis respectively. The data points filled with a color are the data points of the investigations on the 1:3 sloped dike. The reflection coefficients cover a range between 0.26 and 0.71. The reflection coefficients for the 1:6 sloped dike are lower because of less reflection and their values lie between 0.16 and 0.35.

The waves on the 1:3 sloped dike can mainly be classified as plunging breakers. Some tests have to be related to collapsing breakers. The tests on the 1:6 sloped dike contain only plunging breakers.

For the analysis of wave overtopping on the 1:3 sloped dike, it has to be distinguished between breaking and non-breaking waves. On the 1:6 sloped dike only breaking waves are considered. The breaker coefficient was determined using formula (7.6). The surf similarity parameter is given below (cf. (7.7)).

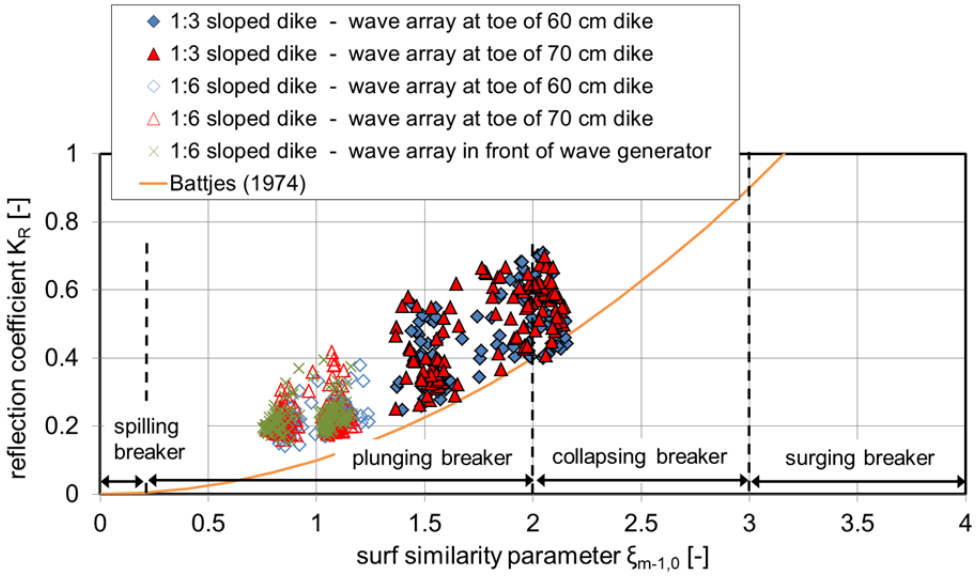

Figure 7.18 Surf similarity parameter $\xi_{m-1,0}$against reflection coefficient K_R of all tests; reflection analysis using five wave gauges

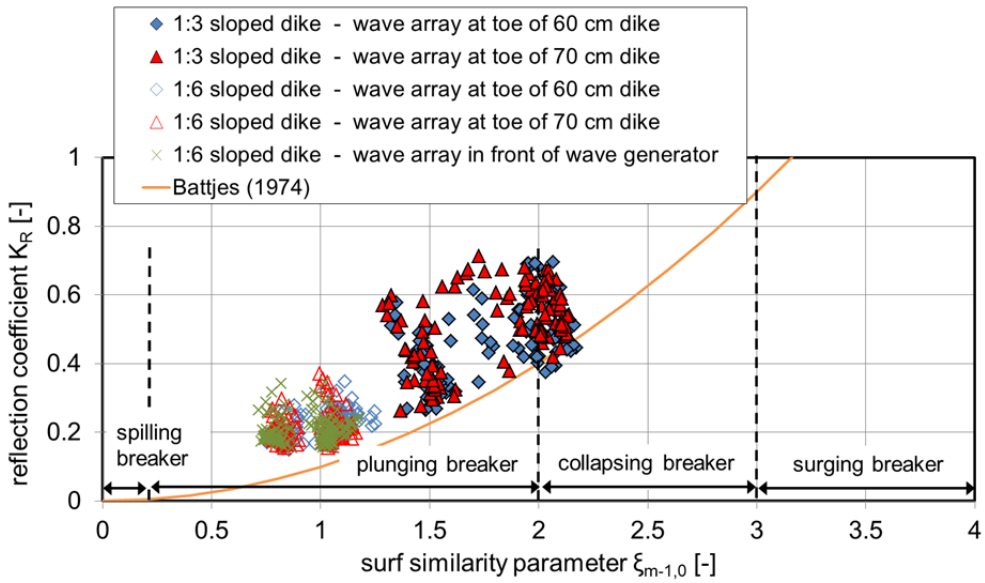

Figure 7.19 Surf similarity parameter $\xi_{m-1,0}$against reflection coefficient K_R of all tests; reflection analysis using three wave gauges

7.4 Detailed analysis of wave gauge array at toe of 0.7 m high and 1:6 sloped dike

The wave height H_{m0} of every wave gauge is determined for all tests from the reflection analysis using five wave gauges. Exemplary the wave heights of the test s6_26 (-30° wave attack, 0.15 m/s current, no wind) are given in Figure 7.22. It becomes obvious that for the first wave gauge of the wave gauge array at toe of 0.7 m high dike higher wave heights have been determined (marked by an orange ellipse). Due to that unclear signal, the reflection analysis for the wave gauge array at the toe of 0.7 m dike was repeated using only the other four wave gauges. The corresponding results for the spectral moments are plotted in Figure 7.21. No big difference is noticeable and the regression coefficient is only slightly higher by using five wave gauges for the reflection analysis (left figure).

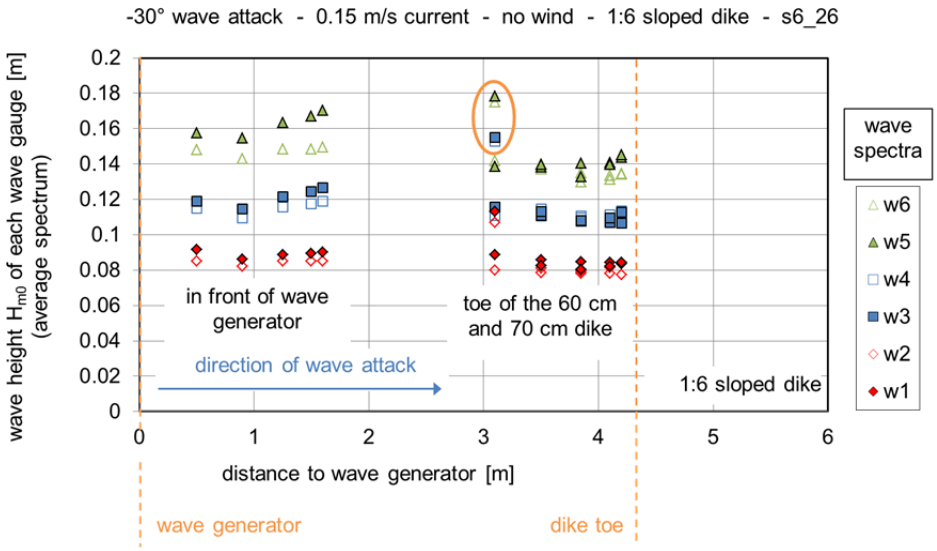

Figure 7.20 Wave heights H_{m0} - s6_26

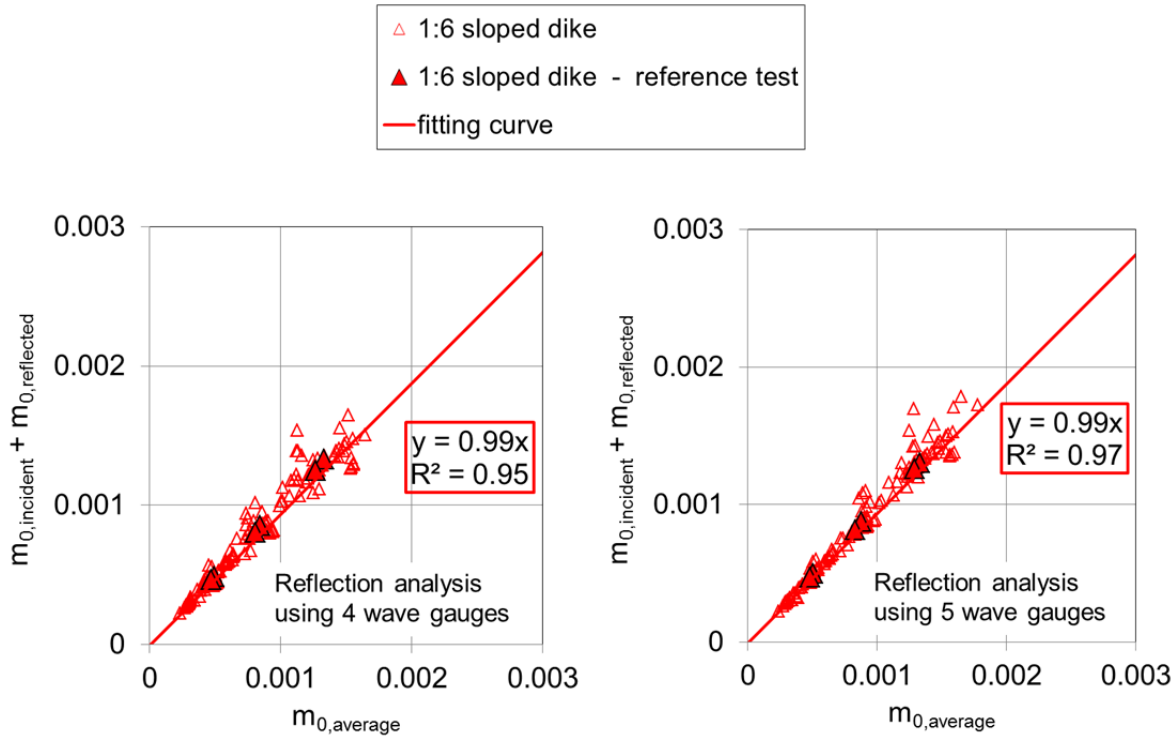

Figure 7.21 $m_{0,average}$ as a function of the sum of $m_{0,incident}$ and $m_{0,reflected}$, analysis with 4 and 5 wave gauges

7.5 Wave field parameters

The reflection analysis was performed using three and five wave gauges of each wave gauge array. The results are given in the previous section. All wave gauge arrays give similar or better results for the reflection analysis using 5 wave gauges. In spite of the higher standard deviation of the $H_{2\%}$-values from the zero-down-crossing analysis while considering all five wave gauges of each wave gauge array, the results of the reflection analysis using five wave gauges will be used for further analysis. An exception is the analysis of the wave gauge array at toe of 0.7 m high and 1:6 sloped dike. Due to the unclear signal of the first wave gauge (no. 55) the corresponding wave gauge array will be analyzed without that wave gauge. The wave parameters from the reflection analysis using only four wave gauges will be used for further analysis.

To guarantee the comparability of all tests the same wave gauges are analyzed in each test. Table 7.1 gives an overview of the wave gauges used for the reflection analysis on the 1:3 and 1:6 sloped dike. In Annex H and Annex I all analyzed data concerning the wave field are listed for the analysis on the 1:3 sloped dike and 1:6 sloped dike respectively.

Table 7.1 Wave gauges used in model tests and for analysis

dike slope	**wave gauge array…**														
	…in front of wave generator number of wave gauge distance to wave generator [m]					**…at toe of 0.6 m dike** number of wave gauge distance to wave generator [m]					**…at toe of 0.7 m dike** number of wave gauge distance to wave generator [m]				
1:3	-	-	-	-	-	14 3.90	13 4.30	12 4.65	11 4.90	10 5.00	9 3.90	8 4.30	7 4.65	6 4.90	5 5.00
1:6	9 0.50	8 0.90	7 1.25	6 1.50	5 1.60	14 3.10	13 3.50	12 3.85	11 4.10	10 4.20	55 not used	54 3.50	53 3.85	52 4.10	51 4.20

7.6 Evolution of wave height and wave period

To determine the influence of a current on wave height, wave heights in front of the wave generator and wave heights measured at the dike toe of the 0.6 m and 0.7 m high dikes were compared. The wave heights in front of the wave generator have only been measured during tests with the 1:6 sloped dike.

Figure 7.22 shows the relation between the wave height in front of the wave generator and the wave height at the dike toe $H_{m0,wave\ generator}/H_{m0,dike\ toe}$ against the absolute wave height in front of the wave generator $H_{m0,wave\ generator}$. The relation $H_{m0,dike\ toe}/H_{m0,wave\ generator}$ is 1.0 if the wave height does not change during wave propagation across the channel width. Values higher than 1.0 indicate an increasing wave height, whereas values smaller than 1.0 represent a decreasing wave height. The relation between the wave period in front of the wave generator and the wave period at the dike toe $T_{m-1,0,dike\ toe}/T_{m-1,0,wave\ generator}$ against the absolute wave period in front of the wave generator $T_{m-1,0,wave\ generator}$ is given in Figure 7.23.

No relation between the behavior of the wave height and the wave period respectively and the angle of wave attack or the longshore current could be determined. Therefor spreading of the wave height is higher than for the wave period.

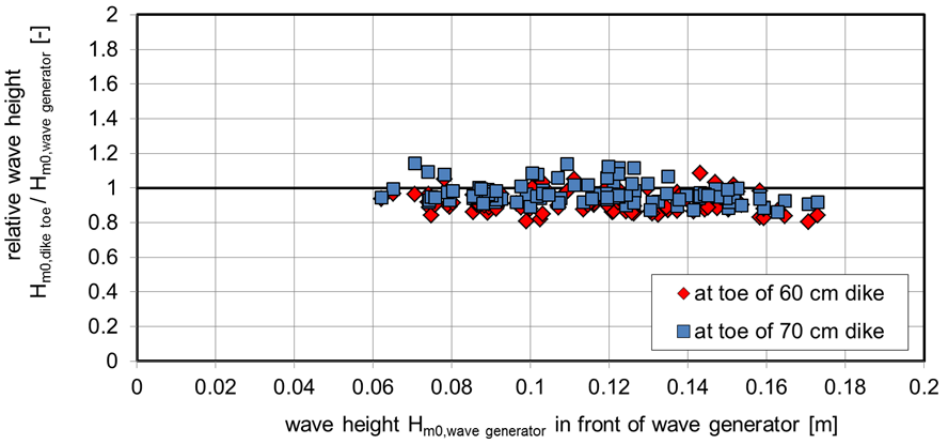

Figure 7.22 Wave height $H_{m0,wave\ generator}$, against relative wave height $H_{m0,dike\ toe}/H_{m0,wave\ generator}$ for all tests on 1:6 sloped dike

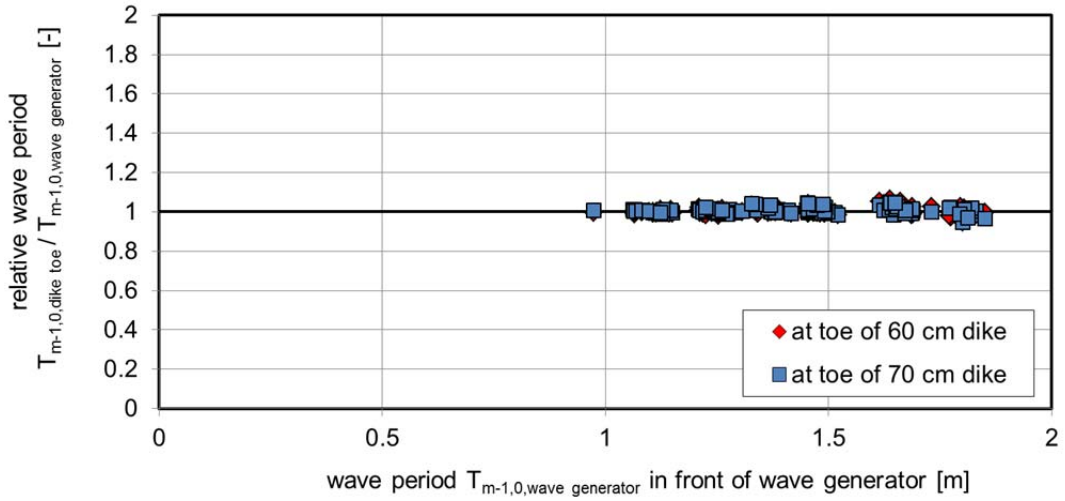

Figure 7.23 Wave period $T_{m-1,0,wave\ generator}$, against relative wave period $T_{m-1,0,dike\ toe}/T_{m-1,0,wave\ generator}$ all test on 1:6 sloped dike

8 Analysis of wave run-up and wave overtopping

8.1 Remarks

This section describes the measured wave run-up and wave overtopping analysis and how these flow processes are influenced by wind, current and oblique wave attack. The studied data set includes different combinations of only two or all influencing parameters, but can be subdivided in four main sub sets:

- perpendicular wave attack – as reference test
- oblique wave attack
- current influence on wave attack
- wind influence on wave attack

The basic set for perpendicular wave attack and the sub set for oblique wave attack are used for a first comparison of the tests to the currently applied formulae and former investigations (e. g. EUROTOP-MANUAL, 2007, OUMERACI ET AL., 2002). This is done first to validate the applied evaluation method. In addition the newly introduced variables, such as current and wind, are analyzed and compared to the basic tests.

The considered parameters are defined as following:

- wind velocity u: 5 m/s 10 m/s (1:3 sloped dike)
  4 m/s 8 m/s (1:6 sloped dike)
- current velocity v: 0.15 m/s 0.3 m/s 0.4 m/s (only 1:6 sloped dike)
- angle of wave attack β: -45° -30° -15° 0° +15° +30°

Positive angles of wave attack describe a wave propagation with the current and negative angles of wave attack describe a wave propagation against the current.

The main objectives of measurement analysis are to estimate the influence of each parameter considered (direction of wave attack, current, wind) on the wave run-up height and to determine correction factors to the commonly used empirical formulae discussed in section 5.4.

The analyzed tests considering wave run-up are listed in Annex J. All results on wave run-up and wave overtopping are summarized in Annex K (wave run-up, 1:3 sloped dike), Annex L(wave run-up, 1:6 sloped dike), Annex M (wave overtopping, 1:3 sloped dike) and Annex N (wave overtopping, 1:6 sloped dike).

8.2 Analysis on wave run-up

8.2.1 Comparison between capacitive gauge and video

Video analysis was processed regarding 10 stripes each 1/10 of the run-up board width. However data analysis does not include stripe 1 and stripe 10 because the measured values here are influenced by laterally flow processes as mentioned before. As brought up previously several regions were excluded from video analysis due to disturbing light reflection (see section 6.3.1). This is the cause that for

many videos of the FlowDike 1 test series (1:3 sloped dike) no values could be detected for stripe 4 and 5.

Figure 8.1 shows the run-up height depending on time obtained by both measurement facilities – the capacitive gauge and video camera (model test 451, s4_01a_00_w1_00_00). Data measured by video camera are represented by the two middle stripes (stripe 5 and stripe 6). Obviously there is a good agreement regarding the run-up process and the maximum values. This indicates that both measurement techniques are suitable to determine wave run-up.

A significant difference has to be acknowledged for the wave run-down. The capacitive gauge always detected a slower run-down process because the down-rushing water was decelerated by the rubber bands which assured a constant distance between the two wires and of course due to the surface tension. On the contrary the detection of run-up tongue by video analysis could not identify the very thin and almost transparent water film during the run-down process because there was no significant change in pixel brightness here. Then the next up rushing wave was identified and its run-up tongue recognized.

The data plot displays also why it was necessary to choose a crossing level higher than zero (see section 6.3.3). The measured data shows that the run-down of the wave tongue could not be sufficiently measured by capacitive gauge. After the wave tongue reaches its maximum height the water level decreases very slowly and a following smaller wave might be missed. Furthermore the measurement data for the time dependent run-up often did not reach the still water level between two up-rushing waves. With a crossing level equal to zero many wave run-up events would be missed.

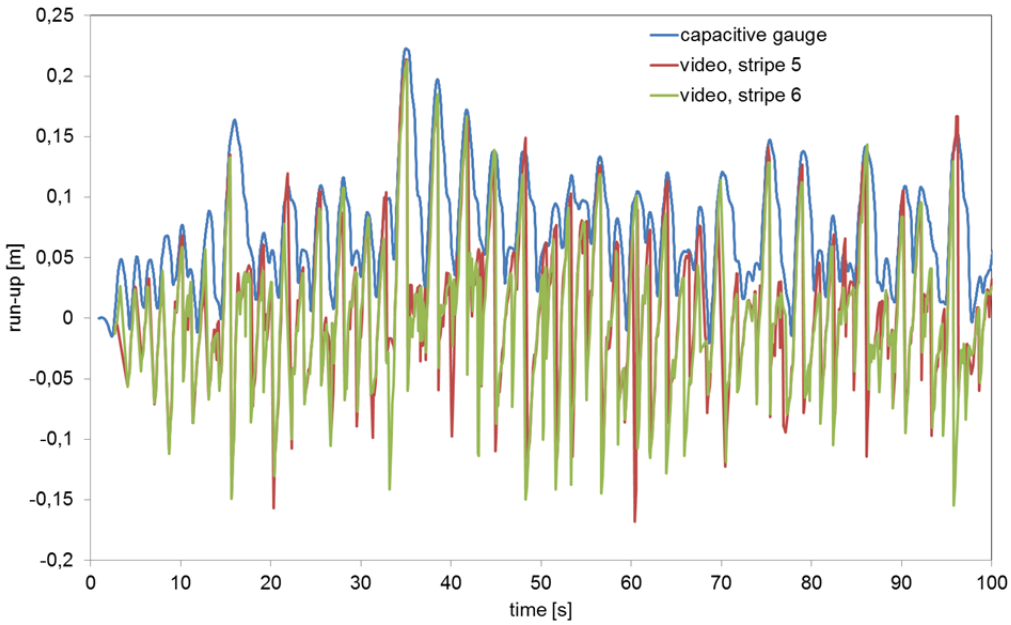

Figure 8.1 Wave run-up depending on time measured by capacitive gauge and video (stripe 5 and 6), model test s4_01a_00_w1_00_00

A comparison between calculated values of $R_{u2\%}$ for both measurement devices for all model tests is presented in Figure 8.2. The values on basis of capacitive gauge measurement are almost all lower than the maximum values obtained by video analysis considering the whole run-up board width. The best fit line shows average differences of about 9 %.

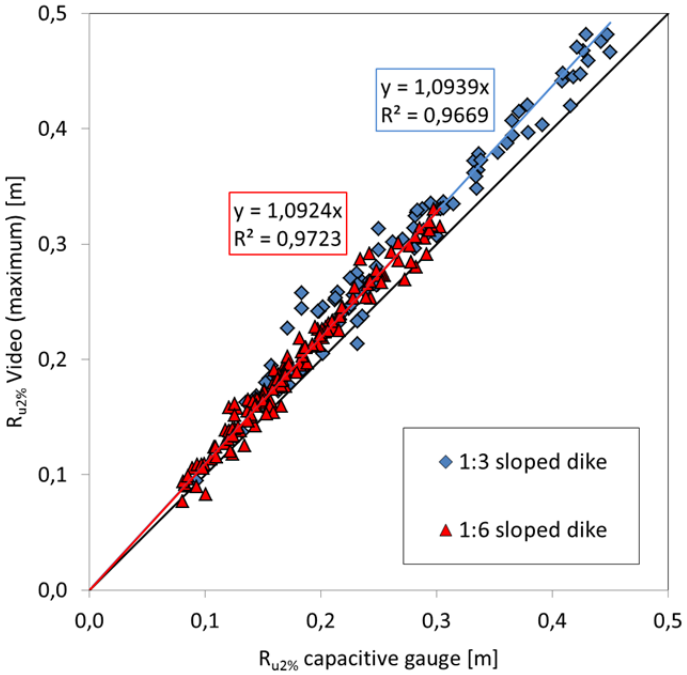

Figure 8.2 Wave run-up height $R_{u2\%}$ for all model tests: comparison between maximum values obtained by video analysis considering the whole run-up board width and measured by capacitive gauge

This is because of the different width of the capacitive gauge and the run-up board. The capacitive gauge was situated in the middle of the run-up plate and could only measure the wave run-up there although the run-up height differed across the plate width. Results from video analysis represent here the maximum run-up height independent of its location across the run-up plate width (see section 6.3.1).

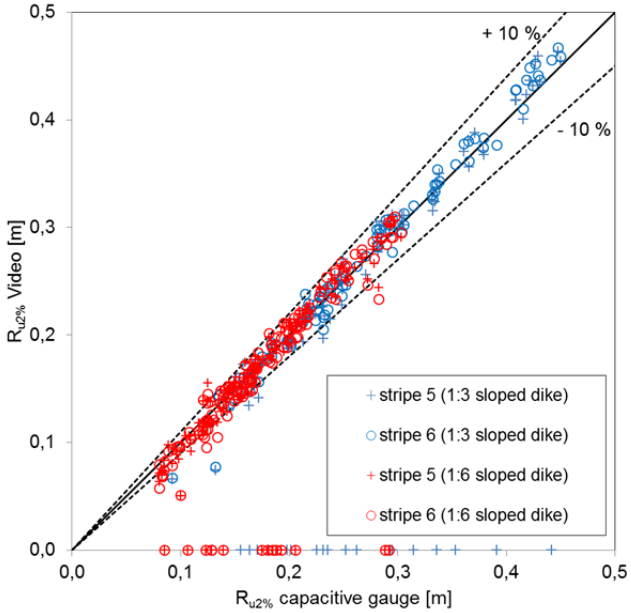

Figure 8.3 Comparison between wave run-up height $R_{u2\%}$ measured by capacitive gauge and extracted from video films for two smaller stripes around the capacitive gauge

A comparison between the result of the capacitive gauge and the two stripes around it (stripe 5 and stripe 6) should show no significant difference. This is proved in Figure 8.3. The diagram shows smaller relative differences for higher values of $R_{u2\%}$ which might indicate measurement errors.

The following discussion includes all $R_{u2\%}$-values obtained by video analysis (1:3 sloped dike: 6 stripes, 1:6 sloped dike: 8 stripes) and measured by the capacitive gauge.

8.2.2 Reference tests

To validate the overall model set-up, results from reference tests (1:3 dike as well as 1:6 dike) are compared to data of former investigations. Figure 8.4 shows calculated values of relative wave run-up height $R_{u2\%}/H_{m0}$ versus surf similarity parameter $\xi_{m-1,0}$. Two functions of former investigations have been added to the figure including equation (5.7) and (5.8) by EUROTOP-MANUAL (2007). Values for H_{m0} were obtained analyzing measurement results of the wave gauge array which was situated closer to the run-up board. All measured values for wave run-up height are plotted within the graph. This gives an impression of the general variance within the model results regarding wave run-up.

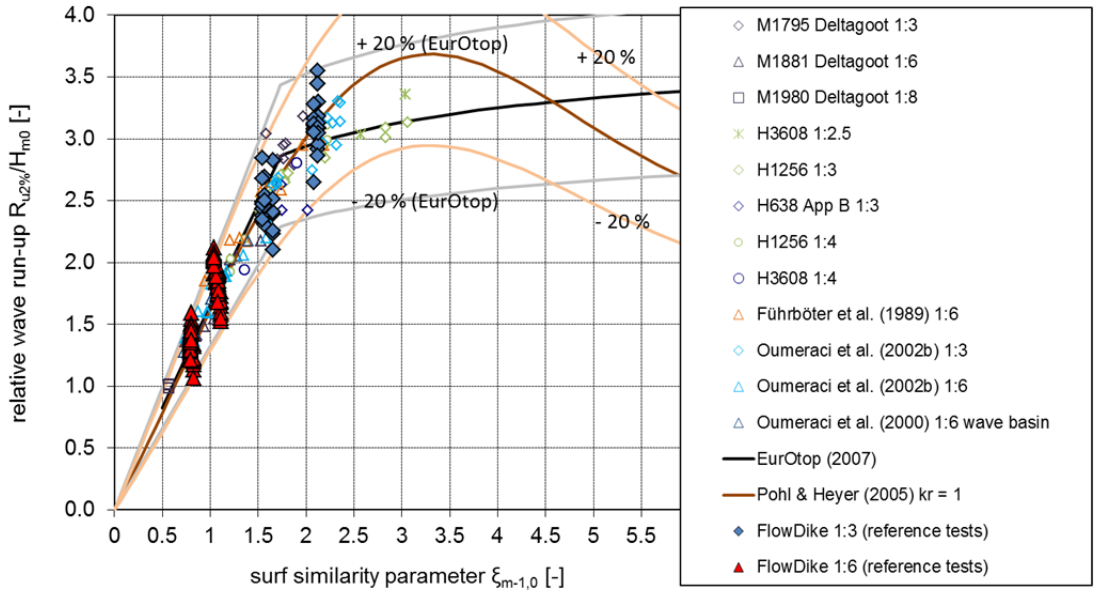

Figure 8.4. Relative wave run-up height $R_{u2\%}/H_{m0}$ versus surf similarity parameter $\xi_{m-1,0}$ – comparison between reference tests and former investigations (the identifiers M1795, M1881, M1980, H3608, H1256, H638, H1256 and H3608 refer to investigations at the wave flume at DELTARES, see EUROTOP-MANUAL, 2007)

The comparison shows a good agreement to former investigation and indicates that the general hydraulic model set-up was appropriate for the investigation planned. Surf similarity parameter $\xi_{m-1,0}$ is between 1.5 and 2.1 for the FlowDike 1 model tests (1:3 sloped dike) and between 0.8 and 1.1 for the FlowDike 2 model tests (1:6 sloped dike).

8.2.3 Influence of angle of wave attack

Figure 8.5 shows calculated values of relative wave run-up height $R_{u2\%}/H_{m0}$ versus surf similarity parameter $\xi_{m-1,0}$ for all model tests with oblique wave attack (tests without current and wind). The two functions by EUROTOP-MANUAL 2007 and by HEYER & POHL 2005 have been added to the figure. Results of the reference model tests (without current, without wind, perpendicular wave attack) were added for comparison reasons.

It is obvious that an oblique wave attack leads to smaller relative run-up heights. If the angle of wave attack is higher the resultant relative run-up height $R_{u2\%}$ is smaller. This tendency is significant for

angles of wave attack β > 40° which is indicated by an arrow in the figure. For smaller angles of wave attack the influence is not obviously.

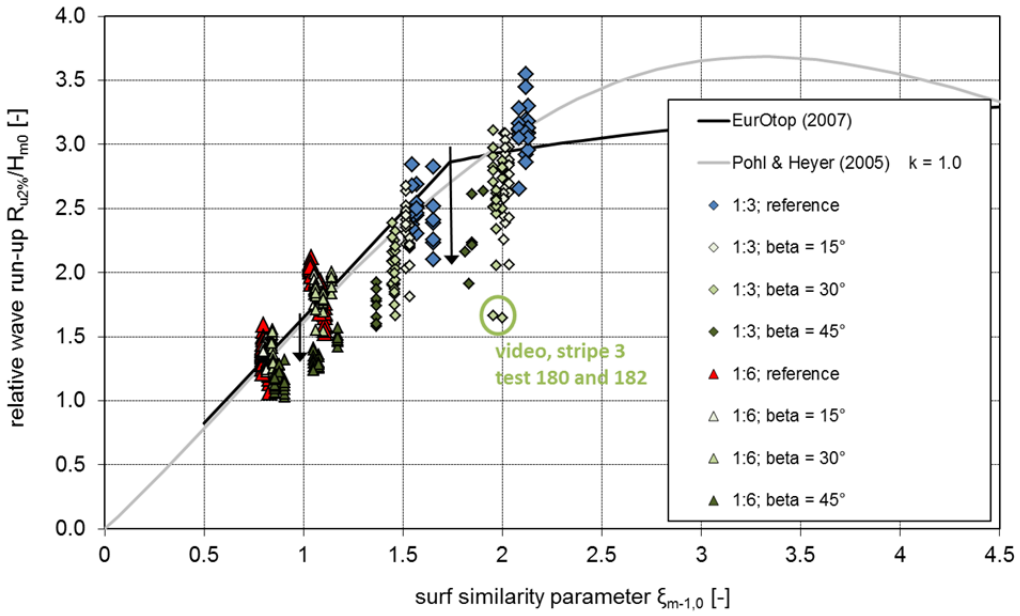

Figure 8.5 Relative run-up height $R_{u2\%}/H_{m0}$ versus surf similarity parameter $\xi_{m-1,0}$ for reference tests and tests with oblique wave attack

To analyze the influence of the angle of wave attack on run-up the ratio γ_β, is defined as follow:

$$\gamma_\beta = \frac{\left(R_{u2\%} / H_{m0}\right)_\beta}{\left(R_{u2\%} / H_{m0}\right)_{\beta=0}} \tag{8.1}$$

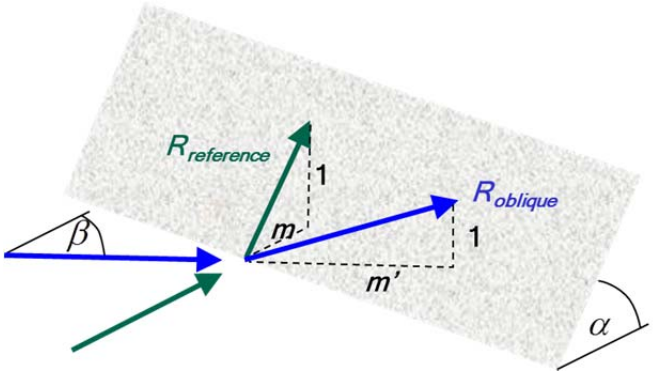

Figure 8.6 Relationship between wave run-up under perpendicular wave attack ($R_{\beta=0}$) and oblique wave attack ($R_{\beta\neq0}$).

The influence of the angle of wave attack on run-up can be described using the function (cos β) because dike slope (tan α = 1/m) for perpendicular wave attack (see Figure 8.6) and the according dike slope (tan(α') = 1/m') considering a wave attack under the angle β are related by:

$$\frac{\tan\alpha'}{\tan\alpha} = \cos\beta \tag{8.2}$$

Because the run-up is proportional to the dike slope the ratio γ_β is proportional to (cos β) too. To estimate boundary value for a function $\gamma_\beta = f(\beta)$ wave run-up on a very flat shore as well as at a

vertical wall should be discussed further. On a very flat shore ($\alpha \rightarrow 0°$) a total refraction is possible. Wave direction in case of shore parallel waves ($\beta = 90°$) would be changed and resulted in an almost perpendicular wave attack and the run-up would be equal to that in case of $\beta = 0°$ (see Figure 8.7, left side). It follows a ratio $\gamma_{\beta=90°}$ ($\alpha \rightarrow 0°$) = 1. Waves propagating in the perpendicular direction ($\beta = 90°$) of a vertical wall ($\alpha = 90°$) create a run-up R = H (see Figure 8.7, right side). If one considers a vertical wall and a wall parallel wave attack ($\beta = 0°$) the waves would be propagate along the wall and create a hypothetical run-up of R = H/2. From this it follows that $\gamma_{\beta=90°}$ ($\alpha \rightarrow 0°$) = 0.5.

A function capturing all these considerations could be:

$$\gamma_\beta = a_r \cdot \cos^2 \beta + b_r \tag{8.3}$$

The coefficients a_r and b_r depending at least on the dike slope (see Figure 8.8) with $a_r + b_r = 1$. The coefficient b_r represents the boundary value $\gamma_{\beta=90°}$. It has to be lower in the case of a steeper slope and higher in the case of a flatter slope (see Figure 8.8).

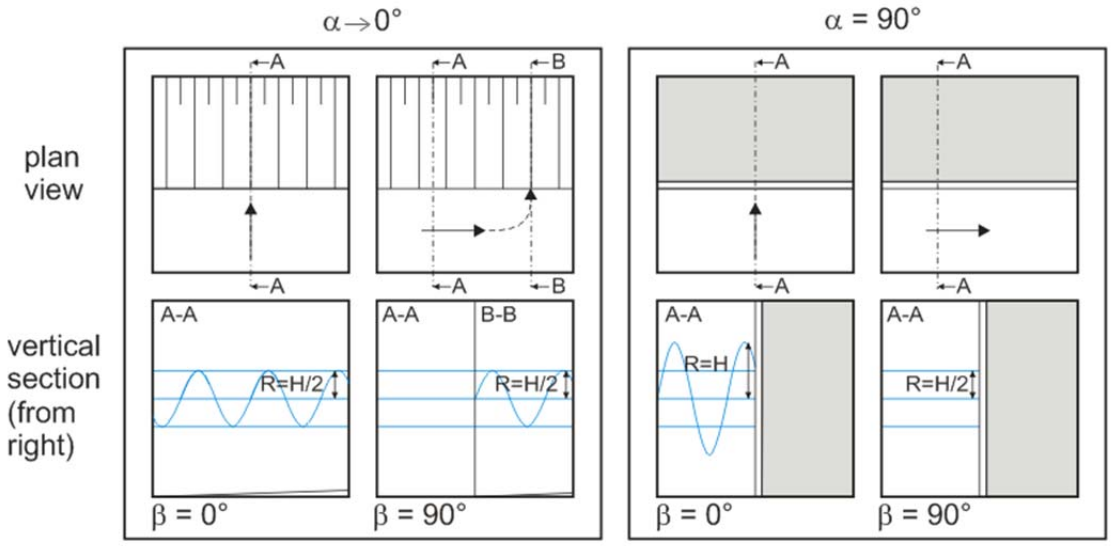

Figure 8.7 Wave run-up height: boundary values for perpendicular or parallel “run-up” und a very flat shore (left) and at a vertical wall (right)

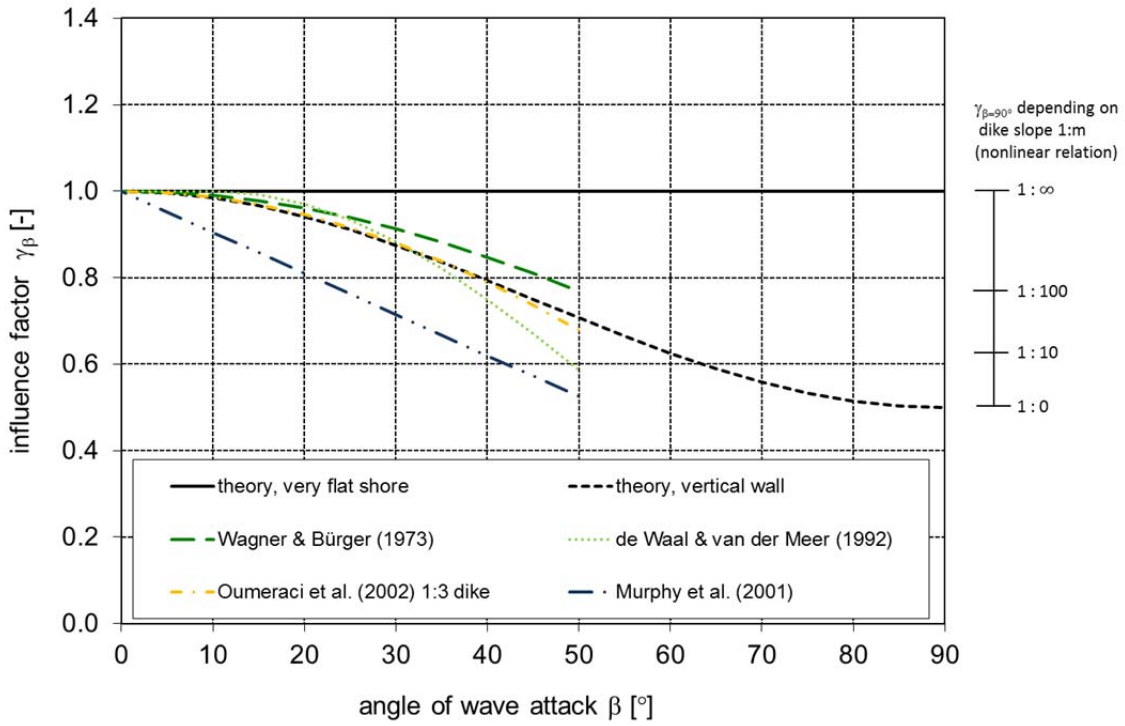

Figure 8.8 Empirical function for the influence factor γ_β in dependence on the angle of wave attack

The calculated values γ_β for all tests with oblique wave attack but without wind and without a longshore current are presented in Figure 8.9. Data includes measured values by capacitive gauge as well as extracted values from video analysis. Results from test 156 and test 445 were not considered within data analysis because they are characterized by significant differences between results from capacitive gauge and video analysis.

In general there is a decreasing tendency of γ_β with higher values of β. Only one data set (1:6 sloped dike, $\beta = 30°$) is not consistent with this tendency and was excluded from regression analysis. It has to be noticed that the measured data represent a more scattered data set.

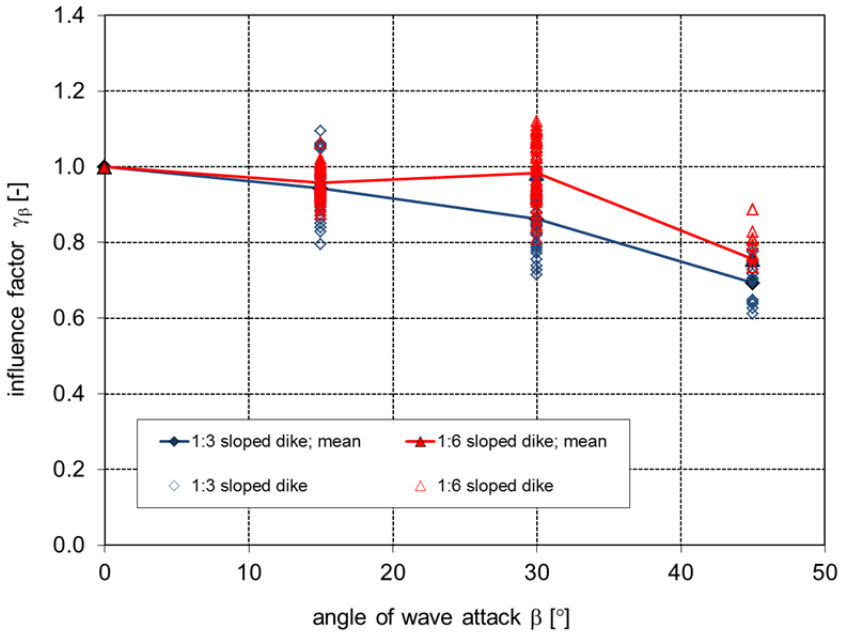

Figure 8.9 Influence factor γ_β in dependence on the angle of wave attack (tests without wind and current)

The results show good agreement with existing empirical functions (see Figure 8.11). In general it could be stated that the results fit in former investigations and could be an additional prove that the hydraulic model set-up was appropriate chosen.

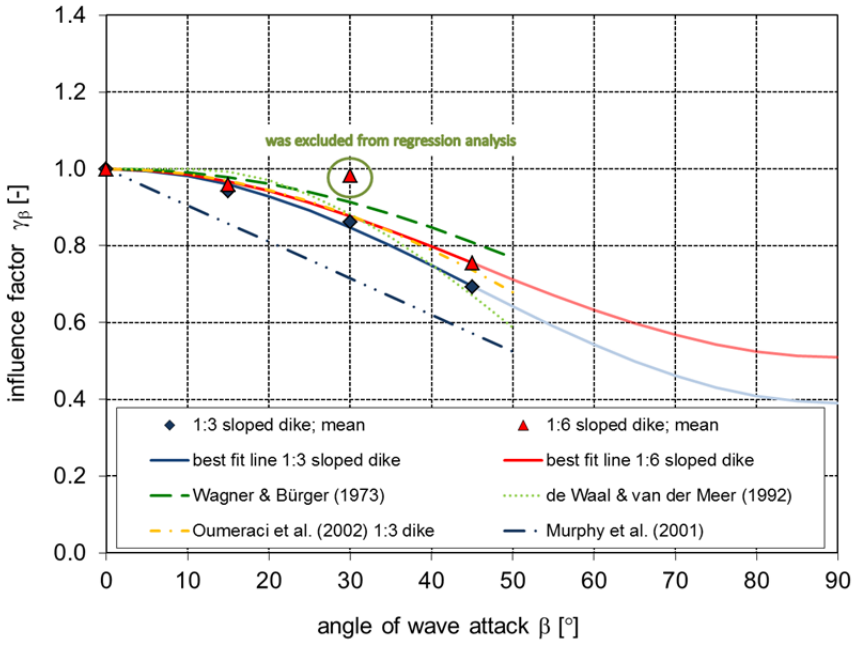

Figure 8.10 Influence factor γ_β in dependence on $\cos^2\beta$

Two equations were fitted to the results according to the form derived above:

$$\gamma_\beta = 0.61 \cdot \cos^2 \beta + 0.39 \quad (1:3 \text{ sloped dike}) \tag{8.4}$$

$$\gamma_\beta = 0.49 \cdot \cos^2 \beta + 0.51 \quad (1:6 \text{ sloped dike}) \tag{8.5}$$

The derived functions confirm the theoretical discussion above. The value $b_r = \gamma_{\beta=90°}$ is higher for the 1:6 sloped dike than for the 1:3 sloped dike. Further investigations for $\beta > 50°$ are still needed to validate the formulae above for this co-domain.

8.2.4 Influence of wind

It is commonly assumed within the literature that onshore wind has an increasing effect on wave run-up (see chapter 5.4).

Figure 8.11 displays the relative run-up height depending on surf similarity parameter for tests with wind and for reference tests. The dots cover similar regions within the diagram and no clear tendency is visible.

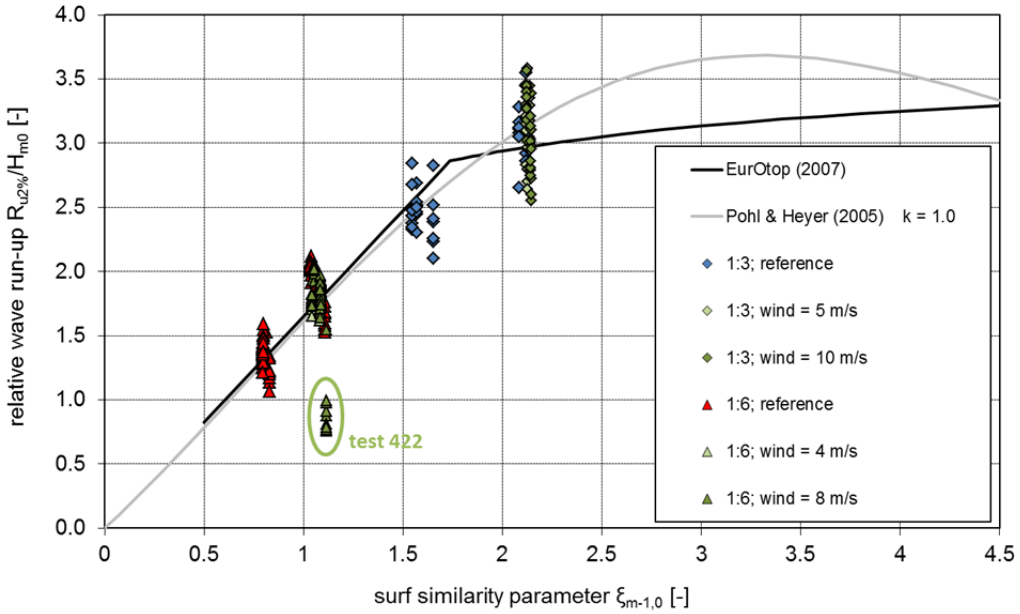

Figure 8.11 Relative run-up height $R_{u2\%}/H_{m0}$ versus surf similarity parameter $\xi_{m-1,0}$ for reference tests and tests with wind

To analyze the influence of onshore wind the ratio γ_w is defined as follow:

$$\gamma_w = \frac{\left(R_{u2\%} / H_{m0}\right)_w}{\left(R_{u2\%} / H_{m0}\right)_{w=0}} \tag{8.6}$$

The calculated factors for each test with wind, rectangular wave attack and without a current are presented in Figure 8.12. Data includes measured values by capacitive gauge as well as extracted values from video analysis.

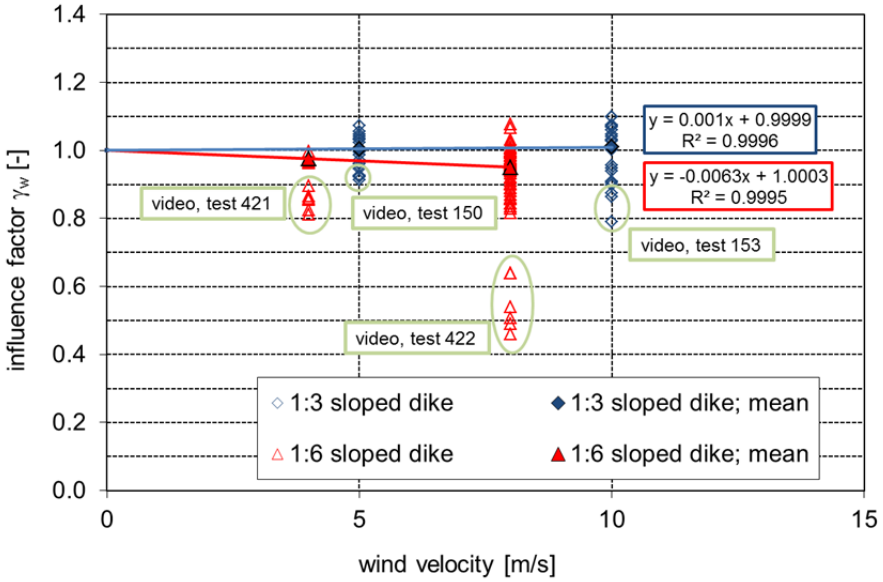

Figure 8.12 Influence factor γ_w in dependence on wind velocity (tests without current and perpendicular wave attack)

Video films for FlowDike 2 (1:6 sloped dike) and wind velocity of 4 m/s were defective as visible in the results of test 421. That's why the mean value was only calculated using data from capacitive gauge. Data extracted by video analysis for test 422 were excluded too because they did not fit with the value of the capacitive gauge and show a significant lower value of γ_w without any comprehensible reason. But it might be possible that reflections of light which occurred on the run-up board have interfered with run-up detection during video analysis. Out of the same reason test 150 and test 153 were not considered within further data analysis.

The results indicate no noteworthy increasing effect of wind on run-up as stated in the literature for wind speeds > 6 m/s to 8 m/s. On the contrary there is a very slightly decreasing effect in case of the 1:6 sloped dike. Because the presented study considered sea state the explanation of these results which are different to those from former investigations with monochromatic waves might lay herein. That the wind pushes a wave tongue up the sloped might be the case for monochromatic waves as well as sea state and would increase the wave run-up. In case of a reducing influence of downwash on the subsequent wave there might be a different effect. Because in a sea state a higher wave is in general followed by a smaller wave so that this effect may not come out so significant considering the wave run-up of higher waves in a sea state. An explanation for a decreasing effect could be that the wind induces an earlier breaking process of the waves on the dike slope and that's why the wave run-up is lower than without wind. It seems that in the case of a sea state these opposing effects balance each other.

To estimate the corresponding prototype wind speed out of model wind speed the formula presented in GONZÁLES-ECRIVÁ (2006) might be useful but very few data were used to establish it:

$$w = \frac{w_p}{c_w} \tag{8.7}$$

with w_p prototype wind speed [m/s]

c_w constant factor c_w = 1.2 to 1.8 [-]

8.2.5 Influence of current

The following ways of interaction between wave and current are possible and are stated here as hypotheses. They are focused on the change in wave height. On a first thought it seems that a current causes only a displacement of every single water drop parallel to the wave crest and no change of any wave parameter is happening, than no effect on run-up would be detectable. But if we consider in a second thought that the current causes a deflection of every water particle moving in circular paths, than every particle would move along a helix and has to travel a longer distance which would cause an additional energy loss and a lower wave run-up. If we consider a sea state we can distinguish further between its smaller and bigger waves. Particles in a smaller wave would have to move in a more stretched helix as particles in a bigger wave. As we are focused on larger waves because they cause the widely known $R_{u2\%}$ a run-up height which would be only exceeded by 2 % of the incoming waves the effect described above may be not so significant in the whole.

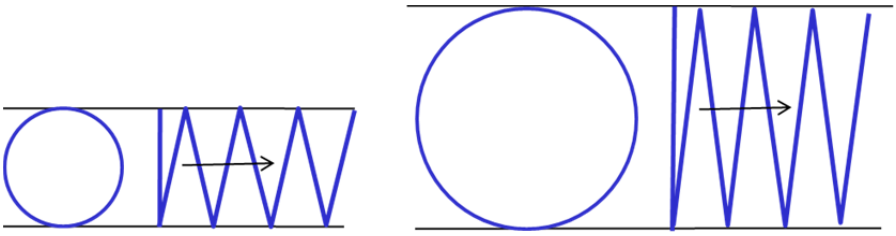

Figure 8.13 moving path of a water drop in a smaller (left) and a bigger (right) wave of a sea state

The change of the angular frequency and connected parameters as wave period and wave length can be calculated according to section 4.2.

But it is also possible that the current provides additional energy and this increases the wave energy and affects a higher wave run-up. The maximum attainable run-up height is equal to the kinetic energy head of the current ($v^2/(2g)$). A component of the current in wave direction may also increase the run-up velocity and leads to a higher run-up.

If there is a component of the current in the direction of wave propagation the wave length would increase which leads to a higher run-up according to equation (5.1) and vice versa. If the component of the current in wave direction is equal to zero (the wave propagates in a perpendicular direction relative to the current) there would be no change in wave length. But there would be still a change in the direction of wave energy transport, because some energy would propagate parallel to the wave crest.

Figure 8.14 shows the relative wave run-up versus surf similarity parameter for both reference tests and test with currents, without wind and perpendicular wave attack. Regarding this diagram it is not obvious if a higher current velocity has any effect on the wave run-up.

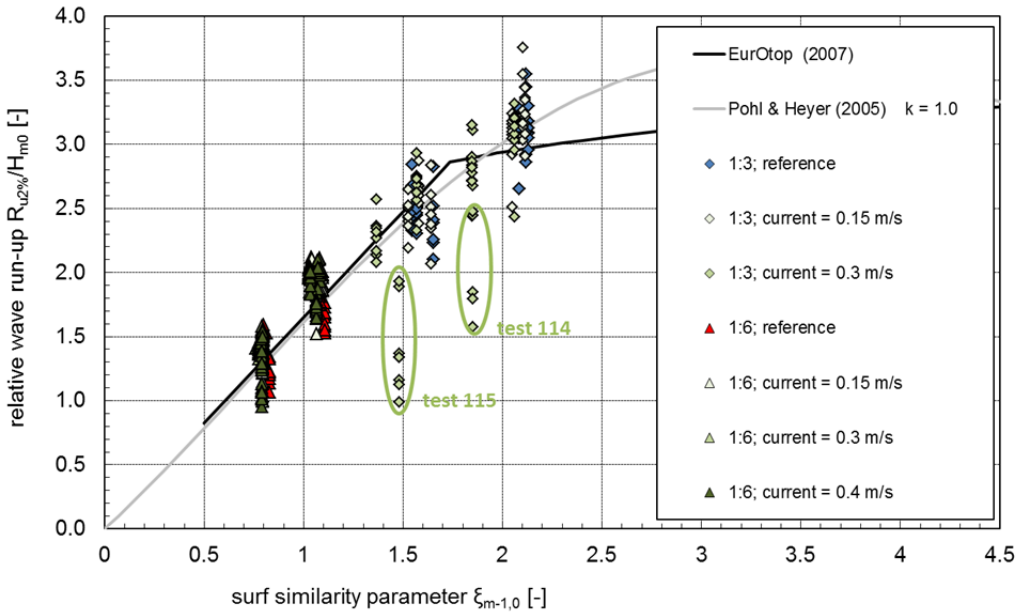

Figure 8.14 Relative run-up height $R_{u2\%}/H_{m0}$ versus surf similarity parameter$\xi_{m-1,0}$ for reference tests and tests with longshore current

To analyze the influence of current on wave run-up the ratio γ_{cu} is defined as follows:

$$\gamma_{cu} = \frac{\left(R_{u2\%} / H_{m0}\right)_{cu}}{\left(R_{u2\%} / H_{m0}\right)_{cu=0}} \tag{8.8}$$

The so calculated influence factor γ_{cu} in dependence on current velocity is presented in Figure 8.15. Green marked tests are characterized by significant differences between results from capacitive gauge and video analysis and were excluded from further analysis. The calculated values show no significant influence of current on run-up considering current velocities up to 0.4 m/s and perpendicular wave attack.

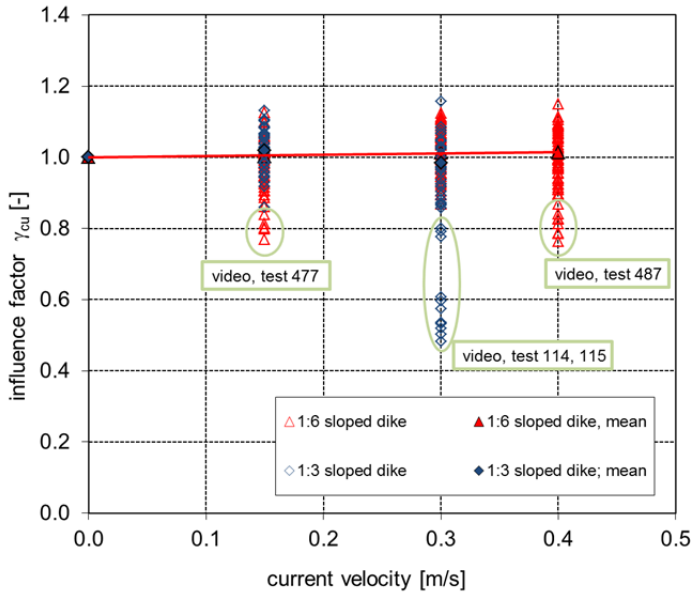

Figure 8.15 Influence factor γ_{cu} in dependence on current velocity (tests with current but without wind and perpendicular wave attack).

It seems that in case of oblique wave attack and longshore current the different and in part opposing effects mentioned above together with refraction and shoaling results in no change of run-up height.

8.2.6 Influence of current and oblique wave attack

In a second step the combined effect of oblique wave attack and a longshore current was investigated. It was described previously (chapter 4.2) that it is possible to include the change of wave parameters due to a longshore current by using the absolute wave parameters together with the angle of wave energy instead of the angle of wave attack.

But it is also possible that additional to the effect that a longshore current causes a deflection of the wave energy direction which decreases the wave run-up it increases the wave run-up velocity which would increase wave run-up. It is not obvious which effect might be dominated. It has to be considered too that all these effects will be superposed by refraction and shoaling as well.

The results of the current investigation show no obvious dependencies (Figure 8.16 and Figure 8.17) but it has to be considered that the relative wave run-up height $R_{u2\%}/H_{m0}$ is a very sensitive parameter. Here no clear advantage is obvious in using absolute wave parameters and the angle of wave energy instead of the relative wave parameters together with the angle of wave attack.

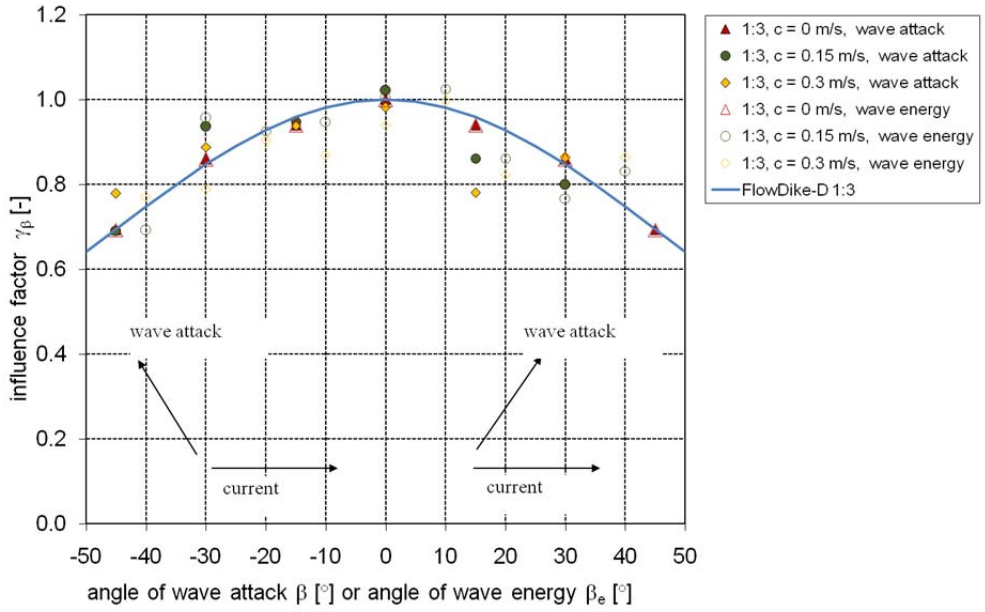

Figure 8.16 Influence factor γ_β in dependence on angle of wave attack or angle of wave energy respectively (1:3 sloped dike, tests with current and perpendicular and oblique wave attack but without wind).

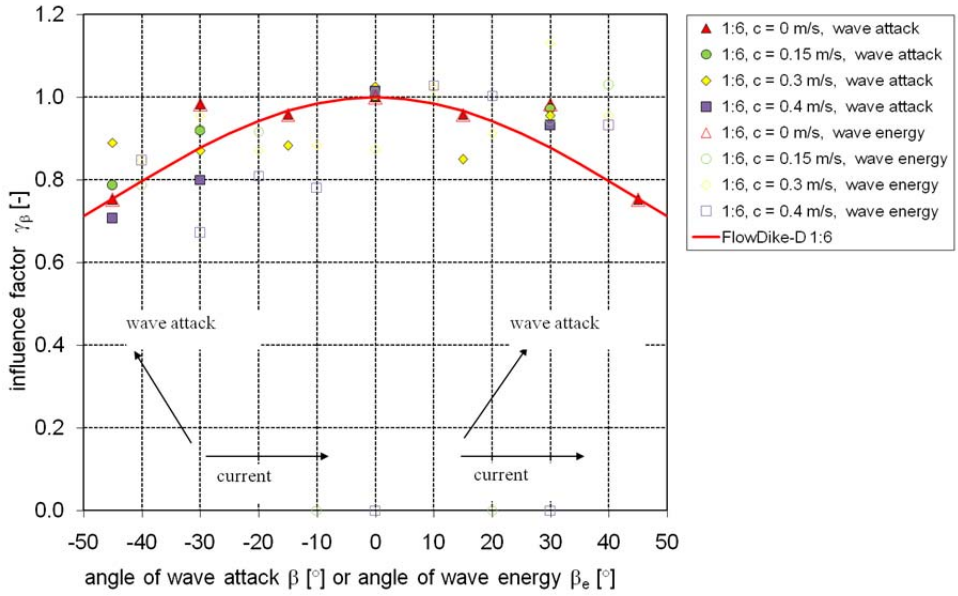

Figure 8.17 Influence factor γ_β in dependence on angle of wave attack or angle of wave energy respectively (1:6 sloped dike, tests with current and perpendicular and oblique wave attack but without wind).

8.2.7 Combination of all influence parameters

The third step within data analysis was the comparison between measured and calculated relative wave run-up. Calculation was done using the formula of EUROTOP-MANUAL (2007) together with the estimated influence factors γ_β, γ_{cu} and γ_w (see chapters 8.2.3 to 8.2.5). Results are presented in Figure 8.18 and Figure 8.19.

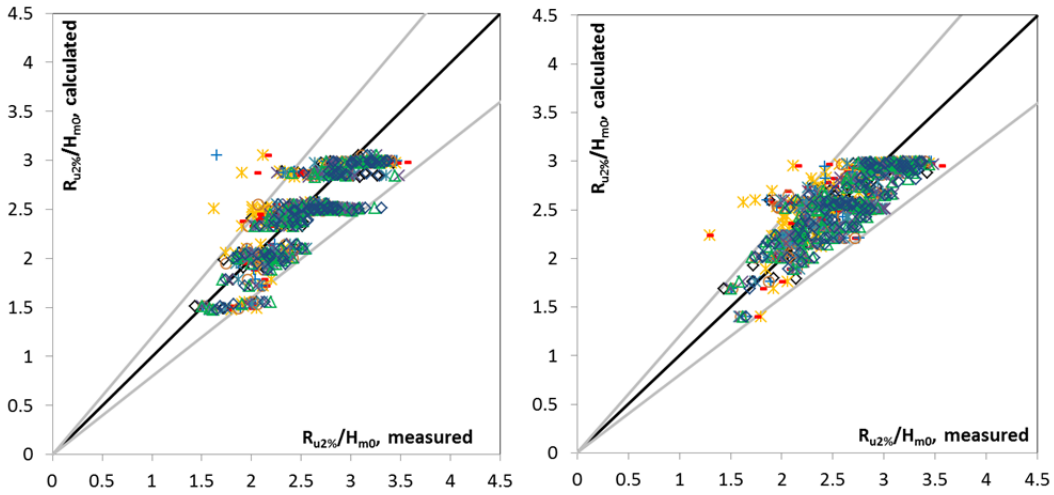

Figure 8.18 Comparison between measured and calculated relative wave run-up (1:3 sloped dike, calculation formulae (5.7) and (5.8) and the influence factors determined above; left: calculation using relative wave parameters and the angle of wave attack; right: calculation using absolute wave parameters and the angle of wave energy)

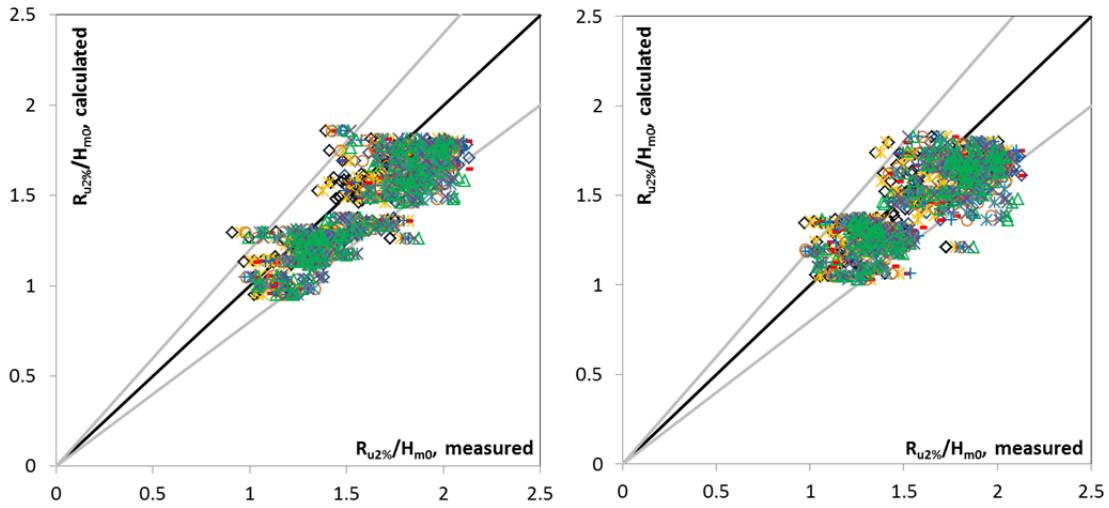

Figure 8.19 Comparison between measured and calculated relative wave run-up (1:6 sloped dike, calculation formulae (5.7) and (5.8) and the influence factors determined above; left: calculation using relative wave parameters and the angle of wave attack; right: calculation using absolute wave parameters and the angle of wave energy)

The comparison shows a good agreement between the measured and the calculated values. All pairs of values are in a range of ± 20 %. The advantage in using absolute wave parameters together with the angle of wave energy instead of relative wave parameters together with the angle of wave attack is not obvious.

8.3 Analysis on wave overtopping

8.3.1 Reference test

In a first step the results from the basic test without wind and current are compared to the existing formulae from the EUROTOP-MANUAL (2007). The results on the 1:3 sloped dike and 1:6 sloped dike are illustrated below, together with the formulae for breaking and non-breaking waves ((5.11), (5.12)) and their 95 % confidence range.

First the results for both configurations fit well within the 95 % confidence range, which are displayed as dotted lines in the graphics. Most of the points fall below the average probabilistic trend (dashed blue line) from the EUROTOP-MANUAL (2007), but validate altogether the formulae.

Interpolated trend lines were added to the following diagrams to make them easier to understand. Due to the relation between the dimensionless overtopping discharge q_* and the dimensionless freebord height R_{c*} given earlier in section 5.2.2 an exponential function was chosen.

After fitting the trend for the basic reference test, all following analysis will be done by regression analysis. For this purpose the inclinations of the slope b for each test series trend are compared to the inclination b of the reference test.

Figure 8.20 shows the results of the reference tests for the 1:3 and 1:6 sloped dikes for breaking waves. In Figure 8.21 the regression curve for non-breaking waves for the 1:3 sloped dike is given. All regression lines of the two dike slopes (dotted graph (1:3 dike) and dashed graph (1:6 dike)) are slightly lower than the recommended formula of the EUROTOP-MANUAL (2007), but still lying within the confidence range of 95 %. In the following analysis the inclination of the graph of the

corresponding reference test is used to determine the influence factors γ_i for the three different conditions:

- 1:3 dike for breaking wave conditions
- 1:6 dike for breaking wave conditions
- 1:3 dike for non-breaking wave conditions

For better comparison with the formulae from the EUROTOP-MANUAL (2007), a regression with a fixed crossing on the y-axis was applied. The fixed interception Q_0 remains the same as the y-axis crossing from formulae (5.11) and (5.12) for each breaking condition.

The following trend was found for the 1:3 sloped dike (blue line):

- breaking waves: $Q_0 = 0.067$ $b = -5.189$
- non-breaking waves: $Q_0 = 0.2$ $b = -2.677$

The 1:6 sloped dike (red line) gives the following parameter:

- breaking waves: $Q_0 = 0.067$ $b = -4.779$

In each case the results follow an average trend, which is just a bit lower than the stated equation from the EUROTOP-MANUAL (2007). Concluding for the analysis on wind, current and oblique wave attack, the crossing with the y-axis of the basic reference test can remain the same as in the formulae from EUROTOP-MANUAL (2007). The inclination of the slope b will influence the designated comparison of the results, as it is used to determine the influence of each variable within a parametric study.

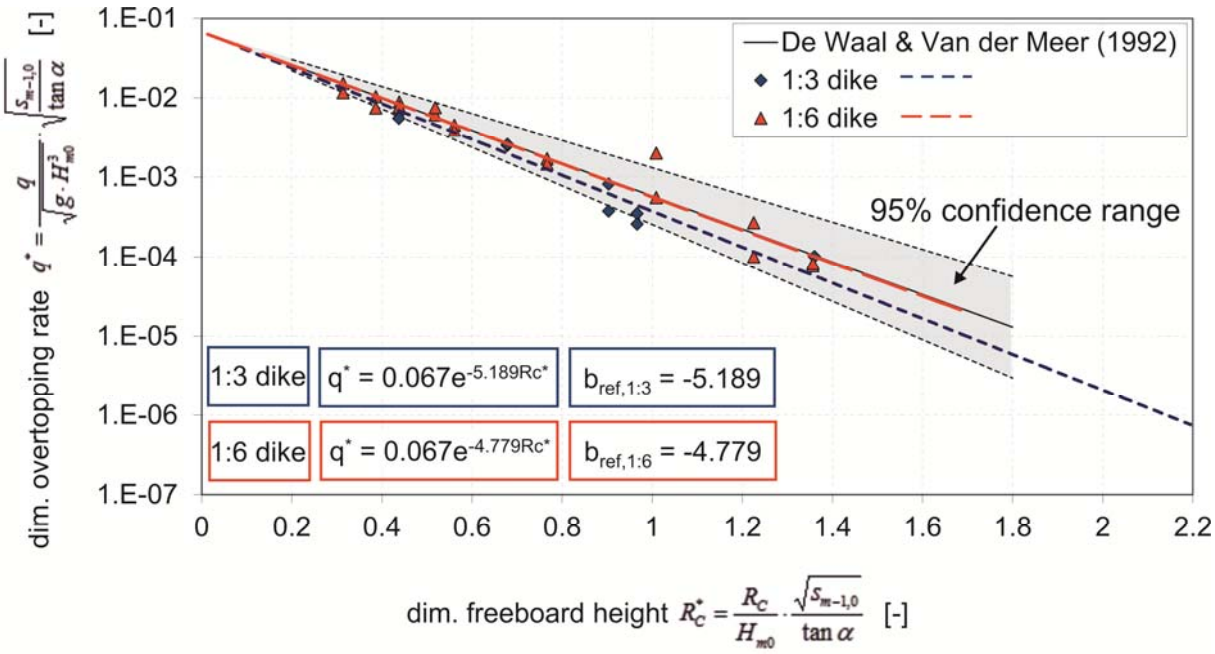

Figure 8.20 Dimensionless overtopping rate - reference tests for breaking wave conditions (1:3 dike, 1:6 dike)

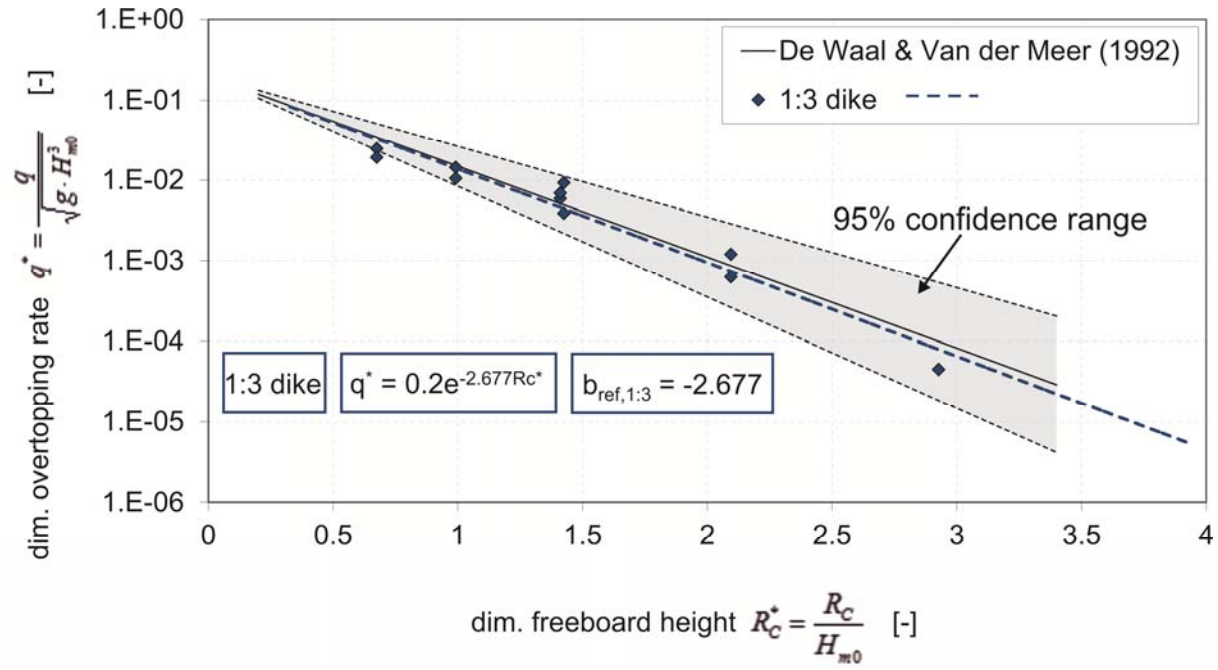

Figure 8.21 Dimensionless overtopping rate - reference test for non-breaking wave conditions (1:3 sloped dike)

Summarizing the first conclusions drawn in this section, it can be stated that:

- The results validate well the theory applied in EUROTOP-MANUAL (2007).
- The overtopping formula underestimates slightly the results found in FlowDike 1, but fits those of FlowDike 2 well.
- The trend lines with fixed interception show an acceptable accuracy.
- The basic trend lines used for regression analysis of the following parametric set can be fixed on the y-axis to the interception values of formulae (5.11) and (5.12).
- Between FlowDike 1 and FlowDike 2 a shift of the results has remained. This variance was about 8 % referring to the slope inclinations ($b_{1:6}/b_{1:3}$) = (-4.779/-5.189) = 92%.

8.3.2 Influence of wave spectra

Figure 8.22 shows the results of former investigations on mostly 1:6 smooth sloped dikes. Most of the listed tests were performed during the German research project “Loading of the inner slope of sea dikes by wave overtopping” (BMBF KIS 009) where the investigation of different wave spectra was part of it. Also the tests results during the project “Influence of oblique wave attack on wave run-up and wave overtopping – 3D model tests at NRC/Canada with long and short crested Waves –“ are included. In the left graph the data points of all tests are given. The corresponding regression curves are given in the right graph. It can be seen that the results for the double peak spectra and the TMA spectra is a bit smoother than the regression curve of FlowDike 1 and FlowDike 2 (1:3 and 1:6 sloped dike) and the sea state test.

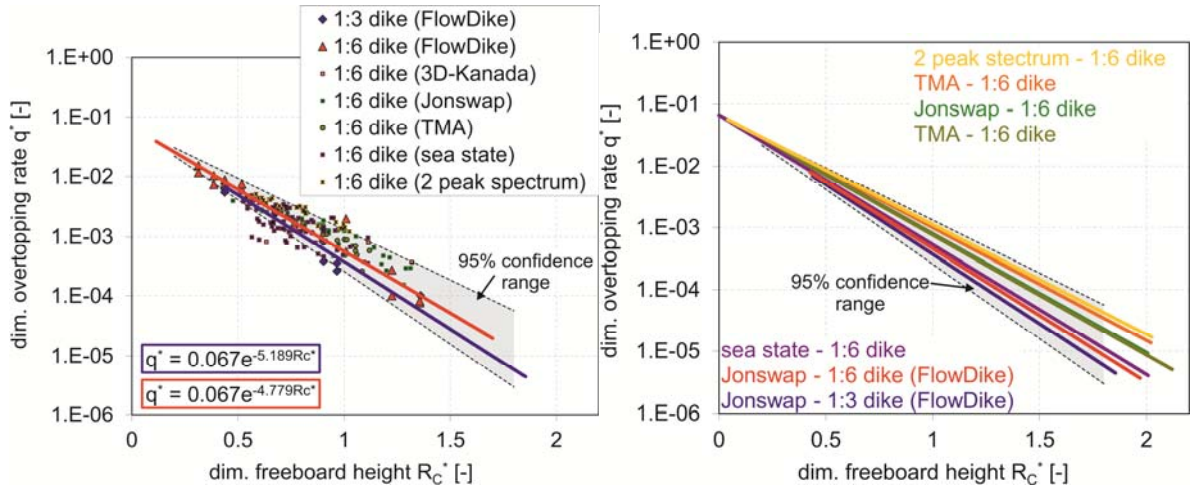

Figure 8.22 Influence of wave spectra on wave overtopping; Comparison of FlowDike 1 and FlowDike 2 results with former investigations by OUMERACI ET AL. (2002)

8.3.3 Influence of oblique wave attack without current

Oblique wave attack has been investigated before, so this section will only be an adaptation and verification. This is done with regard to the following analyses, which will consider the combined effects of obliqueness, currents and wind.

In the following figures (Figure 8.23 to Figure 8.25) all test results for oblique wave attacks are given. The trend lines have been determined with fixed interception for each angle of wave attack.

Again the data points lay very well around their exponential regression. Only the points for non-breaking waves with -15° oblique waves seam to scatter too much (cf. Figure 8.25). There is an obvious trend in both graphs, where the increase of obliqueness results in a reduction of overtopping. For the larger angles the reduction increases, this means between 0° and 15° the reduction is lower than between 30° and 45°.

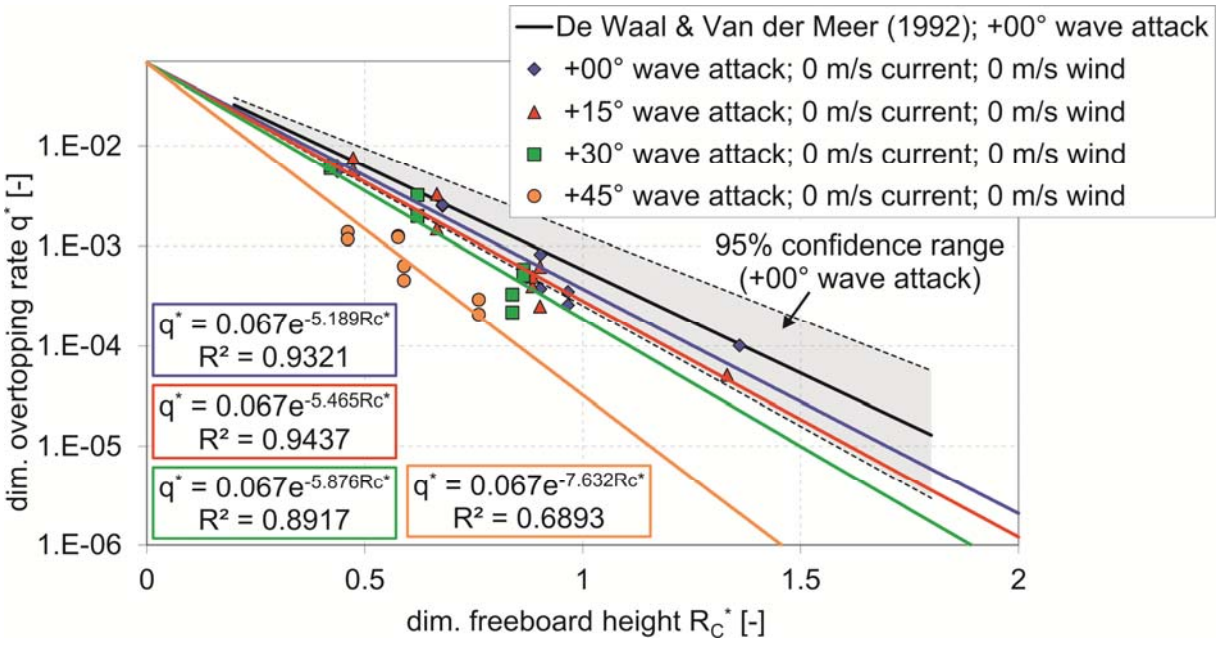

Figure 8.23 Influence of oblique wave attack on wave overtopping; 1:3 sloped dike (breaking conditions)

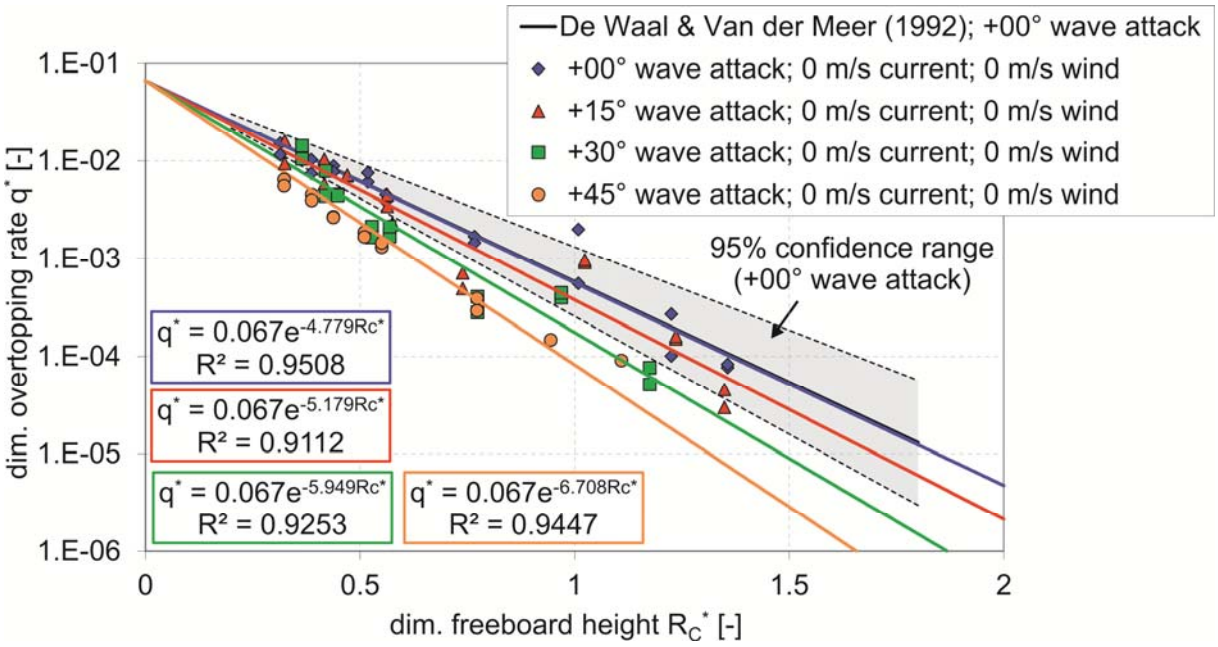

Figure 8.24 Influence of oblique wave attack on wave overtopping; 1:6 sloped dike (breaking conditions)

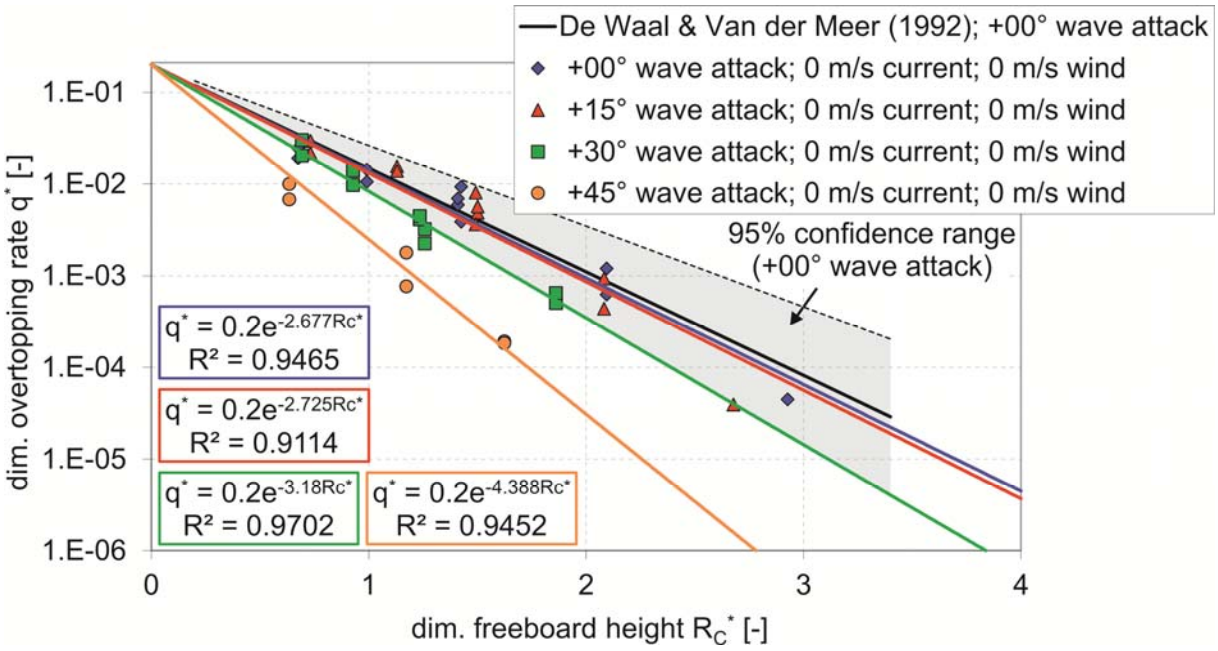

Figure 8.25 Influence of oblique wave attack on wave overtopping; 1:3 sloped dike (non-breaking conditions)

On the 1:6 sloped dike the trend lines and results for oblique wave attack for breaking conditions are illustrated in Figure 8.24. A similar effect is obvious. The increase in obliqueness results in the reduction of overtopping, but this time the reduction, especially between 30° and 45°, is not as large as for the 1:3 sloped dike. It was mentioned before that small overtopping amounts were expected and also recognized during testing due to the slope inclination. An explanation for less difference in the overtopping graphs for FlowDike 2 could be as well the smoother slope of the dike that leads to early breaking on the dike.

At a closer look one finds that the trend line slope b shows for all different angles of wave attack a shift between the 1:3 slope and the 1:6 slope. The shift was already perceived for the perpendicular waves (section 8.3.1) and will stay the same through the whole analysis (Table 8.1).

Table 8.1 Inclinations of the slopes $b_{1:3}$ and $b_{1:6}$oftests without current and wind (cf. Figure 8.23 to Figure 8.24)

dike slope	wave conditions	wave attack			
		0°	15°	30°	45°
1:3	breaking waves	-5.189	-5.465	-5.876	-7.632
1:3	non-breaking waves	-2.677	-2.725	-3.180	-4.388
1:6	breaking waves	-4.779	-5.179	-5.949	-6.708

Statistical spread of tests

The slopes of the trend lines b (cf. figures above) are determined using the regression formula of Microsoft Excel 2010. To determine the statistical spreading of these values b a slope b_i was determined for every measured value separately. The procedure is clarified in Figure 8.29 while b_i can by also calculated with

$$b_i = \frac{\ln\left(\frac{q_*}{a}\right)}{R_{c*}} \quad [-] \tag{8.9}$$

with q_* dimensionless overtopping rate [-]

a regression coefficient with $a = 0.067$ for breaking conditions and $b = 0.2$ for non-breaking conditions [-]

R_{c*} dimensionless freeboard height [-]

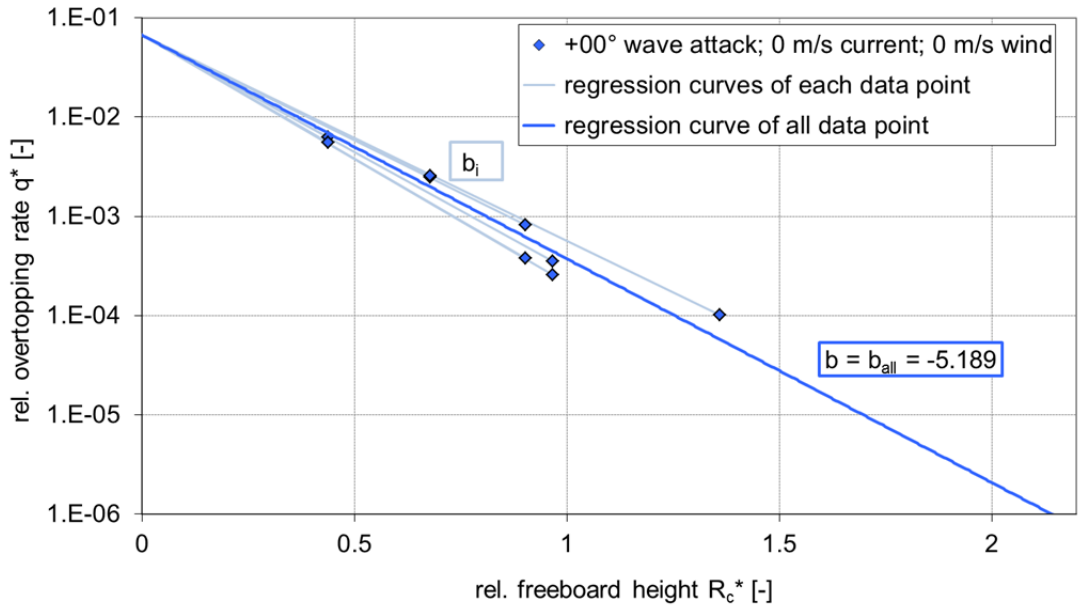

Figure 8.26 Determination of the slopes of the graphs for each data point b_i and the slope of the graph considering all data points $b_{all} = b$ exemplary for the reference test on the 1:3 sloped dike (breaking conditions)

For each data point i and its slope of the graph b_i, an influence factor γ_i is determined separately for each data point and defined by the following formula:

$$\gamma_i = \frac{b_i}{b_{all,0°}} \quad [-] \tag{8.10}$$

Like given in Table 8.1 the parameter $b_{all,0°}$ are determined as follows:

- 1:3 sloped dike, breaking waves: $b_{all,0°} = -5.189$
- 1:3 sloped dike, non-breaking waves: $b_{all,0°} = -2.677$
- 1:3 sloped dike, breaking waves: $b_{all,0°} = -4.779$

These influence factors are plotted in Figure 8.27 to Figure 8.28 against the angle of wave attack.

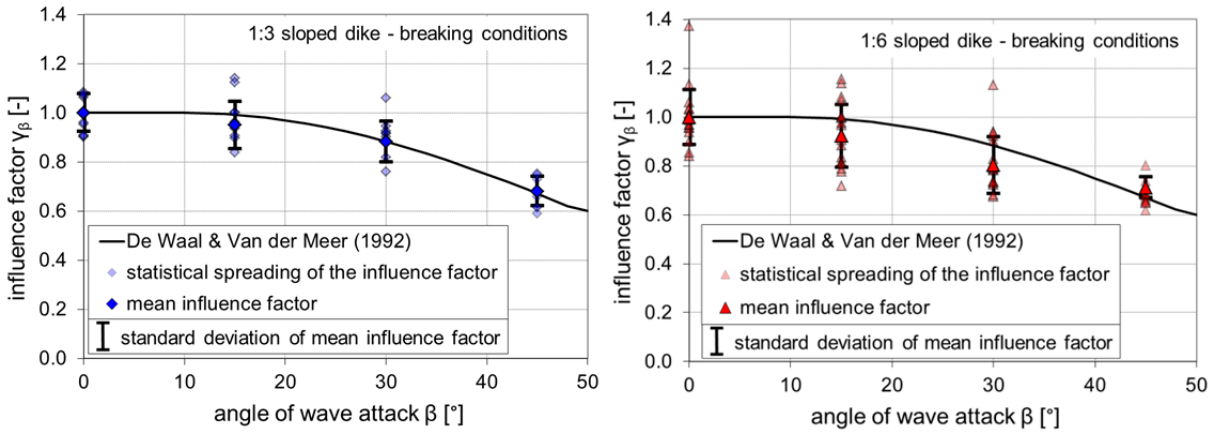

Figure 8.27 Influence of oblique wave attack on wave overtopping: statistical spreading of tests with oblique wave attack; breaking conditions (left: 1:3 sloped dike; right: 1:6 sloped dike)

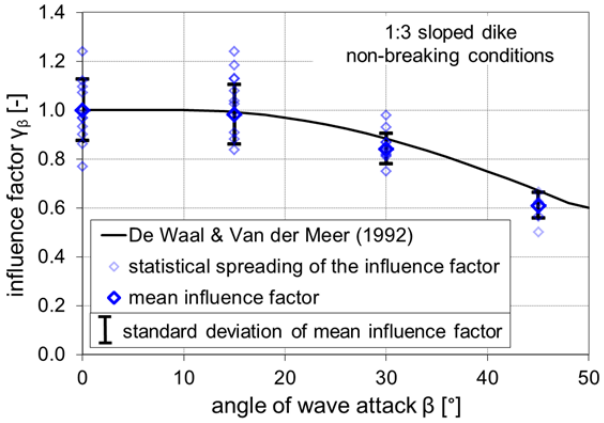

Figure 8.28 Influence of oblique wave attack on wave overtopping: statistical spreading of tests with oblique wave attack; 1:3 sloped dike (non-breaking wave conditions)

Comparison with former investigations

Influence factors for wave overtopping for obliqueness γ_β can be determined by comparing the exponential coefficients b_β for normal wave attack ($\beta = 0$) and oblique wave attack ($\beta \neq 0$):

$$\gamma_i = \frac{b_\beta}{b_{\beta=0°}} \tag{8.11}$$

The results of FlowDike 1 and FlowDike 2 validate well the trend of the former results like DE WAAL & VAN DER MEER (1992) (cf. Figure 8.29). Most data points fall a little bit below the regression line. The description of the formulae given by the other authors is shown in section 5.3 in more detail.

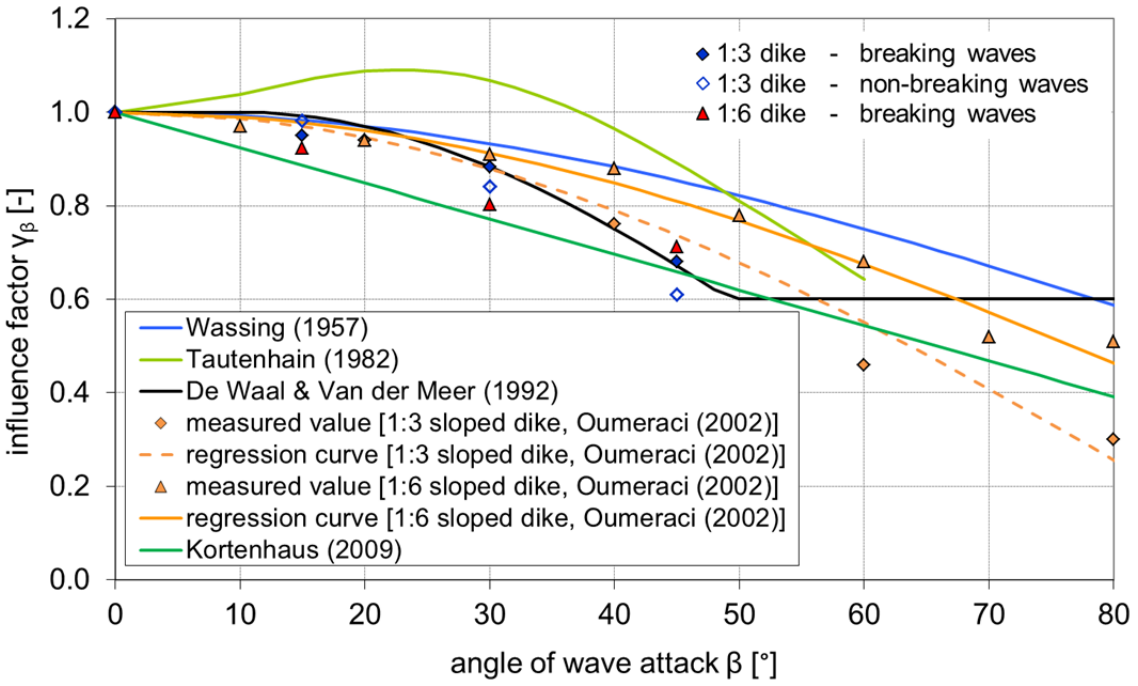

Figure 8.29 Comparison of influence factors for obliqueness – FlowDike 1 and FlowDike 2 (1:3 and 1:6 sloped dike) with former investigations

8.3.4 Influence of current

To determine the influence of the longshore current, the influence factors γ_{cu} was introduced to take the influence of current v_x into account:

$$\gamma_{cu} = \frac{b_{cu}}{b_{cu=0}} \tag{8.12}$$

This influence factor is defined for tests with perpendicular wave attack and without wind. Figure 8.30 gives these influence factors plotted against the current velocity for breaking and non-breaking conditions of each dike. The influence factors differ between 0.965 and 1.025, with the exception of the test on the 1:3 sloped dike under non-breaking wave conditions with a current velocity of 0.3 m/s.

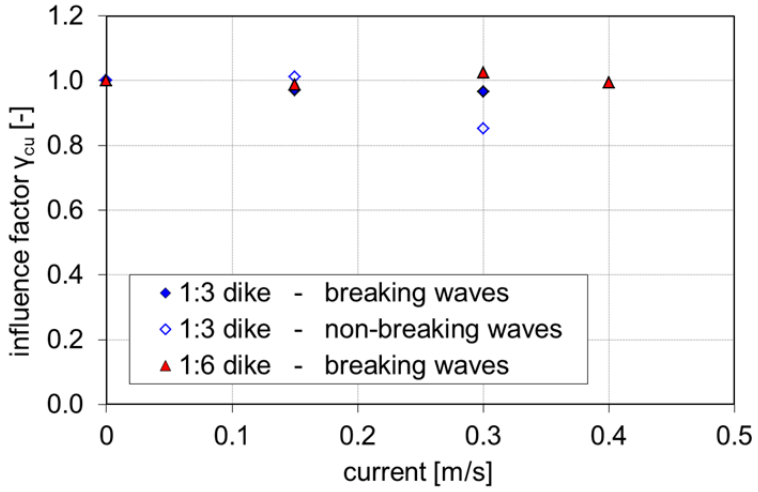

Figure 8.30 Influence of the current on wave overtopping, angle of wave attack β=0°, no wind

These influence factors and their statistical spreading against the current are plotted in Figure 8.31 and Figure 8.32.

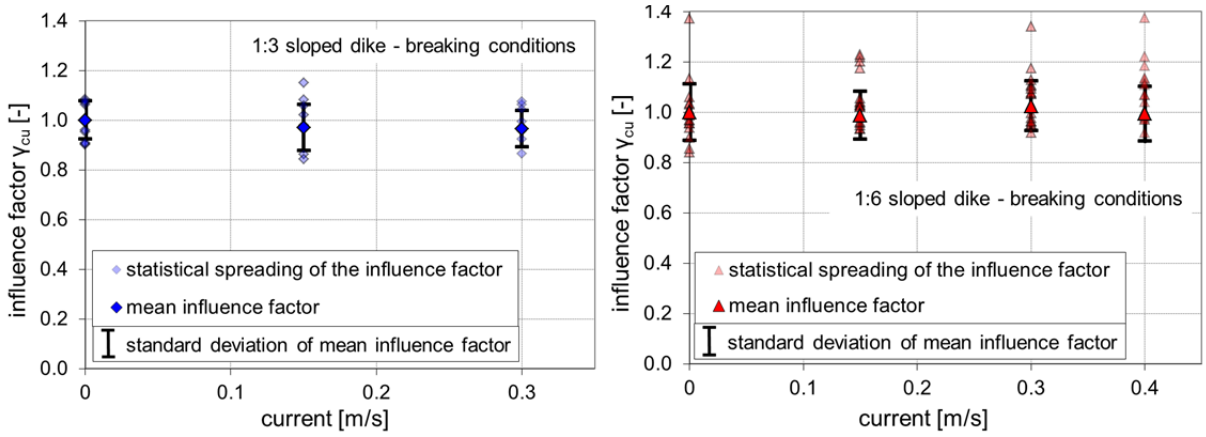

Figure 8.31 Influence of the current on wave overtopping: statistical spreading of tests with current, breaking conditions (left: 1:3 sloped dike; right: 1:6 sloped dike)

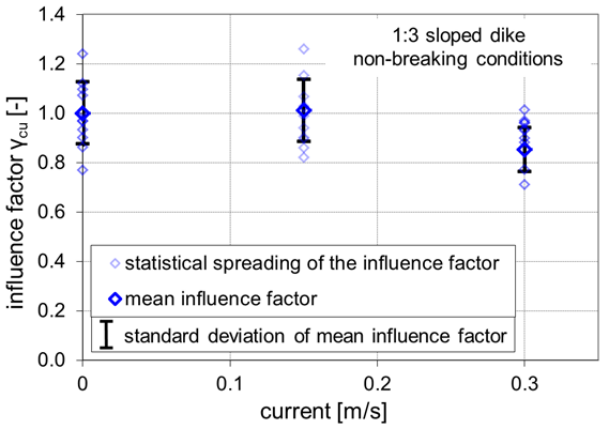

Figure 8.32 Influence of the current on wave overtopping: statistical spreading of tests with current; 1:3 sloped dike (non-breaking wave conditions)

8.3.5 Influence of wind·

From the test program it can be seen that the test series on wind contain merely the wave spectra w1, w3 and w5 with a lower steepness than the wave spectra w2, w4 and w6. The steepness is a limiting factor for the surf similarity parameter, which is a input variable in the overtopping formulae. Due to this the generated waves for wind tests give only results for non-breaking conditions during FlowDike 1. For FlowDike 2 the influence of the slope was governing and still only breaking waves occurred. Another difference between FlowDike 1 and FlowDike 2 is the missing wind tests for u = 4 m/s, only two tests on this wind speed exist.

Though the effect in overtopping could be measured the detected events marked as points in the graphs show almost no influence for small and high overtopping events for the 1:3 sloped dike (cf. Figure 8.33, left; lying nearly on the points of the reference test and in the 95 % confidence range of DE WAAL & VAN DER MEER (1992)). This do not correlate to the statement by WARD ET AL. (1996) and DE WAAL ET AL. (1996) that for smaller overtopping amounts a small increasing trend for the average overtopping can be established while no influence in noticeable for higher overtopping rates.

For FlowDike 2 the effect of increasing average overtopping amounts for the smaller wave spectra, such as w1 can be stated again. The first data points for high waves in the graph match again the points from the reference test. The regression curves are nearly the same, so that no influence of wind is recognizable (cf. Figure 8.33, right).

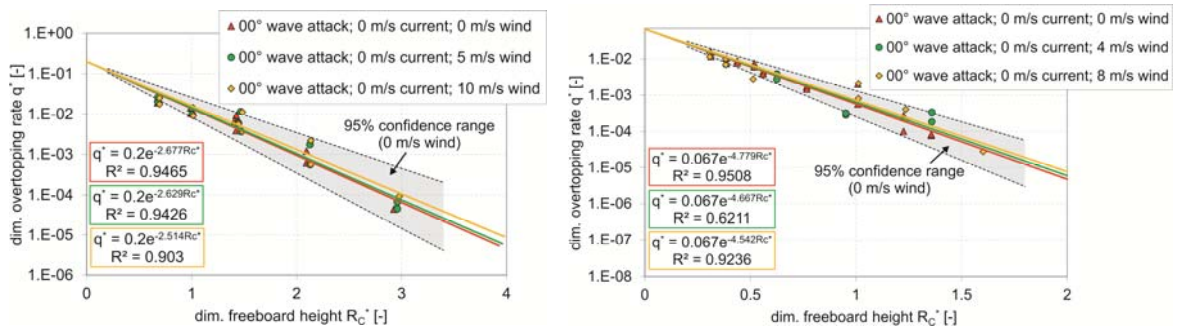

Figure 8.33 Wind influence on wave overtopping; left: 1:3 sloped dike - FlowDike 1; 1:6 sloped dike - FlowDike 2

The influence factors and their statistical spreading are plotted in Figure 8.34 against the wind.

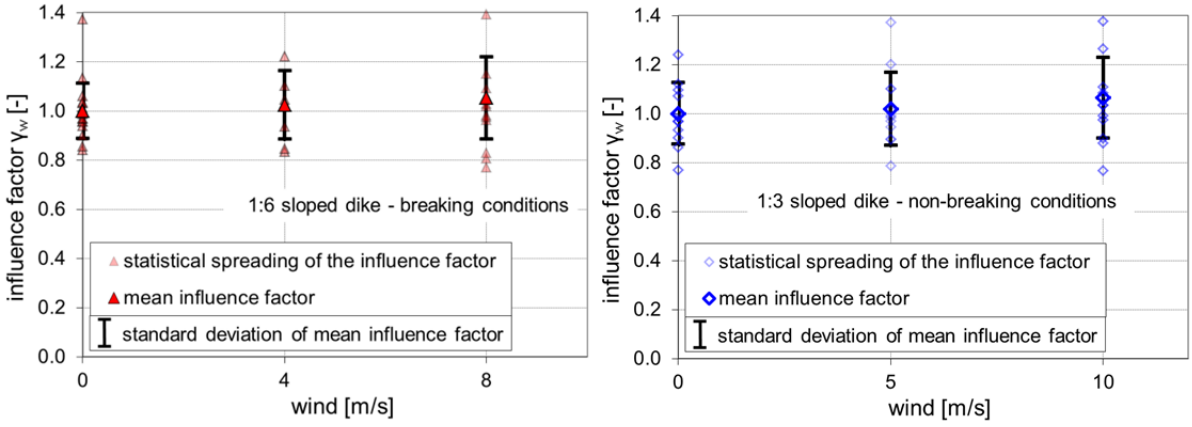

Figure 8.34 Statistical spreading of tests with wind; left: 1:6 sloped dike (breaking conditions); right: 1:3 sloped dike (non-breaking conditions)

8.3.6 Influence of oblique wave attack and current

To present the results of oblique wave attack and current on wave overtopping a distinction has to be done between the results for the 1:3 sloped dike for breaking and non-breaking waves (cf. Figure 8.36) and the results for the breaking waves on the 1:6 sloped dike (cf. Figure 8.37). In the following the results are presented for different combinations of the angle of wave attack and the angle of wave energy respectively the absolute and relative wave parameters (cf. Figure 8.35):

- angle of wave attack and absolute wave parameters
- angle of wave attack and relative wave parameters
- angle of wave energy and absolute wave parameters

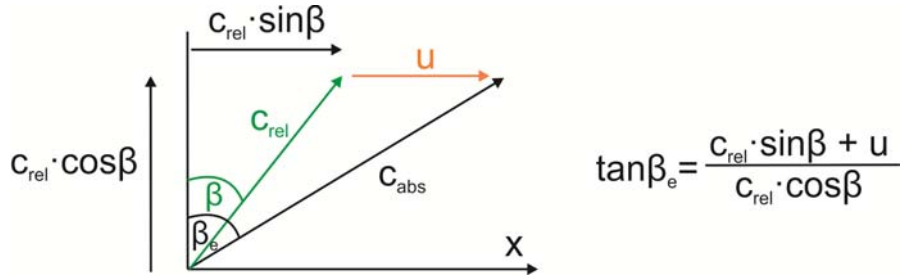

Figure 8.35 Relationship of the angle of wave attack, angle of wave energy, relative group velocity and absolute group velocity (cf. Figure 4.2)

Angle of wave attack and absolute wave parameters

In a first step, a characteristic factor was applied to determine the influence of a combination of oblique waves and longshore current. The absolute wave parameters are used. The triangles show the influence factors for tests without current. An increase of the influence factor for increasing current velocity, shown by the circles (0.15 m/s), diamonds (0.30 m/s) and squares (0.40 m/s only 1:6 dike), is noticeable for breaking wave conditions. For non-breaking wave conditions (1:3 sloped dike) the influence factor increases for angles of wave attack of -45°, -30° and +15° and decreases for angles of wave attack of -15° and +30°. For non-breaking waves the influence factor of the tests under perpendicular wave attack and with a current of 0.30 m/s is quite smaller than with no current or a current of 0.15 m/s.

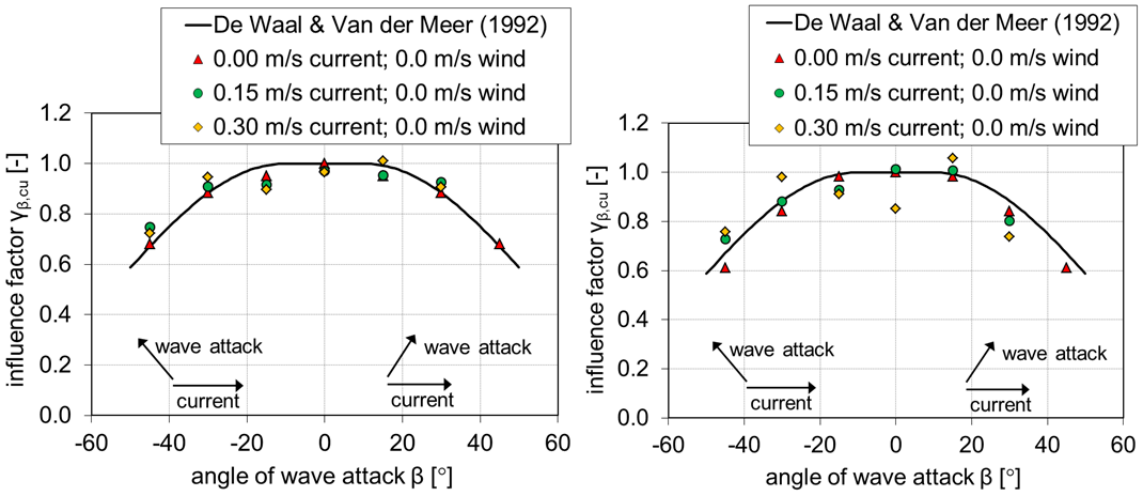

Figure 8.36 Current influence on wave overtopping, 1:3 sloped dike, left: breaking waves; right: non-breaking waves

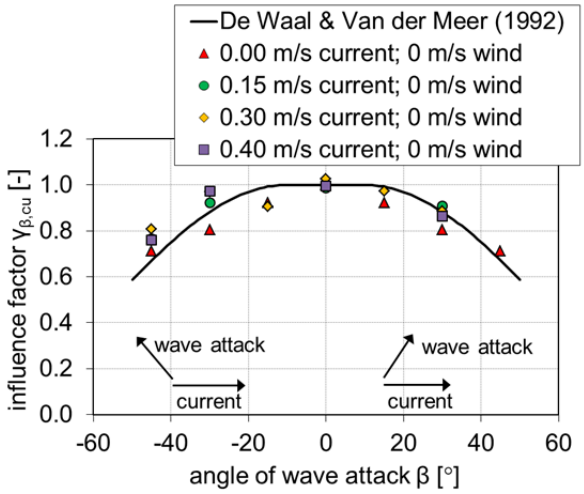

Figure 8.37 Current influence on wave overtopping, 1:6 sloped dike, breaking waves

Angle of wave attack and relative wave parameters

For non-breaking waves the dimensionless overtopping rate and the dimensionless freeboard height was determined independent of the wave period (cf. Figure 8.20 and Figure 8.21). Hence using the relative wave period only changes the influence factor $\gamma_{\beta,cu}$ for breaking wave conditions and not for non-breaking conditions. The corresponding graphs are given below for the 1:3 and the 1:6 sloped dike (Figure 8.38 and Figure 8.39). The filled data points are results considering the absolute wave period $T_{abs,m-1,0}$. The non-filled data points were determined by using the relative wave period $T_{rel,m-1,0}$. The influence factor decreases for positive angles of wave attack. For negative angles of wave attack the relative wave periods become smaller. Consequently the influence factors increase to high values and cannot be used for describing the influence of current. The here presented data corresponding to the relative wave period investigation are preliminary data and do not fit the data of further graphs.

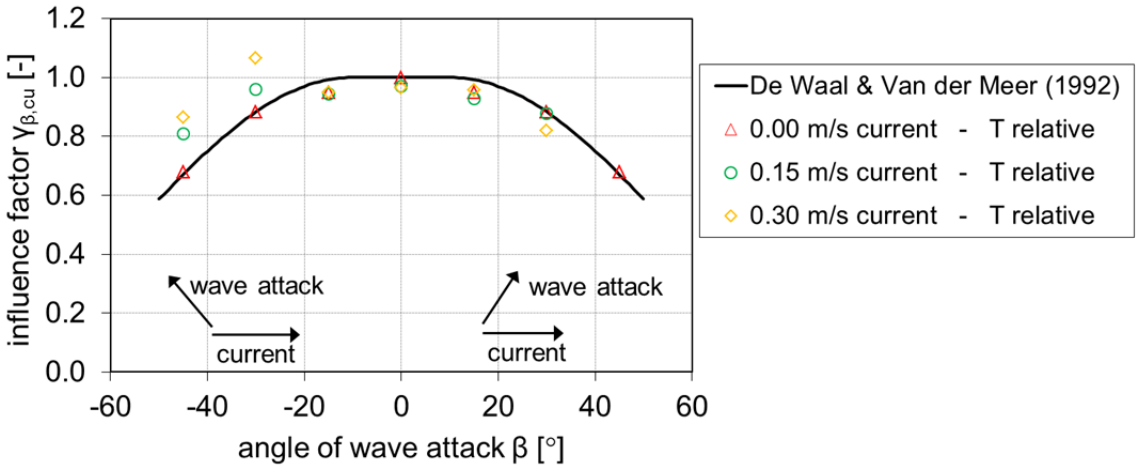

Figure 8.38 Current influence on wave overtopping including the relative wave period, 1:3 sloped dike, br. waves

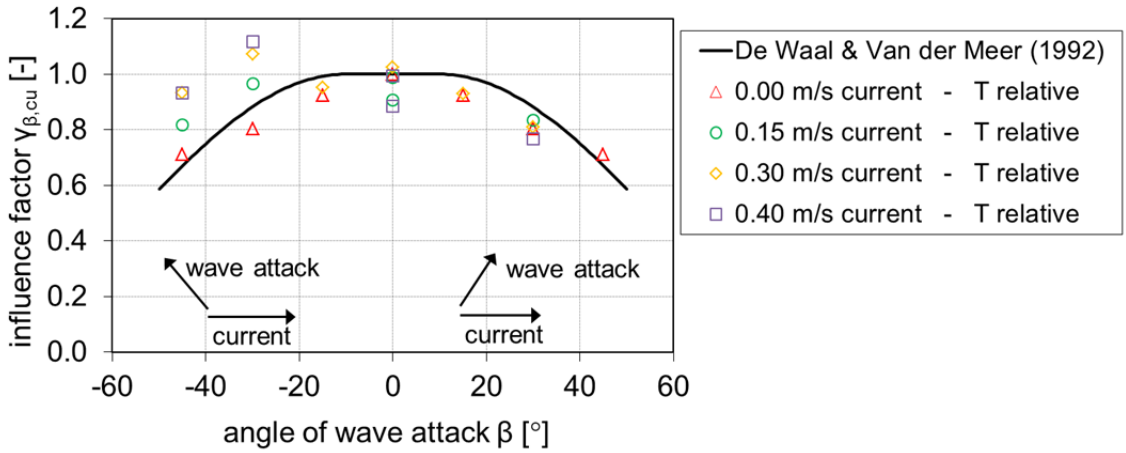

Figure 8.39 Current influence on wave overtopping including the relative wave period, 1:6 sloped dike, br. waves

Angle of wave energy and absolute wave parameters

In the following, the theory of the wave energy direction is applied to the test results in Figure 8.40 to Figure 8.42 for the 1:3 and 1:6 sloped dike for breaking and non-breaking (only 1:3 sloped dike) waves. The filled data points are plotted against the angle of wave energy β_e. The data using the direction of wave energy lie further to the right than the data points that consider only the wave direction and not its energy direction and correspond fairly well to the graph of DE WAAL & VAN DER MEER (1992).

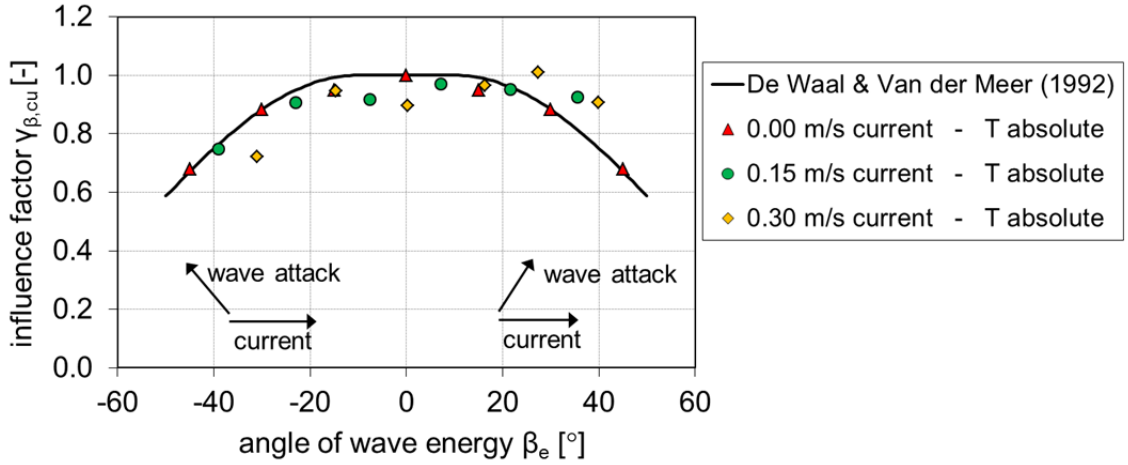

Figure 8.40 Current influence on wave overtopping including the angle of wave energy, 1:3 sloped dike, br. waves

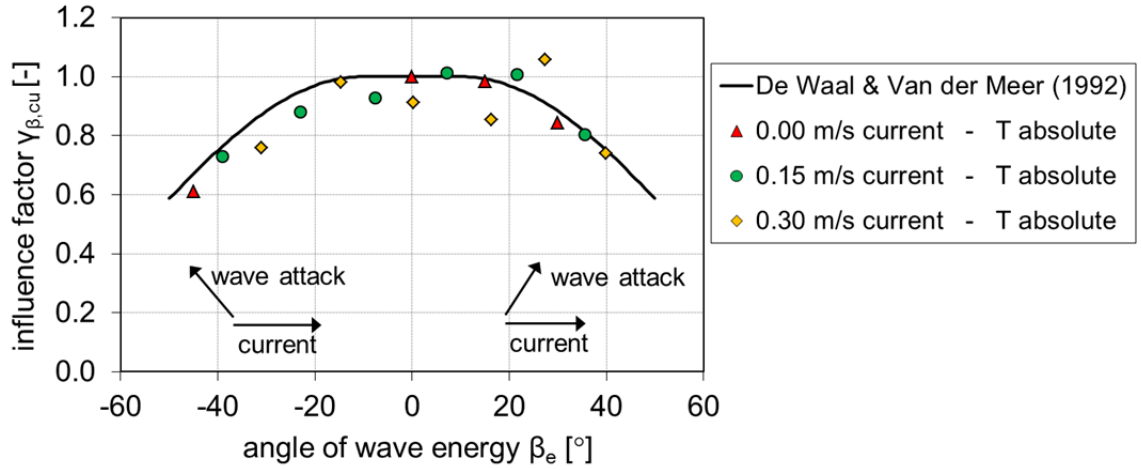

Figure 8.41 Current influence on wave overtopping incl. the angle of wave energy, 1:3 sloped dike, non-br. waves

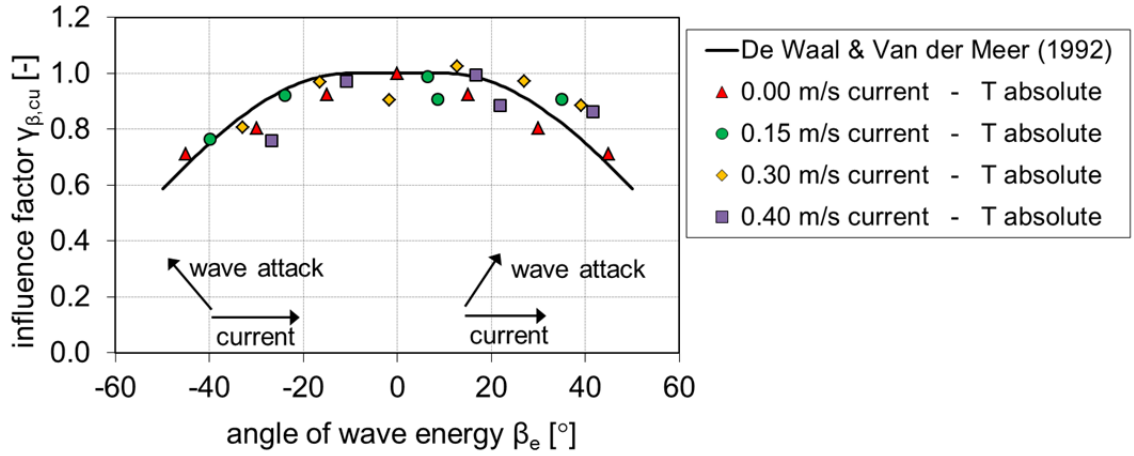

Figure 8.42 Current influence on wave overtopping including the angle of wave energy, 1:6 sloped dike, br. waves

Conclusion

The influence of a longshore current combined with oblique wave attack has been analyzed. In the following a brief conclusion will be given for the three different combinations of the angle of wave attack and the angle of wave energy respectively the absolute and relative wave parameters:

- angle of wave attack and absolute wave parameters:
  - no significant influence of the current on wave overtopping could be measured
  - for breaking waves an insignificant increasing of wave overtopping is identifiable for current > 0 m/s
  - for non-breaking waves (1:3 sloped dike): the wave overtopping increases with a higher current velocity with negative angles of wave attack; the wave overtopping decreases with a higher current velocity with positive angles of wave attack
- angle of wave attack and relative wave parameters
  - the dimensionless overtopping rate increases inexplicable using relative wave parameters
- angle of wave energy and absolute wave parameters
  - influence factors correspond more or less with the formula for γ_β by EUROTOP-MANUAL (2007)

Because of the slightly influence of a longshore current on wave overtopping it is recommended to use the angle of wave attack and absolute wave parameters as analyzing method.

8.4 Comparison of wave run-up and wave overtopping

This section summarizes the influences of the angle of wave attack, the longshore current and wind on wave run-up and wave overtopping. For every data set the influence factor γ is given in Table 8.2 to Table 8.9 for the 1:3 sloped (breaking and non-breaking wave conditions) dike and the 1:6 sloped dike (breaking wave conditions). The influence factors determined by the analysis on wave run-up correspond well with the influence factors determined by wave overtopping analysis. As described in section 8.2 for wave run-up and 8.3 for wave overtopping only some tests give unclear influence factors. These factors are written in gray in the following tables.

Table 8.2 Influence factors γ_β for oblique wave attack

angle of wave attack	1:3 sloped dike			1:6 sloped dike	
	run-up	overtopping br. waves	overtopping non-br. waves	run-up	overtopping br. waves
0°	1.00	1.00	1.00	1.00	1.00
-15°	0.94	0.95	0.98	0.96	0.92
-30°	0.86	0.88	0.84	0.98	0.80
+45°	0.69	0.68	0.61	0.75	0.71

Table 8.3 Influence factors γ_{cu} for current

angle of wave attack	1:3 sloped dike			1:6 sloped dike	
	run-up	overtopping br. waves	overtopping non-br. waves	run-up	overtopping br. waves
0 m/s	1.00	1.00	1.00	1.00	1.00
0.15 m/s	1.02	0.97	1.01	1.00	0.99
0.30 m/s	0.98	0.97	0.85	1.01	1.02
0.40 m/s	-	-	-	1.01	0.99

Table 8.4 Influence factors γ_w for wind

wind	1:3 sloped dike			1:6 sloped dike	
	run-up	overtopping br. waves	overtopping non-br. waves	run-up	overtopping br. waves
0 m/s	1.00	-	1.00	1.00	1.00
4 m/s or 5 m/s	1.00	-	1.02	0.98	1.02
8 m/s or 10 m/s	1.01	-	1.07	0.95	1.05

Table 8.5 Influence factors $\gamma_{\beta,cu}$ for current, oblique wave attack β = -45°, 0 m/s wind

current	1:3 sloped dike			1:6 sloped dike	
	run-up	overtopping br. waves	overtopping non-br. waves	run-up	overtopping br. waves
0 m/s	0.69	0.68	0.61	0.75	0.71
0.15 m/s	0.69	0.75	0.73	0.79	0.76
0.30 m/s	0.78	0.72	0.76	0.89	0.81
0.40 m/s	-	-	-	0.71	0.76

Table 8.6 Influence factors $\gamma_{\beta,cu}$ for current, oblique wave attack β = -30°, 0 m/s wind

current	1:3 sloped dike			1:6 sloped dike	
	run-up	overtopping br. waves	overtopping non-br. waves	run-up	overtopping br. waves
0 m/s	0.86	0.88	0.84	0.98	0.80
0.15 m/s	0.94	0.91	0.88	0.92	0.92
0.30 m/s	0.89	0.95	0.98	0.87	0.97
0.40 m/s	-	-	-	0.80	0.97

Table 8.7 Influence factors $\gamma_{\beta,cu}$ for current, oblique wave attack β = -15°, 0 m/s wind

current	1:3 sloped dike			1:6 sloped dike	
	run-up	overtopping br. waves	overtopping non-br. waves	run-up	overtopping br. waves
0 m/s	0.94	0.95	0.98	0.96	0.92
0.15 m/s	0.95	0.92	0.93	-	-
0.30 m/s	0.94	0.90	0.91	0.88	0.90
0.40 m/s	-	-	-	-	-

Table 8.8 Influence factors $\gamma_{\beta,cu}$ for current, oblique wave attack β = +15°, 0 m/s wind

current	1:3 sloped dike			1:6 sloped dike	
	run-up	overtopping br. waves	overtopping non-br. waves	run-up	overtopping br. waves
0 m/s	0.94	0.95	0.98	0.96	0.92
0.15 m/s	0.86	0.95	1.01	-	-
0.30 m/s	0.78	1.01	1.06	0.85	0.97
0.40 m/s	-	-	-	-	-

Table 8.9 Influence factors $\gamma_{\beta,cu}$ for current, oblique wave attack β = +30°, 0 m/s wind

current	1:3 sloped dike			1:6 sloped dike	
	run-up	overtopping br. waves	overtopping non-br. waves	run-up	overtopping br. waves
0 m/s	0.86	0.88	0.84	0.98	0.80
0.15 m/s	0.80	0.93	0.80	0.97	0.91
0.30 m/s	0.86	0.91	0.74	0.96	0.89
0.40 m/s	-	-	-	0.93	0.86

8.5 Analysis of flow processes on dike crests

8.5.1 Plausibility of the measured data

For each test of the 1:3 and 1:6 sloped dike the coefficients c_h and c_v were determined by using the described formula (5.28) and (5.29) by SCHÜTTRUMPF & VAN GENT (2003). To exclude measuring errors a selection of tests was made: flow velocities of wind tests and with a corresponding flow depth on the crest lower than 1 cm are not usable because the micro propeller was not able to deliver correct results under these conditions. These flow velocities are not considered in the following analysis. Figure 8.43 and Figure 8.44 show the coefficients c_h and c_v for all four dike configurations on the seaward side. These coefficients c_h and c_v are determined using the mentioned formula by SCHÜTTRUMPF & VAN GENT (2003):

$$c_h = \frac{R_{u2\%} - R_c}{H_s} \cdot \frac{H_s}{h_{2\%}} \quad [-] \tag{8.13}$$

with H_s significant wave height [m]

$R_{u2\%}$ run-up height exceeded by 2% of the incoming waves [m]

R_c freeboard height [m]

c_h empirical coefficient determined by model tests[-]

Additionally flow velocities on the seaward dike crest $v_{2\%}$ are given by

$$c_v = \sqrt{\frac{R_{u2\%} - R_c}{H_s}} \cdot \frac{\sqrt{g \cdot H_s}}{v_{2\%}} \quad [-] \tag{8.14}$$

c_v empirical coefficient determined by model tests[-]

In Figure 8.43 and Figure 8.44 the standard-deviations ±σ, ±2σ and ±3σ of the coefficients c_h and c_v are plotted respectively.

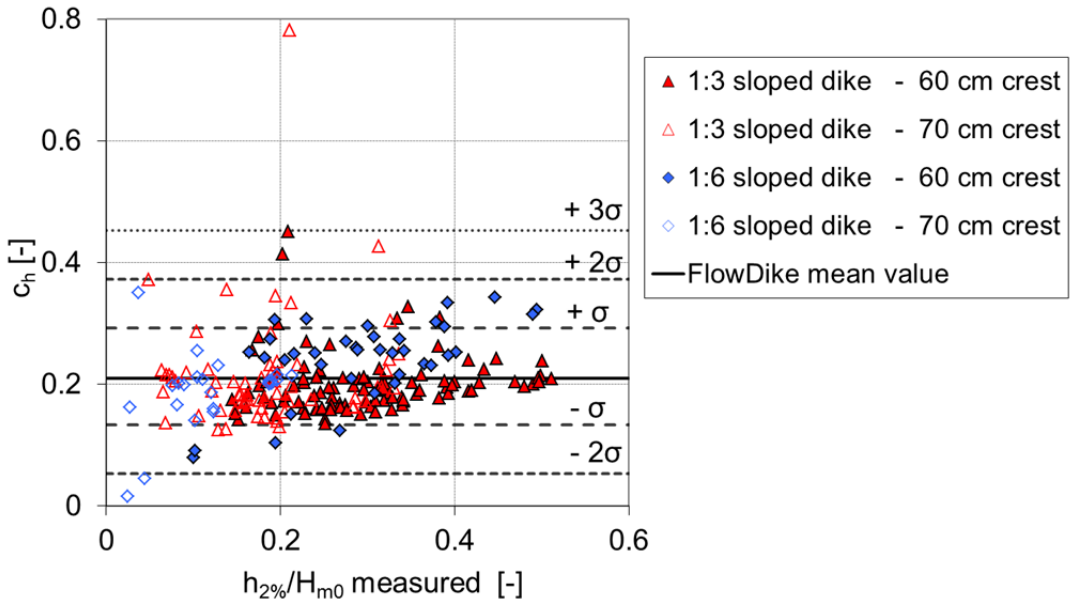

Figure 8.43 Coefficient c_h as a function of $h_{2\%}/H_{m0}$ without tests with wind or flow depth under 1cm

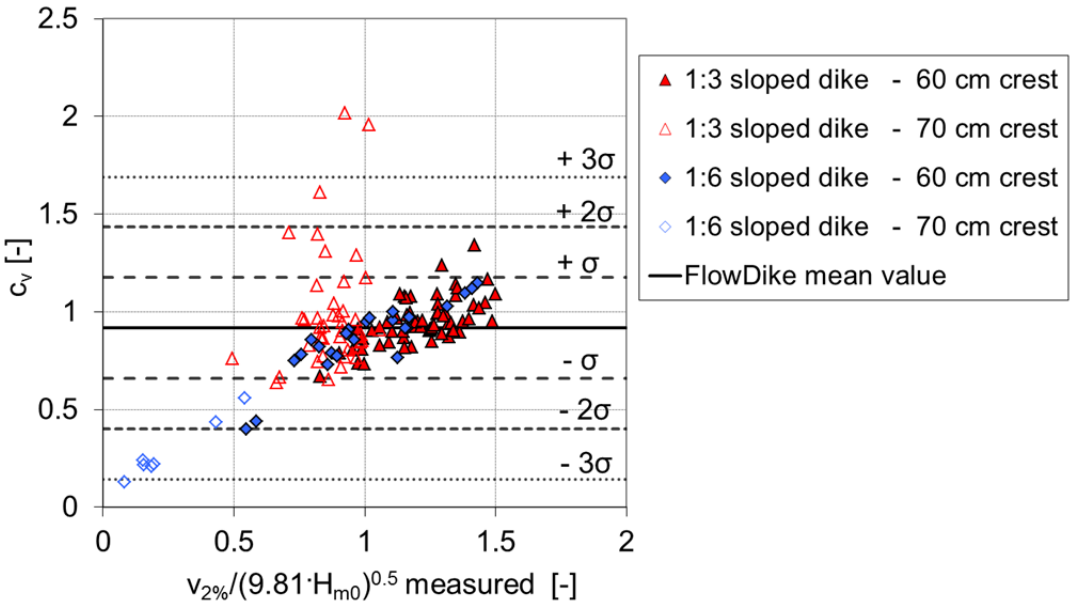

Figure 8.44 Coefficient c_v as a function of $v_{2\%}/(9.81 \cdot H_{m0})^{0,5}$ without tests with wind or flow depth under 1cm

Furthermore as a result of these distributions the data which are located outside the 3σ-interval are excluded from the following analysis and new mean values are determined.

To verify the coefficients for each dike configuration the average coefficient of each dike configuration and the average coefficient of all dike configurations are shown in Figure 8.45. The standard deviation refers to every single test. The coefficient c_v of the 1:6 sloped and 0.7 m high dike give quite different values than the other dike configurations (cf. red-lined circle in Figure 8.34). Therefore this dike configuration will be omitted for the determination of the coefficient c_v. Figure 8.46 shows the new distribution of coefficients and the final constant empirical coefficients c_h and c_v:

$c_h = 0.21$ and $c_v = 0.94$

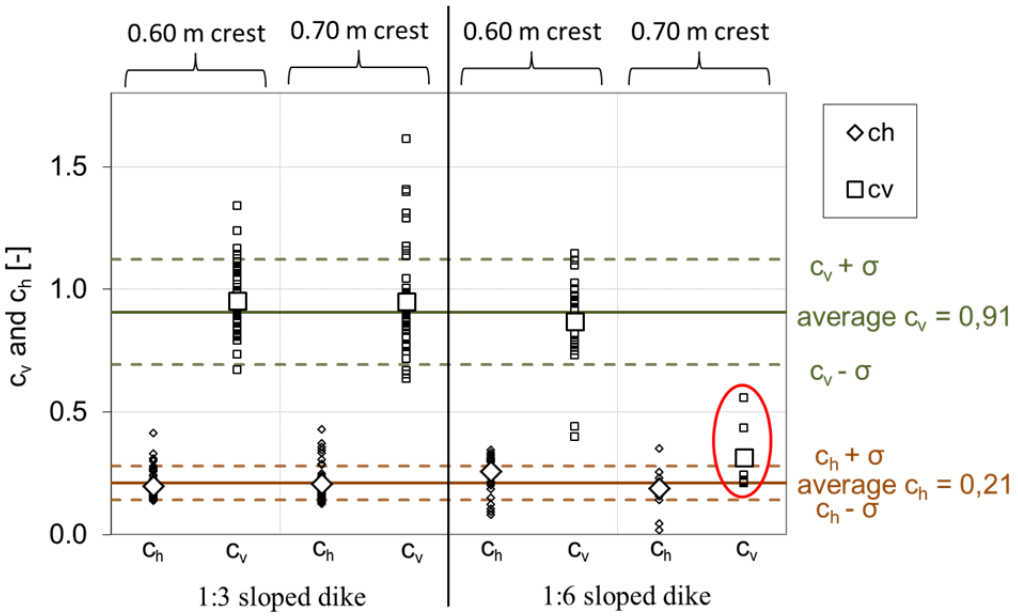

Figure 8.45 Average coefficients of every single dike configuration and of all configurations together

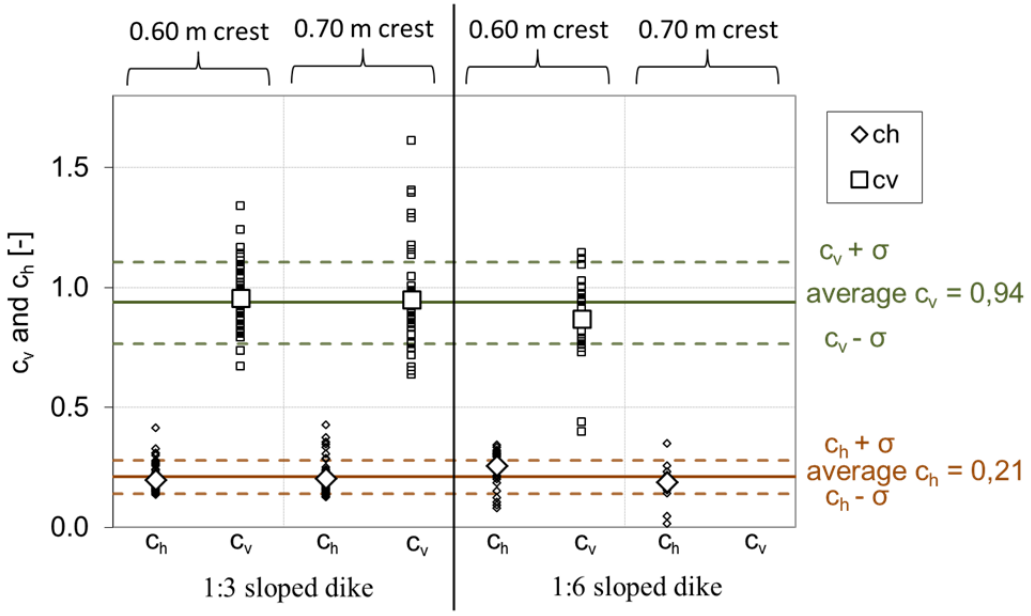

Figure 8.46 Average coefficients of every single dike configuration and of all configurations together excluding c_v of 1:6 sloped and 0.7 m high dike

It is possible to determine the flow depths and flow velocities on the seaward side by using the modification of empirical coefficients used in formula (5.28) and (5.29) by SCHÜTTRUMPF & VAN GENT (2003).

Figure 8.47 shows that the new empirical coefficient $c_h = 0.21$ is lower than the coefficient by SCHÜTTRUMPF (2001) $c_h = 0.33$ and is slightly higher than the value by VAN GENT (2002) $c_h = 0.15$. The coefficient $c_v = 0.94$ for the results of FlowDike 1 and FlowDike 2 is lower than the coefficients by SCHÜTTRUMPF (2001) $c_v = 1.37$ and VAN GENT (2002) $c_v = 1.30$. The coefficients by SCHÜTTRUMPF (2001) have been determined by flow depth and flow velocities on the dike slope, while flow depths on the dike crest have been used in FlowDike 1 and FlowDike 2.

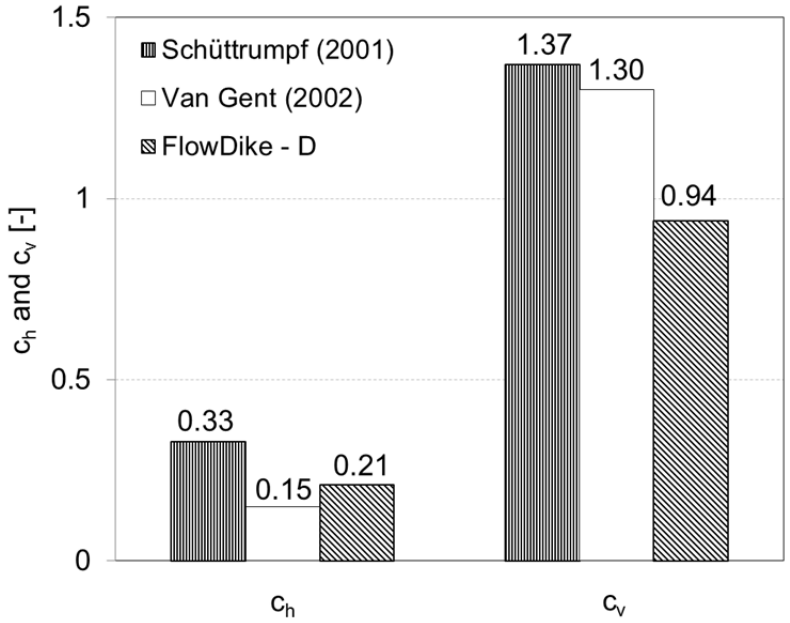

Figure 8.47 Coefficients c_h and c_v of former investigations compared with the new coefficients by FlowDike 1 and FlowDike 2

With the new empirical coefficients c_h and c_v flow depths $h_{2\%}$ and flow velocities $v_{2\%}$ were calculated and plotted against the measured values (Figure 8.48). According to the modification of empirical coefficients used in formula by SCHÜTTRUMPF & VAN GENT (2003) it is possible to determine the flow depths and flow velocities on the seaward side of the crest on the 1:3 sloped dike (Figure 8.48) and 1:6 sloped dike (Figure 8.49). Further analysis considering the influence of current and wind on flow processes on dike crests has not been carried out yet.

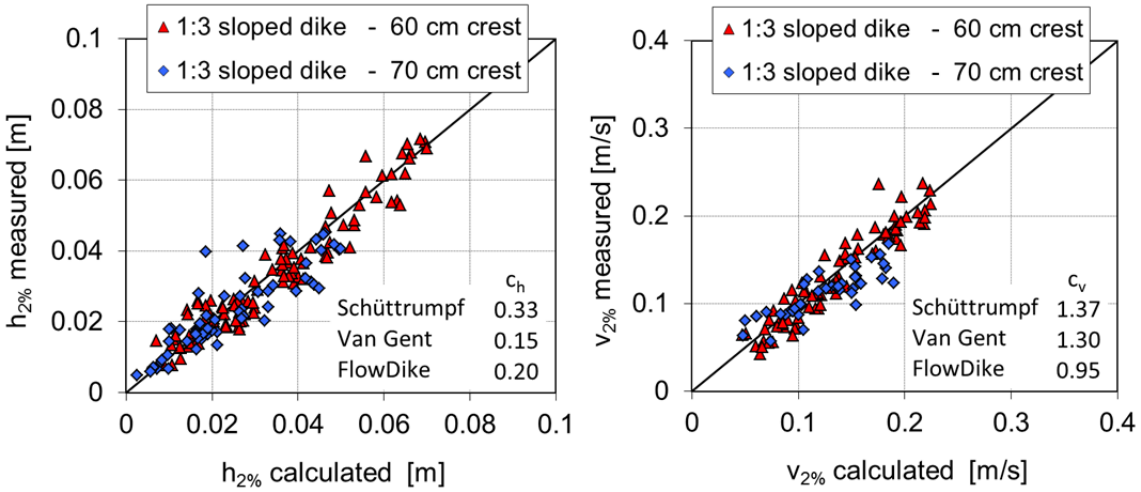

Figure 8.48 Measured and calculated flow depths $h_{2\%}$ and flow velocities $v_{2\%}$ on the seaward side of the dike crests using the new empirical coefficients, 1:3 sloped dike

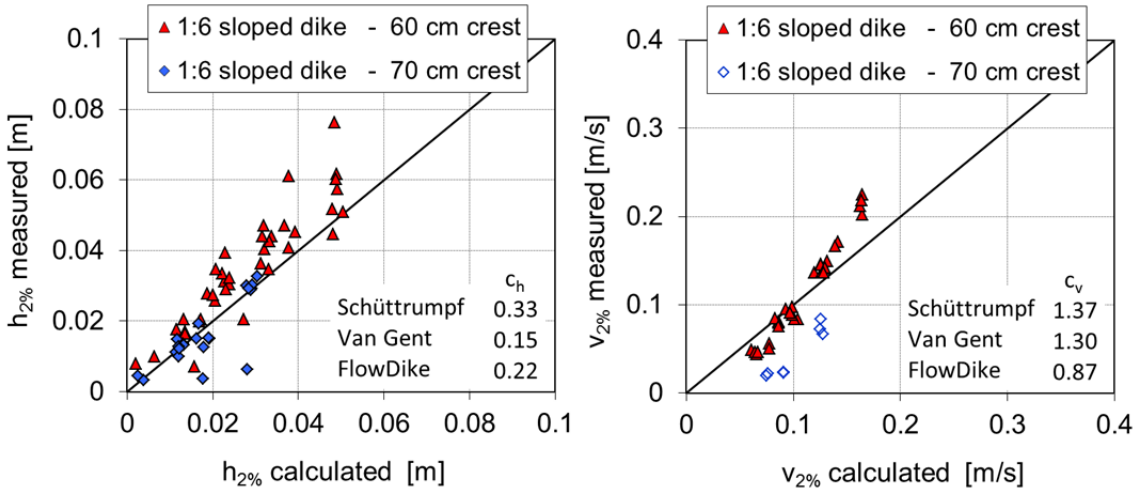

Figure 8.49 Measured and calculated flow depths $h_{2\%}$ and flow velocities $v_{2\%}$ on the seaward side of the dike crests using the new empirical coefficients, 1:6 sloped dike

8.5.2 Influence of oblique wave attack on flow processes on dike crests

In the following section the influence of oblique wave attack on flow depth on dike crests will be analyzed. Following the previous chapter, the flow velocities on the dike crests do not give clear results. Therefore they will not be used for the determination of the influence of oblique wave attack on flow processes on dike crests.

The dimensionless flow depth h* can be determined using the following formula:

$$h^* = \frac{h_{2\%}}{H_s} \quad [-] \tag{8.15}$$

with $h_{2\%}$ flow depths on seaward dike crest, which is exceeded by 2% of the incoming waves [m]

H_s significant wave height [m]

Figure 8.50 and Figure 8.51 give the dependency between the dimensionless flow depth h* and the dimensionless freeboard height R_c* for the different angles of wave attack. The interception with the y-axis of the regression curves is defined as h* = 1. This means that the flow depths on the seaward dike crest $h_{2\%}$ have the same value as the significant wave height H_s. The inclination of the graphs of the tests with perpendicular wave attack is lower than the slopes of the graphs of the test with oblique wave attack. The higher the angle of wave attack the smaller is the dimensionless flow depth h* while unchanged dimensionless freeboard height R_c*. This behavior corresponds well with the characteristic of the wave overtopping rate (cf. section 8.3).

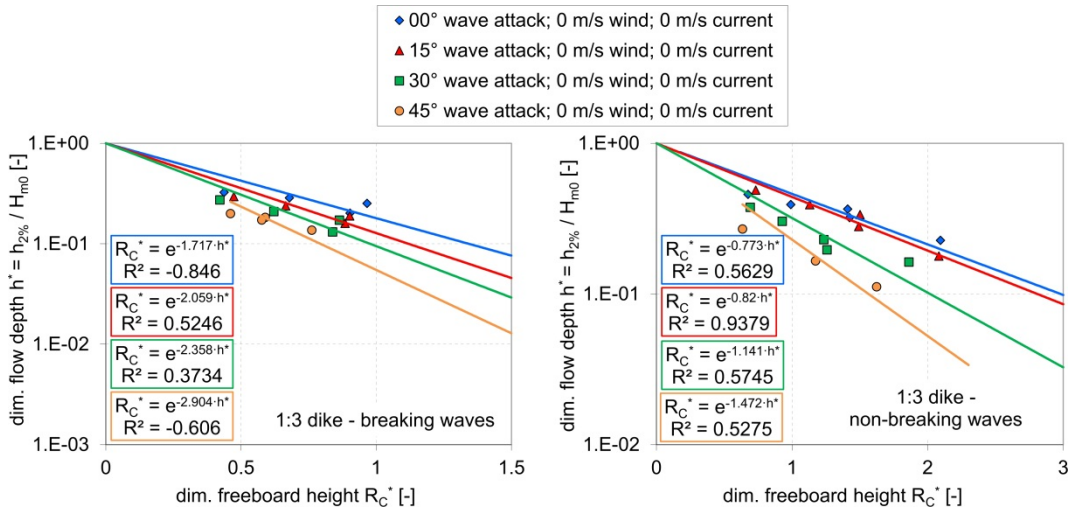

Figure 8.50 Influence of oblique wave attack on flow depth on dike crests; 1:3 sloped dike (left: breaking conditions; right non-breaking conditions)

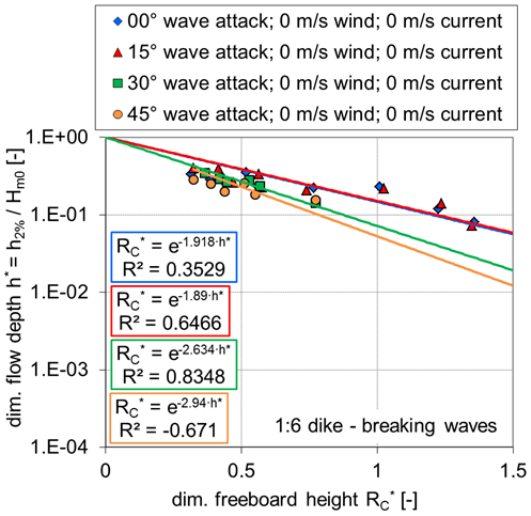

Figure 8.51 Influence of oblique wave attack on flow depth on dike crests; 1:6 sloped dike (breaking conditions)

9 Conclusion

The investigations of FlowDike 1 and FlowDike 2 on the effects of onshore wind and longshore current on wave run-up and wave overtopping for perpendicular and oblique wave attack. These variables were two of the missing effects in freeboard design and therefore a main interest for design purposes. Model tests were carried out in the shallow water wave basin at DHI (Hørsholm, Denmark) and included the configuration of a 1:3 sloped dike (FlowDike 1) and a 1:6 sloped dike (FlowDike 2).

The data analysis on wave run-up was based on an advanced data extraction from video films considering 10 separate stripes of the run-up board which provided additional measurement results. In a first step the measured wave run-up was analyzed with respect to the influence of single parameter oblique wave attack, onshore wind and a longshore current.

Results considering oblique wave attack confirm former empirical investigations. The increasing effect of onshore wind on wave run-up as described regarding former model tests with monochromatic waves could not be validated by the FlowDike test results. The investigated onshore wind speed of < 10 m/s had no significant effect on the wave run-up in the model tests with the 1:3 sloped dike and a very slightly decreasing effect in the model tests with the 1:6 sloped dike. Furthermore no significant effect on wave run-up in case of a longshore current velocity < 0.4 m/s and a perpendicular wave attack was obtained.

In a second step the combined effect of oblique wave attack and a longshore current was investigated. The results show non obvious dependencies but it has to be considered that the relative wave run-up height is a very sensitive parameter.

The third step within data analysis was the comparison between measured and calculated relative wave run-up. Calculation was done using the formula of EURTOP-MANUAL (2007) together with the estimated influence factors $\gamma_{\beta,}$ γ_{cu} and γ_{w}. The comparison shows a good agreement between the measured and the calculated values. All pairs of values are in a range of ± 20 %.

The tests on perpendicular wave attack without influencing parameter validated the existing wave overtopping formulae from the EURTOP-MANUAL (2007). For both model tests the data points of the reference tests fit well within the 95 % confidence range of the formula.

All wind tests confirmed the stated assumptions by GONZÁLEZ-ESCRIVA (2006) and DE WAAL ET AL. (1996) concerning the significant wind impact on small overtopping discharges. For high overtopping discharges practically no influence is noticeable as the data points for wind match those of the reference test, this validates the stated theory of WARD ET AL. (1996).

The influence of oblique waves on overtopping was analyzed as a last resort. In a first attempt the results found for both investigations validate the trend for obliqueness to reduce wave overtopping. The influence factors found for FlowDike 1 validate well the regression trend found for former investigations.

For wave overtopping the combination of oblique wave attack and longshore current was analyzed by determining an influence factor $\gamma_{\beta,cu}$. Using therefore the relative wave period $T_{rel,m-1,0}$ instead of the absolute wave period $T_{abs,m-1,0}$ leads to rather high values and does not account the current influence on wave overtopping. Instead of that the influence-factor $\gamma_{\beta,cu}$ can be determined by using the angle of wave energy β_e instead of the angle of wave attack β.

The influence factors for the angle of wave attack, the longshore current and wind on wave run-up correspond well to the influence factors on wave overtopping. For both analysis on wave run-up and wave overtopping the absolute wave parameters and the angle of wave attack should be used.

According to the modification of empirical coefficients used in formulae by SCHÜTTRUMPF & VAN GENT (2003) it is possible to determine the flow depths and flow velocities on the seaward side of the crest. Additionally the dimensionless flow depths for different dimensionless freeboard height and different angles of wave attack have been analyzed. The higher the angle of wave attack the smaller is the dimensionless flow depth for unchanged dimensionless freeboard heights. This behavior corresponds well with the characteristics of the wave overtopping rate.

Further investigations on very oblique wave attack with $\beta > 45°$ are planned within the HYDRALAB-IV project CornerDike.

10 References

Ahrens, J. P., Heimbaugh, M. S. (1992): **Seawall overtopping model**, Proceedings of the 21st International Conference on Coastal Engineering

Aminti, P., Franco, L. (1988): **Wave overtopping on rubble mound breakwaters**, Proceedings of the 21st International Conference on Coastal Engineering, pp. 770 - 781, New York, United States

Battjes, J. A. (1974): **Computation of set-up, longshore currents, run-up and overtopping due to wind-generated waves**, Vol. 74-2, Delft, Netherlands

Bendat, J.L., Piersol, A.G. (1993): **Engineering Applications of Correlation and Spectral Analysis**, John Wiley & Sons, New York, New York

Bradbury, A. P., Allsop, N. W. H. (1988): **Hydraulic effects of breakwater crown walls**, Proceedings of conference on design of breakwaters, pp. 385 - 396, London

de Rouck, J., Troch, P., van de Walle, B., van Gent, M. R. A., van Damme, L., de Rond, J., Frigaard, P., Murphy, J. (2002): **Wave run-up on sloping coastal structures prototype measurements versus scale model tests**, Proceedings of the international Conference on Breakwaters, coastal structures and coastlines, pp. 233 - 244, London, England

de Waal, J. P., van der Meer, J. W. (1992): **Wave runup and overtopping on coastal structures**, Proceedings of the 23rd International Conference on Coastal Engineering, pp. 1772 - 1784

de Waal, J. P., Tönjes, P., van de Meer, J. W. (1996): **Wave overtopping of vertical structures including wind effect**, Proceedings of the 25th International Conference on Coastal Engineering, pp. 2216 - 2229, Singapore, Singapore

DHI Wasy Water & Environment (2007): **WS Wave Analysis Tools - User Guide**, [DHI Software 2007] website: http://www.hydroasia.org/jahia/webdav/site/hydroasia/shared/Document_public/Project/Manuals/WRS/MIKEZero_WSWAnalysisTools.pdf (access on 27th October 2011)

EurOtop-Manual, Pullen, T., Allsop, N. W. H., Bruce, T., Kortenhaus, A., Schüttrumpf, H., van der Meer, J. W. (2007): **Die Küste - EurOtop, wave overtopping of sea defences and related structures: Assessment manual**, Issue 73, URL: http://www.overtopping-manual.com/-eurotop.pdf (04-18-12)

Franco, L., de Gerloni, M., van der Meer, J. W. (1994): **Wave overtopping on vertical and composite breakwaters**, Proceedings of the 24th International Conference on Coastal Engineering

Gibson, A. H. (1930): **The effect of surface waves on the discharge over weirs**, ICE Selected Engineering Papers, Vol. 1, Issue 99, pp. 5 - 18, London, UK

González-Escriva, J. A. (2006): **The role of wind in wave runup and wave overtopping of coastal structures**, Proceedings of the 30th International Conference, Vol. 5, pp. 4766 - 4778, Singapore, Singapore

Grüne, J., Wang, Z. (2000): **Wave run-up on sloping seadykes and revetments**, Proceedings of the 27th International Conference, Singapore, Singapore

Hedges, T. S. (1987): **Combinations of Waves and Currents - An Introduction**, Proceedings of the Institution of Civil Engineers Part 1-Design and Construction, Vol. 82, pp. 567 - 585, London, England

Hedges, T. S., Reis, M. T. (1998): **Random waves overtopping of simple sea walls: a new regression model**, Proceedings of the Institution of Civil Engineers.Water, maritime & energy, Vol. 130, Issue Telford, pp. 1 - 10, London, United Kingdom

Heyer, T., Pohl, R. (2005): **Der Auflauf unregelmäßiger Wellen im Übergangsbereich zwischen branden und Schwingen**, Wasser und Abfall, Vol. 5, pp. 34 - 38, Sindelfingen, Germany

Holthuijsen, L. H. (2007): **Waves in oceanic and coastal waters**, New York, New York

Hunt, I. A. (1959): **Design of seawalls and breakwaters**, Journal of Waterway Port Coastal and Ocean Engineering-Asce, pp. 123 - 152, New York, New York

Juhl, J., Sloth, P. (1994): **Wave overtopping of breakwaters under oblique waves**, Proceedings of the 24th International Conference on Coastal Engineering, pp. 1182 – 1196

Kortenhaus, A., Fröhle, P., Jensen, J., von Lieberman, N., Mai, S., Miller, C., Peters, K., Schüttrumpf, H. (2009): **Probabilistische Bemessung von Bauwerken**, In:Hafenbautechnische Gesellschaft and Deutsche Gesellschaft für Geotechnik e.V., Unsere Gewässer - Forschungsbedarf aus Sicht der Praxis : eine Dokumentation von HTG und DGGT, Hamburg, pp. 109-122

Le Méhauté, B. (1976) **Similitude in Coastal Engineering**. Journal of the Waterways, Harbors and Coastal Engineering. Vol. 102. p. 317-335

Malcherek, A. (2010): **Gezeiten und Wellen - Die Hydromechanik der Küstengewässer**, Vieweg + Teubner

Oumeraci, H., Schüttrumpf, H., Sauer, W., Möller, J. and Droste, T. (2000): **Physical model tests on wave overtopping with natural sea states - 2D model tests with single, double and multi peak wave energy spectra**, Vol. LWI-Bericht 852, Braunschweig, Germany

Oumeraci, H., Möller, J., Schüttrumpf, H., Zimmermann, C., Daemrich, K.-F., Ohle, N. (2002): **Schräger Wellenauflauf an Seedeichen**, Vol. LWI 881, FI 643/V, Braunschweig, Germany

Owen, M. W. (1980): **Design of seawalls allowing for wave overtopping**, Vol. EX 924, Wallingford, England

Owen, M. W. (1982): **The hydraulic design of sea-wall profiles**, pp. 185 - 192, London, England

Pedersen, J., Burcharth, H. F. (1992): **Wave forces on crown walls**, Proceedings of the 23st international Conference on Coastal Engineering, New York, United States

R. Pohl (1992): **Discussions according to the paper Khader**, M.H.A., Rai, S.P., Yong, D.M. (1991). **An experimental study of wave runup on steep curvilinear slopes,** Journal of Hydraulic Research, Vol. 29, no. 3, pp 403-415. Journal of Hydraulic Research, Vol. 30, no. 3, pp 423-427

Wagner, H. (1974): **Seebau und Küstenschutz 1**. VEB Verlag Technik, Berlin

Sawaragi, T., Deguchi, I., Park, S.-K. (1988): **Reduction of wave overtopping rate by use of artificial reefs**, Proceedings of the 21st International Conference on Coastal Engineering, pp. 335 - 349, New York, United States

Schüttrumpf, H. (2001): **Wellenüberlaufströmung bei Seedeichen - Experimentelle und theoretische Untersuchungen**, Braunschweig, Germany

Schüttrumpf, H., van Gent, M. R. A. (2003): **Wave overtopping at seadikes**, pp. 431 - 443, Vicksburg, MS

Smith, G. M., Seijffert, J. W. W., van der Meer, J. W. (1994): **Erosion and overtopping of a grass dike large scale model tests**, Proceedings of the 24th International Conference on Coastal Engineering, pp. 2639 - 2652

Tautenhain, E., Kohlhase, S., Partenscky, H. W. (1982): **Wave run-up at sea dikes under oblique wave approach**, Proceedings of the 18th International Conference on Coastal Engineering, pp. 804 - 810

Treloar, P. D. (1986): **Spectral wave refraction under the influence of depth and current**, Coastal Engineering, Vol. 9, Issue 5, pp. 439 - 452, Amsterdam, Netherlands

van der Meer, J. W. (1993): **Conceptual design of rubble mound breakwater**, Delft Hydraulics, Vol. 483

van der Meer, J. W., Janssen, J. P. F. M. (1994): **Wave run-up and wave overtopping at dikes and revetments**, Delft, Netherlands

van der Meer, J. W., Janssen, J. P. F. M.(1995): **Wave run-up and wave overtopping at dikes**, In: Wave forces on inclined and vertical wall structures, New York, New York, pp. 1-27

van Gent, M. R. A. (2002): **Wave overtopping events at dikes**, Proceedings of the 28th International Conference, Singapore

Wagner, H., Bürger, W. (1973): **Kennwerte zur Seedeichbemessung**, Wasserwirtschaft Wassertechnik, Vol. 23, Issue 6, pp. 204 - 207, Berlin, Germany

Ward, D. L., Zhang, J., Wibner, C. G., Cinotto, C. M. (1996): **Wind effects on runup and overtopping of coastal structures**, Proceedings of the 29th International Conference on Coastal Engineering, pp. 2206 - 2215, Singapore, Singapore

Wassing, F. (1957): **Model investigation on wave run-up carried out in the Netherlands during the past twenty years**, Issue 42, pp. 700 - 714

Glossary

Average wave: The average wave is a superposition of the incident and reflected wave and therefore it is the actual visible wave.

Breaking waves (plunging) and non-breaking waves (surging): A certain type of breaking is given by the combination of structure slope and wave steepness for the deep water conditions. On sloped structures it can be defined by the surf similarity parameter$\xi_{m-1,0}$ with breaking waves $\xi_{m-1,0} > 2 - 3$ and non-breaking waves $\xi_{m-1,0} > 2 - 3$. The transition between plunging and surging waves is known as collapsing.

Crossing analysis: For most of the processed data a crossing analysis (up or down crossing) was used in time domain. Both options use a defined crossing level within the raw data signal to detect single events and their parameter, such as peak to peak value or event duration. The difference between up or down crossing is the starting direction within the analysis, whether it starts to detect an event first when it is crossing the threshold in upward direction or downwards.

Exceedance curve: An exceedance curve is a tool to visualize the distribution of any parameter, such as run-up heights. The percentage of exceeding is calculated from the number of detected events related to the number of waves N. The curve simply relates the percentage of events to i.e. the run-up height.

Incident wave: The incident wave describes the wave coming from the sea before it hits the structure. In the model tests it is the incidental generated wave from the wave generator without reflection influences.

JONSWAP–spectra: The Joint North Sea Wave Project – spectra describes the empirical distribution of energy with frequency within the ocean. It is one of the most frequently applied spectra and was applied for many model tests before; thus it was used for comparability.

Long crested waves: Surface waves that are nearly two-dimensional, in that the crests appear very long in comparison with the wave length, and the energy propagation is concentrated in a narrow band around the mean wave direction. They do not exist in nature, but can be generated in the laboratory.

Oblique wave attack: Waves that strike the structure at an angle.

Perpendicular wave attack: Waves that strike the structure normally to its face.

Rayleigh distribution: A Raleigh distribution is a continuous probability distribution that can be used to describe the fitting of a density function.

Reflection analysis: The reflection analysis done in frequency domain is used to determine the moments of spectral density for incident and reflected waves.

Reflection coefficient: The reflection coefficient is determined during reflection analysis and describes the intensity of a reflected wave relative to an incident wave.

Reflected waves: Waves that hit the structure and are reflected seaward with little or no breaking. The wave height and wave length decreases depending on the type of structure.

Return period: The average length of time between sea states of a given severity.

Significant wave height: The average height of the highest of one third of the waves in a given sea state.

Short crested waves: Waves that have a small extent in the direction perpendicular to the direction of propagation. Most waves in natural state are short-crested.

Spectral energy density: It describes how the energy (or variance) of a signal or a time series is distributed with frequency.

Wave run-up and wave overtopping: The run-up is the rush of water up a structure as a result of wave attack. Wave overtopping is the mean discharge of water in l/(s·m) that passes over a structure due to wave attack and should be limited to a tolerable amount.

Wave steepness: The wave steepness is defined as the ratio of wave height to wave length (H/L). It includes therefore information about the characteristic and history of the wave. Distinction can be made into swell sea ($s_0 = 0.01$) and wind sea ($s_0 = 0.04$ to 0.06).

Annex A Model set-up

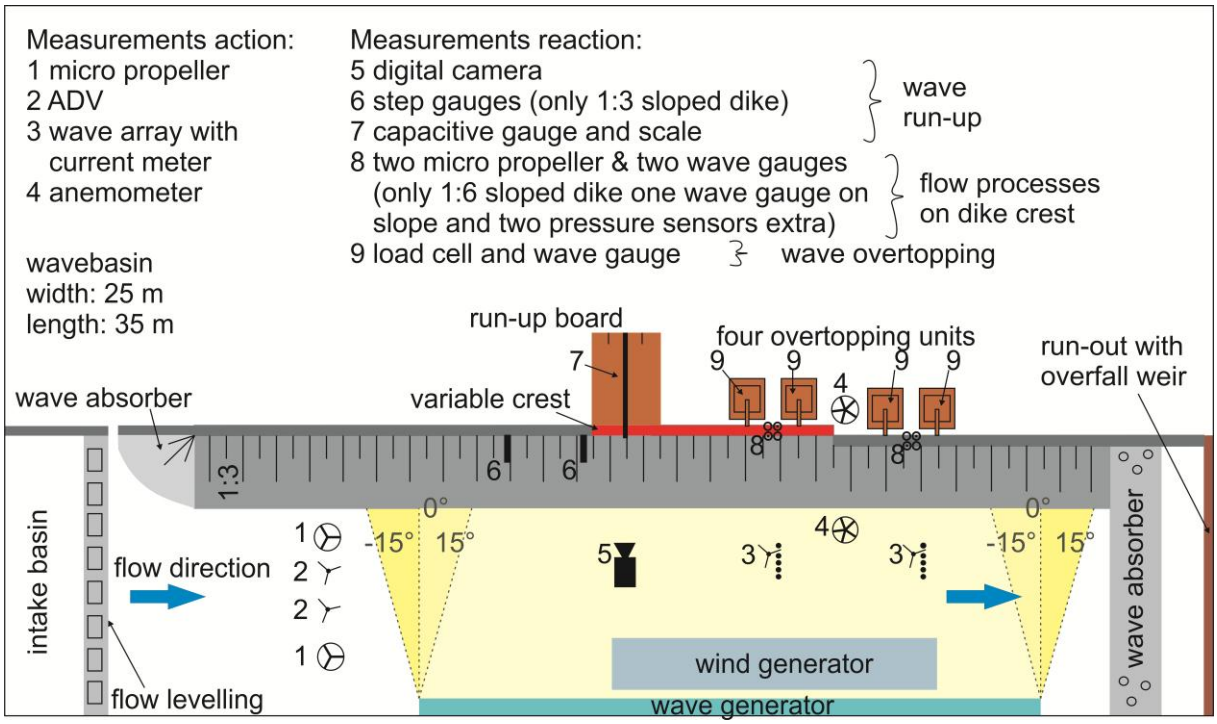

Figure-annex 1 Set-up 1 - angles of wave attack -15°,0° and +15° (1:3 sloped dike - FlowDike 1)

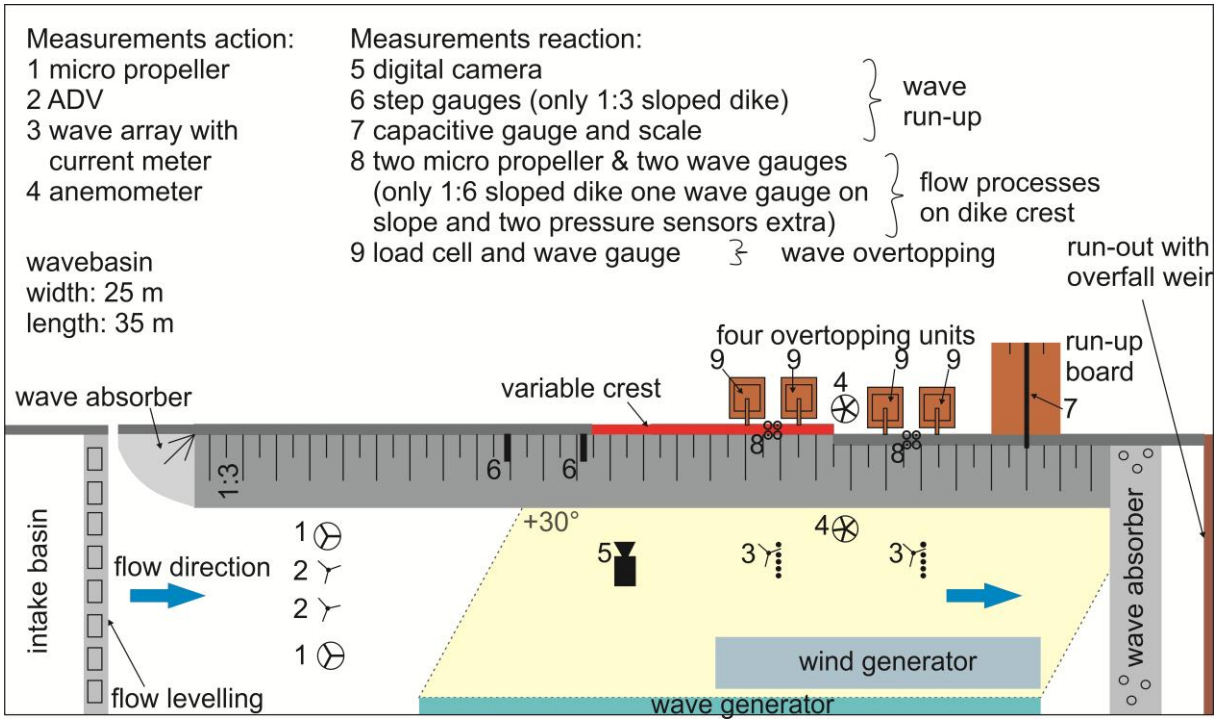

Figure-annex 2 Set-up 2 - angles of wave attack +30° (1:3 sloped dike - FlowDike 1)

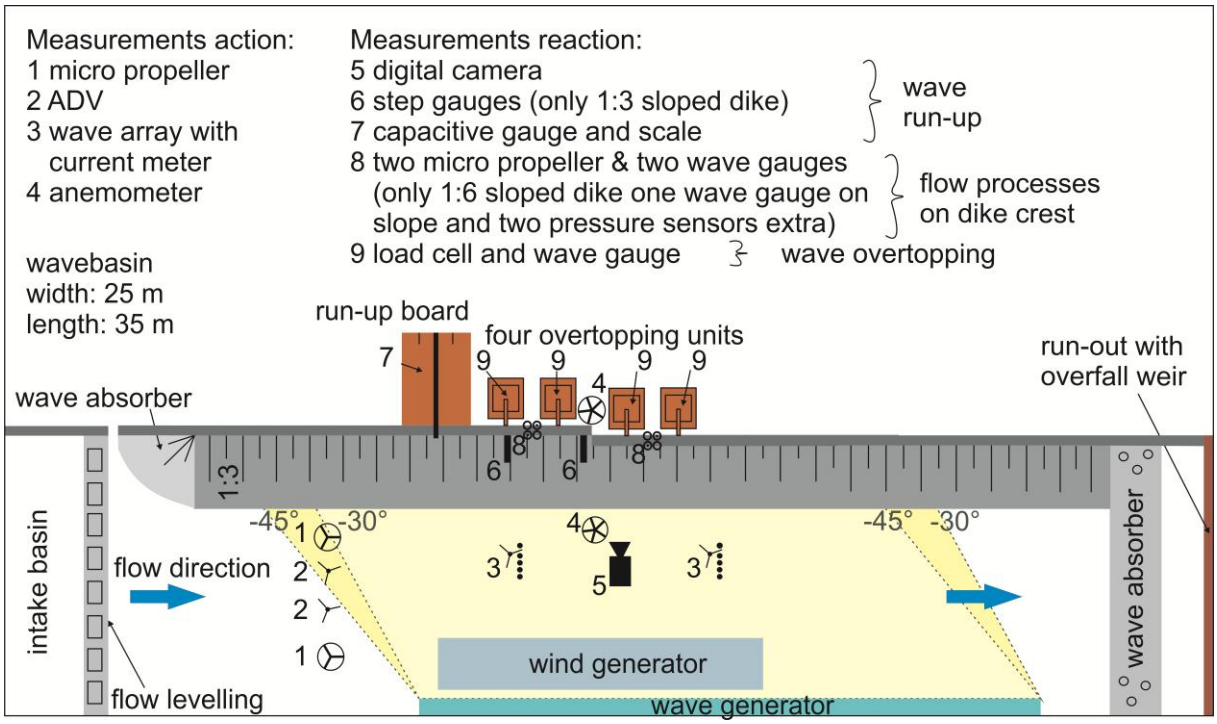

Figure-annex 3 Set-up 3 - angles of wave attack -30° and -45° (1:3 sloped dike - FlowDike 1)

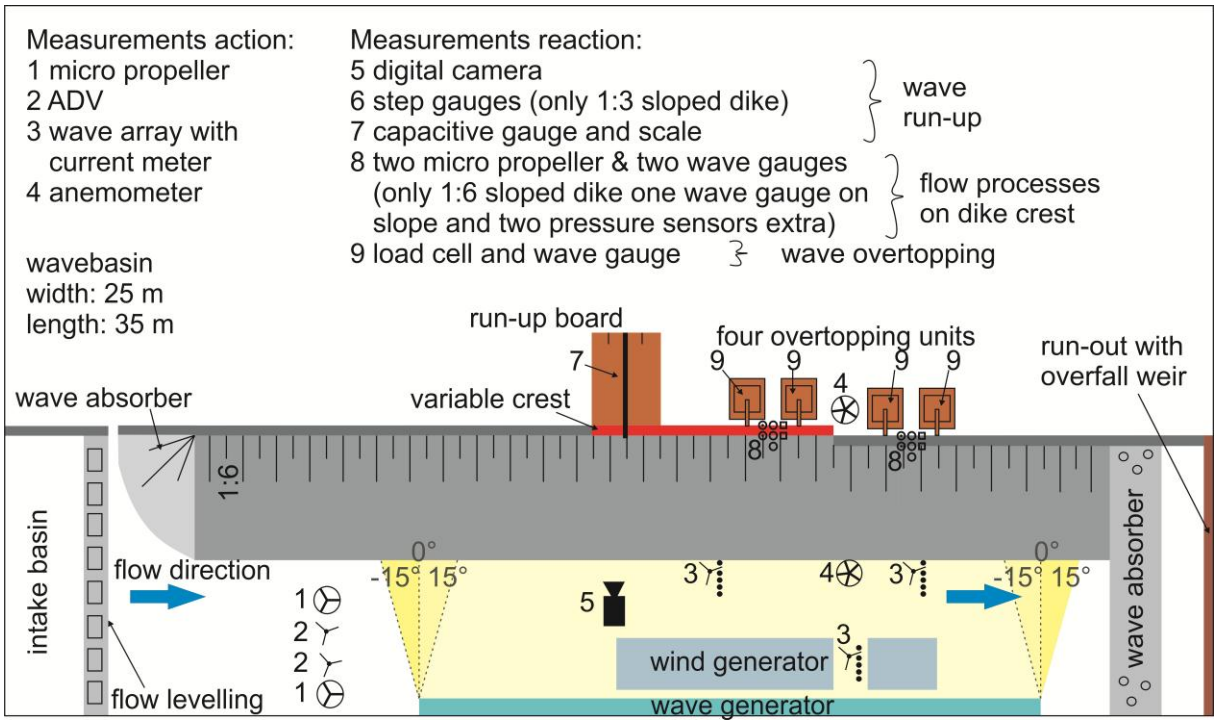

Figure-annex 4 Set-up 4 - angles of wave attack -15°, 0°and +15° (1:6 sloped dike - FlowDike 2)

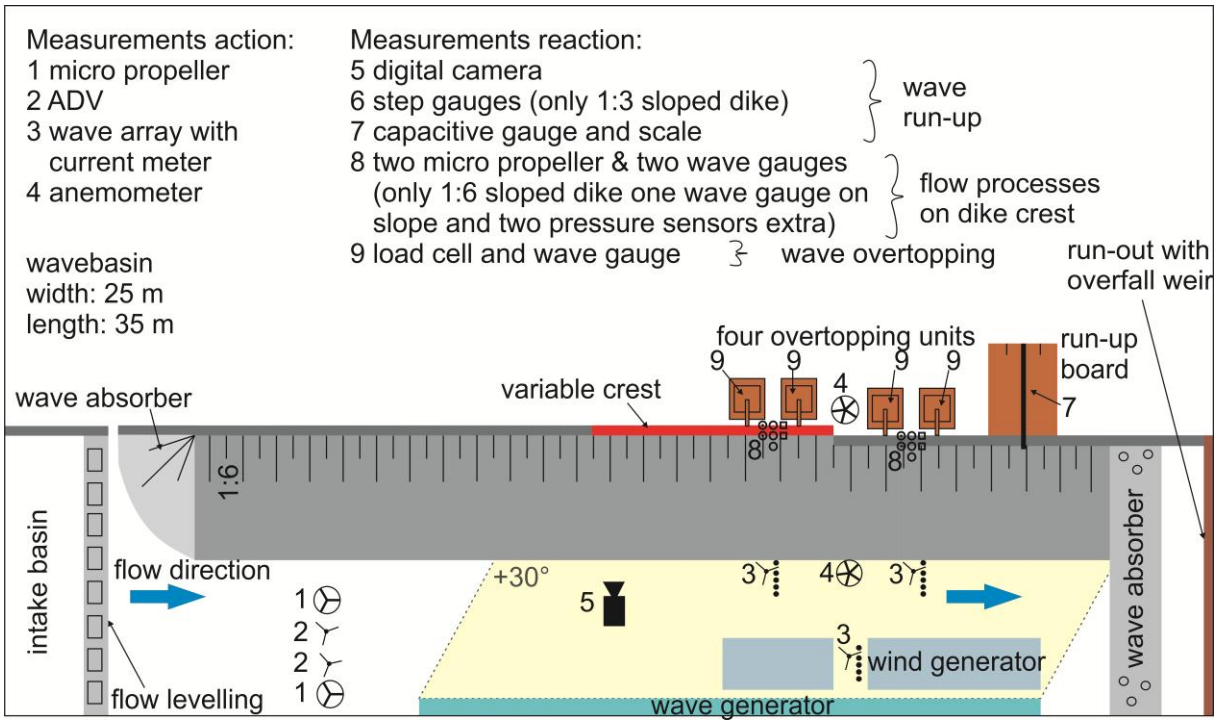

Figure-annex 5 Set-up 5 - angles of wave attack +30° (1:6 sloped dike - FlowDike 2)

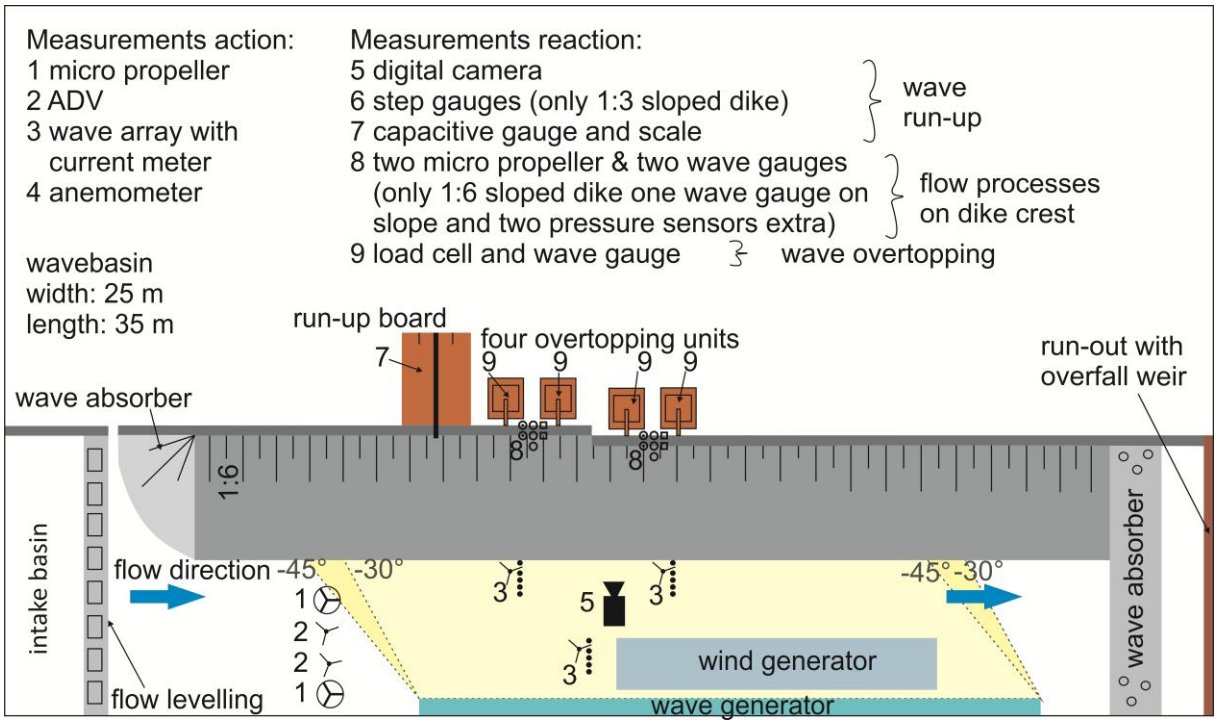

Figure-annex 6 Set-up 6 - angles of wave attack -30° and -45° (1:6 sloped dike - FlowDike 2)

Annex B Channel List - 1:3 sloped dike (FlowDike 1)

Table-annex 1 Channel list – 1:3 sloped dike (FlowDike 1)

channel number	row in *.dfs0-file	item in wave syntheziser	Description	Position	Calibration curve
1	2	1	air temperature		[°C]
2	3	2	water temperature		[°C]
3	4	3	air flow	behind the dike (landwardside)	50 Hz on wind generator correspond to 10 m/s 25 Hz on wind generator correspond to 5 m/s (0.2 m above 0.6 m crest. 0.1 m above 0.7 m crest)
4	5	4	air flow	near ADV in front of 0.7 m crest	
5	6	5	wave gauge in front of the 0.7 m crest	position: 1.1 m (at dike side)	[m]
6	7	6		position: 1 m	[m]
7	8	7		position: 0.75 m	[m]
8	9	8		position: 0.4 m	[m]
9	10	9		position: 0 m (at wave machine side)	[m]
10	11	10	wave gauges in front of the 0.6 m crest	position: 1.1 m (at dike side)	[m]
11	12	11		position: 1 m	[m]
12	13	12		position: 0.75 m	[m]
13	14	13		position: 0.4 m	[m]
14	15	14		position: 0 m (at wave machine side)	[m]
15	16	15	wave gauge	on landward side on the 0.7 m crest	[m]
16	17	16	wave gauge	on seaward side on the 0.7 m crest	[m]
17	18	17	wave gauge	on landward side on the 0.6 m crest	[m]
18	19	18	wave gauge	on seaward side on the 0.6 m crest	[m]
19	20	19	Vx - ADV (DHI)	near wavearray at toe of 0.6 m dike, wg13 (set-up 1, 2 + 3 until test 220) not used after test 220	[m/s]
20	21	20	Vy - ADV (DHI)		[m/s]
21	22	21	Vz - ADV (DHI)		[m/s]
22	23	22	Vx - SD12 (DHI)	near wavearray at toe of 0.7 m dike, wg5 (set-up 1, 2 + 3 until test 220) near wavearray at toe of 0.6 m dike, wg13 (from test 222)	[m/s]
23	24	23	Vy - SD12 (DHI)		[m/s]

channel number	row in *.dfs0-file	item in wave syntheziser	Description	Position	Calibration curve
25	25	24	Vx - ADV (RWTH)	in the middle of the beam (set-up 1, 2 + 3 until test 220) near wavearray at toe of 0.7 m dike, wg5 (from test 222)	[m/s]
26	26	25	Vy - ADV (RWTH)		[m/s]
27	27	26	Vz - ADV (RWTH)		[m/s]
28	28	27	Vx - ADV (RWTH)	in the middle of the beam	[m/s]
29	29	28	Vy - ADV (RWTH)		[m/s]
30	30	29	Vz - ADV (RWTH)		[m/s]
31	31	30	micro propeller	replaced ADV (19-21)	v = 0.8616 · signal
32	32	31	micro propeller	replaced ADV (22-24)	v = 1.09 · signal
33	33	32	micro propeller MiniWater 20	on landward side on the 0.7 m crest	v = 0.8296 · signal
34	34	33	micro propeller MiniWater 20	on seaward side on the 0.7 m crest	v = 0.4871 · signal
35	35	34	micro propeller MiniWater 20	on landward side on the 0.6 m crest	v = 0.4687 · signal
36	36	35	micro propeller MiniWater 20	on seaward side on the 0.6 m crest	v = 0.4913 · signal
37	37	36	load cell Vz	of the overtopping-box behind 0.7 m crest, upstream	[kg]
38	38	37	wavegauge	in the overtopping-box behind 0.7 m crest, upstream	[m]
39	39	38	load cell Vz	of the overtopping-box behind 0.7 m crest, downstream	[kg]
40	40	39	wavegauge	in the overtopping-box behind 0.7 m crest, downstream	[m]
41	41	40	load cell Vz	of the overtopping-box behind 0.6 m crest, upstream	[kg]
42	42	41	wavegauge	in the overtopping-box behind 0.6 m crest, upstream	[m]
43	43	42	load cell Vz	of the overtopping-box behind 0.6 m crest, downstream	[kg]
44	44	43	wavegauge	in the overtopping-box behind 0.6 m crest, downstream	[m]
45	45	44	pump	in the overtopping-box behind 0.7 m crest, upstream (lc37)	q = 1.7845 · signal [l/s]
46	46	45	pump	in the overtopping-box behind 0.7 m crest, downstream (lc39)	q = 1.4010 · signal [l/s]
47	47	46	pump	in the overtopping-box behind 0.6 m crest, upstream (lc41)	q = 1.5942 · signal [l/s]
48	48	47	pump	in the overtopping-box behind 0.6 m crest, downstream	q = 1.5943 · signal [l/s]

channel number	row in *.dfs0-file	item in wave syntheziser	Description	Position	Calibration curve
				(lc43)	
49	49	48	capacitive-gauge	on the run-up-board	set-up 1: R[m] = 0.3748 · signal[V] + 0.4047 set-up 2: R[m] = 0.3674 · signal[V] + 0.2279 set-up 3: R[m] = 0.3708 · signal[V] + 0.4095
50	50	49	pump	in the deep basin (to induce the flow)	[m³/s]
53	51	50	stepgauge	stepgauge at 50 m; 2 m (upstream)	
54	52	51	stepgauge		
55	53	52	stepgauge		
56	54	53	stepgauge		
57	55	54	stepgauge	stepgauge at 50 m; 2 m (downstream)	
58	56	55	stepgauge		
59	57	56	stepgauge		
60	58	57	stepgauge		

Annex C Channel list – 1:6 sloped dike (FlowDike 2)

Table-annex 2 Channel list – 1:6 sloped dike (FlowDike 2)

channel number	**row in *.dfs0-file**	**item in wave synthesizer**	**Description**	**Position**	**Calibration curve Unit**
1	2	1	water temperature		[°C]
2	3	2	air temperature		[°C]
3	4	3	air flow	behind dike	50 Hz on wind generator correspond to 10 m/s 25 Hz on wind generator correspond to 5 m/s (0.2 m above 0.6 m crest. 0.1 m above 0.7 m crest)
4	5	4	air flow	near ADV in front of 0.7 m crest	
5	6	5	wave gauges 0.5 m away from wave generator	position: 1.1 m (at dike side)	[m]
6	7	6		position: 1 m	[m]
7	8	7		position: 0.75 m	[m]
8	9	8		position: 0.4 m	[m]
9	10	9		position: 0 m (at wave generator side)	[m]
10	11	10	wave gauges in front of the 0.6 m crest	position: 1.1 m (at toe of the dike)	[m]
11	12	11		position: 1 m	[m]
12	13	12		position: 0.75 m	[m]
13	14	13		position: 0.4 m	[m]
14	15	14		position: 0 m (at wave generator side)	[m]
15	16	15	wave gauge	on landward side on the 0.7 m crest	[m]
16	17	16	wave gauge	on seaward side on the 0.7 m crest	[m]
17	18	17	wave gauge	on landward side on the 0.6 m crest	[m]
18	19	18	wave gauge	on seaward side on the 0.6 m crest	[m]
19	20	19	Vx - ADV (DHI)	near wavearray at toe of 0.7 m dike	[m/s]
20	21	20	Vy - ADV (DHI)		[m/s]
21	22	21	Vz - ADV (DHI)		[m/s]
22	23	22	Vx - SD-12 (DHI)	near wavearray at toe of 0.7 m dike	[m/s]
23	24	23	Vy - SD-12 (DHI)		[m/s]

channel number	row in *.dfs0-file	item in wave synthesizer	Description	Position	Calibration curve Unit
24	25	24	Vz - SD-12 (DHI)		[m/s]
25	26	25	Vx - ADV (RWTH)	in the middle of the beam	[m/s]
26	27	26	Vy - ADV (RWTH)		[m/s]
27	28	27	Vz - ADV (RWTH)		[m/s]
28	29	28	Vx - ADV (RWTH)	in the middle of the beam	[m/s]
29	30	29	Vy - ADV (RWTH)		[m/s]
30	31	30	Vz - ADV (RWTH)		[m/s]
31	32	31	micro propeller	replaced ADV (19-21)	v = 0.8616 · signal [m/s]
32	33	32	micro propeller	replaced ADV (22-24)	v = 1.09 · signal [m/s]
33	34	33	micro propeller MiniWater 20	on seaward side on the 0.7 m crest	v = 0.1932 · signal [m/s]
34	35	34	micro propeller MiniWater 20	on landward side on the 0.7 m crest	v = 0.1518 · signal [m/s]
35	36	35	micro propeller MiniWater 20	on seaward side on the 0.6 m crest	v = 0.2347 · signal [m/s]
36	37	36	micro propeller MiniWater 20	on landward side on the 0.6 m crest	v = 0.1625 · signal [m/s]
37	38	37	load cell Vz	of the overtopping-box behind 0.7 m crest, upstream	[kg]
38	39	38	wavegauge	in the overtopping-box behind 0.7 m crest, upstream	[m]
39	40	39	load cell Vz	of the overtopping-box behind 0.7 m crest, downstream	[kg]
40	41	40	wavegauge	in the overtopping-box behind 0.7 m crest, downstream	[m]
41	42	41	load cell Vz	of the overtopping-box behind 0.6 m crest, upstream	[kg]
42	43	42	wavegauge	in the overtopping-box behind 0.6 m crest, upstream	[m]
43	44	43	load cell Vz	of the overtopping-box behind 0.6 m crest, downstream	[kg]
44	45	44	wavegauge	in the overtopping-box behind 0.6 m crest, downstream	[m]
45	46	45	pump	in the overtopping-box behind 0.7 m crest, upstream (lc37)	q = 1.7335 · signal [l/s]
46	47	46	pump	in the overtopping-box behind 0.7 m crest, downstream (lc39)	q = 1.5996 · signal [l/s]
47	48	47	pump	in the overtopping-box behind 0.6 m crest, upstream (lc41)	q = 1.6799 · signal [l/s]

channel number	row in *.dfs0-file	item in wave synthesizer	Description	Position	Calibration curve Unit
48	49	48	pump	in the overtopping-box behind 0.6 m crest, downstream (lc43)	q = 1.7456 · signal [l/s]
49	50	49	capacitive-gauge	on the run-up-board	set-up 4: R[m] = 0.1179 · signal[V] + 0.5092 set-up 5: R[m] = 0.1179 · signal[V] + 0.5092 set-up 6: R[m] = 0.1170 · signal[V] + 0.5224
50	51	50	pump	in the deep basin (to induce the flow)	[m³/s]
51	52	51	wave gauges in front of the 0.7 m crest	position: 1.1 m (at toe of the dike)	[m]
52	53	52		position: 1 m	[m]
53	54	53		position: 0.75 m	[m]
54	55	54		position: 0.4 m	[m]
55	56	55		position: 0 m (at wave generator side)	[m]
56	57	56	wave gauge	slope on 0.6 m crest	[m]
57	58	57	wave gauge	slope on 0.7 m crest	[m]
58	59	58	pressure sensor	on seaward side on the 0.7 m crest	[m]
59	60	59	pressure sensor	on landward side on the 0.7 m crest	[m]
60	61	60	pressure sensor	on seaward side on the 0.6 m crest	[m]
61	62	61	pressure sensor	on landward side on the 0.6 m crest	[m]
62	63	62	Vx vectrino		[m/s]
63	64	63	Vy vectrino		[m/s]
64	65	64	Vz vectrino		[m/s]

Annex D Wave conditions – JONSWAP spectrum

Table-annex 3 Wave parameters, flow depth d= 0.50 m, wave characteristics I (1:3 sloped dike)

wave spectra	Hs [m]	Tp [s]	$T_{m-1,0} = \frac{T_p}{1.1}$ [s]	$L_{m-1,0} = \frac{g \cdot T_{m-1,0}^2}{2\pi} \cdot \tanh\left(\frac{2\pi}{L_{m-1,0}} \cdot d\right)$ [m]	steepness $s_{m-1,0} = \frac{H_s}{L_{m-1,0}}$ [-]	duration for 1000 waves [min]
w1	0.07	1.474	1.340	2.416	0.029	25
w2	0.07	1.045	0.950	1.379	0.051	18
w3	0.10	1.76	1.600	3.078	0.032	30
w4	0.10	1.243	1.130	1.862	0.054	21
w5	0.15	2.156	1.960	3.960	0.038	36
w6	0.15	1.529	1.390	2.545	0.059	26

Table-annex 4 Wave parameters, flow depth d = 0.50 m, wave characteristics II (1:3 and 1:6 sloped dike)

wave spectra	Hs [m]	Tp [s]	$T_{m-1,0} = \frac{T_p}{1.1}$ [s]	$L_{m-1,0} = \frac{g \cdot T_{m-1,0}^2}{2\pi} \cdot \tanh\left(\frac{2\pi}{L_{m-1,0}} \cdot d\right)$ [m]	steepness $s_{m-1,0} = \frac{H_s}{L_{m-1,0}}$ [-]	duration for 1000 waves [min]
w1	0.09	1.670	1.518	2.873	0.031	28
w2	0.09	1.181	1.074	1.710	0.053	20
w3	0.12	1.929	1.754	3.459	0.035	33
w4	0.12	1.364	1.240	2.154	0.056	23
w5	0.15	2.156	1.960	3.960	0.038	36
w6	0.15	1.525	1.386	2.535	0.059	26

Table-annex 5 Wave parameters, flow depth d = 0.55 m wave characteristics I (1:3 and 1:6 sloped dike)

wave spectra	Hs [m]	Tp [s]	$T_{m-1,0} = \frac{T_p}{1.1}$ [s]	$L_{m-1,0} = \frac{g \cdot T_{m-1,0}^2}{2\pi} \cdot \tanh\left(\frac{2\pi}{L_{m-1,0}} \cdot d\right)$ [m]	steepness $s_{m-1,0} = \frac{H_s}{L_{m-1,0}}$ [-]	duration for 1000 waves [min]
w1	0.07	1.474	1.340	2.478	0.028	25
w2	0.07	1.045	0.950	1.390	0.050	18
w3	0.10	1.76	1.600	3.180	0.031	30
w4	0.10	1.243	1.130	1.893	0.053	21
w5	0.15	2.156	1.960	4.113	0.036	36
w6	0.15	1.529	1.390	2.614	0.057	26

Table-annex 6 Wave parameters, flow depth d = 0.55 m wave characteristics II (1:6 sloped dike)

wave spectra	Hs [m]	Tp [s]	$T_{m-1,0} = \frac{T_p}{1.1}$ [s]	$L_{m-1,0} = \frac{g \cdot T_{m-1,0}^2}{2\pi} \cdot \tanh\left(\frac{2\pi}{L_{m-1,0}} \cdot d\right)$ [m]	steepness $s_{m-1,0} = \frac{H_s}{L_{m-1,0}}$ [-]	duration for 1000 waves [min]
w1	0.09	1.670	1.518	2.962	0.030	28
w2	0.09	1.181	1.074	1.734	0.052	20
w3	0.12	1.929	1.754	3.581	0.033	33
w4	0.12	1.364	1.240	2.201	0.055	23
w5	0.15	2.156	1.960	4.113	0.036	36
w6	0.15	1.525	1.386	2.605	0.058	26

Annex E Test program - 1:3 sloped dike (FlowDike 1)

Table-annex 7 Test program - 1:3 sloped dike, flow depth d = 0.50 m, wave characteristic I (wc I)

testseries name	experiment date	wave direction [°] (+with current; - against current)	current [m/s]	wind speed [m/s]	wave spectra and its testnumber
s1_03_30_wi_00_00	02.02.09	0	0.30	0	w1 to w6 114, 115, 116, 117, 119, 120
s1_08_30_wi_49_00	03.02.09	0	0.30	10	w1, w3, w5 121, 122, 123
s1_19_30_wi_00_15w	03.02.09	+15	0.30	0	w1 to w6 124, 125, 126, 127, 128, 129
s1_16_30_wi_00_15a	04.02.09	-15	0.30	0	w1 to w6 131, 132, 133, 134, 135, 136
s1_08b_30_wi_25_00	04.02.09	0	0.30	5	w1, w3, w5 137, 138, 140
s1_01_00_wi_00_00	05.02.09	0	0.00	0	w1 to w6 144, 145, 146, 147, 148, 149 (144, 145, 198, 199, 200, 201)
s1_06b_00_wi_25_00	05.02.09	0	0.00	5	w1, w3, w5 150, 151, 152
s1_06_00_wi_49_00	05.02.09	0	0.00	10	w1, w3, w5 153, 154, 155
s1_12_00_wi_00_15w	06.02.09	+15	0.00	0	w1 to w6 156, 157, 158, 159, 160, 161
s1_11_15_wi_00_00	06.02.09	0	0.15	0	w1 to w6 162, 163, 164, 165, 166, 167
s1_13_15_wi_00_15w	09.02.09	+15	0.15	0	w1 to w6 168, 169, 170, 171, 172, 173
s1_15_15_wi_00_15a	09.02.09	-15	0.15	0	w1 to w6 174, 175, 176, 177, 178, 179
s2_02_00_wi_00_30w	11.02.09	+30	0.00	0	w1 to w6 180, 181, 182, 183, 184, 185
s2_07b_00_wi_25_30w	11.02.09	+30	0.00	5	w1, w3, w5 186, 187, 188
s2_07_00_wi_49_30w	11.02.09	+30	0.00	10	w1, w3, w5 189, 190, 191
s2_20_15_wi_00_30w	12.02.09	+30	0.15	0	w1 to w6 192, 193, 194, 195, 196, 197
s2_04_30_wi_00_30w	12.02.09	+30	0.30	0	w1 to w6 202, 203, 204, 205, 206, 207
s2_09b_30_wi_25_30w	13.02.09	+30	0.30	5	w1, w3, w5 208, 209, 210
s2_09_30_wi_49_30w	13.02.09	+30	0.30	10	w1, w3, w5 211, 212, 213
s3_18_00_wi_00_45a	17.02.09	-45	0.00	0	w1 to w5 215, 216, 217, 218, 220
s3_05_30_wi_00_30a	18.02.09	-30	0.30	0	w1 to w6 222, 223, 224, 225, 226, 227
s3_14_30_wi_00_45a	18.02.09	-45	0.30	0	w1 to w6 228, 229, 230, 231, 232, 233
s3_21_15_wi_00_30a	19.02.09	-30	0.15	0	w1 to w6 234, 235, 236, 237, 238, 239
s3_17_15_wi_00_45a	19.02.09	-45	0.15	0	w1 to w6 240, 241, 242, 243, 244, 245

Annex F Test program - 1:6 sloped dike (FlowDike 2)

Table-annex 8 Test program - 1:6 sloped dike

testseries name	experiment date	flow depth [m]	wave characteristic	wave direction [°] (+with current; - against current)	current [m/s]	wind speed [m/s]	wave spectra and its testnumber (wave condition wc I or wave condition wc II)
s4_01_00_wi_00_00	09_11_19	0.50	wc I	0	0	0	w1 to w6 425, 427, 426, 428, 429, 430
s4_01a_00_wi_00_00	09_11_23+24	0.55	wc II	0	0	0	w1 to w6 451, 452, 453, 454, 456, 457
s4_02_00_wi_25_00	09_11_18+19	0.50	wc I	0	0	5	w1, w3, w5 418, 419, 421
s4_03_00_wi_49_00	09_11_19	0.50	wc I	0	0	10	w1, w3, w5 422, 423, 424
s4_03a_00_wi_49_00	09_11_25	0.55	wc II	0	0	10	w1, w3, w5 464, 465, 466,
s4_04_30_wi_00_00	09_11_17	0.50	wc I	0	0.30	0	w1 to w6 411, 410, 409, 408, 407, 406
s4_04a_30_wi_00_00	09_11_25	0.55	wc II	0	0.30	0	w1 to w6 458, 459, 460, 461, 462, 463
s4_05_30_wi_49_00	09_11_18	0.55	wc II	0	0.30	10	w1, w3, w5 412, 413, 414
s4_06_30_wi_25_00	09_11_18	0.50	wc I	0	0.30	5	w1, w3, w5 415, 416, 417
s4_07_15_wi_00_00	09_11_26	0.55	wc II	0	0.15	0	w1 to w6 467, 468, 469, 470, 471, 472
s4_08_15_wi_49_00	09_11_26	0.55	wc II	0	0.15	10	w1, w3, w5 473, 474, 475
s4_10_40_wi_00_00	09_11_27	0.55	wc II	0	0.40	0	w1 to w6 480, 481, 482, 483, 484, 485
s4_11_40_wi_49_00	09_11_27	0.55	wc II	0	0.40	10	w1, w3, w5 488, 489, 490

testseries name	experiment date	flow depth [m]	wave characteristic	wave direction [°] (+with current; -against current)	current [m/s]	wind speed [m/s]	wave spectra and its testnumber (wave condition wc I or wave condition wc II)
s4_32_30_wi_00_15w	09_11_20	0.50	wc I	+15	0.30	0	w1 to w6 432, 433, 434, 435, 437, 438
s4_33_30_wi_00_15a	09_11_20	0.50	wc I	-15	0.30	0	w3 to w6 440, 441, 442, 443
s4_34_00_wi_00_15w	09_11_23	0.55	wc II	+15	0.00	0	w1 to w6 444, 445, 447, 448, 449, 450
s4_35_15_wi_00_00	09_11_26	0.55	wc I	0	0.15	0	w1, w2 476, 477
s4_36_40_wi_00_00	09_11_27	0.55	wc I	0	0.40	0	w1, w2 486, 487
s5_13_00_wi_00_30w	09_12_01+02+03	0.55	wc II	+30	0.00	0	w1 to w6 511, 512, 513, 514, 515, 516
s5_15_00_wi_49_30w	09_12_03	0.55	wc II	+30	0.00	10	w1, w3, w5 536, 537, 538
s5_16_40_wi_00_30w	09_12_01	0.55	wc II	+30	0.40	0	w1 to w6 501, 502, 503, 504, 505, 506
s5_17_40_wi_49_30w	09_12_01	0.55	wc II	+30	0.40	10	w1, w3, w5 508, 509, 510
s5_19_30_wi_00_30w	09_12_02	0.55	wc II	+30	0.30	0	w1 to w6 517, 518, 519, 520, 521, 522
s5_20_30_wi_49_30w	09_12_02	0.55	wc II	+30	0.30	10	w1, w3, w5 523, 524, 525
s5_22_15_wi_00_30w	09_12_03	0.55	wc II	+30	0.15	0	w1 to w6 530, 531, 532, 533, 534, 535
s6_25_00_wi_00_45a	09_12_08+09	0.55	wc II	-45	0.00	0	w1 to w6 613, 614, 615, 616, 617, 618
s6_26_15_wi_00_30a	09_12_07+08	0.55	wc II	-30	0.15	0	w1 to w6 607, 608, 609, 610, 611, 612
s6_27_15_wi_00_45a	09_12_07	0.55	wc II	-45	0.15	0	w1 to w6 601, 602, 603, 604, 605, 606
s6_28_30_wi_00_30a	09_12_08+09	0.55	wc II	-30	0.30	0	w1 to w6 625, 626, 627, 628, 629, 630

testseries name	experiment date	flow depth [m]	wave characteristic	wave direction [°] (+with current; - against current)	current [m/s]	wind speed [m/s]	wave spectra and its testnumber (wave condition wc I or wave condition wc II)
s6_29_30_wi_00_45a	09_12_08	0.55	wc II	-45	0.30	0	w1 to w6 619, 620, 621, 622, 623, 624
s6_30_40_wi_00_30a	09_12_10	0.55	wc II	-30	0.40	0	w1 to w6 637, 638, 639, 640, 641, 642
s6_31_40_wi_00_45a	09_12_09+10	0.55	wc II	-45	0.40	0	w1 to w6 631, 632, 633, 634, 635, 636

Annex G Calibration function - Micro propeller

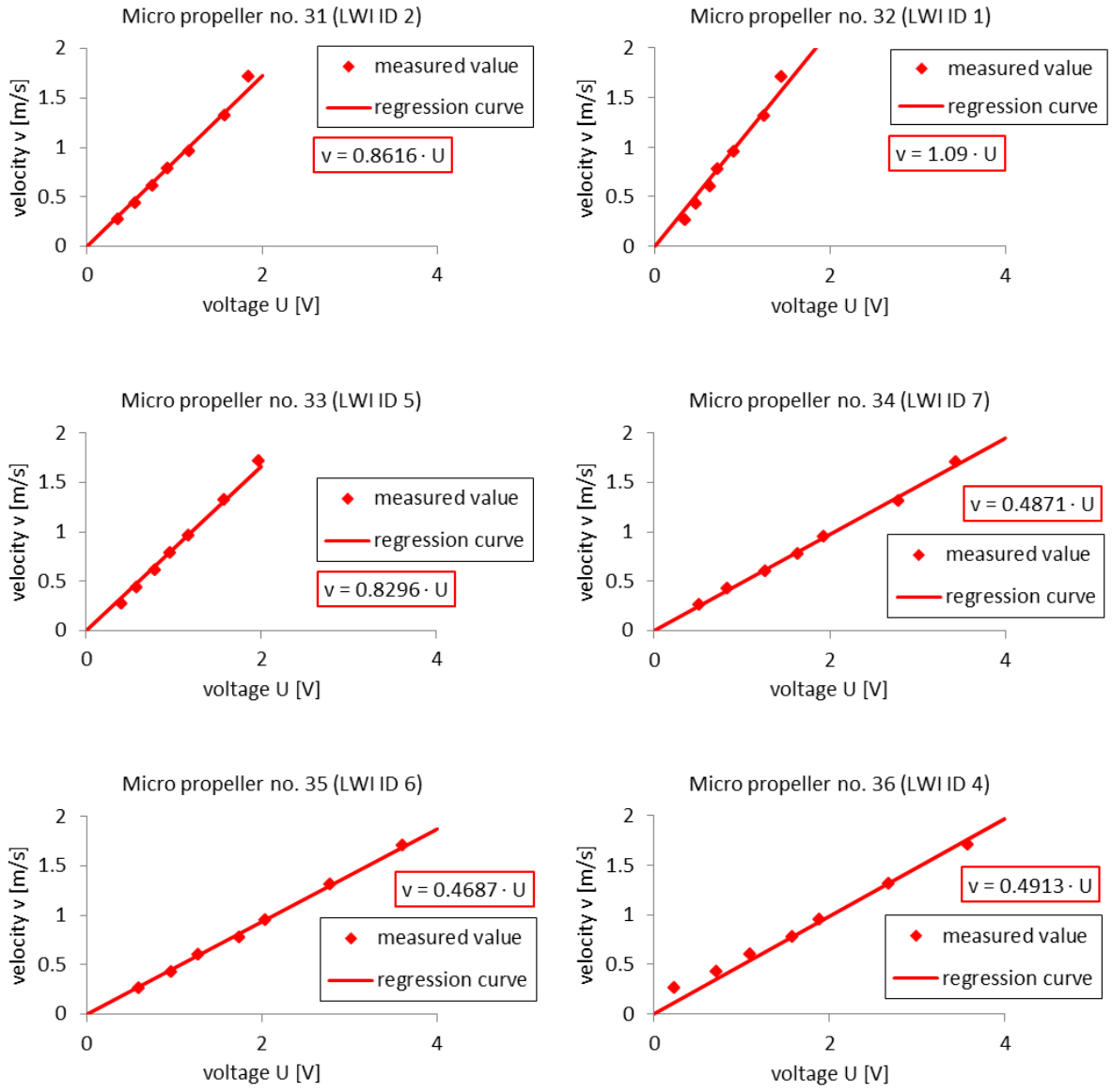

Figure annex 7 Calibration curves for micro propeller in flow direction from LWI, TU Braunschweig (used on 1:3 sloped dike)

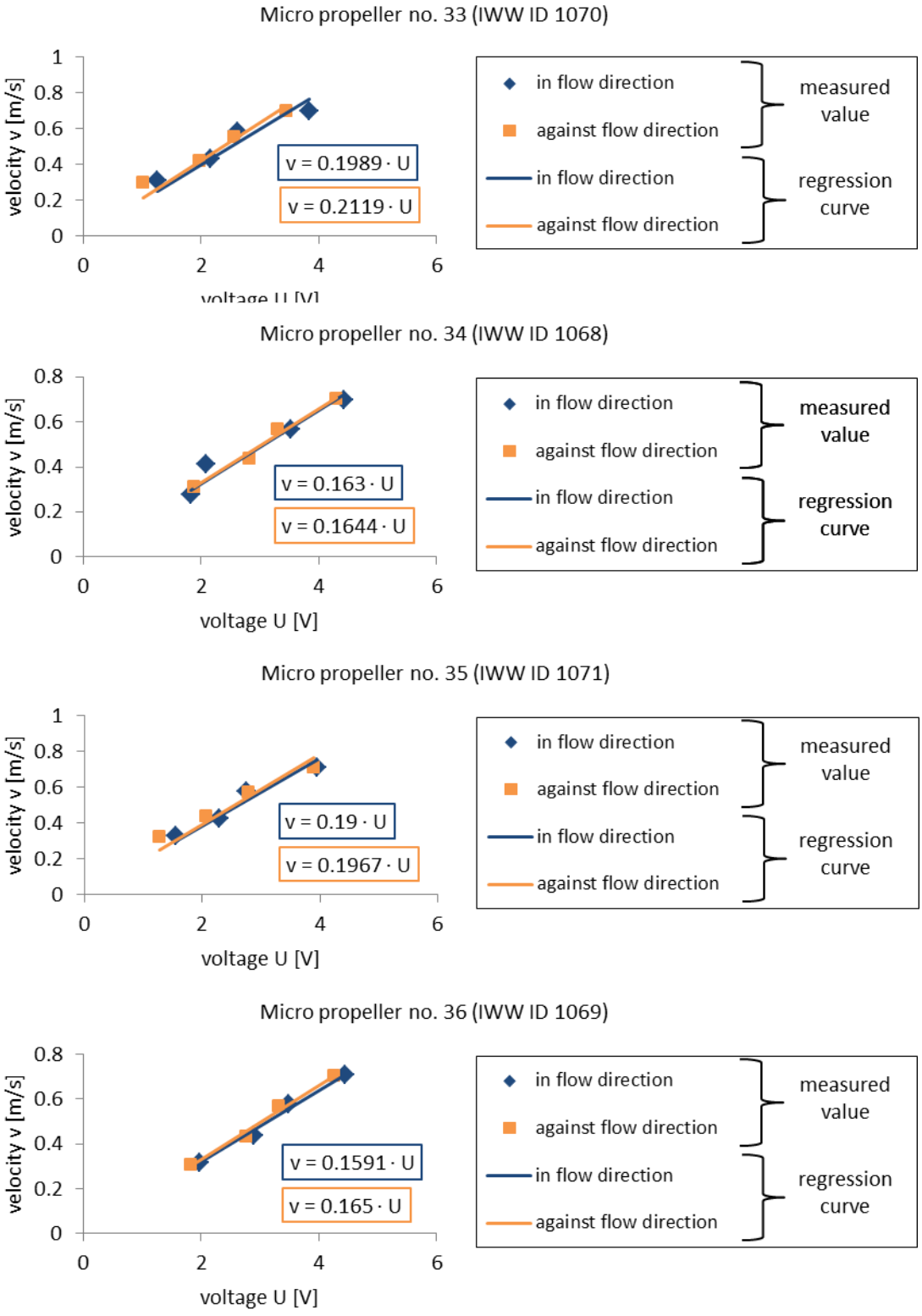

Figure-annex 8 Calibration curves for micro propeller of RWTH Aachen University (used on 1:6 sloped dike)

Annex H Analyzed data - wave field – 1:3 sloped dike (FlowDike 1)

Table-annex 9 Test program - 1:3 sloped dike, flow depth d = 0.50 m, wave characetristics I (wc I)

test-number	testseries name [1]	no. of waves of test	at toe of 0.6 m dike			at toe of 0.7 m dike		
			H_{m0} [m]	T_p [s]	$T_{m-1,0}$ [s]	H_{m0} [m]	T_p [s]	$T_{m-1,0}$ [s]
144	s1_01_00_w1_00_00	1162	0.0706	1.4629	1.3494	0.068	1.4629	1.3271
145	s1_01_00_w2_00_00	1087	0.0588	1.0503	1.0196	0.0649	1.0779	1.0116
198	s1_01_00_w3_00_00	1180	0.1004	1.7809	1.599	0.095	1.7809	1.5762
199	s1_01_00_w4_00_00	1110	0.092	1.28	1.1639	0.0945	1.2047	1.1451
200	s1_01_00_w5_00_00	1283	0.1476	2.1558	1.8882	0.1399	2.1558	1.8722
201	s1_01_00_w6_00_00	1139	0.1449	1.517	1.4384	0.1407	1.517	1.4148
114	s1_03_30_w1_00_00	1364	0.0509	1.1703	1.0392	0.0538	1.1378	1.0333
115	s1_03_30_w2_00_00	1242	0.0466	0.7877	0.7858	0.0493	0.7877	0.787
116	s1_03_30_w3_00_00	1273	0.0966	1.6384	1.4261	0.1043	1.5754	1.4287
117	s1_03_30_w4_00_00	1191	0.1006	1.1703	1.0643	0.1038	1.1378	1.0574
119	s1_03_30_w5_00_00	1311	0.1416	2.1558	1.8873	0.1409	2.1558	1.8584
120	s1_03_30_w6_00_00	1189	0.131	1.517	1.4075	0.1394	1.517	1.4055
153	s1_06_00_w1_49_00	1149	0.069	1.4629	1.3615	0.0672	1.4629	1.3335
154	s1_06_00_w3_49_00	1142	0.0985	1.7809	1.6052	0.0936	1.7809	1.5757
155	s1_06_00_w5_49_00	1261	0.144	2.1558	1.8885	0.1348	2.1558	1.8709
150	s1_06b_00_w1_25_00	1135	0.0693	1.4629	1.3583	0.0676	1.4629	1.3319
151	s1_06b_00_w3_25_00	1141	0.0994	1.7809	1.6019	0.094	1.7809	1.5737
152	s1_06b_00_w5_25_00	1255	0.1467	2.1558	1.8893	0.1363	2.1558	1.8737
121	s1_08_30_w1_49_00	1338	0.0496	1.2412	1.1161	0.0502	1.2412	1.1084
122	s1_08_30_w3_49_00	1204	0.0929	1.7809	1.5663	0.0939	1.7809	1.5493
123	s1_08_30_w5_49_00	1277	0.1447	2.1558	1.9173	0.1423	2.1558	1.8792

[1] Composition of testseries name (e. i. s1_01_00_w1_00_00):
s1 (set-up no.) _ 01 (no. of testseries) _ 00 (current [m/(100s)]) _ w1 (wave no.) _ 00 (wind [Hz (wind generator)]) _ 00 (angle of wave attack [°], w = with or a = against current)

test-number	testseries name [1]	no. of waves of test	at toe of 0.6 m dike			at toe of 0.7 m dike		
			H_{m0} [m]	T_p [s]	$T_{m-1,0}$ [s]	H_{m0} [m]	T_p [s]	$T_{m-1,0}$ [s]
137	s1_08b_30_w1_25_00	1165	0.064	1.517	1.2977	0.0684	1.4629	1.3118
138	s1_08b_30_w3_25_00	1164	0.0947	1.7067	1.5782	0.0958	1.7809	1.5644
140	s1_08b_30_w5_25_00	1275	0.1404	2.1558	1.911	0.1402	2.1558	1.8689
162	s1_11_15_w1_00_00	1173	0.0651	1.4629	1.3187	0.0671	1.4124	1.3084
163	s1_11_15_w2_00_00	1092	0.0663	1.0503	1.0152	0.065	1.024	1.0048
164	s1_11_15_w3_00_00	1186	0.0997	1.7809	1.5933	0.0962	1.7809	1.5732
165	s1_11_15_w4_00_00	1097	0.0907	1.2047	1.127	0.0982	1.28	1.1477
166	s1_11_15_w5_00_00	1301	0.1509	2.1558	1.9067	0.1435	2.1558	1.8659
167	s1_11_15_w6_00_00	1189	0.1395	1.517	1.4266	0.1367	1.517	1.4036
156	s1_12_00_w1_00_15w	1180	0.067	1.4629	1.2898	0.0747	1.4629	1.3191
157	s1_12_00_w2_00_15w	1063	0.0728	1.0503	0.9865	0.0722	1.024	0.9762
158	s1_12_00_w3_00_15w	1252	0.0884	1.7067	1.4861	0.096	1.7067	1.5004
159	s1_12_00_w4_00_15w	1140	0.1008	1.2047	1.1361	0.0992	1.2412	1.1449
160	s1_12_00_w5_00_15w	1414	0.1365	2.1558	1.8386	0.1332	2.1558	1.7817
161	s1_12_00_w6_00_15w	1211	0.1343	1.517	1.3844	0.1473	1.517	1.4134
168	s1_13_15_w1_00_15w	1169	0.0707	1.4124	1.3041	0.0692	1.4124	1.2971
169	s1_13_15_w2_00_15w	1037	0.0697	1.024	0.9793	0.0716	1.0503	0.9859
170	s1_13_15_w3_00_15w	1244	0.0914	1.7067	1.4941	0.0931	1.7809	1.4929
171	s1_13_15_w4_00_15w	1095	0.1037	1.2412	1.152	0.1032	1.2412	1.1451
172	s1_13_15_w5_00_15w	1428	0.1321	2.1558	1.797	0.1273	2.1558	1.7801
173	s1_13_15_w6_00_15w	1199	0.1412	1.517	1.3935	0.1386	1.5754	1.3867
174	s1_15_15_w1_00_15a	1160	0.0785	1.4629	1.3372	0.0713	1.4629	1.3118
175	s1_15_15_w2_00_15a	1043	0.071	1.0503	0.9988	0.0715	1.0503	0.9852
176	s1_15_15_w3_00_15a	1241	0.1036	1.7809	1.5226	0.094	1.7809	1.5084
177	s1_15_15_w4_00_15a	1137	0.1074	1.2412	1.1698	0.0989	1.28	1.1567
178	s1_15_15_w5_00_15a	1405	0.1409	2.1558	1.786	0.1323	2.1558	1.8015
179	s1_15_15_w6_00_15a	1166	0.1525	1.517	1.4042	0.1402	1.517	1.4046
131	s1_16_30_w1_00_15a	1151	0.0762	1.4629	1.351	0.0706	1.517	1.3333
132	s1_16_30_w2_00_15a	1055	0.0692	1.024	0.9893	0.0692	1.024	0.9908

test-number	testseries name [1]	no. of waves of test	at toe of 0.6 m dike			at toe of 0.7 m dike		
			H_{m0} [m]	T_p [s]	$T_{m-1,0}$ [s]	H_{m0} [m]	T_p [s]	$T_{m-1,0}$ [s]
133	s1_16_30_w3_00_15a	1213	0.1068	1.7067	1.554	0.0988	1.7067	1.5314
134	s1_16_30_w4_00_15a	1081	0.0994	1.2412	1.1787	0.0972	1.2412	1.1655
135	s1_16_30_w5_00_15a	1367	0.1474	2.1558	1.8346	0.1322	2.1558	1.8088
136	s1_16_30_w6_00_15a	1139	0.1541	1.517	1.437	0.1465	1.517	1.4381
124	s1_19_30_w1_00_15w	1166	0.071	1.517	1.3281	0.0663	1.4629	1.2914
125	s1_19_30_w2_00_15w	1066	0.0691	1.024	0.9787	0.0696	1.0503	0.9855
126	s1_19_30_w3_00_15w	1213	0.0948	1.7067	1.5225	0.0908	1.7809	1.5114
127	s1_19_30_w4_00_15w	1148	0.0941	1.1703	1.1437	0.0958	1.2412	1.138
128	s1_19_30_w5_00_15w	1407	0.1234	2.048	1.7655	0.1267	2.1558	1.7962
129	s1_19_30_w6_00_15w	1195	0.1449	1.517	1.4161	0.1322	1.517	1.3897
180	s2_02_00_w1_00_30w	1161	0.081	1.4629	1.3234	0.0768	1.4629	1.3028
181	s2_02_00_w2_00_30w	1038	0.0785	1.0503	0.9915	0.0805	0.999	0.9895
182	s2_02_00_w3_00_30w	1169	0.1077	1.7067	1.5331	0.1074	1.7809	1.5711
183	s2_02_00_w4_00_30w	1091	0.1091	1.28	1.1701	0.1112	1.2412	1.1571
184	s2_02_00_w5_00_30w	1297	0.1444	2.048	1.8459	0.159	2.1558	1.8861
185	s2_02_00_w6_00_30w	1143	0.1554	1.517	1.4432	0.1635	1.517	1.4158
202	s2_04_30_w1_00_30w	1128	0.0717	1.4124	1.3305	0.0808	1.4629	1.3393
203	s2_04_30_w2_00_30w	1037	0.072	1.024	1.0121	0.0743	1.0779	1.0389
204	s2_04_30_w3_00_30w	1234	0.1056	1.7809	1.5945	0.1089	1.7067	1.5529
205	s2_04_30_w4_00_30w	1102	0.104	1.28	1.1743	0.1114	1.28	1.1972
206	s2_04_30_w5_00_30w	1256	0.1527	2.1558	1.8652	0.1463	2.1558	1.8172
207	s2_04_30_w6_00_30w	1167	0.1498	1.4629	1.4344	0.1556	1.4629	1.4273
189	s2_07_00_w1_49_30w	1131	0.0808	1.4629	1.3274	0.0743	1.4629	1.3177
190	s2_07_00_w3_49_30w	1150	0.1066	1.7067	1.5336	0.1054	1.7809	1.5813
191	s2_07_00_w5_49_30w	1276	0.1418	2.048	1.846	0.1553	2.1558	1.8883
186	s2_07b_00_w1_25_30w	1124	0.0807	1.4629	1.3233	0.0752	1.4629	1.307
187	s2_07b_00_w3_25_30w	1152	0.1069	1.7067	1.5317	0.1062	1.7809	1.576
188	s2_07b_00_w5_25_30w	1272	0.1435	2.048	1.845	0.1576	2.1558	1.8871
211	s2_09_30_w1_49_30w	1127	0.0714	1.4124	1.3344	0.0811	1.4629	1.3417

test-number	testseries name [1]	no. of waves of test	at toe of 0.6 m dike			at toe of 0.7 m dike		
			H_{m0} [m]	T_p [s]	$T_{m-1,0}$ [s]	H_{m0} [m]	T_p [s]	$T_{m-1,0}$ [s]
212	s2_09_30_w3_49_30w	1228	0.1055	1.7809	1.6022	0.1092	1.7067	1.5555
213	s2_09_30_w5_49_30w	1269	0.1513	2.1558	1.8688	0.1463	2.1558	1.8159
208	s2_09b_30_w1_25_30w	1126	0.072	1.4124	1.3317	0.0812	1.4629	1.3413
209	s2_09b_30_w3_25_30w	1225	0.1058	1.7809	1.5978	0.1095	1.7067	1.5553
210	s2_09b_30_w5_25_30w	1260	0.1519	2.1558	1.8654	0.1469	2.1558	1.817
192	s2_20_15_w1_00_30w	1138	0.0702	1.517	1.302	0.0832	1.517	1.3265
193	s2_20_15_w2_00_30w	1017	0.079	1.0503	0.9998	0.0811	1.0779	1.0158
194	s2_20_15_w3_00_30w	1227	0.1057	1.7809	1.5705	0.1147	1.7067	1.543
195	s2_20_15_w4_00_30w	1076	0.1078	1.2412	1.153	0.1198	1.2047	1.1768
196	s2_20_15_w5_00_30w	1305	0.1482	2.1558	1.8706	0.158	2.1558	1.8391
197	s2_20_15_w6_00_30w	1163	0.1487	1.5754	1.4374	0.1662	1.517	1.4182
222	s3_05_30_w1_00_30a	1173	0.0764	1.4629	1.3276	0.0707	1.4124	1.3361
223	s3_05_30_w2_00_30a	1022	0.0748	1.024	1.0217	0.0723	0.999	1.026
224	s3_05_30_w3_00_30a	1228	0.1034	1.7809	1.531	0.0999	1.7809	1.5597
225	s3_05_30_w4_00_30a	1061	0.1045	1.28	1.1906	0.0989	1.2047	1.1966
226	s3_05_30_w5_00_30a	1200	0.146	2.1558	1.833	0.155	2.1558	1.8948
227	s3_05_30_w6_00_30a	1086	0.1514	1.517	1.4638	0.1416	1.517	1.4998
228	s3_14_30_w1_00_45a	1128	0.0877	1.4124	1.3469	0.0962	1.3653	1.354
229	s3_14_30_w2_00_45a	968	0.0812	1.0503	1.0622	0.0853	1.107	1.0732
230	s3_14_30_w3_00_45a	1212	0.1249	1.7809	1.565	0.1302	1.7809	1.5468
231	s3_14_30_w4_00_45a	1044	0.1155	1.3213	1.2162	0.1244	1.3213	1.2392
232	s3_14_30_w5_00_45a	1323	0.175	2.1558	1.856	0.1668	2.1558	1.8396
233	s3_14_30_w6_00_45a	1105	0.1284	1.4629	1.5008	0.1481	1.517	1.4962
240	s3_17_15_w1_00_45a	1147	0.0902	1.517	1.3363	0.0975	1.4629	1.3348
241	s3_17_15_w2_00_45a	992	0.0885	1.0503	1.026	0.0918	1.024	1.0359
242	s3_17_15_w3_00_45a	1235	0.1255	1.7067	1.5409	0.1282	1.7067	1.5181
243	s3_17_15_w4_00_45a	1037	0.1198	1.2412	1.196	0.1276	1.2412	1.197
244	s3_17_15_w5_00_45a	1367	0.1753	2.1558	1.8442	0.171	2.1558	1.8263
245	s3_17_15_w6_00_45a	1131	0.1362	1.5754	1.4822	0.1384	1.5754	1.4718

test-number	testseries name [1]	no. of waves of test	at toe of 0.6 m dike			at toe of 0.7 m dike		
			H_{m0} [m]	T_p [s]	$T_{m-1,0}$ [s]	H_{m0} [m]	T_p [s]	$T_{m-1,0}$ [s]
215	s3_18_00_w1_00_45a	1195	0.0965	1.4629	1.3101	0.0869	1.517	1.3089
216	s3_18_00_w2_00_45a	1018	0.0957	1.0503	1.0189	0.0937	1.024	1.007
217	s3_18_00_w3_00_45a	1208	0.1232	1.7067	1.4837	0.1231	1.7809	1.5282
218	s3_18_00_w4_00_45a	1082	0.1253	1.2047	1.1761	0.1264	1.2412	1.166
220	s3_18_00_w5_00_45a	1369	0.1575	2.1558	1.7751	0.1704	2.1558	1.8138
234	s3_21_15_w1_00_30a	1180	0.079	1.4629	1.3178	0.0787	1.4124	1.2868
235	s3_21_15_w2_00_30a	1011	0.079	1.024	1.0021	0.0858	1.024	1.0064
236	s3_21_15_w3_00_30a	1255	0.1021	1.7067	1.5068	0.1033	1.7809	1.4957
237	s3_21_15_w4_00_30a	1071	0.1084	1.2412	1.1724	0.1148	1.2047	1.166
238	s3_21_15_w5_00_30a	1289	0.1431	2.1558	1.8129	0.1475	2.1558	1.8249
239	s3_21_15_w6_00_30a	1129	0.1512	1.517	1.439	0.1483	1.517	1.4391

Annex I Analyzed data - wave field – 1:6 sloped dike (FlowDike 2)

Table-annex 10 Test program - 1:6 sloped dike

test-number	testseries name[2]	water depth [m]	no. of waves of test	wave characteristic wc I or wc II	in front of wave generator			at toe of 0.6 m dike			at toe of 0.7 m dike		
					H_{m0} [m]	T_p [s]	$T_{m-1,0}$ [s]	H_{m0} [m]	T_p [s]	$T_{m-1,0}$ [s]	H_{m0} [m]	T_p [s]	$T_{m-1,0}$ [s]
425	s4_01_00_w1_00_00	0.5	1240	wc I	0.0658	1.5059	1.3736	0.0653	1.5059	1.3547	0.0698	1.4222	1.3496
427	s4_01_00_w2_00_00	0.5	1210	wc I	0.0614	1.024	0.9836	0.0633	1.024	0.9968	0.0652	1.024	1.0011
426	s4_01_00_w3_00_00	0.5	1259	wc I	0.0995	1.7067	1.6411	0.0957	1.7067	1.6051	0.1024	1.7067	1.6125
428	s4_01_00_w4_00_00	0.5	1157	wc I	0.0868	1.219	1.1858	0.0946	1.219	1.178	0.0994	1.219	1.1764
429	s4_01_00_w5_00_00	0.5	1270	wc I	0.1538	2.1333	1.9538	0.1422	2.1333	1.8747	0.1522	2.1333	1.9465
430	s4_01_00_w6_00_00	0.5	1194	wc I	0.1366	1.5059	1.4722	0.1349	1.5059	1.4332	0.1425	1.5059	1.4187
451	s4_01a_00_w1_00_00	0.55	1333	wc II	0.0896	1.7067	1.5472	0.0865	1.6	1.5275	0.0929	1.7067	1.5221
452	s4_01a_00_w2_00_00	0.55	1242	wc II	0.0802	1.219	1.1055	0.0849	1.219	1.1159	0.0914	1.1636	1.1063
453	s4_01a_00_w3_00_00	0.55	1386	wc II	0.1222	1.8286	1.7765	0.1146	1.8286	1.7364	0.1225	1.9692	1.7326
454	s4_01a_00_w4_00_00	0.55	1253	wc II	0.1098	1.3474	1.2924	0.111	1.28	1.272	0.1191	1.3474	1.2636
456	s4_01a_00_w5_00_00	0.55	1000	wc II	0.1538	2.1333	1.9499	0.1429	2.1333	1.8882	0.1498	2.1333	1.9204
457	s4_01a_00_w6_00_00	0.55	1261	wc II	0.1408	1.5059	1.4588	0.1384	1.5059	1.4266	0.1468	1.5059	1.4176
418	s4_02_00_w1_25_00	0.5	1210	wc I	0.0649	1.5059	1.3616	0.0656	1.5059	1.334	0.0694	1.4222	1.329
419	s4_02_00_w3_25_00	0.5	1201	wc I	0.0961	1.7067	1.6266	0.0937	1.7067	1.5797	0.0985	1.7067	1.5764
421	s4_02_00_w5_25_00	0.5	1205	wc I	0.1537	2.1333	1.9587	0.1415	2.1333	1.8791	0.1523	2.1333	1.9447
422	s4_03_00_w1_49_00	0.5	1167	wc I	0.0652	1.5059	1.3868	0.0652	1.5059	1.364	0.0692	1.4222	1.3637
423	s4_03_00_w3_49_00	0.5	1143	wc I	0.0999	1.7067	1.6533	0.0957	1.7067	1.6123	0.1033	1.7067	1.6214
424	s4_03_00_w5_49_00	0.5	1182	wc I	0.1532	2.1333	1.9622	0.1408	2.1333	1.8812	0.1532	2.1333	1.9475
464	s4_03a_00_w1_49_00	0.55	1263	wc II	0.0882	1.7067	1.5739	0.0861	1.6	1.5315	0.0928	1.6	1.5353

[2] Composition of testseries name (e. i. s1_01_00_w1_00_00):
s1 (set-up no.) _ 01 (no. of testseries) _ 00 (current [m/(100s)]) _ w1 (wave no.) _ 00 (wind [Hz (wind generator)]) _ 00 (angle of wave attack [°], w = with or a = against current)

test-number	testseries name[2]	water depth [m]	no. of waves of test	wave characteristic wc I or wc II	in front of wave generator			at toe of 0.6 m dike			at toe of 0.7 m dike		
					H_{m0} [m]	T_p [s]	$T_{m-1,0}$ [s]	H_{m0} [m]	T_p [s]	$T_{m-1,0}$ [s]	H_{m0} [m]	T_p [s]	$T_{m-1,0}$ [s]
465	s4_03a_00_w3_49_00	0.55	1341	wc II	0.1207	1.8286	1.8021	0.1122	1.8286	1.7404	0.1225	1.9692	1.7424
466	s4_03a_00_w5_49_00	0.55	1306	wc II	0.1566	2.1333	1.9714	0.1409	2.1333	1.8966	0.1534	2.1333	1.9365
411	s4_04_30_w1_00_00	0.5	1266	wc I	0.064	1.4222	1.3204	0.0699	1.4222	1.3172	0.0723	1.5059	1.3579
410	s4_04_30_w2_00_00	0.5	1089	wc I	0.0631	1.0667	1.051	0.0686	1.024	1	0.0654	1.024	1.0795
409	s4_04_30_w3_00_00	0.5	1247	wc I	0.0923	1.7067	1.5974	0.0948	1.7067	1.564	0.1002	1.7067	1.6124
408	s4_04_30_w4_00_00	0.5	1101	wc I	0.0954	1.219	1.1526	0.0986	1.219	1.1488	0.095	1.219	1.1883
407	s4_04_30_w5_00_00	0.5	1240	wc I	0.1434	2.1333	1.9302	0.1444	2.1333	1.8734	0.1501	2.1333	1.9922
406	s4_04_30_w6_00_00	0.5	1168	wc I	0.1308	1.5059	1.4179	0.1415	1.5059	1.3985	0.1457	1.5059	1.4772
458	s4_04a_30_w1_00_00	0.55	1350	wc II	0.0813	1.7067	1.5293	0.0839	1.6	1.5049	0.0889	1.7067	1.5154
459	s4_04a_30_w2_00_00	0.55	1266	wc II	0.0848	1.1636	1.111	0.0855	1.219	1.1056	0.0905	1.1636	1.1068
460	s4_04a_30_w3_00_00	0.55	1375	wc II	0.119	1.9692	1.7985	0.1168	1.9692	1.7592	0.1249	1.9692	1.755
461	s4_04a_30_w4_00_00	0.55	1258	wc II	0.1056	1.3474	1.2673	0.1136	1.3474	1.2691	0.1211	1.3474	1.2659
462	s4_04a_30_w5_00_00	0.55	1359	wc II	0.1538	2.1333	1.9781	0.1511	2.1333	1.9211	0.1571	2.1333	1.9402
463	s4_04a_30_w6_00_00	0.55	1276	wc II	0.1309	1.5059	1.4372	0.1388	1.5059	1.4134	0.148	1.5059	1.4117
412	s4_05_30_w1_49_00	0.55	1207	wc II	0.0621	1.4222	1.3244	0.0663	1.5059	1.3294	0.07	1.4222	1.3352
413	s4_05_30_w3_49_00	0.55	1182	wc II	0.0901	1.7067	1.6039	0.0898	1.7067	1.5738	0.0964	1.7067	1.5752
414	s4_05_30_w5_49_00	0.55	1175	wc II	0.1404	2.1333	1.9312	0.1371	2.1333	1.8786	0.1443	2.1333	1.9164
415	s4_06_30_w1_25_00	0.5	1237	wc I	0.0624	1.4222	1.32	0.0665	1.5059	1.324	0.0707	1.4222	1.332
416	s4_06_30_w3_25_00	0.5	1245	wc I	0.0903	1.8286	1.6016	0.0902	1.7067	1.5697	0.0969	1.7067	1.5722
417	s4_06_30_w5_25_00	0.5	1224	wc I	0.1414	2.1333	1.9318	0.138	2.1333	1.8778	0.145	2.1333	1.9142
467	s4_07_15_w1_00_00	0.55	1351	wc II	0.0839	1.6	1.5486	0.083	1.7067	1.5153	0.0884	1.6	1.5202
468	s4_07_15_w2_00_00	0.55	1246	wc II	0.0803	1.1636	1.0994	0.0842	1.1636	1.1078	0.0888	1.219	1.1089
469	s4_07_15_w3_00_00	0.55	1392	wc II	0.1198	1.9692	1.8043	0.115	1.9692	1.76	0.1215	1.9692	1.753
470	s4_07_15_w4_00_00	0.55	1259	wc II	0.1039	1.3474	1.2749	0.1126	1.3474	1.276	0.1174	1.3474	1.267
471	s4_07_15_w5_00_00	0.55	1375	wc II	0.1558	2.1333	1.9805	0.1472	2.1333	1.9182	0.1532	2.1333	1.9421
472	s4_07_15_w6_00_00	0.55	1292	wc II	0.1351	1.5059	1.4524	0.1369	1.5059	1.4158	0.1428	1.5059	1.4177
473	s4_08_15_w1_49_00	0.55	1284	wc II	0.084	1.6	1.5549	0.0828	1.7067	1.5231	0.0882	1.6	1.5279

test-number	testseries name[2]	water depth [m]	no. of waves of test	wave characteristic wc I or wc II	in front of wave generator			at toe of 0.6 m dike			at toe of 0.7 m dike		
					H_{m0} [m]	T_p [s]	$T_{m-1,0}$ [s]	H_{m0} [m]	T_p [s]	$T_{m-1,0}$ [s]	H_{m0} [m]	T_p [s]	$T_{m-1,0}$ [s]
474	s4_08_15_w3_49_00	0.55	1312	wc II	0.1197	1.9692	1.8084	0.1144	1.9692	1.7688	0.1213	1.9692	1.7629
475	s4_08_15_w5_49_00	0.55	1297	wc II	0.1559	2.1333	1.9809	0.147	2.1333	1.9263	0.1534	2.1333	1.9491
480	s4_10_40_w1_00_00	0.55	1361	wc II	0.0789	1.7067	1.5182	0.0853	1.6	1.5183	0.0877	1.7067	1.516
481	s4_10_40_w2_00_00	0.55	1273	wc II	0.0829	1.219	1.1212	0.0856	1.1636	1.1112	0.0896	1.1636	1.109
482	s4_10_40_w3_00_00	0.55	1388	wc II	0.1134	1.9692	1.7912	0.1158	1.9692	1.7548	0.123	1.9692	1.7523
483	s4_10_40_w4_00_00	0.55	1281	wc II	0.1093	1.3474	1.2733	0.113	1.3474	1.2688	0.1194	1.4222	1.2707
484	s4_10_40_w5_00_00	0.55	1359	wc II	0.1479	2.1333	1.9785	0.1497	2.1333	1.921	0.1546	2.1333	1.9438
485	s4_10_40_w6_00_00	0.55	1274	wc II	0.128	1.5059	1.4292	0.138	1.5059	1.4198	0.1465	1.5059	1.4088
488	s4_11_40_w1_49_00	0.55	1297	wc II	0.0793	1.7067	1.5281	0.085	1.6	1.5297	0.0883	1.6	1.5209
489	s4_11_40_w3_49_00	0.55	1335	wc II	0.1133	1.9692	1.8032	0.1151	1.9692	1.7676	0.1234	1.9692	1.76
490	s4_11_40_w5_49_00	0.55	1304	wc II	0.1479	2.1333	1.9877	0.1495	2.1333	1.9315	0.1554	2.1333	1.9511
432	s4_32_30_w1_00_15w	0.5	1185	wc I	0.0652	1.4222	1.3675	0.0648	1.4222	1.3582	0.0666	1.5059	1.3601
433	s4_32_30_w2_00_15w	0.5	1044	wc I	0.0577	1.0667	1.0088	0.0589	1.024	1.0085	0.0626	1.024	1.0063
434	s4_32_30_w3_00_15w	0.5	1311	wc I	0.0821	1.7067	1.529	0.0865	1.7067	1.5515	0.0897	1.7067	1.5346
435	s4_32_30_w4_00_15w	0.5	1092	wc I	0.0864	1.28	1.1876	0.0896	1.219	1.1822	0.0925	1.28	1.1721
437	s4_32_30_w5_00_15w	0.5	1337	wc I	0.1229	2.1333	1.824	0.1228	2.1333	1.7823	0.1403	2.1333	1.8995
438	s4_32_30_w6_00_15w	0.5	1172	wc I	0.1344	1.5059	1.4375	0.1335	1.5059	1.4172	0.1424	1.5059	1.4201
440	s4_33_30_w3_00_15a	0.5	1232	wc I	0.1051	1.7067	1.611	0.0993	1.7067	1.5908	0.1026	1.7067	1.5656
441	s4_33_30_w4_00_15a	0.5	1086	wc I	0.0933	1.28	1.2051	0.0941	1.219	1.1909	0.1001	1.219	1.1835
442	s4_33_30_w5_00_15a	0.5	1309	wc I	0.1565	2.1333	1.8908	0.1363	2.1333	1.8171	0.1416	2.1333	1.8313
443	s4_33_30_w6_00_15a	0.5	1131	wc I	0.1537	1.5059	1.4778	0.1442	1.5059	1.4457	0.1555	1.5059	1.4257
444	s4_34_00_w1_00_15w	0.55	1342	wc II	0.0796	1.6	1.5099	0.0873	1.7067	1.5303	0.089	1.6	1.5193
445	s4_34_00_w2_00_15w	0.55	1204	wc II	0.0838	1.219	1.1215	0.0819	1.1636	1.1213	0.0869	1.1636	1.1194
447	s4_34_00_w3_00_15w	0.55	1405	wc II	0.1067	1.9692	1.764	0.1127	1.9692	1.7362	0.1168	1.9692	1.7551
448	s4_34_00_w4_00_15w	0.55	1235	wc II	0.109	1.3474	1.2631	0.1082	1.3474	1.2797	0.1167	1.3474	1.275
449	s4_34_00_w5_00_15w	0.55	1362	wc II	0.1403	2.1333	1.974	0.1394	2.1333	1.884	0.1539	2.1333	1.9745
450	s4_34_00_w6_00_15w	0.55	1246	wc II	0.1304	1.5059	1.4127	0.1389	1.5059	1.4322	0.1472	1.5059	1.4144

test-number	testseries name[2]	water depth [m]	no. of waves of test	wave characteristic wc I or wc II	in front of wave generator			at toe of 0.6 m dike			at toe of 0.7 m dike		
					H_{m0} [m]	T_p [s]	$T_{m-1,0}$ [s]	H_{m0} [m]	T_p [s]	$T_{m-1,0}$ [s]	H_{m0} [m]	T_p [s]	$T_{m-1,0}$ [s]
476	s4_35_15_w1_00_00	0.55	1271	wc II	0.0643	1.5059	1.3516	0.0677	1.4222	1.3331	0.0695	1.5059	1.3339
477	s4_35_15_w2_00_00	0.55	1106	wc II	0.0652	1.024	0.9826	0.0656	1.024	0.9818	0.0696	1.024	0.979
486	s4_36_40_w1_00_00	0.55	1345	wc II	0.0642	1.4222	1.3297	0.0675	1.5059	1.3327	0.0725	1.4222	1.3443
487	s4_36_40_w2_00_00	0.55	1144	wc II	0.065	1.024	0.996	0.0669	1.024	0.9852	0.0696	1.024	0.9833
511	s5_13_00_w1_00_30w	0.55	1317	wc II	0.0854	1.7067	1.5558	0.0796	1.7067	1.5517	0.0878	1.7067	1.5593
512	s5_13_00_w2_00_30w	0.55	1169	wc II	0.0737	1.1636	1.1434	0.0778	1.1636	1.1379	0.0789	1.1636	1.1393
513	s5_13_00_w3_00_30w	0.55	1363	wc II	0.1082	1.9692	1.7383	0.1164	1.9692	1.7969	0.1178	1.9692	1.7524
514	s5_13_00_w4_00_30w	0.55	1211	wc II	0.1029	1.4222	1.3144	0.1006	1.3474	1.2829	0.1049	1.3474	1.296
515	s5_13_00_w5_00_30w	0.55	1379	wc II	0.1239	2.1333	1.8695	0.1461	2.1333	1.9454	0.1374	2.1333	1.9244
516	s5_13_00_w6_00_30w	0.55	1217	wc II	0.1355	1.5059	1.4565	0.1265	1.5059	1.4409	0.1339	1.5059	1.4465
536	s5_15_00_w1_49_30w	0.55	1254	wc II	0.0821	1.7067	1.5608	0.0778	1.7067	1.5557	0.0848	1.7067	1.5644
537	s5_15_00_w3_49_30w	0.55	1295	wc II	0.1043	1.9692	1.7466	0.113	1.9692	1.8022	0.1155	1.9692	1.7626
538	s5_15_00_w5_49_30w	0.55	1306	wc II	0.1226	2.1333	1.8765	0.1442	2.1333	1.9431	0.1368	2.1333	1.9259
501	s5_16_40_w1_00_30w	0.55	1292	wc II	0.0703	1.7067	1.576	0.0813	1.7067	1.5678	0.0737	1.6	1.5103
502	s5_16_40_w2_00_30w	0.55	1165	wc II	0.068	1.1636	1.1583	0.0721	1.1636	1.1423	0.0782	1.1636	1.1684
503	s5_16_40_w3_00_30w	0.55	1348	wc II	0.1035	1.9692	1.7966	0.1111	1.9692	1.7548	0.1016	1.9692	1.747
504	s5_16_40_w4_00_30w	0.55	1204	wc II	0.0922	1.3474	1.3024	0.101	1.3474	1.3012	0.1055	1.3474	1.2932
505	s5_16_40_w5_00_30w	0.55	1285	wc II	0.1277	2.1333	1.9382	0.1375	2.1333	1.8625	0.1263	2.1333	1.9453
506	s5_16_40_w6_00_30w	0.55	1282	wc II	0.112	1.6	1.4528	0.1298	1.5059	1.4513	0.1263	1.5059	1.4053
508	s5_17_40_w1_49_30w	0.55	1258	wc II	0.0704	1.7067	1.5824	0.0822	1.7067	1.5698	0.0746	1.6	1.5113
509	s5_17_40_w3_49_30w	0.55	1342	wc II	0.1029	1.9692	1.7977	0.1118	1.9692	1.7592	0.1027	1.9692	1.7477
510	s5_17_40_w5_49_30w	0.55	1290	wc II	0.1271	2.1333	1.9404	0.1382	2.1333	1.8621	0.1281	2.1333	1.9491
517	s5_19_30_w1_00_30w	0.55	1296	wc II	0.0713	1.6	1.548	0.0802	1.7067	1.5754	0.0768	1.6	1.5165
518	s5_19_30_w2_00_30w	0.55	1172	wc II	0.0708	1.219	1.1576	0.0695	1.1636	1.1386	0.0743	1.1636	1.1593
519	s5_19_30_w3_00_30w	0.55	1360	wc II	0.0994	1.9692	1.7621	0.1107	1.9692	1.7723	0.1033	1.9692	1.7319
520	s5_19_30_w4_00_30w	0.55	1201	wc II	0.095	1.3474	1.2955	0.0999	1.4222	1.2999	0.1073	1.3474	1.3018
521	s5_19_30_w5_00_30w	0.55	1326	wc II	0.1214	2.1333	1.9048	0.1398	2.1333	1.8843	0.1252	2.1333	1.923

test-number	testseries name[2]	water depth [m]	no. of waves of test	wave characteristic wc I or wc II	in front of wave generator			at toe of 0.6 m dike			at toe of 0.7 m dike		
					H_{m0} [m]	T_p [s]	$T_{m-1,0}$ [s]	H_{m0} [m]	T_p [s]	$T_{m-1,0}$ [s]	H_{m0} [m]	T_p [s]	$T_{m-1,0}$ [s]
522	s5_19_30_w6_00_30w	0.55	1250	wc II	0.114	1.6	1.4385	0.1292	1.5059	1.4496	0.1321	1.5059	1.4153
523	s5_20_30_w1_49_30w	0.55	1245	wc II	0.0715	1.6	1.5529	0.0813	1.7067	1.5758	0.0768	1.6	1.5163
524	s5_20_30_w3_49_30w	0.55	1310	wc II	0.0993	1.9692	1.768	0.1114	1.9692	1.7738	0.1035	1.9692	1.7342
525	s5_20_30_w5_49_30w	0.55	1299	wc II	0.1213	2.1333	1.9102	0.1404	2.1333	1.8859	0.1254	2.1333	1.9253
530	s5_22_15_w1_00_30w	0.55	1286	wc II	0.0779	1.6	1.5387	0.0778	1.7067	1.5769	0.082	1.7067	1.5413
531	s5_22_15_w2_00_30w	0.55	1166	wc II	0.0734	1.1636	1.1488	0.0681	1.1636	1.1332	0.0741	1.1636	1.14
532	s5_22_15_w3_00_30w	0.55	1392	wc II	0.1003	1.9692	1.7247	0.1125	1.9692	1.8012	0.1104	1.9692	1.7398
533	s5_22_15_w4_00_30w	0.55	1200	wc II	0.1003	1.3474	1.2972	0.0972	1.3474	1.2922	0.1062	1.4222	1.3025
534	s5_22_15_w5_00_30w	0.55	1377	wc II	0.1188	2.1333	1.8662	0.1432	2.1333	1.9267	0.1301	2.1333	1.9092
535	s5_22_15_w6_00_30w	0.55	1222	wc II	0.1271	1.5059	1.4398	0.1284	1.5059	1.4497	0.1369	1.5059	1.4322
613	s6_25_00_w1_00_45a	0.55	1229	wc II	0.0868	1.7067	1.5968	0.0819	1.7067	1.6142	0.0771	1.7067	1.5552
614	s6_25_00_w2_00_45a	0.55	1144	wc II	0.0701	1.219	1.1733	0.0702	1.219	1.1486	0.0751	1.1636	1.1608
615	s6_25_00_w3_00_45a	0.55	1280	wc II	0.1185	1.9692	1.8004	0.1256	1.9692	1.8328	0.1124	1.8286	1.7857
616	s6_25_00_w4_00_45a	0.55	1162	wc II	0.1061	1.3474	1.338	0.097	1.3474	1.3107	0.1044	1.3474	1.306
617	s6_25_00_w5_00_45a	0.55	1267	wc II	0.1471	2.1333	1.9359	0.1514	2.1333	1.9599	0.1407	2.1333	1.9801
618	s6_25_00_w6_00_45a	0.55	1204	wc II	0.138	1.6	1.4758	0.1287	1.6	1.4754	0.1284	1.5059	1.4297
607	s6_26_15_w1_00_30a	0.55	1272	wc II	0.0838	1.7067	1.5466	0.0823	1.7067	1.5344	0.0867	1.6	1.551
608	s6_26_15_w2_00_30a	0.55	1153	wc II	0.0759	1.1636	1.1414	0.0798	1.1636	1.1525	0.0808	1.1636	1.1521
609	s6_26_15_w3_00_30a	0.55	1347	wc II	0.108	1.8286	1.7595	0.1115	1.9692	1.7661	0.1181	1.9692	1.7901
610	s6_26_15_w4_00_30a	0.55	1164	wc II	0.1068	1.3474	1.3047	0.1116	1.3474	1.3013	0.1103	1.4222	1.3026
611	s6_26_15_w5_00_30a	0.55	1313	wc II	0.1353	2.1333	1.9403	0.1413	2.1333	1.9224	0.1563	2.1333	1.9753
612	s6_26_15_w6_00_30a	0.55	1204	wc II	0.1337	1.5059	1.4493	0.1349	1.5059	1.4359	0.1427	1.5059	1.4391
601	s6_27_15_w1_00_45a	0.55	1224	wc II	0.0821	1.7067	1.6194	0.0821	1.7067	1.5765	0.0839	1.7067	1.5848
602	s6_27_15_w2_00_45a	0.55	1126	wc II	0.0669	1.1636	1.1623	0.0707	1.1636	1.165	0.0701	1.1636	1.1741
603	s6_27_15_w3_00_45a	0.55	1313	wc II	0.1209	1.9692	1.8506	0.1149	1.9692	1.7967	0.1116	1.9692	1.7862
604	s6_27_15_w4_00_45a	0.55	1158	wc II	0.0938	1.3474	1.3306	0.1011	1.4222	1.3232	0.1026	1.3474	1.3346
605	s6_27_15_w5_00_45a	0.55	1294	wc II	0.1546	2.1333	1.9978	0.1394	2.1333	1.944	0.1376	2.1333	1.9761

test-number	testseries name[2]	water depth [m]	no. of waves of test	wave characteristic wc I or wc II	in front of wave generator			at toe of 0.6 m dike			at toe of 0.7 m dike		
					H_{m0} [m]	T_p [s]	$T_{m-1,0}$ [s]	H_{m0} [m]	T_p [s]	$T_{m-1,0}$ [s]	H_{m0} [m]	T_p [s]	$T_{m-1,0}$ [s]
606	s6_27_15_w6_00_45a	0.55	1182	wc II	0.1296	1.5059	1.4975	0.1313	1.5059	1.4662	0.1323	1.5059	1.4664
625	s6_28_30_w1_00_30a	0.55	1286	wc II	0.0872	1.7067	1.5727	0.0848	1.6	1.5414	0.0879	1.6	1.5696
626	s6_28_30_w2_00_30a	0.55	1145	wc II	0.0753	1.1636	1.1566	0.0822	1.1636	1.1436	0.0777	1.1636	1.1645
627	s6_28_30_w3_00_30a	0.55	1325	wc II	0.1134	1.8286	1.7818	0.1159	1.9692	1.8005	0.121	1.9692	1.8012
628	s6_28_30_w4_00_30a	0.55	1180	wc II	0.1043	1.3474	1.3217	0.1104	1.3474	1.2937	0.1114	1.3474	1.3203
629	s6_28_30_w5_00_30a	0.55	1291	wc II	0.1407	2.1333	1.9542	0.1537	2.1333	1.9767	0.1632	2.1333	1.9929
630	s6_28_30_w6_00_30a	0.55	1202	wc II	0.137	1.6	1.4803	0.1349	1.5059	1.4416	0.1455	1.5059	1.4528
619	s6_29_30_w1_00_45a	0.55	1215	wc II	0.0761	1.7067	1.6128	0.0907	1.7067	1.5904	0.0878	1.7067	1.627
620	s6_29_30_w2_00_45a	0.55	1121	wc II	0.0638	1.1636	1.1874	0.071	1.219	1.1863	0.0648	1.219	1.207
621	s6_29_30_w3_00_45a	0.55	1303	wc II	0.1169	1.9692	1.8643	0.1156	1.9692	1.7761	0.1185	1.9692	1.8044
622	s6_29_30_w4_00_45a	0.55	1136	wc II	0.0964	1.3474	1.3424	0.1073	1.3474	1.348	0.1006	1.3474	1.3566
623	s6_29_30_w5_00_45a	0.55	1282	wc II	0.1549	2.1333	2.0352	0.1398	2.1333	1.9454	0.1459	2.1333	1.9816
624	s6_29_30_w6_00_45a	0.55	1161	wc II	0.1245	1.5059	1.4989	0.1431	1.5059	1.489	0.1357	1.6	1.5079
637	s6_30_40_w1_00_30a	0.55	1349	wc II	0.0847	1.6	1.5851	0.0851	1.7067	1.5664	0.0882	1.6	1.5822
638	s6_30_40_w2_00_30a	0.55	1283	wc II	0.0743	1.1636	1.1713	0.0805	1.1636	1.1506	0.0755	1.1636	1.1754
639	s6_30_40_w3_00_30a	0.55	1349	wc II	0.1185	1.8286	1.8094	0.1197	1.9692	1.8182	0.1254	1.9692	1.8084
640	s6_30_40_w4_00_30a	0.55	1246	wc II	0.1059	1.4222	1.3421	0.1081	1.3474	1.3125	0.1113	1.3474	1.3358
641	s6_30_40_w5_00_30a	0.55	1282	wc II	0.1487	2.1333	1.9792	0.1578	2.1333	2.0076	0.1652	2.1333	1.9978
642	s6_30_40_w6_00_30a	0.55	1211	wc II	0.1362	1.5059	1.4902	0.1337	1.5059	1.4674	0.1452	1.5059	1.4616
631	s6_31_40_w1_00_45a	0.55	1298	wc II	0.0786	1.6	1.6201	0.0905	1.7067	1.5913	0.0873	1.7067	1.6476
632	s6_31_40_w2_00_45a	0.55	1242	wc II	0.0616	1.1636	1.2011	0.0756	1.219	1.2009	0.061	1.219	1.2264
633	s6_31_40_w3_00_45a	0.55	1359	wc II	0.1115	1.9692	1.8604	0.1204	1.9692	1.7791	0.1218	1.9692	1.8376
634	s6_31_40_w4_00_45a	0.55	1157	wc II	0.0949	1.3474	1.3651	0.1132	1.3474	1.3492	0.098	1.3474	1.3814
635	s6_31_40_w5_00_45a	0.55	1308	wc II	0.1503	2.1333	2.0496	0.146	2.1333	1.9582	0.1548	2.1333	2.0029
636	s6_31_40_w6_00_45a	0.55	1184	wc II	0.1282	1.5059	1.514	0.144	1.5059	1.4847	0.1363	1.5059	1.524

Annex J Wave run-up – analyzed tests

Table-annex 11 Wave run-up – overview of analyzed tests

Overview about available run-up data, test numbers

FlowDike 1 (1:3 sloped dike)

	beta = 0, wind = 0			
wave	v = 0,0	v = 0,15	v = 0,3	v = 0,4
1	**144**	162	114	
2	**145**	163	115	
3	**146**	164	116	
4	**147**	165	117	
5	**148**	166	119	
6	**149**	167	120	

	beta = 30, wind = 0			
wave	v = 0,0	v = 0,15	v = 0,3	v = 0,4
1	180	192	202	
2	181	193	203	
3	182	194	204	
4	183	195	205	
5	184	196	206	
6	185	197	207	

	beta = 0, wind = 5 m/s			
wave	v = 0,0	v = 0,15	v = 0,3	v = 0,4
1	150		137	
2				
3	151		138	
4				
5	152		140	
6				

	beta = 30, wind = 5 m/s			
wave	v = 0,0	v = 0,15	v = 0,3	v = 0,4
1	186		208	
2				
3	187		209	
4				
5	188		210	
6				

	beta = 15, wind = 0			
wave	v = 0,0	v = 0,15	v = 0,3	v = 0,4
1	156	168	124	
2	157	169	125	
3	158	170	126	
4	159	171	127	
5	160	172	128	
6	161	173	129	

	beta = -30, wind = 0			
wave	v = 0,0	v = 0,15	v = 0,3	v = 0,4
1	*	234	222	
2	*	235	223	
3	*	236	224	
4	*	237	225	
5	*	238	226	
6	*	239	227	

	beta = 0, wind = 10 m/s			
wave	v = 0,0	v = 0,15	v = 0,3	v = 0,4
1	153		121	
2				
3	154		122	
4				
5	155		123	
6				

	beta = 30, wind = 10 m/s			
wave	v = 0,0	v = 0,15	v = 0,3	v = 0,4
1	189		211	
2				
3	190		212	
4				
5	191		213	
6				

	beta = -15, wind = 0			
wave	v = 0,0	v = 0,15	v = 0,3	v = 0,4
1	*	174	131	
2	*	175	132	
3	*	176	133	
4	*	177	134	
5	*	178	135	
6	*	179	136	

	beta = -45, wind = 0			
wave	v = 0,0	v = 0,15	v = 0,3	v = 0,4
1	215	240	228	
2	216	241	229	
3	217	242	230	
4	218	243	231	
5	220	244	232	
6	221	245	233	

FlowDike 2 (1:6 1:3 sloped dike)

	beta = 0, wind = 0			
wave	v = 0,0	v = 0,15	v = 0,3	v = 0,4
1	***451***	*467*	*458*	*480*
2	***452***	*468*	*459*	*481*
3	***453***	*469*	*460*	*482*
4	***454***	*470*	*461*	*483*
5	***456***	*471*	*462*	*484*
6	***457***	*472*	*463*	*485*

	beta = 30, wind = 0			
wave	v = 0,0	v = 0,15	v = 0,3	v = 0,4
1	*511*	*530*	*517*	*501*
2	*512*	*531*	*518*	*502*
3	*513*	*532*	*519*	*503*
4	*517*	*533*	*520*	*504*
5	*515*	*534*	*521*	*505*
6	*516*	*535*	*522*	*506*

	beta = 0, wind = 0 (doppelt)			
wave	v = 0,0	v = 0,15	v = 0,3	v = 0,4
1	**425**	*476*	411	*486*
2	**427**	*477*	410	*487*
3	**426**		409	
4	**428**		408	
5	**429**		407	
6	**430**		406	

	beta = 15, wind = 0			
wave	v = 0,0	v = 0,15	v = 0,3	v = 0,4
1	*444*		432	
2	*445*		433	
3	*447*		434	
4	*448*		435	
5	*449*		437	
6	*450*		438	

	beta = -30, wind = 0			
wave	v = 0,0	v = 0,15	v = 0,3	v = 0,4
1	*	*607*	*625*	*637*
2	*	*608*	*626*	*638*
3	*	*609*	*627*	*639*
4	*	*610*	*628*	*640*
5	*	*611*	*629*	*641*
6	*	*612*	*630*	*642*

	beta = 0, wind = 4 m/s			
wave	v = 0,0	v = 0,15	v = 0,3	v = 0,4
1	418		415	
2				
3	419		416	
4				
5	421		417	
6				

	beta = 30, wind = 8 m/s			
wave	v = 0,0	v = 0,15	v = 0,3	v = 0,4
1	*536*		*523*	*508*
2				
3	*537*		*524*	*509*
4				
5	*538*		*525*	*510*
6				

	beta = -15, wind = 0			
wave	v = 0,0	v = 0,15	v = 0,3	v = 0,4
1	*			
2	*			
3	*		440	
4	*		441	
5	*		442	
6	*		443	

	beta = -45, wind 0			
wave	v = 0,0	v = 0,15	v = 0,3	v = 0,4
1	*613*	*601*	*619*	*631*
2	*614*	*602*	*620*	*632*
3	*615*	*603*	*621*	*633*
4	*616*	*604*	*622*	*634*
5	*617*	*605*	*623*	*635*
6	*618*	*606*	*624*	*636*

	beta = 0, wind = 8 m/s			
wave	v = 0,0	v = 0,15	v = 0,3	v = 0,4
1	*464*	*473*	*412*	*488*
2				
3	*465*	*474*	*413*	*489*
4				
5	*466*	*475*	*414*	*490*
6				

	beta = 0, wind = 8 m/s (doppelt)			
wave	v = 0,0	v = 0,15	v = 0,3	v = 0,4
1	422			
2				
3	423			
4				
5	424			
6				

	no test
	video camera problems, but there are still enough data available
	video malfunction, no data
	capacitive gauge malfunction, no data
	capacitive gauge and video malfunction, no data
* same tests as beta = 15 and 30 respectively (v = 0 m/s, wind = 0)	
italic = water depth h = 0,55 m (else h = 0,5 m)	
test 221 has been stoped, no data	
reference tests	

data analysis:	
	tests with current (without wind, perpendicular wave attack)
	oblique wave attack (without current and wind)
	tests with wind (without current, perpendicular wave attack)

Annex K Analyzed data - wave run-up – 1:3 sloped dike (FlowDike 1)

Table-annex 11 Analyzed data – wave run-up - 1:3 sloped dike[3]

test-number	testseries name[4]	water depth [m]	H_{m0} [m]	$T_{m-1,0}$ [s]	run-up height $R_{u2\%}$ [m]										
					capacitive gauge	video stripe 1	video stripe 2	video stripe 3	video stripe 4	video stripe 5	video stripe 6	video stripe 7	video stripe 8	video stripe 9	video stripe 10
114	s1_03_00_w1_00	0.5	0.054	1.033	0.145	0.085	0.100	0.097	-	0.132	0.134	0.134	0.150	0.147	0.141
115	s1_03_00_w2_00	0.5	0.049	0.787	0.093	0.048	0.057	0.055	-	0.066	0.067	0.066	0.077	0.074	0.077
116	s1_03_00_w3_00	0.5	0.104	1.429	0.283	0.254	0.282	0.289	0.295	0.301	0.298	0.293	0.306	0.313	0.310
117	s1_03_00_w4_00	0.5	0.104	1.057	0.236	0.222	0.222	0.216	0.225	0.245	0.244	0.241	0.255	0.252	0.247
119	s1_03_00_w5_00	0.5	0.141	1.858	0.427	0.343	0.417	0.434	0.450	0.453	0.452	0.443	0.446	0.450	0.445
120	s1_03_00_w6_00	0.5	0.139	1.405	0.365	0.323	0.356	0.373	0.383	0.381	0.380	0.365	0.381	0.383	0.381
121	s1_08_30_w1_49_+00	0.5	0.050	1.108	0.154	0.096	0.106	0.107	0.083	0.155	0.160	0.163	0.163	0.158	0.146
122	s1_08_30_w3_49_+00	0.5	0.094	1.549	0.288	0.252	0.289	0.307	0.315	0.306	0.297	0.291	0.307	0.310	0.301
123	s1_08_30_w5_49_+00	0.5	0.142	1.879	0.448	0.329	0.414	0.437	0.456	0.464	0.467	0.465	0.460	0.458	0.447
124	s1_19_30_w1_00_-15	0.5	0.066	1.291	0.172	-	-	-	-	-	-	-	-	-	-
125	s1_19_30_w2_00_-15	0.5	0.070	0.985	0.132	0.027	0.050	0.054	0.047	0.074	0.077	0.083	0.116	0.124	0.127
126	s1_19_30_w3_00_-15	0.5	0.091	1.511	0.225	0.154	0.174	0.186	0.212	0.219	0.213	0.205	0.219	0.230	0.239
127	s1_19_30_w4_00_-15	0.5	0.096	1.138	0.193	-	-	-	-	-	-	-	-	-	-
128	s1_19_30_w5_00_-15	0.5	0.127	1.796	0.293	-	-	-	-	-	-	-	-	-	-
129	s1_19_30_w6_00_-15	0.5	0.132	1.390	0.284	-	-	-	-	-	-	-	-	-	-
131	s1_16_30_w1_00_+15	0.5	0.071	1.333	0.215	0.226	0.209	0.199	0.208	0.212	0.238	0.247	0.244	0.234	0.240

[3] italic: uncertain values

[4] Composition of testseries name (e. i. s1_01_00_w1_00_00):
s1 (set-up no.) _ 01 (no. of testseries) _ 00 (current [m/(100s)]) _ w1 (wave no.) _ 00 (wind [Hz (wind generator)]) _ 00 (angle of wave attack [°], w = with or a = against current)

test-number	testseries name[4]	water depth [m]	H_{m0} [m]	$T_{m-1,0}$ [s]	run-up height $R_{u2\%}$ [m]										
					capacitive gauge	video stripe 1	video stripe 2	video stripe 3	video stripe 4	video stripe 5	video stripe 6	video stripe 7	video stripe 8	video stripe 9	video stripe 10
132	s1_16_30_w2_00_+15	0.5	0.069	0.991	0.163	0.159	0.156	0.131	0.169	0.163	0.164	0.168	0.174	0.177	0.166
133	s1_16_30_w3_00_+15	0.5	0.099	1.531	0.271	0.269	0.254	0.242	-	0.256	0.273	0.278	0.278	0.281	0.294
134	s1_16_30_w4_00_+15	0.5	0.097	1.165	0.231	0.206	0.206	0.199	-	0.226	0.235	0.238	0.244	0.249	0.262
135	s1_16_30_w5_00_+15	0.5	0.132	1.809	0.379	0.396	0.393	0.381	-	0.371	0.374	0.371	0.378	0.379	0.371
136	s1_16_30_w6_00_+15	0.5	0.147	1.438	0.332	0.314	0.327	0.317	-	0.325	0.330	0.340	0.342	0.358	0.340
137	s1_08b_30_w1_25_+00	0.5	0.068	1.312	0.233	0.171	0.193	-	-	0.217	0.219	0.214	0.224	0.220	0.217
138	s1_08b_30_w3_25_+00	0.5	0.096	1.564	0.306	0.250	0.287	0.284	-	0.302	0.302	0.292	0.313	0.320	0.312
140	s1_08b_30_w5_25_+00	0.5	0.140	1.869	0.442	0.340	0.401	0.429	-	-	0.455	0.449	0.459	0.451	0.451
144	s1_01_00_w1_00	0.5	0.068	1.327	0.199	0.217	0.234	0.234	-	-	0.195	0.210	0.212	0.205	0.186
145	s1_01_00_w2_00	0.5	0.065	1.012	0.155	0.137	0.157	0.145	-	-	0.147	0.163	0.172	0.172	0.168
146	s1_01_00_w3_00	0.5	0.095	1.576	0.293	0.281	0.297	0.302	0.293	-	0.297	0.290	0.277	0.268	0.264
147	s1_01_00_w4_00	0.5	0.095	1.145	0.226	0.221	0.237	0.254	0.231	-	0.223	0.235	0.240	0.238	0.242
148	s1_01_00_w5_00	0.5	0.140	1.872	0.431	0.371	0.427	0.443	-	0.435	0.437	0.427	0.433	0.427	0.411
149	s1_01_00_w6_00	0.5	0.141	1.415	0.353	0.325	0.345	0.354	0.347	-	0.358	0.353	0.356	0.336	0.336
150	s1_06b_00_w1_49_+00	0.5	0.068	1.332	0.184	0.233	0.231	0.214	-	0.190	0.180	0.202	0.211	0.195	0.181
151	s1_06b_00_w3_49_+00	0.5	0.094	1.574	0.282	0.298	0.315	0.309	-	0.277	0.282	0.264	0.259	0.266	0.255
152	s1_06b_00_w5_49_+00	0.5	0.136	1.874	0.422	0.385	0.432	0.444	-	0.436	0.448	0.428	0.430	0.434	0.430
153	s1_06_00_w1_49_+00	0.5	0.067	1.333	0.171	0.208	0.200	0.183	-	-	0.174	0.198	0.215	0.210	0.193
154	s1_06_00_w3_49_+00	0.5	0.094	1.576	0.262	0.285	0.294	0.283	0.258	-	0.264	0.269	0.282	0.283	0.273
155	s1_06_00_w5_49_+00	0.5	0.135	1.871	0.430	0.407	0.443	0.453	0.465	0.459	0.441	0.453	0.447	0.453	0.443
155a	s1_06_00_w5_49_+00	0.5	0.135	1.871		0.410	0.454	0.456	0.468	0.460	0.445	0.445	0.452	0.456	0.449
156	s1_12_00_w1_00_-15	0.5	0.075	1.319	0.231	0.169	0.183	0.193	-	0.196	0.205	0.193	0.198	0.208	0.205
157	s1_12_00_w2_00_-15	0.5	0.072	0.976	0.181	0.146	0.166	0.169	-	-	0.178	0.171	0.174	0.176	0.174
158	s1_12_00_w3_00_-15	0.5	0.096	1.500	0.281	0.229	0.255	0.273	-	0.286	0.291	0.286	0.273	0.284	0.293

test-number	testseries name[4]	water depth [m]	H_{m0} [m]	$T_{m-1,0}$ [s]	run-up height $R_{u2\%}$ [m]										
					capacitive gauge	video stripe 1	video stripe 2	video stripe 3	video stripe 4	video stripe 5	video stripe 6	video stripe 7	video stripe 8	video stripe 9	video stripe 10
159	s1_12_00_w4_00_-15	0.5	0.099	1.145	0.249	0.220	0.235	0.239	-	0.242	0.246	0.242	0.240	0.247	0.251
160	s1_12_00_w5_00_-15	0.5	0.133	1.782	0.379	0.274	0.323	0.349	0.358	0.368	0.383	0.377	0.377	0.383	0.383
161	s1_12_00_w6_00_-15	0.5	0.147	1.413	0.334	0.266	0.302	0.322	0.328	0.324	0.333	0.326	0.320	0.328	0.333
162	s1_11_15_w1_00_+00	0.5	0.067	1.308	0.212	0.205	0.219	0.238	-	0.210	0.212	0.203	0.205	0.215	0.208
163	s1_11_15_w2_00_+00	0.5	0.065	1.005	0.163	0.153	0.169	0.153	-	0.134	0.159	0.154	0.158	0.148	0.144
164	s1_11_15_w3_00_+00	0.5	0.096	1.573	0.304	0.279	0.308	0.323	0.321	0.310	0.296	0.296	0.308	0.307	0.297
165	s1_11_15_w4_00_+00	0.5	0.098	1.148	0.238	0.235	0.246	0.247	-	0.215	0.239	0.232	0.230	0.239	0.237
166	s1_11_15_w5_00_+00	0.5	0.144	1.866	0.450	0.362	0.421	0.442	0.438	0.454	0.458	0.446	0.448	0.450	0.438
167	s1_11_15_w6_00_+00	0.5	0.137	1.404	0.366	0.326	0.356	0.367	0.367	0.356	0.361	0.348	0.356	0.360	0.352
168	s1_13_15_w1_00_-15	0.5	0.069	1.297	0.202	0.145	0.164	0.173	-	-	0.190	0.186	0.191	0.198	0.198
169	s1_13_15_w2_00_-15	0.5	0.072	0.986	0.164	0.092	0.093	0.092	-	-	0.147	0.149	0.159	0.166	0.171
170	s1_13_15_w3_00_-15	0.5	0.093	1.493	0.253	0.200	0.215	0.226	-	-	0.246	0.239	0.245	0.262	0.268
171	s1_13_15_w4_00_-15	0.5	0.103	1.145	0.236	0.178	0.196	0.205	-	-	0.223	0.220	0.222	0.229	0.232
172	s1_13_15_w5_00_-15	0.5	0.127	1.780	0.336	0.247	0.291	0.316	0.309	-	0.340	0.342	0.345	0.353	0.362
173	s1_13_15_w6_00_-15	0.5	0.139	1.387	0.315	0.247	0.281	0.288	-	-	0.320	0.304	0.304	0.317	0.318
174	s1_15_15_w1_00_+15	0.5	0.071	1.312	0.232	0.187	0.189	0.192	-	-	0.216	0.216	0.209	0.209	0.214
175	s1_15_15_w2_00_+15	0.5	0.072	0.985	0.172	0.160	0.153	0.156	-	0.142	0.156	0.147	0.147	0.150	0.138
176	s1_15_15_w3_00_+15	0.5	0.094	1.508	0.295	0.258	0.250	0.250	-	-	0.277	0.272	0.272	0.297	0.299
177	s1_15_15_w4_00_+15	0.5	0.099	1.157	0.248	0.235	0.224	0.236	-	0.228	0.236	0.233	0.233	0.240	0.231
178	s1_15_15_w5_00_+15	0.5	0.132	1.801	0.391	0.376	0.371	0.365	0.320	-	0.376	0.376	0.374	0.384	0.373
179	s1_15_15_w6_00_+15	0.5	0.140	1.405	0.332	0.319	0.324	0.317	0.310	0.315	0.326	0.328	0.345	0.354	0.337
180	s2_02_00_w1_00	0.5	0.077	1.303	0.218	0.128	0.193	0.208	0.215	0.224	0.229	0.229	0.219	0.220	0.215
181	s2_02_00_w2_00	0.5	0.080	0.990	0.153	0.146	-	0.153	0.150	0.140	0.148	0.160	0.160	0.165	0.168
182	s2_02_00_w3_00	0.5	0.107	1.571	0.300	0.176	-	0.268	0.293	0.300	0.302	0.302	0.291	0.280	0.284

test-number	testseries name[4]	water depth [m]	H_{m0} [m]	$T_{m-1,0}$ [s]	run-up height $R_{u2\%}$ [m]										
					capacitive gauge	video stripe 1	video stripe 2	video stripe 3	video stripe 4	video stripe 5	video stripe 6	video stripe 7	video stripe 8	video stripe 9	video stripe 10
183	s2_02_00_w4_00	0.5	0.111	1.157	0.232	0.211	-	0.212	0.223	0.231	0.240	0.252	0.256	0.258	0.247
184	s2_02_00_w5_00	0.5	0.159	1.886	0.416	0.327	-	0.372	0.391	0.400	0.410	0.408	0.414	0.410	0.391
185	s2_02_00_w6_00	0.5	0.163	1.416	0.337	0.271	-	0.316	0.331	0.342	0.353	0.359	0.363	0.355	0.346
186	s2_07b_00_w1_25_-30	0.5	0.075	1.307	0.216	-	0.197	0.212	0.214	0.215	0.224	0.226	0.215	0.212	0.217
187	s2_07b_00_w3_25_-30	0.5	0.106	1.576	0.289	0.169	0.259	0.280	0.296	0.301	0.307	0.309	0.296	0.280	0.283
188	s2_07b_00_w5_25_-30	0.5	0.158	1.887	0.409	0.330	0.360	0.389	0.406	0.418	0.427	0.431	0.437	0.425	0.416
189	s2_07_00_w1_49_-30	0.5	0.074	1.318	0.216	0.104	0.185	0.204	0.209	0.218	0.220	0.223	0.218	0.213	0.213
190	s2_07_00_w3_49_-30	0.5	0.105	1.581	0.293	0.175	0.223	0.279	0.295	0.302	0.302	0.300	0.288	0.282	0.281
191	s2_07_00_w5_49_-30	0.5	0.155	1.888	0.419	0.332	0.252	0.384	0.404	0.423	0.437	0.437	0.439	0.429	0.419
192	s2_20_15_w1_00_-30	0.5	0.083	1.326	0.191	-	-	-	-	-	-	-	-	-	-
193	s2_20_15_w2_00_-30	0.5	0.081	1.016	0.173	-	-	-	-	-	-	-	-	-	-
194	s2_20_15_w3_00_-30	0.5	0.115	1.543	0.282	-	-	-	-	-	-	-	-	-	-
195	s2_20_15_w4_00_-30	0.5	0.120	1.177	0.231	-	-	-	-	-	-	-	-	-	-
196	s2_20_15_w5_00_-30	0.5	0.158	1.839	0.398	-	-	-	-	-	-	-	-	-	-
197	s2_20_15_w6_00_-30	0.5	0.166	1.418	0.286	-	-	-	-	-	-	-	-	-	-
202	s2_04_30_w1_00_-30	0.5	0.081	1.339	-	0.171	0.203	0.218	0.223	0.220	0.211	0.210	0.203	0.208	0.217
203	s2_04_30_w2_00_-30	0.5	0.074	1.039	-	0.176	0.178	0.189	0.191	0.188	0.183	0.179	0.178	0.173	0.173
204	s2_04_30_w3_00_-30	0.5	0.109	1.553	-	0.231	0.238	0.259	0.269	0.274	0.289	0.296	0.301	0.298	0.289
205	s2_04_30_w4_00_-30	0.5	0.111	1.197	-	0.239	0.221	0.246	0.254	0.258	0.256	0.253	0.256	0.258	0.254
206	s2_04_30_w5_00_-30	0.5	0.146	1.817	-	0.335	0.315	0.357	0.380	0.391	0.403	0.414	0.414	0.412	0.416
207	s2_04_30_w6_00_-30	0.5	0.156	1.427	-	0.303	0.288	0.321	0.330	0.335	0.339	0.333	0.330	0.322	0.315
208	s2_09b_00_w1_25_-30	0.5	0.081	1.341	-	0.151	0.192	0.205	0.209	0.207	0.205	0.200	0.195	0.198	0.205
209	s2_09b_00_w3_25_-30	0.5	0.110	1.555	-	0.238	0.229	0.259	0.266	0.275	0.284	0.296	0.296	0.296	0.289
210	s2_09b_00_w5_25_-30	0.5	0.147	1.817	-	0.328	0.296	0.347	0.373	0.381	0.390	0.400	0.404	0.408	0.404

test-number	testseries name[4]	water depth [m]	H_{m0} [m]	$T_{m-1,0}$ [s]	run-up height $R_{u2\%}$ [m]										
					capacitive gauge	video stripe 1	video stripe 2	video stripe 3	video stripe 4	video stripe 5	video stripe 6	video stripe 7	video stripe 8	video stripe 9	video stripe 10
211	s2_09_00_w1_49_-30	0.5	0.081	1.342	-	0.139	0.189	0.205	0.212	0.212	0.203	0.200	0.191	0.196	0.201
212	s2_09_00_w3_49_-30	0.5	0.109	1.555	-	0.230	0.219	0.245	0.256	0.259	0.272	0.279	0.288	0.286	0.272
213	s2_09_00_w5_49_-30	0.5	0.146	1.816	-	0.331	0.294	0.348	0.370	0.380	0.386	0.403	0.407	0.405	0.399
215	s3_18_00_w1_00_+45	0.5	0.087	1.309	-	0.194	0.193	0.194	0.194	0.193	0.193	0.193	0.191	0.191	0.191
216	s3_18_00_w2_00_+45	0.5	0.094	1.007	-	0.167	0.169	0.164	0.155	0.150	0.149	0.150	0.152	0.155	0.169
217	s3_18_00_w3_00_+45	0.5	0.123	1.528	-	-	-	-	-	-	-	-	-	-	-
218	s3_18_00_w4_00_+45	0.5	0.126	1.166	-	-	-	-	-	-	-	-	-	-	-
220	s3_18_00_w5_00_+45	0.5	0.170	1.814	-	-	-	-	-	-	-	-	-	-	-
222	s3_05_30_w1_00_+30	0.5	0.071	1.336	0.202	0.182	0.187	*0.192*	*0.192*	*0.192*	*0.192*	*0.192*	0.230	0.235	0.240
223	s3_05_30_w2_00_+30	0.5	0.072	1.026	0.135	0.119	0.126	0.134	0.134	0.139	0.144	0.146	0.156	0.154	0.149
224	s3_05_30_w3_00_+30	0.5	0.100	1.560	0.283	0.253	0.266	0.266	0.274	0.282	0.294	0.307	0.309	0.314	0.323
225	s3_05_30_w4_00_+30	0.5	0.099	1.197	0.213	*0.193*[4]	*0.193*[4]	*0.193*	*0.193*	*0.193*	0.219	0.222	0.227	0.227	0.250
226	s3_05_30_w5_00_+30	0.5	0.155	1.895	0.409	0.376	0.389	0.404	0.416	0.418	0.428	0.432	0.438	0.430	0.428
227	s3_05_30_w6_00_+30	0.5	0.142	1.500	0.334	0.296	0.298	0.309	0.318	0.332	0.340	0.342	0.351	0.349	0.351
228	s3_14_30_w1_00_+45	0.5	0.096	1.354	0.226	0.225	0.226	0.225	0.230	0.231	0.230	0.233	0.231	0.223	0.225
229	s3_14_30_w2_00_+45	0.5	0.085	1.073	0.175	0.161	0.165	0.165	0.170	0.171	0.180	0.183	0.186	0.181	0.175
230	s3_14_30_w3_00_+45	0.5	0.130	1.547	0.281	0.299	0.299	0.298	0.307	0.305	0.298	0.287	0.287	0.281	0.296
231	s3_14_30_w4_00_+45	0.5	0.124	1.239	0.242	0.234	0.236	0.246	0.250	0.255	0.248	0.243	0.236	0.226	0.238
232	s3_14_30_w5_00_+45	0.5	0.167	1.840	0.371	0.394	0.397	0.399	0.399	0.388	0.382	0.375	0.361	0.365	0.363
233	s3_14_30_w6_00_+45	0.5	0.148	1.496	0.295	0.312	0.314	0.315	0.312	0.312	0.308	0.303	0.292	0.287	0.363
234	s3_21_15_w1_00_+30	0.5	0.079	1.287	0.228	0.224	0.229	0.231	0.231	0.236	0.236	0.236	0.238	0.238	0.238
235	s3_21_15_w2_00_+30	0.5	0.086	1.006	0.185	0.159	0.176	0.173	0.174	0.183	0.188	0.186	0.189	0.186	0.191
236	s3_21_15_w3_00_+30	0.5	0.103	1.496	0.306	0.291	0.295	0.300	0.307	0.311	0.313	0.318	0.317	0.317	0.320
237	s3_21_15_w4_00_+30	0.5	0.115	1.166	0.248	0.242	0.240	0.242	0.243	0.250	0.252	0.256	0.259	0.270	0.273

test-number	testseries name[4]	water depth [m]	H_{m0} [m]	$T_{m-1,0}$ [s]	run-up height $R_{u2\%}$ [m]										
					capacitive gauge	video stripe 1	video stripe 2	video stripe 3	video stripe 4	video stripe 5	video stripe 6	video stripe 7	video stripe 8	video stripe 9	video stripe 10
238	s3_21_15_w5_00_+30	0.5	0.148	1.825	0.425	0.404	0.408	0.420	0.427	0.431	0.431	0.431	0.423	0.422	0.416
239	s3_21_15_w6_00_+30	0.5	0.148	1.439	0.361	0.342	0.344	0.353	0.361	0.370	0.378	0.374	0.376	0.372	0.361
240	s3_17_15_w1_00_+45	0.5	0.097	1.335	0.197	0.240	0.231	0.221	0.194	0.194	0.192	0.189	0.180	0.177	0.185
241	s3_17_15_w2_00_+45	0.5	0.092	1.036	0.158	0.188	0.189	0.182	0.174	0.172	0.161	0.149	0.146	0.159	0.176
242	s3_17_15_w3_00_+45	0.5	0.128	1.518	0.250	0.291	0.289	0.277	0.270	0.266	0.254	0.244	0.237	0.238	0.249
243	s3_17_15_w4_00_+45	0.5	0.128	1.197	0.184	0.254	0.246	0.230	*0.194*	*0.194*	*0.193*	*0.193*	*0.193*	0.216	0.228
244	s3_17_15_w5_00_+45	0.5	0.171	1.826	0.339	0.365	0.361	0.352	0.352	0.350	0.343	0.335	0.330	0.332	0.332
245	s3_17_15_w6_00_+45	0.5	0.138	1.472	0.250	0.306	0.304	0.292	0.281	0.270	0.258	0.244	0.236	0.241	0.253

Annex L Analyzed data - wave run-up – 1:6 sloped dike (FlowDike 2)

Table-annex 12 Analyzed data – wave run-up - 1:6 sloped dike[5]

test-number	testseries name[6]	water depth [m]	H_{m0} [m]	$T_{m-1,0}$ [s]	run-up height $R_{u2\%}$ [m]										
					capacitive gauge	video stripe 1	video stripe 2	video stripe 3	video stripe 4	video stripe 5	video stripe 6	video stripe 7	video stripe 8	video stripe 9	video stripe 10
451	s4_01a_00_w1_00_00	0.55	0.086	1.528	0.163	0.146	0.157	0.167	0.164	0.166	0.156	0.165	0.159	0.152	0.140
452	s4_01a_00_w2_00_00	0.55	0.085	1.116	0.108	0.099	0.106	0.110	0.111	0.106	0.110	0.116	0.112	0.110	0.103
453	s4_01a_00_w3_00_00	0.55	0.115	1.736	0.216	0.185	0.212	0.213	0.223	0.227	0.221	0.228	0.222	0.217	0.205
454	s4_01a_00_w4_00_00	0.55	0.111	1.272	0.151	0.153	0.155	0.160	0.158	0.154	0.153	0.157	0.153	0.150	0.145
456	s4_01a_00_w5_00_00	0.55	0.143	1.888	0.303	0.217	0.274	0.289	0.292	0.291	0.295	0.290	0.292	0.282	0.259
457	s4_01a_00_w6_00_00	0.55	0.138	1.427	0.207	0.178	0.208	0.213	0.220	0.207	0.197	0.204	0.199	0.189	0.179
425	s4_01_00_w1_00_00	0.5	0.065	1.355	0.109	0.101	0.107	0.112	0.115	0.103	0.104	0.110	0.099	0.101	0.099
427	s4_01_00_w2_00_00	0.5	0.063	0.997	0.085	0.064	0.072	0.077	0.078	0.083	0.074	0.076	0.077	0.067	0.061
426	s4_01_00_w3_00_00	0.5	0.096	1.605	0.185	0.165	0.168	0.172	0.178	0.177	0.174	0.181	0.168	0.161	0.152
428	s4_01_00_w4_00_00	0.5	0.095	1.178	0.122	0.117	0.123	0.124	0.126	0.118	0.119	0.127	0.122	0.115	0.115
429	s4_01_00_w5_00_00	0.5	0.142	1.875	0.285	0.254	0.290	0.293	0.291	0.287	0.289	0.295	0.294	0.290	0.270
430	s4_01_00_w6_00_00	0.5	0.135	1.433	0.206	-	-	-	-	-	-	-	-	-	-
467	s4_07_15_w1_00_00	0.55	0.083	1.515	0.159	0.158	0.166	0.164	0.163	0.164	0.154	0.157	0.157	0.155	0.148
468	s4_07_15_w2_00_00	0.55	0.084	1.108	0.117	0.105	0.110	0.111	0.112	0.118	0.111	0.109	0.109	0.102	0.097
469	s4_07_15_w3_00_00	0.55	0.115	1.760	0.219	0.198	0.225	0.228	0.227	0.229	0.224	0.222	0.223	0.216	0.201
470	s4_07_15_w4_00_00	0.55	0.113	1.276	0.169	0.155	0.162	0.164	0.163	0.159	0.156	0.160	0.157	0.151	0.136

[5] italic: uncertain values

[6] Composition of testseries name: test series (i.e. s1_01) _ current [1/100 m/s] _ wave number _ wind [Hz] _ angle of wave attack [°] w = with or a = against the current

test-number	testseries name[6]	water depth [m]	H_{m0} [m]	$T_{m-1,0}$ [s]	run-up height $R_{u2\%}$ [m]										
					capacitive gauge	video stripe 1	video stripe 2	video stripe 3	video stripe 4	video stripe 5	video stripe 6	video stripe 7	video stripe 8	video stripe 9	video stripe 10
471	s4_07_15_w5_00_00	0.55	0.147	1.918	0.296	0.233	0.288	0.302	0.305	0.310	0.291	0.295	0.296	0.294	0.278
472	s4_07_15_w6_00_00	0.55	0.137	1.416	0.208	0.186	0.209	0.203	0.211	0.211	0.198	0.210	0.209	0.201	0.185
458	s4_04a_30_w1_00_00	0.55	0.084	1.505	0.169	0.156	0.170	0.172	0.178	0.177	0.169	0.168	0.168	0.167	0.152
459	s4_04a_30_w2_00_00	0.55	0.085	1.106	0.117	0.108	0.114	0.118	0.120	0.118	0.108	0.110	0.116	0.110	0.099
460	s4_04a_30_w3_00_00	0.55	0.117	1.759	0.228	0.206	0.230	0.239	0.241	0.244	0.235	0.231	0.235	0.231	0.213
461	s4_04a_30_w4_00_00	0.55	0.114	1.269	0.166	0.153	0.161	0.163	0.168	0.166	0.158	0.162	0.166	0.157	0.150
462	s4_04a_30_w5_00_00	0.55	0.151	1.921	0.297	0.211	0.279	0.296	0.301	0.306	0.310	0.299	0.306	0.302	0.291
463	s4_04a_30_w6_00_00	0.55	0.139	1.413	0.216	0.187	0.213	0.214	0.215	0.220	0.210	0.206	0.201	0.202	0.197
480	s4_10_40_w1_00_00	0.55	0.085	1.518	0.171	0.151	0.164	0.171	0.171	0.169	0.168	0.168	0.171	0.173	0.161
481	s4_10_40_w2_00_00	0.55	0.086	1.111	0.121	0.101	0.109	0.112	0.116	0.119	0.111	0.119	0.119	0.119	0.108
482	s4_10_40_w3_00_00	0.55	0.116	1.755	0.243	0.180	0.217	0.229	0.231	0.235	0.233	0.232	0.236	0.236	0.222
483	s4_10_40_w4_00_00	0.55	0.113	1.269	0.163	0.147	0.156	0.160	0.160	0.161	0.157	0.164	0.169	0.168	0.159
484	s4_10_40_w5_00_00	0.55	0.150	1.921	0.291	0.198	0.274	0.284	0.299	0.303	0.305	0.294	0.300	0.301	0.286
485	s4_10_40_w6_00_00	0.55	0.138	1.420	0.211	0.169	0.194	0.201	0.203	0.209	0.208	0.215	0.212	0.207	0.199
432	s4_32_30_w1_00_15m	0.5	0.065	1.358	0.124	0.086	0.092	0.096	0.106	0.114	0.095	0.108	0.109	0.116	0.115
433	s4_32_30_w2_00_15m	0.5	0.059	1.008	0.081	0.051	0.054	0.057	0.065	0.064	0.058	0.062	0.063	0.064	0.064
434	s4_32_30_w3_00_15m	0.5	0.086	1.551	0.157	0.131	0.140	0.144	0.146	0.154	0.143	0.145	0.152	0.156	0.154
435	s4_32_30_w4_00_15m	0.5	0.090	1.182	0.134	0.101	0.106	0.109	0.114	0.118	0.105	0.116	0.117	0.119	0.114
437	s4_32_30_w5_00_15m	0.5	0.123	1.782	0.182	0.162	0.172	0.176	0.175	0.181	0.175	0.180	0.187	0.186	0.187
438	s4_32_30_w6_00_15m	0.5	0.133	1.417	0.229	0.222	0.230	0.237	0.238	0.242	0.240	0.240	0.246	0.249	0.246
418	s4_02_00_w1_25_00	0.5	0.066	1.334	0.107	-	-	-	-	-	-	-	-	-	-
419	s4_02_00_w3_25_00	0.5	0.094	1.580	0.175	-	-	-	-	-	-	-	-	-	-
421	s4_02_00_w5_25_00	0.5	0.141	1.879	0.282	0.215	0.248	0.240	0.245	0.244	0.233	0.253	0.250	0.258	0.250
422	s4_03_00_w1_49_00	0.5	0.065	1.364	0.100	0.051	0.049	0.057	0.053	0.050	0.051	0.059	0.063	0.065	0.067

test-number	testseries name[6]	water depth [m]	H_{m0} [m]	$T_{m-1,0}$ [s]	run-up height $R_{u2\%}$ [m]										
					capacitive gauge	video stripe 1	video stripe 2	video stripe 3	video stripe 4	video stripe 5	video stripe 6	video stripe 7	video stripe 8	video stripe 9	video stripe 10
423	s4_03_00_w3_49_00	0.5	0.096	1.612	0.167	0.157	0.163	0.161	0.169	0.166	0.164	0.173	0.170	0.157	0.152
424	s4_03_00_w5_49_00	0.5	0.141	1.881	0.272	0.233	0.248	0.253	0.257	0.252	0.246	0.247	0.244	0.256	0.240
464	s4_03a_00_w1_49_00	0.55	0.086	1.531	0.144	0.141	0.148	0.153	0.158	0.148	0.151	0.156	0.153	0.150	0.141
465	s4_03a_00_w3_49_00	0.55	0.112	1.740	0.210	0.186	0.206	0.214	0.216	0.219	0.220	0.221	0.214	0.208	0.195
466	s4_03a_00_w5_49_00	0.55	0.141	1.897	0.289	0.205	0.272	0.280	0.284	0.291	0.284	0.283	0.288	0.285	0.272
411	s4_04_30_w1_00_00	0.5	0.070	1.317	0.129	-	-	-	-	-	-	-	-	-	-
410	s4_04_30_w2_00_00	0.5	0.069	1.000	0.086	-	-	-	-	-	-	-	-	-	-
409	s4_04_30_w3_00_00	0.5	0.095	1.564	0.181	-	-	-	-	-	-	-	-	-	-
408	s4_04_30_w4_00_00	0.5	0.099	1.149	0.140	-	-	-	-	-	-	-	-	-	-
407	s4_04_30_w5_00_00	0.5	0.144	1.873	0.282	0.245	0.281	0.288	0.293	0.291	0.284	0.283	0.282	0.285	0.271
406	s4_04_30_w6_00_00	0.5	0.141	1.398	0.202	0.180	0.197	0.201	0.206	0.205	0.194	0.192	0.192	0.187	0.182
412	s4_05_30_w1_49_00	0.5	0.066	1.329	0.129	-	-	-	-	-	-	-	-	-	-
413	s4_05_30_w3_49_00	0.5	0.090	1.574	0.185	-	-	-	-	-	-	-	-	-	-
414	s4_05_30_w5_49_00	0.5	0.137	1.879	0.292	-	-	-	-	-	-	-	-	-	-
415	s4_06_30_w1_25_00	0.5	0.066	1.324	0.124	-	-	-	-	-	-	-	-	-	-
416	s4_06_30_w3_25_00	0.5	0.090	1.570	0.188	-	-	-	-	-	-	-	-	-	-
417	s4_06_30_w5_25_00	0.5	0.138	1.878	0.289	-	-	-	-	-	-	-	-	-	-
473	s4_08_15_w1_49_00	0.55	0.083	1.523	0.151	0.156	0.161	0.162	0.162	0.161	0.148	0.156	0.159	0.154	0.141
474	s4_08_15_w3_49_00	0.55	0.114	1.769	0.210	0.199	0.225	0.224	0.223	0.222	0.209	0.210	0.211	0.211	0.195
475	s4_08_15_w5_49_00	0.55	0.147	1.926	0.294	0.224	0.291	0.302	0.312	0.302	0.291	0.285	0.283	0.280	0.269
488	s4_11_40_w1_49_00	0.55	0.085	1.530	0.164	0.154	0.166	0.172	0.175	0.174	0.162	0.166	0.169	0.171	0.161
489	s4_11_40_w3_49_00	0.55	0.115	1.768	0.239	0.188	0.226	0.230	0.237	0.237	0.234	0.231	0.229	0.226	0.217
490	s4_11_40_w5_49_00	0.55	0.149	1.931	0.294	0.192	0.280	0.286	0.297	0.301	0.304	0.288	0.288	0.295	0.287
440	s4_33_30_w3_00_15p	0.5	0.099	1.591	0.166	0.145	0.147	0.151	0.145	0.146	0.156	0.165	0.164	0.164	0.162

test-number	testseries name[6]	water depth [m]	H_{m0} [m]	$T_{m-1,0}$ [s]	run-up height $R_{u2\%}$ [m]										
					capacitive gauge	video stripe 1	video stripe 2	video stripe 3	video stripe 4	video stripe 5	video stripe 6	video stripe 7	video stripe 8	video stripe 9	video stripe 10
441	s4_33_30_w4_00_15p	0.5	0.094	1.191	0.130	0.109	0.118	0.112	0.116	0.118	0.121	0.124	0.116	0.116	0.111
442	s4_33_30_w5_00_15p	0.5	0.136	1.817	0.255	0.233	0.253	0.240	0.248	0.252	0.251	0.258	0.248	0.246	0.241
443	s4_33_30_w6_00_15p	0.5	0.144	1.446	0.195	0.169	0.176	0.180	0.188	0.185	0.188	0.193	0.193	0.188	0.185
444	s4_34_00_w1_00_15m	0.55	0.087	1.530	0.150	0.141	0.148	0.159	0.157	0.155	0.153	0.154	0.152	0.153	0.151
445	s4_34_00_w2_00_15m	0.55	0.082	1.121	0.122	0.093	0.101	0.104	0.107	0.114	0.105	0.103	0.102	0.102	0.097
447	s4_34_00_w3_00_15m	0.55	0.113	1.736	0.216	0.176	0.202	0.203	0.208	0.211	0.217	0.211	0.214	0.218	0.210
448	s4_34_00_w4_00_15m	0.55	0.108	1.280	0.157	0.139	0.150	0.150	0.153	0.151	0.149	0.145	0.150	0.148	0.148
449	s4_34_00_w5_00_15m	0.55	0.139	1.884	0.278	0.199	0.243	0.258	0.264	0.266	0.271	0.268	0.276	0.270	0.272
450	s4_34_00_w6_00_15m	0.55	0.139	1.432	0.198	0.166	0.187	0.190	0.193	0.193	0.188	0.188	0.189	0.192	0.182
476	s4_35_15_w1_00_00	0.55	0.068	1.333	0.124	0.106	0.116	0.117	0.120	0.117	0.112	0.121	0.115	0.104	0.093
477	s4_35_15_w2_00_00	0.55	0.066	0.982	0.084	0.063	0.066	0.074	0.083	0.074	0.068	0.076	0.071	0.065	0.064
486	s4_36_40_w1_00_00	0.55	0.068	1.333	0.125	0.099	0.113	0.118	0.116	0.121	0.112	0.117	0.120	0.119	0.108
487	s4_36_40_w2_00_00	0.55	0.067	0.985	0.083	0.060	0.064	0.068	0.074	0.073	0.068	0.076	0.072	0.071	0.063
511	s5_13_00_w1_00_30m	0.55	0.080	1.552	0.159	0.123	0.147	0.155	0.157	0.160	0.161	0.157	0.147	0.151	0.149
512	s5_13_00_w2_00_30m	0.55	0.078	1.138	0.105	0.080	0.088	0.096	0.101	0.106	0.100	0.098	0.103	0.101	0.099
513	s5_13_00_w3_00_30m	0.55	0.116	1.797	0.204	0.150	0.179	0.196	0.207	0.214	0.215	0.214	0.209	0.208	0.200
514	s5_13_00_w4_00_30m	0.55	0.101	1.283	0.150	0.117	0.135	0.145	0.153	0.155	0.152	0.150	0.148	0.147	0.142
515	s5_13_00_w5_00_30m	0.55	0.146	1.945	0.267	0.184	0.227	0.249	0.265	0.272	0.275	0.278	0.275	0.268	0.250
516	s5_13_00_w6_00_30m	0.55	0.126	1.441	0.187	0.146	0.167	0.178	0.185	0.191	0.191	0.196	0.196	0.194	0.184
530	s5_22_15_w1_00_30m	0.55	0.078	1.577	0.145	0.114	0.132	0.142	0.146	0.151	0.149	0.150	0.144	0.147	0.148
531	s5_22_15_w2_00_30m	0.55	0.068	1.133	0.099	0.084	0.089	0.092	0.091	0.092	0.096	0.093	0.092	0.098	0.099
532	s5_22_15_w3_00_30m	0.55	0.113	1.801	0.201	0.143	0.167	0.185	0.202	0.209	0.211	0.212	0.207	0.208	0.207
533	s5_22_15_w4_00_30m	0.55	0.097	1.292	0.137	0.112	0.121	0.128	0.129	0.133	0.137	0.140	0.140	0.143	0.146
534	s5_22_15_w5_00_30m	0.55	0.143	1.927	0.277	0.184	0.220	0.247	0.265	0.279	0.286	0.292	0.283	0.278	0.274

test-number	testseries name[6]	water depth [m]	H_{m0} [m]	$T_{m-1,0}$ [s]	run-up height $R_{u2\%}$ [m]										
					capacitive gauge	video stripe 1	video stripe 2	video stripe 3	video stripe 4	video stripe 5	video stripe 6	video stripe 7	video stripe 8	video stripe 9	video stripe 10
535	s5_22_15_w6_00_30m	0.55	0.128	1.450	0.171	0.144	0.154	0.161	0.171	0.174	0.183	0.189	0.190	0.192	0.191
517	s5_19_30_w1_00_30m	0.55	0.080	1.575	0.137	0.114	0.126	0.137	0.145	0.149	0.148	0.150	0.149	0.146	0.145
518	s5_19_30_w2_00_30m	0.55	0.070	1.139	0.089	0.086	0.095	0.098	0.097	0.097	0.092	0.090	0.088	0.089	0.090
519	s5_19_30_w3_00_30m	0.55	0.111	1.772	0.197	0.154	0.175	0.188	0.203	0.211	0.210	0.208	0.208	0.210	0.208
520	s5_19_30_w4_00_30m	0.55	0.100	1.300	0.127	0.126	0.136	0.138	0.145	0.138	0.138	0.133	0.128	0.136	0.135
521	s5_19_30_w5_00_30m	0.55	0.140	1.884	0.267	0.181	0.211	0.234	0.252	0.268	0.279	0.285	0.287	0.295	0.291
522	s5_19_30_w6_00_30m	0.55	0.129	1.450	0.160	0.154	0.161	0.170	0.177	0.175	0.172	0.175	0.177	0.177	0.177
501	s5_16_40_w1_00_30m	0.55	0.081	1.568	0.121	0.118	0.129	0.132	0.140	0.138	0.140	0.143	0.143	0.140	0.143
502	s5_16_40_w2_00_30m	0.55	0.072	1.142	0.093	0.086	0.092	0.095	0.095	0.093	0.094	0.091	0.087	0.090	0.083
503	s5_16_40_w3_00_30m	0.55	0.111	1.755	0.195	0.153	0.165	0.181	0.196	0.207	0.211	0.214	0.212	0.213	0.210
504	s5_16_40_w4_00_30m	0.55	0.101	1.301	0.125	0.125	0.141	0.149	0.152	0.155	0.145	0.143	0.132	0.132	0.130
505	s5_16_40_w5_00_30m	0.55	0.137	1.863	0.242	0.176	0.197	0.213	0.232	0.248	0.260	0.272	0.282	0.285	0.282
506	s5_16_40_w6_00_30m	0.55	0.130	1.451	0.169	0.158	0.168	0.175	0.177	0.180	0.178	0.181	0.173	0.169	0.168
536	s5_15_00_w1_49_30m	0.55	0.078	1.556	0.145	0.118	0.141	0.151	0.153	0.156	0.152	0.150	0.145	0.147	0.141
537	s5_15_00_w3_49_30m	0.55	0.113	1.802	0.204	0.146	0.179	0.201	0.206	0.204	0.210	0.214	0.209	0.205	0.194
538	s5_15_00_w5_49_30m	0.55	0.144	1.943	0.253	0.179	0.225	0.245	0.255	0.259	0.264	0.266	0.265	0.256	0.241
523	s5_20_30_w1_49_30m	0.55	0.081	1.576	0.141	0.110	0.126	0.131	0.138	0.142	0.149	0.152	0.147	0.141	0.138
524	s5_20_30_w3_49_30m	0.55	0.111	1.774	0.193	-	-	-	-	-	-	-	-	-	-
525	s5_20_30_w5_49_30m	0.55	0.140	1.886	0.261	0.180	0.203	0.233	0.248	0.263	0.275	0.283	0.287	0.288	0.281
508	s5_17_40_w1_49_30m	0.55	0.082	1.570	0.125	0.112	0.124	0.133	0.138	0.139	0.137	0.141	0.142	0.139	0.141
509	s5_17_40_w3_49_30m	0.55	0.112	1.759	0.182	0.152	0.162	0.177	0.189	0.198	0.201	0.206	0.209	0.210	0.205
510	s5_17_40_w5_49_30m	0.55	0.138	1.862	0.234	0.177	0.202	0.218	0.232	0.242	0.254	0.268	0.278	0.284	0.279
601	s6_27_15_w1_00_45p	0.55	0.082	1.577	0.143	0.133	0.128	0.122	0.131	0.129	0.125	0.125	0.121	0.118	0.115
602	s6_27_15_w2_00_45p	0.55	0.071	1.165	0.083	0.087	0.081	0.079	0.072	0.069	0.070	0.072	0.072	0.074	0.074

test-number	testseries name[6]	water depth [m]	H_{m0} [m]	$T_{m-1,0}$ [s]	run-up height $R_{u2\%}$ [m]										
					capacitive gauge	video stripe 1	video stripe 2	video stripe 3	video stripe 4	video stripe 5	video stripe 6	video stripe 7	video stripe 8	video stripe 9	video stripe 10
603	s6_27_15_w3_00_45p	0.55	0.115	1.797	0.189	0.183	0.179	0.187	0.188	0.186	0.179	0.174	0.165	0.160	0.154
604	s6_27_15_w4_00_45p	0.55	0.101	1.323	0.120	0.126	0.119	0.116	0.114	0.110	0.107	0.108	0.107	0.106	0.107
605	s6_27_15_w5_00_45p	0.55	0.139	1.944	0.218	0.237	0.238	0.236	0.232	0.223	0.217	0.210	0.202	0.194	0.192
606	s6_27_15_w6_00_45p	0.55	0.131	1.466	0.150	0.155	0.149	0.149	0.146	0.140	0.138	0.137	0.137	0.136	0.141
607	s6_26_15_w1_00_30p	0.55	0.082	1.534	0.166	0.135	0.135	0.139	0.137	0.146	0.149	0.147	0.147	0.146	0.151
608	s6_26_15_w2_00_30p	0.55	0.080	1.153	0.110	0.088	0.092	0.088	0.093	0.092	0.103	0.107	0.105	0.102	0.094
609	s6_26_15_w3_00_30p	0.55	0.112	1.766	0.206	0.189	0.187	0.193	0.199	0.211	0.207	0.209	0.205	0.205	0.199
610	s6_26_15_w4_00_30p	0.55	0.112	1.301	0.155	0.137	0.136	0.132	0.139	0.143	0.148	0.148	0.146	0.147	0.141
611	s6_26_15_w5_00_30p	0.55	0.141	1.922	0.251	0.238	0.243	0.251	0.255	0.262	0.264	0.266	0.263	0.258	0.252
612	s6_26_15_w6_00_30p	0.55	0.135	1.436	0.184	0.167	0.171	0.171	0.179	0.187	0.189	0.186	0.187	0.187	0.183
613	s6_25_00_w1_00_45p	0.55	0.082	1.614	0.124	0.129	0.124	0.122	0.120	0.116	0.120	0.121	0.122	0.129	0.130
614	s6_25_00_w2_00_45p	0.55	0.070	1.149	0.092	0.073	0.072	0.074	0.076	0.080	0.078	0.082	0.082	0.080	0.079
615	s6_25_00_w3_00_45p	0.55	0.126	1.833	0.163	0.177	0.171	0.170	0.164	0.160	0.158	0.158	0.160	0.162	0.161
616	s6_25_00_w4_00_45p	0.55	0.097	1.311	0.124	0.108	0.106	0.111	0.113	0.114	0.121	0.124	0.125	0.119	0.119
617	s6_25_00_w5_00_45p	0.55	0.151	1.960	0.200	0.215	0.214	0.211	0.204	0.199	0.196	0.191	0.188	0.187	0.198
618	s6_25_00_w6_00_45p	0.55	0.129	1.475	0.156	0.138	0.136	0.137	0.141	0.143	0.145	0.151	0.153	0.152	0.155
625	s6_28_30_w1_00_30p	0.55	0.085	1.541	0.145	0.128	0.133	0.132	0.136	0.144	0.146	0.150	0.153	0.152	0.150
626	s6_28_30_w2_00_30p	0.55	0.082	1.144	0.097	0.080	0.080	0.086	0.084	0.089	0.096	0.097	0.100	0.102	0.097
627	s6_28_30_w3_00_30p	0.55	0.116	1.801	0.199	0.175	0.174	0.175	0.185	0.191	0.201	0.208	0.205	0.206	0.212
628	s6_28_30_w4_00_30p	0.55	0.110	1.294	0.143	0.119	0.124	0.124	0.124	0.140	0.143	0.145	0.148	0.148	0.146
629	s6_28_30_w5_00_30p	0.55	0.154	1.977	0.248	0.228	0.238	0.246	0.255	0.265	0.267	0.265	0.267	0.268	0.257
630	s6_28_30_w6_00_30p	0.55	0.135	1.442	0.172	0.152	0.152	0.155	0.164	0.170	0.173	0.180	0.184	0.182	0.182
619	s6_29_30_w1_00_45p	0.55	0.091	1.590	0.159	0.141	0.138	0.134	0.137	0.144	0.146	0.145	0.141	0.139	0.135
620	s6_29_30_w2_00_45p	0.55	0.071	1.186	0.098	0.088	0.082	0.084	0.083	0.084	0.096	0.098	0.097	0.093	0.085

test-number	testseries name[6]	water depth [m]	H_{m0} [m]	$T_{m-1,0}$ [s]	run-up height $R_{u2\%}$ [m]										
					capacitive gauge	video stripe 1	video stripe 2	video stripe 3	video stripe 4	video stripe 5	video stripe 6	video stripe 7	video stripe 8	video stripe 9	video stripe 10
621	s6_29_30_w3_00_45p	0.55	0.116	1.776	0.193	0.177	0.177	0.186	0.196	0.202	0.197	0.196	0.193	0.193	0.187
622	s6_29_30_w4_00_45p	0.55	0.107	1.348	0.139	0.130	0.131	0.134	0.133	0.139	0.143	0.143	0.139	0.135	0.128
623	s6_29_30_w5_00_45p	0.55	0.140	1.945	0.240	0.241	0.245	0.255	0.254	0.252	0.247	0.239	0.233	0.228	0.226
624	s6_29_30_w6_00_45p	0.55	0.143	1.489	0.179	0.163	0.167	0.166	0.170	0.177	0.177	0.178	0.171	0.163	0.157
637	s6_30_40_w1_00_30p	0.55	0.085	1.566	0.140	0.114	0.121	0.120	0.128	0.131	0.137	0.145	0.148	0.145	0.145
638	s6_30_40_w2_00_30p	0.55	0.080	1.151	0.081	0.067	0.068	0.069	0.068	0.071	0.080	0.083	0.085	0.089	0.084
639	s6_30_40_w3_00_30p	0.55	0.120	1.818	0.183	0.156	0.162	0.165	0.179	0.180	0.190	0.195	0.194	0.194	0.197
640	s6_30_40_w4_00_30p	0.55	0.108	1.313	0.129	0.106	0.111	0.109	0.114	0.120	0.126	0.130	0.134	0.134	0.136
641	s6_30_40_w5_00_30p	0.55	0.158	2.008	0.243	0.214	0.231	0.237	0.246	0.250	0.257	0.255	0.257	0.258	0.251
642	s6_30_40_w6_00_30p	0.55	0.134	1.467	0.166	0.140	0.143	0.147	0.158	0.160	0.167	0.171	0.176	0.172	0.174
631	s6_31_40_w1_00_45p	0.55	0.091	1.591	0.153	0.129	0.130	0.126	0.133	0.143	0.141	0.142	0.144	0.141	0.138
632	s6_31_40_w2_00_45p	0.55	0.076	1.201	0.085	0.070	0.070	0.070	0.069	0.073	0.082	0.087	0.086	0.089	0.081
633	s6_31_40_w3_00_45p	0.55	0.120	1.779	0.187	0.167	0.168	0.173	0.185	0.186	0.197	0.198	0.198	0.192	0.189
634	s6_31_40_w4_00_45p	0.55	0.113	1.349	0.137	0.116	0.117	0.116	0.124	0.129	0.135	0.138	0.139	0.138	0.135
635	s6_31_40_w5_00_45p	0.55	0.146	1.958	0.252	0.229	0.247	0.248	0.245	0.250	0.254	0.254	0.251	0.250	0.245
636	s6_31_40_w6_00_45p	0.55	0.144	1.485	0.169	0.148	0.148	0.154	0.161	0.167	0.170	0.176	0.176	0.177	0.169

Annex M Analyzed data - wave overtopping – 1:3 sloped dike (FlowDike 1)

Table-annex 13 Analyzed data – wave overtopping - 1:3 sloped dike

test-number	testseries name[7]	start time	end time	at toe of 60 cm dike				at toe of 70 cm dike			
				H_{m0} [m]	$T_{m-1,0}$ [s]	loadcell 41 upstream [l/(s·m)]	loadcell 43 downstream [l/(s·m)]	H_{m0} [m]	$T_{m-1,0}$ [s]	loadcell 37 upstream [l/(s·m)]	loadcell 39 downstream [l/(s·m)]
144	s1_01_00_w1_00_00	10	1400	0.0706	1.3494	0.3485	0.4080	0.068	1.3271	-	0.0025
145	s1_01_00_w2_00_00	10	1000	0.0588	1.0196	0.0478	0.0354	0.0649	1.0116	-	-
198	s1_01_00_w3_00_00	5	1650	0.1004	1.599	1.4388	1.0522	0.095	1.5762	0.0574	0.1107
199	s1_01_00_w4_00_00	5	1170	0.092	1.1639	0.6039	0.6199	0.0945	1.1451	-	0.0248
200	s1_01_00_w5_00_00	0	2010	0.1476	1.8882	4.3908	3.4169	0.1399	1.8722	0.6362	1.5236
201	s1_01_00_w6_00_00	5	1470	0.1449	1.4384	2.9798	2.5997	0.1407	1.4148	0.1696	0.3692
114	s1_03_30_w1_00_00	10	1400	0.0509	1.0392	0.0209	0.0079	0.0538	1.0333	-	-
115	s1_03_30_w2_00_00	10	1000	0.0466	0.7858	-	-	0.0493	0.787	-	-
116	s1_03_30_w3_00_00	10	1650	0.0966	1.4261	0.9605	1.2201	0.1043	1.4287	0.0156	0.0633
117	s1_03_30_w4_00_00	10	1200	0.1006	1.0643	0.5052	0.2997	0.1038	1.0574	-	0.0079
119	s1_03_30_w5_00_00	15	2050	0.1416	1.8873	4.6864	4.6638	0.1409	1.8584	0.6586	0.5706
120	s1_03_30_w6_00_00	5	1500	0.131	1.4075	2.3851	2.8664	0.1394	1.4055	0.1224	0.3120
153	s1_06_00_w1_49_00	10	1400	0.069	1.3615	0.3435	0.3175	0.0672	1.3335	-	0.0050
154	s1_06_00_w3_49_00	10	1650	0.0985	1.6052	1.3902	0.8805	0.0936	1.5757	0.0512	0.1964
155	s1_06_00_w5_49_00	15	2050	0.144	1.8885	4.3270	3.0374	0.1348	1.8709	0.5667	1.7329
150	s1_06b_00_w1_25_00	10	1400	0.0693	1.3583	0.3448	0.3435	0.0676	1.3319	0.0025	0.0037
151	s1_06b_00_w3_25_00	10	1650	0.0994	1.6019	1.3759	0.9655	0.094	1.5737	0.0512	0.1577
152	s1_06b_00_w5_25_00	15	2050	0.1467	1.8893	4.6155	3.4745	0.1363	1.8737	0.5835	1.8077
121	s1_08_30_w1_49_00	10	1400	0.0496	1.1161	0.0615	0.0079	0.0502	1.1084	-	-

[7] Composition of testseries name (e. i. s1_01_00_w1_00_00):
s1 (set-up no.) _ 01 (no. of testseries) _ 00 (current [m/(100s)]) _ w1 (wave no.) _ 00 (wind [Hz (wind generator)]) _ 00 (angle of wave attack [°], w = with or a = against current)

test-number	testseries name[7]	start time	end time	at toe of 60 cm dike				at toe of 70 cm dike			
				H_{m0} [m]	$T_{m-1,0}$ [s]	loadcell 41 upstream [l/(s·m)]	loadcell 43 downstream [l/(s·m)]	H_{m0} [m]	$T_{m-1,0}$ [s]	loadcell 37 upstream [l/(s·m)]	loadcell 39 downstream [l/(s·m)]
122	s1_08_30_w3_49_00	10	1650	0.0929	1.5663	1.1768	1.2667	0.0939	1.5493	0.0275	0.0844
123	s1_08_30_w5_49_00	15	2050	0.1447	1.9173	5.0719	4.6257	0.1423	1.8792	0.7668	0.6924
137	s1_08b_30_w1_25_00	10	1400	0.064	1.2977	0.2604	0.2406	0.0684	1.3118	-	0.0037
138	s1_08b_30_w3_25_00	10	1650	0.0947	1.5782	1.2076	1.3532	0.0958	1.5644	0.0292	0.1024
140	s1_08b_30_w5_25_00	15	2050	0.1404	1.911	4.8252	4.8021	0.1402	1.8689	0.7484	0.7026
162	s1_11_15_w1_00_00	10	1400	0.0651	1.3187	0.2939	0.3981	0.0671	1.3084	-	0.0062
163	s1_11_15_w2_00_00	10	1000	0.0663	1.0152	0.0744	0.0354	0.065	1.0048	-	-
164	s1_11_15_w3_00_00	10	1650	0.0997	1.5933	1.3061	1.4345	0.0962	1.5732	0.0292	0.0836
165	s1_11_15_w4_00_00	5	1170	0.0907	1.127	0.4828	0.6360	0.0982	1.1477	-	0.0146
166	s1_11_15_w5_00_00	0	2010	0.1509	1.9067	5.1216	4.2199	0.1435	1.8659	0.5320	0.6463
167	s1_11_15_w6_00_00	5	1470	0.1395	1.4266	2.6988	3.0547	0.1367	1.4036	0.1108	0.3427
156	s1_12_00_w1_00_15w	10	1400	0.067	1.2898	0.4353	0.1959	0.0747	1.3191	0.0025	-
157	s1_12_00_w2_00_15w	10	1000	0.0728	0.9865	0.1009	0.0407	0.0722	0.9762	-	-
158	s1_12_00_w3_00_15w	10	1650	0.0884	1.4861	1.2788	1.1336	0.096	1.5004	0.0407	0.0867
159	s1_12_00_w4_00_15w	10	1200	0.1008	1.1361	0.8417	0.3836	0.0992	1.1449	-	0.0131
160	s1_12_00_w5_00_15w	15	2050	0.1365	1.8386	3.4290	4.6666	0.1332	1.7817	0.7329	0.8614
161	s1_12_00_w6_00_15w	5	1500	0.1343	1.3844	3.1702	2.4240	0.1473	1.4134	0.1881	0.2331
168	s1_13_15_w1_00_15w	10	1400	0.0707	1.3041	0.4427	0.1823	0.0692	1.2971	0.0025	0.0050
169	s1_13_15_w2_00_15w	10	1000	0.0697	0.9793	0.1009	0.0443	0.0716	0.9859	-	-
170	s1_13_15_w3_00_15w	10	1650	0.0914	1.4941	1.2638	0.7385	0.0931	1.4929	0.0595	0.0564
171	s1_13_15_w4_00_15w	10	1200	0.1037	1.152	0.7279	0.5718	0.1032	1.1451	0.0088	0.0102
172	s1_13_15_w5_00_15w	15	2050	0.1321	1.797	3.0645	3.2890	0.1273	1.7801	1.0050	1.0309
173	s1_13_15_w6_00_15w	5	1500	0.1412	1.3935	3.0113	2.1870	0.1386	1.3867	0.2238	0.3634
174	s1_15_15_w1_00_15a	10	1400	0.0785	1.3372	0.3956	0.1228	0.0713	1.3118	-	-
175	s1_15_15_w2_00_15a	10	1000	0.071	0.9988	0.0779	0.0266	0.0715	0.9852	-	-
176	s1_15_15_w3_00_15a	10	1650	0.1036	1.5226	0.9668	0.3792	0.094	1.5084	0.0324	0.0919
177	s1_15_15_w4_00_15a	10	1200	0.1074	1.1698	0.7473	0.2626	0.0989	1.1567	-	0.0146

test-number	testseries name[7]	start time	end time	at toe of 60 cm dike				at toe of 70 cm dike			
				H_{m0} [m]	$T_{m-1,0}$ [s]	loadcell 41 upstream [l/(s·m)]	loadcell 43 downstream [l/(s·m)]	H_{m0} [m]	$T_{m-1,0}$ [s]	loadcell 37 upstream [l/(s·m)]	loadcell 39 downstream [l/(s·m)]
178	s1_15_15_w5_00_15a	15	2050	0.1409	1.786	2.9564	1.4516	0.1323	1.8015	0.7539	0.8988
179	s1_15_15_w6_00_15a	5	1500	0.1525	1.4042	2.6104	1.3067	0.1402	1.4046	0.1973	0.3300
131	s1_16_30_w1_00_15a	10	1400	0.0762	1.351	0.3869	0.2480	0.0706	1.3333	-	-
132	s1_16_30_w2_00_15a	10	1000	0.0692	0.9893	0.0761	0.0460	0.0692	0.9908	-	-
133	s1_16_30_w3_00_15a	10	1650	0.1068	1.554	1.1276	0.7427	0.0988	1.5314	0.0188	0.0637
134	s1_16_30_w4_00_15a	10	1200	0.0994	1.1787	0.6593	0.4522	0.0972	1.1655	-	0.0073
135	s1_16_30_w5_00_15a	15	2050	0.1474	1.8346	3.8898	2.5679	0.1322	1.8088	0.7822	0.9031
136	s1_16_30_w6_00_15a	5	1500	0.1541	1.437	2.8749	1.8971	0.1465	1.4381	0.0923	0.2896
124	s1_19_30_w1_00_15w	10	1400	0.071	1.3281	0.2592	0.2617	0.0663	1.2914	-	-
125	s1_19_30_w2_00_15w	10	1000	0.0691	0.9787	0.0903	0.0567	0.0696	0.9855	-	-
126	s1_19_30_w3_00_15w	10	1650	0.0948	1.5225	1.2168	0.6570	0.0908	1.5114	0.0522	0.0951
127	s1_19_30_w4_00_15w	10	1200	0.0941	1.1437	0.6331	0.5776	0.0958	1.138	-	0.0117
128	s1_19_30_w5_00_15w	15	2050	0.1234	1.7655	3.1721	2.5538	0.1267	1.7962	0.7539	0.8979
129	s1_19_30_w6_00_15w	5	1500	0.1449	1.4161	2.3203	2.2927	0.1322	1.3897	0.2181	0.3796
180	s2_02_00_w1_00_30w	5	1415	0.081	1.3234	0.2956	0.3205	0.0768	1.3028	-	-
181	s2_02_00_w2_00_30w	5	1000	0.0785	0.9915	0.1024	0.0898	0.0805	0.9895	-	-
182	s2_02_00_w3_00_30w	5	1652	0.1077	1.5331	1.5367	1.0703	0.1074	1.5711	0.0555	0.0715
183	s2_02_00_w4_00_30w	8	1174	0.1091	1.1701	0.9230	0.5679	0.1112	1.1571	-	-
184	s2_02_00_w5_00_30w	0	2010	0.1444	1.8459	5.1917	3.5031	0.159	1.8861	0.4442	0.6376
185	s2_02_00_w6_00_30w	5	1470	0.1554	1.4432	3.0031	3.1883	0.1635	1.4158	0.1144	0.1729
202	s2_04_30_w1_00_30w	10	1400	0.0717	1.3305	0.3966	0.4171	0.0808	1.3393	-	-
203	s2_04_30_w2_00_30w	10	1000	0.072	1.0121	0.1379	0.1442	0.0743	1.0389	-	-
204	s2_04_30_w3_00_30w	10	1650	0.1056	1.5945	1.4155	1.5750	0.1089	1.5529	0.0037	0.0136
205	s2_04_30_w4_00_30w	10	1200	0.104	1.1743	0.8968	0.9691	0.1114	1.1972	-	-
206	s2_04_30_w5_00_30w	15	2050	0.1527	1.8652	3.8287	4.2699	0.1463	1.8172	0.1080	0.2494
207	s2_04_30_w6_00_30w	5	1500	0.1498	1.4344	2.9268	3.2107	0.1556	1.4273	0.0517	0.0967
189	s2_07_00_w1_49_30w	10	1400	0.0808	1.3274	0.3512	0.3205	0.0743	1.3177	0.0044	0.0044

test-number	testseries name[7]	start time	end time	at toe of 60 cm dike				at toe of 70 cm dike			
				H_{m0} [m]	$T_{m-1,0}$ [s]	loadcell 41 upstream [l/(s·m)]	loadcell 43 downstream [l/(s·m)]	H_{m0} [m]	$T_{m-1,0}$ [s]	loadcell 37 upstream [l/(s·m)]	loadcell 39 downstream [l/(s·m)]
190	s2_07_00_w3_49_30w	10	1650	0.1066	1.5336	1.6186	1.0535	0.1054	1.5813	0.1060	0.0850
191	s2_07_00_w5_49_30w	15	2050	0.1418	1.846	5.0982	3.4159	0.1553	1.8883	0.6247	0.6770
186	s2_07b_00_w1_25_30w	10	1400	0.0807	1.3233	0.2502	0.2561	0.0752	1.307	0.0044	0.0029
187	s2_07b_00_w3_25_30w	10	1650	0.1069	1.5317	1.5223	1.0032	0.1062	1.576	0.0666	0.0715
188	s2_07b_00_w5_25_30w	15	2050	0.1435	1.845	5.0663	3.3932	0.1576	1.8871	0.5144	0.6378
211	s2_09_30_w1_49_30w	10	1400	0.0714	1.3344	0.4434	0.4375	0.0811	1.3417	-	-
212	s2_09_30_w3_49_30w	10	1650	0.1055	1.6022	1.4321	1.5641	0.1092	1.5555	0.0099	0.0320
213	s2_09_30_w5_49_30w	15	2050	0.1513	1.8688	3.8075	4.2388	0.1463	1.8159	0.1565	0.2857
208	s2_09b_30_w1_25_30w	10	1400	0.072	1.3317	0.4156	0.4185	0.0812	1.3413	-	-
209	s2_09b_30_w3_25_30w	10	1650	0.1058	1.5978	1.4137	1.5616	0.1095	1.5553	0.0049	0.0197
210	s2_09b_30_w5_25_30w	15	2050	0.1519	1.8654	3.8457	4.2479	0.1469	1.817	0.1161	0.2665
192	s2_20_15_w1_00_30w	5	1410	0.0702	1.302	0.5502	0.3468	0.0832	1.3265	-	-
193	s2_20_15_w2_00_30w	10	1000	0.079	0.9998	0.1818	0.1337	0.0811	1.0158	-	-
194	s2_20_15_w3_00_30w	10	1650	0.1057	1.5705	1.5425	1.7315	0.1147	1.543	0.0197	0.0320
195	s2_20_15_w4_00_30w	10	1200	0.1078	1.153	0.9243	0.9157	0.1198	1.1768	-	-
196	s2_20_15_w5_00_30w	15	2050	0.1482	1.8706	4.8512	4.2058	0.158	1.8391	0.1938	0.3988
197	s2_20_15_w6_00_30w	5	1500	0.1487	1.4374	3.5034	3.2044	0.1662	1.4182	0.0994	0.1661
222	s3_05_30_w1_00_30a	5	1420	0.0764	1.3276	0.2795	0.3863	0.0707	1.3361	0.0176	0.0029
223	s3_05_30_w2_00_30a	5	1000	0.0748	1.0217	0.0731	0.1107	0.0723	1.026	-	-
224	s3_05_30_w3_00_30a	5	1660	0.1034	1.531	1.3020	1.0124	0.0999	1.5597	0.1800	0.0382
225	s3_05_30_w4_00_30a	5	1180	0.1045	1.1906	0.5439	0.7522	0.0989	1.1966	0.0293	0.0138
226	s3_05_30_w5_00_30a	5	2010	0.146	1.833	4.4395	4.6321	0.155	1.8948	1.9016	0.3524
227	s3_05_30_w6_00_30a	5	1470	0.1514	1.4638	2.6547	3.0236	0.1416	1.4998	0.4697	0.1511
228	s3_14_30_w1_00_45a	10	1400	0.0877	1.3469	0.3615	0.4083	0.0962	1.354	-	-
229	s3_14_30_w2_00_45a	10	1000	0.0812	1.0622	0.0773	0.0919	0.0853	1.0732	-	-
230	s3_14_30_w3_00_45a	10	1650	0.1249	1.565	1.2870	1.5618	0.1302	1.5468	0.0185	0.0653
231	s3_14_30_w4_00_45a	10	1200	0.1155	1.2162	0.5474	0.5818	0.1244	1.2392	-	-

test-number	testseries name[7]	start time	end time	at toe of 60 cm dike				at toe of 70 cm dike			
				H_{m0} [m]	$T_{m-1,0}$ [s]	loadcell 41 upstream [l/(s·m)]	loadcell 43 downstream [l/(s·m)]	H_{m0} [m]	$T_{m-1,0}$ [s]	loadcell 37 upstream [l/(s·m)]	loadcell 39 downstream [l/(s·m)]
232	s3_14_30_w5_00_45a	15	2050	0.175	1.856	3.6647	4.1455	0.1668	1.8396	0.4139	1.0034
233	s3_14_30_w6_00_45a	5	1500	0.1284	1.5008	1.6133	1.7911	0.1481	1.4962	0.0368	0.0613
240	s3_17_15_w1_00_45a	10	1400	0.0902	1.3363	0.3629	0.4639	0.0975	1.3348	-	-
241	s3_17_15_w2_00_45a	10	1000	0.0885	1.026	0.0710	0.1149	0.0918	1.0359	-	-
242	s3_17_15_w3_00_45a	10	1650	0.1255	1.5409	1.4103	1.2354	0.1282	1.5181	0.0542	0.0296
243	s3_17_15_w4_00_45a	10	1200	0.1198	1.196	0.5680	0.7246	0.1276	1.197	-	-
244	s3_17_15_w5_00_45a	15	2050	0.1753	1.8442	3.3877	3.3756	0.171	1.8263	0.4351	0.8218
245	s3_17_15_w6_00_45a	5	1500	0.1362	1.4822	1.5261	1.5733	0.1384	1.4718	0.0545	0.0517
215	s3_18_00_w1_00_45a	10	1400	0.0965	1.3101	0.1815	0.1302	0.0869	1.3089	-	-
216	s3_18_00_w2_00_45a	10	1000	0.0957	1.0189	0.0648	0.0460	0.0937	1.007	-	-
217	s3_18_00_w3_00_45a	10	1650	0.1232	1.4837	0.5670	0.4807	0.1231	1.5282	0.0259	0.0247
218	s3_18_00_w4_00_45a	10	1200	0.1253	1.1761	0.4165	0.4062	0.1264	1.166	-	-
220	s3_18_00_w5_00_45a	15	2050	0.1575	1.7751	1.9492	1.3247	0.1704	1.8138	0.3917	0.1686
234	s3_21_15_w1_00_30a	0	1415	0.079	1.3178	0.3058	0.3834	0.0787	1.2868	-	0.0044
235	s3_21_15_w2_00_30a	0	985	0.079	1.0021	0.0898	0.0898	0.0858	1.0064	-	-
236	s3_21_15_w3_00_30a	3	1660	0.1021	1.5068	1.0959	1.6166	0.1033	1.4957	0.0431	0.0567
237	s3_21_15_w4_00_30a	5	1180	0.1084	1.1724	0.7126	0.6610	0.1148	1.166	-	0.0120
238	s3_21_15_w5_00_30a	5	2050	0.1431	1.8129	4.8153	4.3449	0.1475	1.8249	0.8684	0.5200
239	s3_21_15_w6_00_30a	5	1480	0.1512	1.439	2.5577	3.5569	0.1483	1.4391	0.1960	0.3703

Annex N Analyzed data - wave overtopping – 1:6 sloped dike (FlowDike 2)

Table-annex 14 Analyzed data – wave overtopping - 1:6 sloped dike

test-number	testseries name[8]	water depth [m]	start time of analysis	end time of analysis	at toe of 60 cm dike				at toe of 70 cm dike			
					H_{m0} [m]	$T_{m-1,0}$ [s]	loadcell 41 upstream [l/(s·m)]	loadcell 43 downstream [l/(s·m)]	H_{m0} [m]	$T_{m-1,0}$ [s]	loadcell 37 upstream [l/(s·m)]	loadcell 39 downstream [l/(s·m)]
425	s4_01_00_w1_00_00	0.5	8	1400	0.0653	1.3547	-	-	0.0698	1.3496	-	-
427	s4_01_00_w2_00_00	0.5	10	1000	0.0633	0.9968	-	-	0.0652	1.0011	-	-
426	s4_01_00_w3_00_00	0.5	8	1680	0.0957	1.6051	0.1670	0.0910	0.1024	1.6125	-	-
428	s4_01_00_w4_00_00	0.5	12	1185	0.0946	1.178	0.0136	0.0068	0.0994	1.1764	-	-
429	s4_01_00_w5_00_00	0.5	16	2025	0.1422	1.8747	0.4148	0.4140	0.1522	1.9465	0.0603	0.1259
430	s4_01_00_w6_00_00	0.5	6	1490	0.1349	1.4332	0.3144	0.2385	0.1425	1.4187	-	-
451	s4_01a_00_w1_00_00	0.55	0	1690	0.0865	1.5275	1.3411	1.6670	0.0929	1.5221	-	-
452	s4_01a_00_w2_00_00	0.55	0	1210	0.0849	1.1159	0.2398	0.2059	0.0914	1.1063	-	-
453	s4_01a_00_w3_00_00	0.55	0	1990	0.1146	1.7364	3.5752	2.5777	0.1225	1.7326	0.0319	0.0854
454	s4_01a_00_w4_00_00	0.55	0	1390	0.111	1.272	1.0218	0.8728	0.1191	1.2636	-	-
456	s4_01a_00_w5_00_00	0.55	5	2180	0.1429	1.8882	7.2737	5.5398	0.1498	1.9204	0.2385	0.8590
457	s4_01a_00_w6_00_00	0.55	5	1580	0.1384	1.4266	2.9044	2.5337	0.1468	1.4176	0.0242	0.0260
418	s4_02_00_w1_25_00	0.5	0	1390	0.0656	1.334	-	-	0.0694	1.329	-	-
419	s4_02_00_w3_25_00	0.5	0	1630	0.0937	1.5797	0.0713	0.0773	0.0985	1.5764	-	-
421	s4_02_00_w5_25_00	0.5	0	1990	0.1415	1.8791	1.8477	1.3227	0.1523	1.9447	0.0780	0.1394
422	s4_03_00_w1_49_00	0.5	10	1400	0.0652	1.364	-	-	0.0692	1.3637	-	-
423	s4_03_00_w3_49_00	0.5	5	1640	0.0957	1.6123	-	-	0.1033	1.6214	-	-
424	s4_03_00_w5_49_00	0.5	5	2000	0.1408	1.8812	1.0407	0.6853	0.1532	1.9475	-	-
464	s4_03a_00_w1_49_00	0.55	3	1695	0.0861	1.5315	1.3372	0.6131	0.0928	1.5353	0.0058	-

[8] Composition of testseries name (e. i. s1_01_00_w1_00_00):
s1 (set-up no.) _ 01 (no. of testseries) _ 00 (current [m/(100s)]) _ w1 (wave no.) _ 00 (wind [Hz (wind generator)]) _ 00 (angle of wave attack [°], w = with or a = against current)

test-number	testseries name[8]	water depth [m]	start time of analysis	end time of analysis	at toe of 60 cm dike				at toe of 70 cm dike			
					H_{m0} [m]	$T_{m-1,0}$ [s]	loadcell 41 upstream [l/(s·m)]	loadcell 43 downstream [l/(s·m)]	H_{m0} [m]	$T_{m-1,0}$ [s]	loadcell 37 upstream [l/(s·m)]	loadcell 39 downstream [l/(s·m)]
465	s4_03a_00_w3_49_00	0.55	6	2000	0.1122	1.7404	3.4651	2.3995	0.1225	1.7424	0.0671	0.1230
466	s4_03a_00_w5_49_00	0.55	6	2175	0.1409	1.8966	7.3205	5.6092	0.1534	1.9365	0.3405	0.8861
411	s4_04_30_w1_00_00	0.5	0	1395	0.0699	1.3172	-	0.0049	0.0723	1.3579	-	-
410	s4_04_30_w2_00_00	0.5	0	980	0.0686	1	-	-	0.0654	1.0795	-	-
409	s4_04_30_w3_00_00	0.5	0	1635	0.0948	1.564	0.0633	0.1619	0.1002	1.6124	-	-
408	s4_04_30_w4_00_00	0.5	2	1155	0.0986	1.1488	-	0.0161	0.095	1.1883	-	-
407	s4_04_30_w5_00_00	0.5	0	1990	0.1444	1.8734	0.3026	0.4510	0.1501	1.9922	0.1031	0.0776
406	s4_04_30_w6_00_00	0.5	0	1450	0.1415	1.3985	0.1698	0.3671	0.1457	1.4772	-	-
458	s4_04a_30_w1_00_00	0.55	0	1690	0.0839	1.5049	0.7560	1.2905	0.0889	1.5154	-	-
459	s4_04a_30_w2_00_00	0.55	5	1220	0.0855	1.1056	0.2460	0.2540	0.0905	1.1068	-	-
460	s4_04a_30_w3_00_00	0.55	7	2000	0.1168	1.7592	3.4586	3.8123	0.1249	1.755	0.0583	0.0524
461	s4_04a_30_w4_00_00	0.55	6	1400	0.1136	1.2691	0.9256	1.3382	0.1211	1.2659	-	-
462	s4_04a_30_w5_00_00	0.55	6	2180	0.1511	1.9211	8.2892	8.4188	0.1571	1.9402	0.4241	0.4264
463	s4_04a_30_w6_00_00	0.55	7	1580	0.1388	1.4134	2.7288	3.8893	0.148	1.4117	0.0298	0.0578
412	s4_05_30_w1_49_00	0.55	0	1390	0.0663	1.3294	-	0.0049	0.07	1.3352	-	-
413	s4_05_30_w3_49_00	0.55	0	1630	0.0898	1.5738	0.0743	0.1169	0.0964	1.5752	-	-
414	s4_05_30_w5_49_00	0.55	3	1995	0.1371	1.8786	0.0645	0.2312	0.1443	1.9164	0.1216	0.0956
415	s4_06_30_w1_25_00	0.5	0	1400	0.0665	1.324	-	-	0.0707	1.332	-	-
416	s4_06_30_w3_25_00	0.5	0	1650	0.0902	1.5697	0.0687	0.1373	0.0969	1.5722	-	-
417	s4_06_30_w5_25_00	0.5	2	2000	0.138	1.8778	0.0482	0.1409	0.145	1.9142	0.1022	0.0719
467	s4_07_15_w1_00_00	0.55	0	1690	0.083	1.5153	1.2000	1.2354	0.0884	1.5202	-	-
468	s4_07_15_w2_00_00	0.55	8	1220	0.0842	1.1078	0.1934	0.2571	0.0888	1.1089	-	-
469	s4_07_15_w3_00_00	0.55	0	1995	0.115	1.76	3.5755	3.4314	0.1215	1.753	0.0446	0.0529
470	s4_07_15_w4_00_00	0.55	8	1405	0.1126	1.276	1.3166	1.4645	0.1174	1.267	-	-
471	s4_07_15_w5_00_00	0.55	6	2185	0.1472	1.9182	7.8643	7.5151	0.1532	1.9421	0.2035	0.3228
472	s4_07_15_w6_00_00	0.55	6	1580	0.1369	1.4158	3.6010	3.5102	0.1428	1.4177	0.0348	0.0372
473	s4_08_15_w1_49_00	0.55	7	1700	0.0828	1.5231	1.1894	1.1950	0.0882	1.5279	-	0.0058

test-number	testseries name[8]	water depth [m]	start time of analysis	end time of analysis	at toe of 60 cm dike				at toe of 70 cm dike			
					H_{m0} [m]	$T_{m-1,0}$ [s]	loadcell 41 upstream [l/(s·m)]	loadcell 43 downstream [l/(s·m)]	H_{m0} [m]	$T_{m-1,0}$ [s]	loadcell 37 upstream [l/(s·m)]	loadcell 39 downstream [l/(s·m)]
474	s4_08_15_w3_49_00	0.55	6	2000	0.1144	1.7688	3.5722	3.4794	0.1213	1.7629	0.0686	0.0823
475	s4_08_15_w5_49_00	0.55	6	2180	0.147	1.9263	8.4080	7.5388	0.1534	1.9491	0.3792	0.5360
480	s4_10_40_w1_00_00	0.55	5	1695	0.0853	1.5183	1.0339	1.3247	0.0877	1.516	-	-
481	s4_10_40_w2_00_00	0.55	2	1215	0.0856	1.1112	0.2754	0.2078	0.0896	1.109	-	-
482	s4_10_40_w3_00_00	0.55	8	2000	0.1158	1.7548	3.1147	3.9118	0.123	1.7523	0.0637	0.0574
483	s4_10_40_w4_00_00	0.55	9	1405	0.113	1.2688	0.9922	0.9796	0.1194	1.2707	-	-
484	s4_10_40_w5_00_00	0.55	7	2180	0.1497	1.921	8.3000	9.1107	0.1546	1.9438	0.5111	0.4032
485	s4_10_40_w6_00_00	0.55	9	1580	0.138	1.4198	2.6215	3.8348	0.1465	1.4088	0.0255	0.0398
488	s4_11_40_w1_49_00	0.55	13	1700	0.085	1.5297	0.7574	0.8668	0.0883	1.5209	0.0069	0.0064
489	s4_11_40_w3_49_00	0.55	7	2000	0.1151	1.7676	3.0510	3.7794	0.1234	1.76	0.0907	0.0931
490	s4_11_40_w5_49_00	0.55	7	2180	0.1495	1.9315	9.1309	9.0287	0.1554	1.9511	0.5439	0.4711
432	s4_32_30_w1_00_15w	0.5	0	1385	0.0648	1.3582	-	-	0.0666	1.3601	-	-
433	s4_32_30_w2_00_15w	0.5	9	980	0.0589	1.0085	-	-	0.0626	1.0063	-	-
434	s4_32_30_w3_00_15w	0.5	8	1650	0.0865	1.5515	0.0405	0.0232	0.0897	1.5346	-	-
435	s4_32_30_w4_00_15w	0.5	9	1160	0.0896	1.1822	0.0068	0.0059	0.0925	1.1721	-	-
437	s4_32_30_w5_00_15w	0.5	7	2000	0.1228	1.7823	0.2843	0.5561	0.1403	1.8995	0.0676	0.0426
438	s4_32_30_w6_00_15w	0.5	5	1460	0.1335	1.4172	0.1920	0.1772	0.1424	1.4201	-	-
440	s4_33_30_w3_00_15a	0.5	8	1650	0.0993	1.5908	0.1130	0.0797	0.1026	1.5656	-	-
441	s4_33_30_w4_00_15a	0.5	10	1170	0.0941	1.1909	0.0067	0.0059	0.1001	1.1835	-	-
442	s4_33_30_w5_00_15a	0.5	14	2010	0.1363	1.8171	2.1205	1.0155	0.1416	1.8313	0.0328	0.0338
443	s4_33_30_w6_00_15a	0.5	5	1460	0.1442	1.4457	0.2746	0.1940	0.1555	1.4257	-	-
444	s4_34_00_w1_00_15w	0.55	4	1690	0.0873	1.5303	0.6607	0.8653	0.089	1.5193	-	-
445	s4_34_00_w2_00_15w	0.55	0	1210	0.0819	1.1213	0.1066	0.0735	0.0869	1.1194	-	-
447	s4_34_00_w3_00_15w	0.55	8	2000	0.1127	1.7362	1.7283	3.1175	0.1168	1.7551	0.0471	0.0500
448	s4_34_00_w4_00_15w	0.55	9	1405	0.1082	1.2797	0.5108	0.4919	0.1167	1.275	-	-
449	s4_34_00_w5_00_15w	0.55	8	2175	0.1394	1.884	4.1430	7.0727	0.1539	1.9745	0.3827	0.4079
450	s4_34_00_w6_00_15w	0.55	0	1565	0.1389	1.4322	2.0614	2.0973	0.1472	1.4144	0.0144	0.0094

test-number	testseries name[8]	water depth [m]	start time of analysis	end time of analysis	at toe of 60 cm dike				at toe of 70 cm dike			
					H_{m0} [m]	$T_{m-1,0}$ [s]	loadcell 41 upstream [l/(s·m)]	loadcell 43 downstream [l/(s·m)]	H_{m0} [m]	$T_{m-1,0}$ [s]	loadcell 37 upstream [l/(s·m)]	loadcell 39 downstream [l/(s·m)]
476	s4_35_15_w1_00_00	0.55	0	1395	0.0677	1.3331	0.2724	0.3172	0.0695	1.3339	-	-
477	s4_35_15_w2_00_00	0.55	7	980	0.0656	0.9818	0.0341	0.0412	0.0696	0.979	-	-
486	s4_36_40_w1_00_00	0.55	8	1400	0.0675	1.3327	0.2624	0.2702	0.0725	1.3443	-	-
487	s4_36_40_w2_00_00	0.55	3	980	0.0669	0.9852	0.0420	0.0260	0.0696	0.9833	-	-
511	s5_13_00_w1_00_30w	0.55	7	1705	0.0796	1.5517	0.4516	0.3515	0.0878	1.5593	-	-
512	s5_13_00_w2_00_30w	0.55	8	1225	0.0778	1.1379	0.0377	0.0546	0.0789	1.1393	-	-
513	s5_13_00_w3_00_30w	0.55	7	2010	0.1164	1.7969	2.3627	1.3202	0.1178	1.7524	0.0171	0.0254
514	s5_13_00_w4_00_30w	0.55	10	1405	0.1006	1.2829	0.3648	0.4600	0.1049	1.296	-	-
515	s5_13_00_w5_00_30w	0.55	7	2190	0.1461	1.9454	5.3020	3.8739	0.1374	1.9244	0.1803	0.2018
516	s5_13_00_w6_00_30w	0.55	3	1580	0.1265	1.4409	1.4300	1.3974	0.1339	1.4465	-	-
536	s5_15_00_w1_49_30w	0.55	8	1700	0.0778	1.5557	0.4948	0.3343	0.0848	1.5644	-	-
537	s5_15_00_w3_49_30w	0.55	7	2000	0.113	1.8022	2.4106	1.2857	0.1155	1.7626	0.0255	0.0402
538	s5_15_00_w5_49_30w	0.55	8	2180	0.1442	1.9431	5.4362	3.5624	0.1368	1.9259	0.2096	0.2208
501	s5_16_40_w1_00_30w	0.55	12	1705	0.0813	1.5678	0.4633	0.5302	0.0737	1.5103	-	-
502	s5_16_40_w2_00_30w	0.55	7	1225	0.0721	1.1423	0.0441	0.0754	0.0782	1.1684	-	-
503	s5_16_40_w3_00_30w	0.55	7	2000	0.1111	1.7548	1.7566	2.6477	0.1016	1.747	-	-
504	s5_16_40_w4_00_30w	0.55	7	1405	0.101	1.3012	0.6722	0.5282	0.1055	1.2932	-	-
505	s5_16_40_w5_00_30w	0.55	7	2180	0.1375	1.8625	3.9073	5.3336	0.1263	1.9453	0.0638	0.1218
506	s5_16_40_w6_00_30w	0.55	4	1580	0.1298	1.4513	1.5639	1.5999	0.1263	1.4053	-	-
508	s5_17_40_w1_49_30w	0.55	9	1705	0.0822	1.5698	0.5921	0.4469	0.0746	1.5113	-	-
509	s5_17_40_w3_49_30w	0.55	8	2005	0.1118	1.7592	2.3456	2.2695	0.1027	1.7477	0.0083	0.0171
510	s5_17_40_w5_49_30w	0.55	7	2185	0.1382	1.8621	4.5066	5.5440	0.1281	1.9491	0.1197	0.1951
517	s5_19_30_w1_00_30w	0.55	1	1700	0.0802	1.5754	0.7578	0.6094	0.0768	1.5165	-	-
518	s5_19_30_w2_00_30w	0.55	8	1230	0.0695	1.1386	0.1127	0.0727	0.0743	1.1593	-	-
519	s5_19_30_w3_00_30w	0.55	8	2000	0.1107	1.7723	2.6986	2.7762	0.1033	1.7319	-	0.0098
520	s5_19_30_w4_00_30w	0.55	1	1395	0.0999	1.2999	0.6124	0.5410	0.1073	1.3018	-	-
521	s5_19_30_w5_00_30w	0.55	1	2175	0.1398	1.8843	5.4766	5.3970	0.1252	1.923	0.0926	0.1981

test-number	testseries name[8]	water depth [m]	start time of analysis	end time of analysis	at toe of 60 cm dike				at toe of 70 cm dike			
					H_{m0} [m]	$T_{m-1,0}$ [s]	loadcell 41 upstream [l/(s·m)]	loadcell 43 downstream [l/(s·m)]	H_{m0} [m]	$T_{m-1,0}$ [s]	loadcell 37 upstream [l/(s·m)]	loadcell 39 downstream [l/(s·m)]
522	s5_19_30_w6_00_30w	0.55	7	1580	0.1292	1.4496	1.8840	1.8970	0.1321	1.4153	-	-
523	s5_20_30_w1_49_30w	0.55	8	1700	0.0813	1.5758	0.6016	0.5369	0.0768	1.5163	-	-
524	s5_20_30_w3_49_30w	0.55	8	2000	0.1114	1.7738	2.4932	2.6234	0.1035	1.7342	0.0137	0.0309
525	s5_20_30_w5_49_30w	0.55	8	2185	0.1404	1.8859	5.3593	5.5724	0.1254	1.9253	0.1463	0.2611
530	s5_22_15_w1_00_30w	0.55	7	1700	0.0778	1.5769	0.4662	0.4085	0.082	1.5413	-	-
531	s5_22_15_w2_00_30w	0.55	8	1220	0.0681	1.1332	0.0387	0.0443	0.0741	1.14	-	-
532	s5_22_15_w3_00_30w	0.55	7	2000	0.1125	1.8012	2.3834	1.8039	0.1104	1.7398	0.0088	0.0201
533	s5_22_15_w4_00_30w	0.55	7	1405	0.0972	1.2922	0.3515	0.3368	0.1062	1.3025	-	-
534	s5_22_15_w5_00_30w	0.55	3	2180	0.1432	1.9267	5.5261	4.3000	0.1301	1.9092	0.1234	0.1997
535	s5_22_15_w6_00_30w	0.55	9	1585	0.1284	1.4497	1.3563	1.3207	0.1369	1.4322	-	-
613	s6_25_00_w1_00_45a	0.55	8	1705	0.0819	1.6142	0.4139	0.3707	0.0771	1.5552	-	-
614	s6_25_00_w2_00_45a	0.55	8	1230	0.0702	1.1486	0.0384	0.0512	0.0751	1.1608	-	-
615	s6_25_00_w3_00_45a	0.55	11	2005	0.1256	1.8328	1.5332	1.3437	0.1124	1.7857	0.0333	-
616	s6_25_00_w4_00_45a	0.55	7	1405	0.097	1.3107	0.2984	0.3291	0.1044	1.306	-	-
617	s6_25_00_w5_00_45a	0.55	7	2185	0.1514	1.9599	2.9336	2.5135	0.1407	1.9801	-	0.0695
618	s6_25_00_w6_00_45a	0.55	1	1580	0.1287	1.4754	0.8741	0.8611	0.1284	1.4297	-	-
607	s6_26_15_w1_00_30a	0.55	6	1670	0.0823	1.5344	0.6604	1.2491	0.0867	1.551	-	-
608	s6_26_15_w2_00_30a	0.55	7	1225	0.0798	1.1525	0.0850	0.1812	0.0808	1.1521	-	-
609	s6_26_15_w3_00_30a	0.55	6	2000	0.1115	1.7661	2.9695	3.6044	0.1181	1.7901	0.0583	0.0304
610	s6_26_15_w4_00_30a	0.55	7	1400	0.1116	1.3013	0.5869	0.8064	0.1103	1.3026	-	-
611	s6_26_15_w5_00_30a	0.55	1	2175	0.1413	1.9224	6.4911	6.3955	0.1563	1.9753	0.3922	0.1748
612	s6_26_15_w6_00_30a	0.55	7	1580	0.1349	1.4359	2.0335	2.5192	0.1427	1.4391	0.0112	0.0118
601	s6_27_15_w1_00_45a	0.55	7	1700	0.0821	1.5765	0.4950	0.6220	0.0839	1.5848	-	-
602	s6_27_15_w2_00_45a	0.55	6	1225	0.0707	1.165	0.0248	0.0529	0.0701	1.1741	-	-
603	s6_27_15_w3_00_45a	0.55	7	2000	0.1149	1.7967	2.0554	1.7551	0.1116	1.7862	0.0167	0.0127
604	s6_27_15_w4_00_45a	0.55	7	1405	0.1011	1.3232	0.2879	0.3885	0.1026	1.3346	-	-
605	s6_27_15_w5_00_45a	0.55	7	2180	0.1394	1.944	3.4241	3.2686	0.1376	1.9761	0.0778	0.1016

test-number	testseries name[8]	water depth [m]	start time of analysis	end time of analysis	at toe of 60 cm dike				at toe of 70 cm dike			
					H_{m0} [m]	$T_{m-1,0}$ [s]	loadcell 41 upstream [l/(s·m)]	loadcell 43 downstream [l/(s·m)]	H_{m0} [m]	$T_{m-1,0}$ [s]	loadcell 37 upstream [l/(s·m)]	loadcell 39 downstream [l/(s·m)]
606	s6_27_15_w6_00_45a	0.55	7	1585	0.1313	1.4662	1.3133	1.5855	0.1323	1.4664	-	-
625	s6_28_30_w1_00_30a	0.55	2	1695	0.0848	1.5414	0.7674	1.1632	0.0879	1.5696	0.0058	-
626	s6_28_30_w2_00_30a	0.55	8	1225	0.0822	1.1436	0.1372	0.2480	0.0777	1.1645	-	-
627	s6_28_30_w3_00_30a	0.55	2	1995	0.1159	1.8005	3.3499	3.4673	0.121	1.8012	0.1157	0.0417
628	s6_28_30_w4_00_30a	0.55	8	1405	0.1104	1.2937	0.7761	0.9055	0.1114	1.3203	-	-
629	s6_28_30_w5_00_30a	0.55	8	2180	0.1537	1.9767	6.3696	7.5252	0.1632	1.9929	0.5725	0.2190
630	s6_28_30_w6_00_30a	0.55	7	1580	0.1349	1.4416	2.3237	2.7667	0.1455	1.4528	0.0385	0.0168
619	s6_29_30_w1_00_45a	0.55	4	1700	0.0907	1.5904	0.6330	0.7556	0.0878	1.627	-	-
620	s6_29_30_w2_00_45a	0.55	3	1220	0.071	1.1863	0.0369	0.0835	0.0648	1.207	-	-
621	s6_29_30_w3_00_45a	0.55	7	2000	0.1156	1.7761	2.2714	2.7331	0.1185	1.8044	0.0118	0.0284
622	s6_29_30_w4_00_45a	0.55	8	1405	0.1073	1.348	0.3028	0.5083	0.1006	1.3566	-	-
623	s6_29_30_w5_00_45a	0.55	8	2180	0.1398	1.9454	4.0121	4.9922	0.1459	1.9816	0.0720	0.1484
624	s6_29_30_w6_00_45a	0.55	8	1580	0.1431	1.489	1.2336	1.6796	0.1357	1.5079	-	-
637	s6_30_40_w1_00_30a	0.55	9	1705	0.0851	1.5664	0.8512	0.8466	0.0882	1.5822	0.0132	-
638	s6_30_40_w2_00_30a	0.55	8	1225	0.0805	1.1506	0.1268	0.1822	0.0755	1.1754	-	-
639	s6_30_40_w3_00_30a	0.55	9	2000	0.1197	1.8182	2.8761	3.2906	0.1254	1.8084	0.1472	0.0392
640	s6_30_40_w4_00_30a	0.55	5	1400	0.1081	1.3125	0.6519	0.9208	0.1113	1.3358	0.0063	-
641	s6_30_40_w5_00_30a	0.55	7	2180	0.1578	2.0076	5.1934	7.3840	0.1652	1.9978	1.0241	0.2549
642	s6_30_40_w6_00_30a	0.55	4	1580	0.1337	1.4674	2.3979	2.5195	0.1452	1.4616	0.0595	0.0081
631	s6_31_40_w1_00_45a	0.55	9	1705	0.0905	1.5913	0.5051	0.6923	0.0873	1.6476	-	-
632	s6_31_40_w2_00_45a	0.55	8	1225	0.0756	1.2009	0.0385	0.0698	0.061	1.2264	-	-
633	s6_31_40_w3_00_45a	0.55	8	2005	0.1204	1.7791	1.9815	2.8726	0.1218	1.8376	0.0088	0.0127
634	s6_31_40_w4_00_45a	0.55	5	1400	0.1132	1.3492	0.3606	0.5210	0.098	1.3814	-	-
635	s6_31_40_w5_00_45a	0.55	6	2180	0.146	1.9582	4.0148	5.0046	0.1548	2.0029	0.0800	0.0921
636	s6_31_40_w6_00_45a	0.55	15	1590	0.144	1.4847	1.0475	1.4448	0.1363	1.524	-	-